The evolution of the anti-HIV envelope antibody response

Katie McFaul
Imperial College London
Centre for Immunology and Vaccinology
Department of Medicine

Supervisors: Dr Peter Kelleher, Prof Xiao-Ning Xu

Thesis submitted for the Degree of Doctor of Philosophy

Declaration of originality

I, Katie McFaul, declare the work presented in this thesis is my own work. Where information has derived from other published or unpublished source, or collaboration, I confirm this has been referenced appropriately.

Copyright Declaration

The copyright of this thesis rests with the author and is made available under a Creative Commons Attribution Non-Commercial No Derivatives licence. Researchers are free to copy, distribute or transmit the thesis on the condition that they attribute it, that they do not use it for commercial purposes and that they do not alter, transform or build upon it. For any reuse or redistribution, researchers must make clear to others the licence terms of this work.

Acknowledgments

One of the enjoyable things about coming to the end of a project is the opportunity to look back on the last few years and consider all factors contributing to the work. To my mind, there are three essential components for successful research- a robust proposal to define the project, a supportive place in which to execute the work, and the people involved in delivering the project outcomes- I am privileged to have had top quality material and support in all three.

This project was made possible by the foresight and collaborative work of a group of clinicians and researchers to whom I am incredibly grateful for the opportunity to pursue this work. My work locations of the Dean Street Clinic in Soho and the Centre for Immunology and Vaccinology (CIV) at Imperial College are unique and special places, and vanguards in their respective arenas. I have learned so much and consider myself lucky to be part of your teams.

My thanks to the people who helped this project come alive. To the participants of the Dean Street cohort, I thank you for your selfless sacrifice of time and tissue. To Dr Nneka Nwokolo, Dr Alan McOwan and Dr Emma Devitt- thank you for the opportunity to undertake this work. To the CIV team, my thanks for allowing a physician to explore the deepest realms of immunology and molecular biology. Prof Xiao-Ning Xu and Dr Nesrina Imami for guidance, Parisa Amjadi for hours of cell sorting assistance, Dominic Smith for unflappable capability, and the CIV extended family for support during the past few years. And my wholehearted gratitude to Dr Peter Kelleher for his insight, patience, and endless support. Finally to my friends and family, I thank you for your unwavering support, capacity for listening, and ability to grant me perspective when things don't proceed according to "established protocols".

In summary, the lessons learned from this endeavour include an appreciation of perseverance, patience, and stamina. I leave the final words here to Seamus Heaney; "The next move is always the test".

Abstract

IgG and IgA antibodies against HIV-1 envelope protein in the absence of infection is well documented in highly exposed seronegative individuals. The origin of these immune responses may be due to cross reactivity with intestinal commensal bacteria or result from ongoing exposure to viral particles. Pre-HIV-1 infection immune responses against envelope glycoproteins may influence the future trajectory of disease. This project aimed to describe anti-HIV-1 gp140 envelope antibody responses in exposed seronegative individuals and track their development before and after HIV-1 infection. I screened sera from a cohort of highly exposed seronegative men who have sex with men with a yeast displayed HIV-1 gp140 envelope antigen fragment library to map discrete epitopes responsible for anti-HIV-1 humoral responses.

Using batched seronegative serum aliquots, I found humoral immune responses against V1/V2 and C2 gp120 epitopes, and the C helical region, membrane proximal external region, transmembrane domain and endodomain of gp41. Stratification of cohort according to risk region of acquisition of HIV-1 infection revealed no significant changes in the distribution of envelope epitope detected. Immune response to gp41 envelope epitopes were significantly greater in high risk compared with low risk individuals. Antibody response to HIV-1 gp140 envelope protein were assessed longitudinally in five individuals before and after HIV-1 infection. I showed the same HIV-1 gp140 epitopes were recognized in pre and post seroconversion samples suggesting previous antigen exposure lays a template for future humoral responses. In addition, certain pre-exposure gp140 epitopes had amino sequence similarity to intestinal bacterial antigens.

I then used gp140 envelope fragments expressed by yeast cells to isolate single antigen-specific B cells, followed by expression cloning to generate monoclonal envelope antibodies. Antibody dependent cytotoxic function of a single pre-infection monoclonal envelope antibody was assessed. This technology may help increase understanding of humoral immunity to HIV-1.

1. Contents

1. Background and introduction 26
1.1 Human Immunodeficiency Virus (HIV) 26
1.1.1 HIV as the causative agent of the acquired immune deficiency syndrome (AIDS) 26
1.2 HIV Transmission and acute infection 28
1.3 HIV Envelope protein 28
1.3.1 Establishing the viral reservoir 31
1.3.2 Chronic infection and progression to AIDS 31
1.3.3 HIV Testing 33
1.3.4 HIV Treatment 33
1.3.5 HIV Prevention 34
1.3.6 Potential for a HIV vaccine 38
1.4 Humoral immunity 38
1.4.1 B cells 38
1.4.2 Antibody structure and function 39
1.5 Humoral responses in HIV infection 43
1.5.1 B cells in HIV infection 43
1.5.2 B cell responses to HIV infection 44
1.5.3 Control of viraemia in HIV-infected people 46
1.6 Broadly Neutralising Antibodies 47
1.7 Non neutralising antibodies 49
1.8 Anti-HIV responses in seronegative exposed individuals 51
1.8.1 Innate 51
1.8.2 Adaptive immune response- cellular 53
1.8.3 Adaptive immune response- humoral 54
1.8.4 Do HESN protective responses vary according to frequency of exposure? 55
1.10 Antibody responses in HIV vaccination trials 56
1.11 HIV eradication strategies 61
1.12 Anti-Env antibodies 62
1.12.1 The first responder 62
1.12.2 The second coming? 63
1.12.3 Significance of anti-Env response 65
1.13 Summary 66
1.14. Hypothesis 67
1.14.1 Anti-Env in HIV-uninfected people 67
1.14.2 Origin of anti-Env antibodies in HIV pathogenesis 67
1.14.3 Role of anti-Env antibodies in HIV disease and progression 67
1.14.4 Hypothesis 69

1.15 Objectives 70
1.15.1 Cohort 70
1.15.2 Analysis 70
1.15.3 Function 70
2. Background and introduction 61
2.1 Project details 61
2.1.1 Project design 61
2.2 Ethical approval 61
2.2.1 Local Biosafety approval 61
2.3 Cohort details 61
2.3.1 Cohort characteristics 63
2.3.2 Cohort management 66
2.4 Experimental techniques 66
SCHEMATIC OF YEAST SURFACE DISPLAY TECHNOLOGY 67
2.5 Yeast Display System construction 68
2.6 Genomic sequence 68
2.6.1 Primers 68
2.6.2 Preparation of patient samples- plasma and serum 87
2.6.3 Preparation of patient samples - PBMC 88
2.6.4 PBMC counting 88
2.6.5 PBMC freezing and storage 89
2.6.6 Tissue bank depository 89
2.6.7 CD20 adsorption of patient serum pools 89
2.6.8 Flow cytometry 90
2.6.9 Monoclonal antibody work 94
2.6.10 Protocol for yeast antigen baiting 95
2.6.11 Monoclonal antibody production 133
2.6.12 IgG enzyme-linked immunosorbent assay (ELISA) to test for the presence of antibody 153
2.6.13 Polyacrylamide gel electrophoresis (PAGE) to assess antibody molecular weight 157
2.6.14 Screening supernatant antibodies for HIV specific responses 159
2.6.15 Identification of cross reactivity with gut microbiota 161
2.6.16 Functional assessments 161
3. Seronegative cohort 130
3.1 Introduction 130
3.2 Aims 133
3.3 Baseline demographics 134
3.3.1 Group A seronegative 134

3.3.2 Group E seropositive 135
3.4 Selection of participant serum samples 136
3.5 Serum aliquot allocation 136
3.6 HIV gp160 library analysis of seronegative serum aliquots 137
3.6.1 Preparation of the patient serum samples 138
3.6.2 Sample preparation for HIV Envelope library analysis of seronegative aliquots 138
3.6.3 Initial FACS gp160 screening of serum aliquots 139
3.6.4 Sequential enrichment 143
3.6.5 Single clone analysis 146
3.6.6 Sequential enrichment summary 151
3.6.7 Sequence analysis plots 153
3.6.8 Sequence analysis histograms 155
3.6.9 Single clone analysis of individual participant serum 160
3.6.10 Summary of HIV gp160 epitope recognition 163
3.7 HIV gp41 library analysis of seronegative serum aliquots 167
3.7.1 Aims 167
3.7.2 Sample preparation for HIV gp41 library analysis of seronegative serum aliquots 168
3.7.3 Initial FACS gp41 screening of serum aliquots 168
3.7.4 Single clone analysis 174
3.7.5 Sequential enrichment summary 176
3.7.6 Sequence analysis plots 177
3.7.7 Sequence analysis histogram 179
3.8 HIV-1 gp41 epitope recognition in low-risk vs high-risk serum aliquots 185
3.8.1 Overall gp41 sequence recognition 185
3.8.2 Proportion of gp41 sequences recognised by fragments from each risk group 186
3.8.3 HIV-1 gp41 epitope recognition in low-risk vs high-risk serum aliquots 187
3.9 Discussion 188
3.9.1 Summary 188
3.9.2 Cohort recruitment 188
3.9.3 HIV gp160 library analysis of seronegative serum aliquots 188
3.9.4 HIV gp41 library analysis of seronegative serum aliquots 191
3.9.5 HIV-1 gp41 epitope recognition in low-risk vs high-risk serum aliquots 192
3.9.6 Limitations of work 193
3.9.7 Future Work 195
3.10 Conclusion 195
4. Seroconverter cohort 198
4.1 Introduction 198
4.2 Aims 200

4.3 Group B cohort 200
4.3.1 Identification of candidate samples 200
4.3.2 Baseline demographics group B 201
4.3.3 Group B visits 203
4.3.4 HIV seroconversion assessment 203
4.3.5 Group B antiretroviral therapy 207
4.3.6 Group B baseline HIV characteristics 208
4.3.7 Viral load dynamics of Group B 209
4.4 gp160 library analysis of seroconverter serum aliquots 210
4.4.1 Seroconverter serum FACS results 211
4.4.2 Sequential enrichment plots 212
4.4.3 Sequential enrichment graph 217
4.4.4 Single clone analysis 219
4.4.5 Sequential enrichment summary 224
4.4.6 Sequence analysis plots 225
4.4.7 Sequence analysis histograms 229
4.4.8 Single clone sequence analysis 236
4.5 Major antigenic domain/determinant for selected samples 237
4.6 Direct comparison of all samples and stages 239
4.6.1 Individual gp120 vs gp41 responses 240
4.6.2 All infection samples- gp120 individual epitope recognition 241
4.6.3 All infection samples- gp41 epitope recognition 245
4.7 Cross reactivity with gut microbiota 249
4.7.1 Pre infection serum selected epitopes and *E.coli* RNA polymerase 249
4.8 Summary 247
4.8.1 Serum antibody responses to HIV envelope antigens at pre, early and late infection 247
4.8.2 Identification of antigens recognised by host immune responses 247
4.8.3 Overlapping epitope recognition 252
4.8.4 Intestinal microbiota 253
4.8.5 Limitations 255
4.8.6 Future work 256
4.8.7 Conclusion 257
5. Monoclonal antibody production 248
5.1 Introduction 248
5.2 Aims 250
5.3 Basic experiment setup 251
5.3.1 Experimental controls and samples 251

5.3.2 Optimisation of sorting experiment 257
5.4 Experimental B cell antigen baiting 262
5.4.1 Flow sorting plots- experimental 264
5.5 Monoclonal antibody optimisation 266
5.5.1 Single cell reverse transcriptase (RT-PCR) and cloning polymerase chain reaction 266
5.5.2 Cloning PCR 266
5.6 Monoclonal antibody- experimental results 267
5.6.1 Cloning PCR results 267
5.6.2 Kappa chain sequence analysis 269
5.6.3 Flow sorting and PCR cloning yields 270
5.6.4 PreB3 anti-gp41 monoclonal antibody production- digestion, ligation 273
5.6.5 PreB3 anti-gp41 monoclonal antibody production- miniprep and digest outcome 274
5.6.6 Transfection of HEK293 cells 299
5.6.7 ELISA screening of supernatants 299
5.6.8 Sodium dodecyl sulphate (SDS) polyacrylamide gel electrophoresis 303
5.6.9 Monoclonal antibody anti-HIV specificity screening 304
5.7 Review of HIV specific monoclonal antibody properties 309
5.7.1 Gene family usage 309
5.7.2 Variable region analysis 310
5.9 Functional assay using rapid fluorometric ADCC assay 312
5.10 Summary 313
5.10.1 B cell antigen baiting and monoclonal antibody production 313
5.10.2 Monoclonal antibody anti-HIV specificity 315
5.10.3 Monoclonal antibody properties 315
5.10.4 Functional assay using Rapid Fluorometric ADCC 316
5.10.5 Assessment of mAb binding specificity 317
5.11 Summary 317
6. Discussion 300
7. References 312
8. Appendices 362

Tables

Table 1.9-1 Summary of HIV vaccine trials to date 59
Table 2.2-1 Primer sequences used for HIV gp160 envelope PCR 69
Table 2.2-2 HIV Envelope and gp41 primer optimisation products 71
Table 2.2-3 Digested library product concentrations 73
Table 2.2-4 A-tailed PCR library fragments 74
Table 2.2-5 pCTCON2-T vector digest concentration 75
Table 2.2-6 Ligated fragment/vector yield 76
Table 2.2-7 Bacterial transformation efficacy 78
Table 2.3-8 Library fragment plasmids 81
Table 2.3-9 Yeast transformation efficacy 83
Table 2.3-10 Flow cytometry panel setup 92
Table 2.3-11 Flow cytometry gating strategies 93
Table 2.3-12 PBMC cell surface markers 97
Table 2.3-13 Flow sorting experiment samples 129
Table 2.3-14 Gating strategy for yeast sorting of B cells 130
Table 2.4-1 Reagents and volumes for RT-PCR reaction 135
Table 2.6-2 Nested kappa PCR primers 135
Table 2.4-3 Nested kappa chain variable region PCR 136
Table 2.3-18 Heavy chain cloning PCR primers 140
Table 2.3-19 Lambda chain cloning PCR primers 140
Table 2.3-20 Kappa chain cloning PCR primers 140
Table 2.3-21 Vector digestion components 141
Table 2.3-22 Variable chain insert digestion product concentration 142
Table 2.3-23 Vector insert molecular weight 143
Table 2.3-24 Ligation reaction components 144
Table 2.3-25 Minidigest reagent list and volumes 147
Table 3.3-1 1 Group A details 134
Table 3.3-2 Group E details 135
Table 3.6-1 Proportion of low and high-risk MSM sera which react with gp160 yeast expressing clones 141
Table 3.6-2 Mean and standard deviation (SD) of percentage of total yeast population expressing gp160 envelope library recognized by low and high-risk MSM sera 142
Table 3.6-3 Number of single clones which bind to yeast gp160 envelope library 149
Table 3.6-4 Summary sequential FACS sorting and single yeast clone analysis 152
Table 3.6-5 5 Summary of findings for gp160 envelope epitopes detected in LR and HR sera 157
Table 3.6-6 Proportions of fragments recognising discrete region of HIV-1 envelope 165
Table 3.7-1 Proportion of low and high-risk MSM sera which react with gp41 yeast expressing clones 170
Table 3.7-2 Mean and standard deviation (SD) of percentage of total yeast population expressing gp41 envelope library recognized by low and high-risk MSM sera 170
Table 3.7-3 Summary sequential FACS sorting and single yeast clone analysis 177
Table 3.7-4 Summary table of epitope recognition and sequences for gp41 yeast library sorting 181
Table 3.8-1 Seronegative sera recognition of discrete gp41 epitope 187
Table 3.9-1 Proportions of total AUC found in each region of gp160 as per aliquot. 192
Table 4.3-1 Group B baseline information 202
Table 4.3-2 Distribution of baseline patient characteristics 202
Table 4.3-3 Western blot analysis of Group B participants 204
Table 4.3-4 Chronology of Group B HIV infection 206
Table 4.3-5 Group B longitudinal follow-up schedule 206
Table 4.3-6 Details of antiretroviral initiation 207

Table 4.3-7 Characteristics of HIV infection in Group B 208
Table 4.3-8 Viral load dynamics Group B 209
Table 4.4-1 Percentage of gp160 envelope expressing yeast cell reactive with patient sera 212
Table 4.4-2 Percentage of gp160 envelope positive yeast cells which bind to control and patient sera following sequential FACS sort enrichment 217
Table 4.4-3 No of single yeast gp160 envelope clones which react with patient sera 221
Table 4.4-4 Summary table of proportion of yeast gp160 envelope yeast cells which react with patient sera following sequential FACS sort and enrichment 224
Table 4.4-5 Number of sequences available from 50 clones submitted 226
Table 4.4-6 Summary of gp160 epitope recognition by seroconverter serum 235
Table 4.4-7 Single clone analysis of seroconverter samples 236
Table 4.5-1 Summary table of major antigenic determinants for B003 238
Table 4.6-1 Pre, early and late infection sequence fragment review 240
Table 4.6-2 gp120 epitope recognition 243
Table 4.6-3 gp41 epitope recognition 247
Table 4.7-1 Pre infection serum gp41 epitopes 250
Table 4.8-1 Endodomain epitope locations 249
Table 4.8-2 Review of gp41 epitope and *E.coli* alignment 255
Table 5.3-1 FACS experiment setup 251
Table 5.3-2 Q2 cell population 258
Table 5.3-3 Sorted population proportions 260
Table 5.3-4 Index sorting yield 261
Table 5.4-1 Yeast clones selected for B cell baiting 263
Table 5.4-2 Summary of APC high/Pacific Blue high sorted population 264
Table 5.5-1 Outcomes for chain pairs 267
Table 5.6-1 Cloning PCR outcomes 268
Table 5.6-2 Antibody gene family, framework region and complementarity determining lengths for all anti-gp41 antibodies (continued) 276
Table 5.6-2 ELISA plate setup 299
Table 5.6-3 ELISA plate readout for transfection 1 300
Table 5.6-4 ELISA plate readout for transfection 2 300
Table 5.6-5 Standards for ELISA and mean optical density 301
Table 5.6-6 ELISA concentration calculations 302
Table 5.6-7 Analysis of mean fluorescence intensity of control and HIV monoclonal antibodies to gp140 coated CEM.NKr cells 307
Table 5.6-8 Paired t-tests for comparison of control and experimental monoclonal antibodies 308
Table 5.7-1 MAb gene family usage 309
Table 5.7-2 MAb heavy and light chain framework regions 310
Table 5.7-3 MAb heavy and light chain complementarity determining regions 311

Figures

Figure 1.3-1 HIV envelope protein- trimer....29
Figure 1.3-2 Env protein forms....29
Figure 1.4-1 Schematic of antibody structure....40
Figure 1.4-2 Schematic of variable region....41
Figure 1.6-1 Sites of vulnerability on HIV-1 envelope glycoprotein....48
Figure 2.4-1 Schematic of yeast surface display technology....67
Figure 2.6-1 TBE gel electrophoresis of HIV envelope PCR target products....69
Figure 2.6-2 Temperature gradient PCR optimisation....70
Figure 2.6-3 TBE gel electrophoresis of gp41 envelope PCR target products....71
Figure 2.6-4 Gel electrophoresis of digested HIV envelope and gp41....73
Figure 2.6-5 Digested pCTCON2-T vector....75
Figure 2.6-6 HIV envelope library coverage....79
Figure 2.6-7 HIV gp41 small library coverage....80
Figure 2.6-8 HIV gp41 big library coverage....80
Figure 2.6-9 Gating strategy for yeast serum sorting....93
Figure 2.6-10 Gating strategy for B cell baiting using yeast library....130
Figure 2.6-11 Yeast B cell baiting schematic....132
Figure 2.6-12 Reverse transcriptase PCR primers....134
Figure 2.6-13 TBE gel electrophoresis of RT-PCR sorted chain inserts....138
Figure 2.6-14 HEK293A cell growth....149
Figure 2.6-15 ELISA plate layout....155
Figure 2.6-16 96-well plate for supernatant screening....160
Figure 2.6-17 RFADCC assay- courtesy Dr Scarlett Turner....163
Figure 3.5-1 Schematic of seronegative aliquot creation....136
Figure 3.6-1 HIV envelope gp160 schematic....137
Figure 3.6-2 Controls for seronegative FACS analysis....140
Figure 3.6-3 3 Representative flow cytometry dot plots of low and high-risk MSM sera sorted with gp160 yeast library....141
Figure 3.6-4 Mean and standard deviation (SD) of percentage of total yeast population expressing gp160 envelope library recognized by low and high-risk MSM sera....142
Figure 3.6-5 Serial enrichment of seronegative serum binding to the yeast gp160 envelope library following sequential FACS sorting....144
Figure 3.6-6 Mean and standard deviation (SD) of percentage of total yeast population expressing gp160 envelope library recognized by low and high-risk sera....145
Figure 3.6-7 FACS plate analysis....147
Figure 3.6-8 Flow cytometric analysis of single yeast clones....148
Figure 3.6-9 Histograms of single yeast clones which bind to the gp160 envelope library....150
Figure 3.6-10 Sequences aligned to gp160 parent sequence....154
Figure 3.6-11 Histograms of gp160 library sorted by serum samples:....156
Figure 3.6-12 HIV gp160 library sorted by seronegative serum samples....158
Figure 3.6-13 Overlay of HIV-1 amino acid sequences detected in HSEN and laboratory control....159
Figure 3.6-14 FACS plot and histograms individual serum from low-risk gp160 single clone analysis- low-risk....162
Figure 3.6-15 FACS plot and histograms individual gp160 single clone analysis- high-risk....162
Figure 3.6-16 Figure 3.6 16 Proportions of fragments recognising discrete region of HIV-1 envelope 165
Figure 3.7-1 HIV gp41 sequence schematic....167
Figure 3.7-2 Representative flow cytometry dot plots of low and high-risk MSM sera sorted with gp160 yeast library....169

Figure 3.7-3 Mean and standard deviation (SD) of percentage of total yeast population expressing gp41 envelope library recognized by low and high-risk MSM sera 170
Figure 3.7-4 Serial enrichment of seronegative serum binding to the yeast gp41 envelope library following sequential FACS sorting 172
Figure 3.7-5 Mean and standard deviation (SD) of percentage of total yeast population expressing gp41 envelope library recognized by low and high-risk sera 173
Figure 3.7-6 96 well plate with selected yeast clones for analysis by flow cytometry 174
Figure 3.7-7 Flow cytometric analysis of single yeast clones 174
Figure 3.7-8 Histograms for single clone analysis 175
Figure 3.7-9 Yeast clone sequence fragment analysis of H5, H9, L6, L10 and positive control 178
Figure 3.7-10 Histograms of gp41 library sorted by serum samples 180
Figure 3.7-11 HIV gp41 library sorted by seronegative serum samples 182
Figure 3.7-12 Overlay of HIV-1 gp41 amino acid sequences detected in HESN and controls 183
Figure 3.7-13 All HIV-gp41 amino acid sequences detected in all samples 184
Figure 3.8-1 Low and high-risk sequences combined 185
Figure 3.8-2 Proportion of gp41 epitope identified by low and high-risk MSM serum aliquots 186
Figure 3.8-3 Seronegative sera recognition of discrete gp41 epitope 187
Figure 3.9-1 Proportions of total AUC found in each region of gp160 192
Figure 4.2-1 HIV gp160 envelope sequence schematic 200
Figure 4.3-1 Group B viral load dynamics 209
Figure 4.4-1 Flow cytometric dot plots of proportion of yeast cell expressing HIV gp160 envelope which react with patient sera before and during HIV infection after 1st round of FACS sorting 213
Figure 4.4-2 Flow cytometric dot plots of proportion of yeast cell expressing HIV gp160 envelope which react with patient sera before and during HIV infection after 2nd round of FACS sorting 214
Figure 4.4-3 FACS analysis of seroconverter samples 3rd round flow cytometric dot plots of proportion of yeast cell expressing HIV gp160 envelope which react with patient sera before and during HIV infection after 3rd round of FACS sorting 215
Figure 4.4-4 Sequential enrichment of yeast gp160 envelope positive cells which bind to patient sera 216
Figure 4.4-5 Mean and standard deviation (SD) of gp160 envelope positive yeast cells which bind to control and patient sera after sequential FACS sort enrichment 218
Figure 4.4-6 Single clone analysis gating and controls 220
Figure 4.4-7 Representative histograms of single gp160 envelope yeast cells which react with patient sera (1) 222
Figure 4.4-8 Representative histograms of single gp160 envelope yeast cells which react with patient sera (2) 223
Figure 4.4-9 HIV gp160 library sorted by pre- infection samples 226
Figure 4.4-10 HIV gp160 library sorted by early infection samples 227
Figure 4.4-11 HIV gp160 library sorted by late infection samples 228
Figure 4.4-12 Control and seroconverter sequence analysis histogram- timepoints 232
Figure 4.4-13 Control and seroconverter sequence analysis histogram- participant 234
Figure 4.5-1 Sequence histograms for PC and B003 237
Figure 4.6-1 Seroconverter differential response to gp120 and gp41 240
Figure 4.6-2 Seroconverter gp120 epitope recognition 244
Figure 4.6-3 Seroconverter gp41 epitope recognition 248
Figure 4.7-1 *E.coli* subunit beta AA and gp41-1 sequences aligned 249
Figure 4.8-1 Schematic representation of gp41 endodomain 248
Figure 4.8-2 MPER and group B epitopes aligned 251
Figure 5.3-1 PBMC controls 252
Figure 5.3-2 Yeast controls 253
Figure 5.3-3 PBMC and yeast controls 254

Figure 5.3-4 PBMC and yeast increasing ratio control....255
Figure 5.3-5 PBMC cell surface marker and unstained yeast cell control....256
Figure 5.3-6 Double positive PBMC/yeast Q2 cell population....258
Figure 5.3-7 Backgating on APC and FITC channels....259
Figure 5.3-8 Backgated FITC/APC high Q2 population....259
Figure 5.4-1 FACS plots for B cell baiting....265
Figure 5.5-1 Positive control cloning PCR TBE gel analysis....267
Figure 5.6-1 Yields from successive experiments....271
Figure 5.6-2 TBE digest gels;....273
Figure 5.6-3 Standard curve to determine IgG concentration....301
Figure 5.6-4 Monoclonal antibody concentrations....302
Figure 5.6-5 SDS-PAGE gel of transfection 1....303
Figure 5.6-6 Transfection controls....305
Figure 5.6-7 Monoclonal antibody anti-HIV specificity screening FACS plots....306
Figure 5.6-8 Mean and standard deviation of mean fluorescence intensity of control and HIV monoclonal antibodies to gp140 coated CEM.NKr cells....308
Figure 5.7-1 Amino acid length of pre infection HIV heavy and light chain framework regions....310
Figure 5.7-2 Amino acid of pre-infection HIV monoclonal MAb heavy and light chain complementarity determining regions....311
Figure 5.9-1 RFDACC results- plots....312
Figure 5.9-2 RFDACC results- graph....312

List of abbreviations used

3’	3 prime
5’	5 prime
ADCC	Antibody Dependent Cellular Cytotoxicity
ADCVI	Antibody dependent cellular viral inhibition
ADP	Antibody dependent phagocytosis
AGA	Anti-gp41 antibodies
AIDS	Acquired Immune Deficiency Syndrome
APC	Antigen Presenting Cell
APC	Allophycocyanin
APOBEC3G	apolipoprotein B mRNA editing enzyme, catalytic polypeptide-like 3G
ARP	AIDS Reagent Program
ARV	Antiretroviral therapy
BLAST	Basic Local Alignment Search Tool
BNAb	Broadly Neutralising Antibody
bp	Base Pairs
BST-2,	Tetherin/bone marrow stromal antigen 2
BV421	Brilliant Violet 421
CA	Capsid
cART	Combined Antiretroviral Therapy
CD	Cluster of Differentiation
cDNA	Complementary DNA
CDR	Complementarity Determining Region
CEM.NKr	CD4+ lymphocytes resistant to natural killer cell-mediated lysis
CFSE	Carboxyfluorescein Diacetate Succinimidyl Ester
CH	Constant Heavy
CL2/3	Containment level two/three
CMV	Cytomegalovirus
CRF	Circulating Recombinant Form
DMEM	Dulbecco's Modified Eagle Medium
DMSO	Dimethyl Sulfoxide
DNA	Deoxyribonucleic acid
dNTP	Deoxynucleotide
EDTA	Ethylenediaminetetraacetic acid
ELISA	Enzyme-linked immunosorbent assays
Env	Envelope
ERP	Escherichia coli RNA polymerase
Fab	Fragment Antigen Binding
FACS	Fluorescence Activated Cell Sorting
FBS	Foetal bovine serum
Fc	Fragment Crystallisable
FcR	Fragmentable crystallisable receptor
FITC	Fluorescein Isothiocyanate
FR	Framework Region
FSC	Forward Scatter

g	Unit of gravity (for relative centrifugal force)
ɣ	Gamma
GALT	Gut-associated lymphoid tissue
gp	Glycoprotein
HDAC	Histone Deacetylase
HEK	Human Embryonic Kidney Cells
HESN	Highly exposed seronegative people
HIV	Human Immunodeficiency Virus
HIV	Human Immunodeficiency Virus
HIVIG	Anti-HIV Immune Globulin
HRP	Horseradish peroxidase
IFN	Interferon
Ig	Immunoglobulin
IMA	Intestinal microbiota
IMGT	International immunogenetics information system
IN	Integrase
J	Joining
Kb	Kilobase
kbp	kilobase pairs
LB	Lysogeny broth
M	molar (concentration)
MA	matrix
mAb	Monoclonal antibodies
mAb	Monoclonal Antibody
MAD	Major antigenic determinant
MFI	Median Fluorescence Intensity
mg/ml	Milligrams/ml
MHC	Major Histocompatibility Complex
mM	Milimolar (concentration)
MPER	Membrane Proximal External Region
mRNA	Messenger RNA
MSM	Men who have sex with men
NC	Nucleocapsid
NEAA	Non-essential amino acids
ng/ml	Nanograms/ml
NIAIDs	National Institutes of Health AIDS Reagent Program
NIBSC	National Institute for Biological Standards
NK	Natural Killer
NK	Natural killer cell
OD600	Optical density at 600nm wavelength
PAGE	polyacrylamide agarose gel electrophoresis
PBMC	Peripheral blood mononuclear cell
PBMC	Peripheral Blood Mononuclear Cell
PBMC	Peripheral blood mononuclear cell
PBS	Phosphate buffered saline
PBS	Phosphate Buffered Saline

PBS-T	Phosphate Buffered Saline with Tween 20
PCR	Polymerase chain reaction
PE	R-phycoerythrin
PEI	Polyethylenimine
PIC	pre-integration complex
PLWH	people living with HIV
PR,	protease
RFADCC	Rapid Fluorometric Antibody Dependent Cellular Cytotoxicity Assay
RNA	Ribonucleic Acid
R0	Mean basic reproductive number
RPM	Revolutions per minute
RPMI	Roswell Park Memorial Institute
RT	Reverse Transcriptase
RT-PCR	Reverse Transcriptase Polymerase Chain Reaction
SAMHD1	Sterile alpha motif + histidine aspartate domain-containing protein 1
SARS	Severe Acute Respiratory Syndrome
SDCAA	Selective growth yeast media + dextrose
SGCAA	Selective growth yeast media + galactose
SIV	Simian Immunodeficiency Virus
SSC	Side Scatter
STI	Sexually transmitted infection
TBE	Tris-Borate EDTA Buffer
TRIM-5α	Tripartite motif 5α
TZM-bl	CXCR4-positive HeLa cell clone expressing CD4 and CCR5
U	Unit
VH	Variable Heavy
VHDJH	Variable region of the immunoglobulin heavy chain
WHO	World Health Organisation
YPD	Yeast extract peptone dextrose
YSD	Yeast surface display
α	Alpha
δ	Delta
ε	Epsilon
κ	Kappa
λ	Lambda
μ	Mu
μg/ml	Micrograms/m

List of materials used

Product	Company	Catalogue number
96 well low profile skirted PCR plate	Appleton Woods	BS261
PCR cap strips	Appleton Woods	BP001
CD14 FITC	BD	561806
CD16 FITC	BD	555397
CD3 FITC	BD	561647
FACS Tubes	BD	552843
Trypan Blue Solution (0.4%)	BD Falcon	352054
BD FACS Aria III	BD LifeSciences	-
APC Mouse Anti-Human CD19	BD Pharmingen	555415
Blood collection tubes	BD Vacutainer	Assorted
INSTI HIV-1/HIV-2 Antibody Test	Biolytical Labs, WA, USA	-
10x Tris/Glycine/SDS Buffer	Biorad	1610710
2-Mercaptoethanol	Biorad	1610737
Falcon 96 well round bottom plates	Biorad	MSF1001
Gel Doc XR+ imager	Biorad	-
Gene Pulser Xcell^{TM} Electroporator	Biorad	-
IgG1	Biorad	1610732
12 well tissue culture plates	Corning	430641U
Anti-Human CD16 FITC	eBioscience	11-0168-42
2ml microcentrifuge tubes	Fisher Scientific	3621
96 well PCR plates	Fisher Scientific	10320551
AgeI-HF	Fisher Scientific	3453
Terrific Broth	Fisher Scientific	101R20
Ab buffer kit	GE Healthcare	28-4083-47
10% Mini-PROTEAN TGX Stain-Free Protein Gels	Grenier Bio-One	SYR50LS
15cm tissue culture plates	Grenier Bio-One	657160
15ml centrifuge tube	Grenier Bio-One	188261
50ml centrifuge tube	Grenier Bio-One	227270
6 well tissue culture plates	Grenier Bio-One	665180
Histopaque	Histopaque	Histopaque
Goat anti-human IgG Fc Secondary Antibody, FITC	Immune Tech	IT-001-173Δ
gp140 (Clade B/C consensus)	Immune Tech	IT-001-0024ΔTMp
gp140 (JRFL Clade B)	Immune Tech	IT-001-0028p
HEK293A cells	Invitrogen	85120602
Pacific Blue (450 wavelength)	Invitrogen	18942321
Saccharomyces cerevisiae EBY100 yeast cells	Invitrogen	MYA-4941
SOC Media	Invitrogen	18265-017
UltraDOMA Serum-free Hybridoma Medium	Invitrogen	11965092
UltraPure™ DEPC-Treated Water	Invitrogen	10813012
CFSE	Invitrogen	H10101C
LB Broth with agar	Invitrogen	15544-034

QIAquick Gel Extraction Kit	Invitrogen	S33102
RNase free water	Life Technologies	AM9855G
100X MEM NEAA	Lonza	12-727F
Ab Spin Trap	Merck Millipore	UFC901008
6X gel loading dye	NEB	B7024S
BsiWi-HF	NEB	R0553S
DH5alpha competent cells	NEB	R3553S
DNAse I	NEB	M0303S
HindIII-HF	NEB	R3138S
Phusion® High-Fidelity DNA Polymerase	NEB	M0530S
SalI-HF	NEB	R3552L
T4 DNA Ligase	NEB	R3553S
1kb Quickload DNA ladder	NEB	N0467S
BsiWi	NEB	R3101S
EcoRI-HF	NEB	R3104S
Sybr Safe	NEB	N0468S
XhoI	NEB	M0202S
Tris 1M pH8	Promega	N2615
1.5ml Microcentrifuge tube	Qiagen	28204
Ampicillin sodium salt	Qiagen	201901
Microseal Foil	Qiagen	129115
MiniElute reaction clean up kit	Qiagen	28106
Nuclease Free Water	Qiagen	129112
PEI	Qiagen	27106
Qiagen OneStep RT-PCR kit	Qiagen	210212
Qiagen Plasmid Midi Kit	Qiagen	12941
QIAquick PCR Purification Kit	Qiagen	28706
QuickLyse Miniprep Kit	Qiagen	27406
Taq DNA Polymerase	Qiagen	M0273S
10mM dNTP mix	Qiagen	201205
Polyethylenimine (PEI)	Sigma	9002-98-6
1.1ml microtubes	Sigma Aldrich	MINI26-1KT
10x TBE	Sigma Aldrich	A9539-50G
Agar Plates	Sigma Aldrich	L3022
CD19 BV421	Sigma Aldrich	T4049
DMEM (high glucose)	Sigma Aldrich	408727
DMSO	Sigma Aldrich	F4135
Foetal bovine serum	Sigma Aldrich	G7513
LB Broth	Sigma Aldrich	L2897
L-glutamine	Sigma Aldrich	P4333
PenStrep	Sigma Aldrich	H8889
Reservoir	Sigma Aldrich	T8154-100ML
Trypsin-EDTA	Sigma Aldrich	D2650
100bp DNA quick load ladder	Sigma Aldrich	T4415-4L
2.2ml deep well plate	Sigma Aldrich	T5574-500ML
Agarose	Sigma Aldrich	A9518

PBS	Sigma Aldrich	R0883
RPMI	Sigma Aldrich	M7145
T75 flasks	Sigma Aldrich	D8537
Total IgG ELISA kit	Sigma Aldrich	CLS430599-60EA
HEPES	Sigma Aldrich UK	7365-45-9
Mr. Frosty™ freezing containers	Sigma Aldrich/Nalgene	C1562
Haemocytometer	SLS Ltd	353077
QIAprep Spin Miniprep Kit	Starlab	E2896-0220
10ul, 20ul, 100ul, 1000ul pipette tips	Starlab	-
Primers Oligo Design Tools	Thermo Fisher Scientific UK	-
NanoDrop 1000 Spectrophotometer	Thermo Scientific	-
RNase OUT	ThermoFisher Scientific	10777019
PKH-26	ThermoFisher Scientific	C34554
eFluor450 (Pacific Blue)	ThermoFisher UK	65-0842-85
Serological pipettes	VWR	-
One-step RT PCR	VWR	630-1506
YeaStar Genomic DNA kit	Zymo Research Labs	D2002
Laemmli sample buffer	Sigma-Aldrich	

Chapter 1
Background and introduction

Chapter 1 Background and introduction

1.1. Human Immunodeficiency Virus (HIV)

1.1.1. HIV as the causative agent of the acquired immune deficiency syndrome (AIDS)

From 1981, the United States Centers for Disease Control received reports of opportunistic infections such as Kaposi's sarcoma and *Pneumocystis carinii* pneumonia occurring primarily within men who have sex with men, intravenous drug users and Haitian immigrant populations (1–3). In 1983, two groups of researchers independently isolated a new retrovirus from patients with clinical presentations of the recently described acquired immunodeficiency syndrome (4,5). This retrovirus was thought to belong to the human T-cell leukaemia virus (HTLV) family, with tropism for T cells, and was suggested as the aetiology for AIDS after being isolated from the majority of patients with this clinical presentation (6,7).

Since then, HIV has infected 75 million people, claimed the lives of 32 million people, with an estimated prevalence of 0.8% in adults aged 15–49 years worldwide (8). Data from year end 2019 show 37.9 million people worldwide are living with HIV, with 1.7 million new infections acquired in 2018 (9). Geographical variations in incidence result in areas of increased acquisition risk, particularly Sub-Saharan Africa where nearly 5% of adults live with HIV but comprise 71% of those affected globally (10). Men who have sex with men (MSM) are particularly vulnerable to HIV infection, accounting for significant proportions of new HIV infection; 57% in western/central Europe and North America, 41% in Latin America, over 25% in Asia Pacific and Caribbean regions, 20% in eastern Europe, central Asia, Middle East and North Africa, and 12% in western and central Africa (11). Data from the US Centres for Disease Control in the United States show that in 2017, MSM accounted for 70% of all new HIV infections, with young black males aged 25-34 at highest risk (12). Reasons include a greater risk of transmission per sexual act, sexual role versatility, and sexual network effects, all of which assist rapid HIV transmission amongst sexual networks (13–16).HIV viral structure

In this project I focus on HIV-1, with all references to HIV studied here intended as HIV-1.

HIV is a retrovirus within the lentivirus genus (17). Retroviruses are ribonucleic acid (RNA) viruses, where genomic material in the form of RNA undergoes reverse transcription prior to insertion into a host cell genome (18,19). Lentiviruses are characterised by long incubation periods which precede development of chronic illness, and HIV is no exception (20).

HIV is a single stranded RNA virus containing nine open reading frames encoding viral proteins essential for replication and life cycle. Three of these encode polyproteins which are proteolyzed to proteins supporting viral structure and function- Gag, Pol, and Env. There are four structural proteins encoded by Gag (matrix (MA), capsid (CA), nucleocapsid (NC) and p6 protein), and two encoded by Env (gp120 and gp41); these make up the virus core and envelope. Pol is proteolyzed to produce three enzymatic proteins- protease (PR), reverse transcriptase (RT) and integrase (IN). The HIV genome also encodes six accessory proteins; Vif, Vpr and Nef are located in the viral particle, Tat and Rev provide gene regulation functions, and Vpu assists virion assembly (21,22).

Viral fusion to host cells is facilitated by HIV envelope protein and is discussed in section 1.3. Viral fusion is followed by release of viral core into host cell cytoplasm (23). Viral RNA is reverse transcribed into deoxyribonucleic acid (DNA) by the viral enzyme RT. This newly formed viral DNA is co-packaged with viral integrase, capsid protein, and some cellular proteins to form a pre-integration complex (PIC), which enters the host cell nucleus to incorporate the proviral DNA into the host cell genome. (24). HIV integration occurs mainly in actively transcribed regions of the host genome (25). This may be due to the increased accessibility to chromatin in transcribed regions, or favourable interactions between the PIC and transcription factors (26,27). Ultimately, viral integration at areas of high expression will probably result in more active production of proviruses (28).

The retroviral genetic information is now part of the host genome and is transcribed to produce enzymes necessary for production of new viral particles which are released from the cell to continue the life cycle (29–32).

1.2. HIV Transmission and acute infection

HIV transmission occurs by mucosal tissue exposure to cell-free or cell-associated virus. Sexual transmission is the predominant mode of HIV acquisition worldwide, (33–35), accounting for 4 of 5 infections and involves viral exposure at vaginal or rectal mucosa (36). Transmission likelihood per sexual act is influenced by several factors, including transmission partner's HIV viral load, recipient partner genital mucosal condition, and the presence of sexually transmitted infections (37–39). HIV acute infection will be discussed in the context of sexual transmission as it is the globally predominant form of transmission (8).

Despite the presence of a diverse viral population within the inoculum from the infecting partner, mathematical modelling suggests HIV infection is caused by a single virion in the majority of infections (40). The period between initial viral exposure until viral RNA becomes detectable in the bloodstream is termed the eclipse phase and is dominated by a rapidly increasing HIV viral load due to local expansion of HIV founder clones (41–43). The mean basic reproductive number (R(O)) of each newly infected HIV cell is 19.3, causing a mean initial viral doubling time of 10 hours, and the average time from initial HIV exposure to peak viraemia is 21 days, followed by a decay phase over the next ten days (44).

1.3. HIV Envelope protein

HIV virus entry to host cells is facilitated by HIV envelope protein (Env), a trimeric protein constructed of three of each of the glycoproteins (gp) 120 and 41 derived from the precursor gp160 (45). Env is present in various forms on the outer virion surface and may exist as a full functional trimer spike, a partially decayed non-functional conformationally rearranged molecule, or a gp41 stump which has shed gp120 (46,47) This is shown below in Figure 1.3-1 and Figure 1.3-2.

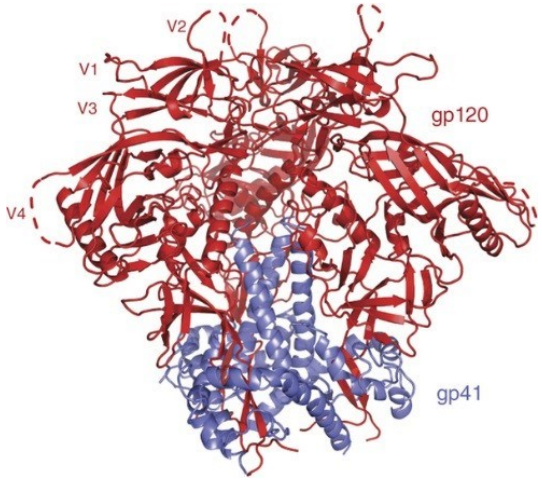


Figure 1.3-1 HIV envelope protein- trimer

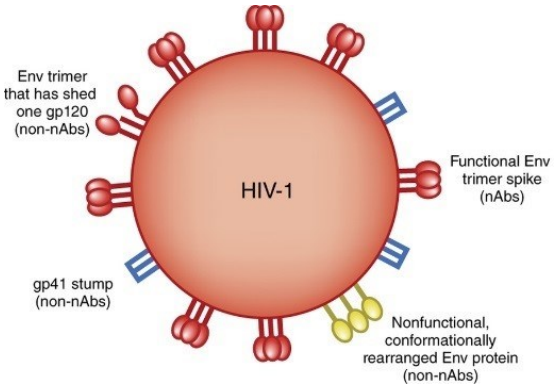


Figure 1.3-2 Env protein forms

Reprinted by permission from: Springer Nature Customer Service Centre GmbH: Springer Nature Antibody responses to envelope glycoproteins in HIV-1 infection, Dennis R Burton, John R Mascola Copyright 2015, see RightsLink Printable Licence in Appendix

Env protein is essential for virus entry as it mediates recognition and infection of host CD4 T-cells (48). The gp120 glycoprotein binds the T cell CD4 glycoprotein, causing a conformational change in the HIV envelope protein, exposing the V1V2 (aa 127-195) and V3 (aa 300-328) (49) loop structures of gp120 which then allows binding to the host cell chemokine receptors CCR5 and CXCR4, which now act as co-receptors for HIV envelope protein (50).

These transmembrane coreceptors are usually CCR5 or CXCR4 (51). Previously, viruses were thought to be tropic for either one of these two coreceptors, with R5 virus predominating in at the seroconversion stage and progressing to R4 tropism as immunodeficiency progressed (52). More recent data suggest HIV presents varying coreceptor preference; R5 tropic, and X4 or M-tropic, where viral evolution occurs to allow new use of new coreceptors or ongoing cellular infection in CD4 limited settings (53).

Gp120 swings away to expose gp41 which will facilitate viral fusion with the host cell membrane (54,55). A hydrophobic fusion peptide at the gp41 N-terminus forms a 6 helix bundle containing a base and an outer part. The outer part attaches to the host cell membrane to create a bridge between the host and viral cell membranes. The bundle helices now refold into a hairpin structure which brings the host cell and viral membranes together, creating fusion pores and allowing transit of virus contents

into the host lymphocyte (56). In this fashion, HIV envelope protein facilitates viral infection of host CD4 T cells.

HIV viral particles are presented to partner genital mucosa in either cell-free or cell associated form, and can penetrate the epithelium to reach the submucosal space (57). Here, cells including Langerhans cells, dendritic cells and fibroblasts transmit virus particles to $CD4^+$T cells (58–60). There may also be direct transcytosis of virus into subepithelial memory $CD4^+$ cells (61,62). As most transmitted virus is CCR5 tropic, and the majority of genital mucosa $CD4^+$T cells express surface receptor CCR5, these form a susceptible population for infection (63,64).

Propagation of infection throughout the lymphatic system is illustrated by a macaque model of SIV intravaginal inoculation which study showed increasing levels of viral RNA in cervical tissue at days 3 and 7, with detectable levels found in vaginal tissue, draining and distal lymph nodes and other lymph tissue by day 12 (65). Viral dissemination throughout the lymphatic system predominantly targets $CD4^+$T cells, with 20% infected and 60% dying via apoptosis (66). Mass recruitment of lymphoid tissue for viral replication creates an exponential rise in HIV plasma virus levels, with peak viraemia occurring approximately 14 days after transmission (67). This exponential rise in plasma viral load usually causes symptoms ranging from mild coryza to systemic features and is called the “seroconversion illness”.

Myeloid cells displaying the coreceptors $CD4^+$, CCR5 and CXCR4 including macrophages, dendritic cells and osteoclasts are another tissue target for HIV infection. This is thought to occur by cell-to-cell transfer of HIV from infected T-cells and contributes to the formation of the viral reservoir (68,69) (see section 1.3.1) . Other tissues implicated in viral infection include blood monocytes, lung tissue macrophages, gut-associated lymphoid tissue, genital tract, bone marrow and the central nervous system (70).

These initial stages of HIV infection were described by Fiebig et al according to the sequential appearance of viral markers in blood; (I) HIV viral RNA at 5 days, (II) p24 antigen at 10 days, (III) positive IgM enzyme immunoassay at 14 days, (IV) indeterminate Western blot for HIV proteins at day 19, (V)

Western blot positive without p31 band at 87 days, and (VI) Western blot positive with a p31 band (100 days and greater) (36).

1.3.1. Establishing the viral reservoir

During acute HIV infection, active $CD4^+$T cells are preferentially targeted as these favour viral replication (71). Certain subsets survive and harbour infection, creating a long term repository for viral DNA called the "viral reservoir", occuring by infection of active cells that transition back to a resting state, or direct infection of resting cells. Some actively infected cells may survive with integrated proviral DNA and return to a resting memory state, remaining quiescent, with viral gene expression subdued and productive infection restricted (72–74). Conversely, some *in vitro* models suggest direct infection of resting $CD4^+$T cells is possible (75,76). *In vitro* studies which reverse T cell latency have demonstrated the replication potential of this proviral DNA reservoir and provides insight into the inability of antiretroviral medication to eradicate infection (77). In addition, infection of myeloid cells is thought to contribute to the HIV reservoir.

1.3.2. Chronic infection and progression to AIDS

Untreated HIV infection is characterised by falling $CD4^+$T cell counts and a rising plasma viral load. Massive depletion of $CD4^+$T cells occurs in gut-associated lymphoid tissue (GALT), peripheral blood, and lymph nodes, and is countered by increased cell turnover, thought to be due to immune activation (78). This can be partially reversed by combined antiretroviral therapy (cART) initiation, but $CD3^+/CD4^+$ and $CD3^+/CD8^+$T cell ratios remain impaired, even in treated individuals (79). In addition to quantitative effects, chronic infection also causes qualitative defects in $CD4^+$ and $CD8^+$T cell function; $CD4^+$ T cell proliferation in response to new and recalled antigens is impaired, as is the supportive role $CD4^+$ T cells provide to $CD8^+$T cell function, B cells, monocytes and macrophages (80).

Generalised immune activation is a feature of chronic HIV infection, resulting in increased cell turnover, alterations in lymphocyte subset proportions towards increasingly activated and differentiated subpopulations, and cellular exhaustion. The cause of immune activation appears to be

an excess secretion of soluble immune factors, arising during acute infection and persisting into chronic. These include pro-inflammatory cytokines TNF-α, IL-1, IL-12, IL-6, chemokines, lipopolysaccharide and type 1 IFN-α (66). These factors drive local and systemic inflammatory processes. Possible causes of immune activation include direct effect by viral proteins, co-infection with conventional or opportunistic infections, microbial translocation from the gastro-intestinal tract, and the reduced efficacy of counter-regulatory immune suppressive responses, such as regulatory T $CD4^+$ T cells (80). In addition, abortive HIV-1 infection in lymphoid cells leads to activation of caspase 1 pathways and pyroptosis, continuing the inflammatory insult (81,82).

Defective T cell regenerative capacity is also a feature of chronic infection, due to a constellation of the following. Central memory T cells are unable to regenerate due to excessive differentiation, viral-mediated cell death, and destruction of lymph node architecture from chronic inflammation. There is also a loss of naïve cells due to excessive differentiation to memory cells, and thymic suppression which reduces availability of naïve cells to replenish those cells lost to differentiation (83).

Chronic HIV infection is also associated with loss of naïve and memory $CD8^+$ T cells. In health, $CD8^+$ T cells combat viral replication but their function is impaired in HIV. Features include a reduced capacity for proliferation, decrease in secretion of inhibitory cytokines and a loss of cytotoxic activity.

As disease progresses, phenotypic changes consistent with exhaustion or senescence arise in $CD4^+$ and $CD8^+$ T cells, as well as in B cells. Exhaustion is characterised by the appearance of inhibitory receptors. Exhaustion can be attenuated by blocking certain ligands; anti-PDL -1 antibodies have been shown to enhance T cell responses in previously “exhausted” cells (84)

Another feature of disease chronicity is a switch in viral co-receptor tropism. As outlined, HIV uses CCR5 together with the CD4 receptor for entry. In chronic infection, tropism may evolve to produce a CXCR4 tropic virus (53) . This now extends the range of viral infection and killing to naïve and resting central memory cells, perpetuating further viral spread and disease progression (83).

Progression to AIDS is marked by the appearance of opportunistic infections and an increased risk of HIV associated cancers. This usually occurs at a CD4 count of 200 cells/mm^3 but may occur at higher CD4 counts in certain individuals, hence it is a clinical and laboratory diagnosis. Opportunistic infections are a constellation of microbial diseases causing illness in an immunocompromised host, and their presence should prompt HIV testing in those of unknown serostatus.

1.3.3. HIV Testing

HIV testing is now a routine part of healthcare and is offered in a variety of settings, including primary care, antenatal care and in emergency departments where local HIV prevalence is greater than 2 per 1000 population (85). Public Health England recommends that groups at increased risk of HIV acquisition should test frequently and testing opportunities should be increased for these communities (86). Outside of traditional clinic testing, people can opt to submit samples for testing via post and receive results accordingly. HIV testing is now available in a point of care format for people with an exposure risk of 6 weeks or more. A fingerprick sample of blood is placed in a well and the results are immediately apparent. The goal of improving access to testing is to reduce the proportion of people living with undiagnosed HIV. As part of a global strategy to reduce HIV transmission, the UNAIDS Program Coordination Board set a target for 90% of people living with HIV (PLWH) to know their status (87). Data released by PHE in November 2018 show the UK has surpassed this target to achieve a diagnosis rate of 92% (88).

1.3.4. HIV Treatment

Initial management of HIV focussed on symptom control and management of opportunistic infections, with progressive replication of virus and declining immune function. A minority of PLWH ("elite controllers") can maintain long term viral suppression through immune control of virus, but this occurs in less than 1% of people (89). The first antiretroviral medications with the power to suppress viral replication arrived in 1986 with the nucleoside reverse transcriptase inhibitor zidovudine (90) but successful viral control was not achieved until 1996, when triple-drug regimens demonstrated durable virologic suppression (91). Initial combined antiretroviral therapy (cART) consisted of multiple doses,

multiple pills, and multiple side effects in the efforts to achieve and maintain viral suppression. Over the past two decades, cART regimens have become more convenient and acceptable for PLWH, with a decrease in medication related side effects. In the UK, 92% of PLWH are aware of their diagnosis, 98% are taking cART, and 97% have an undetectable viral load (92). Where cART is available, it has caused a decline in morbidity and mortality from HIV (93).

The benefits of cART are not restricted to the immunosuppressed population. Our understanding of the benefits of early treatment has been helped by data demonstrating the benefit of early cART initiation on both individual and population-based levels. On an individual level, the Strategic Timing of AntiRetroviral Treatment (START) study revealed that early cART treatment significantly reduced development of both AIDS and non-AIDS events such as cardiovascular, renal and liver comorbidities (94). At a population level, the concept of Treatment as Prevention (TAsP) has shown benefits in reducing onward HIV transmission. Treating a HIV-partner person in a serodiscordant relationship reduces transmission to HIV-uninfected partners (95). Treating HIV-infected patients to achieve undetectable viral loads leads to reduced transmission at population levels, suggesting that early testing and treatment of HIV could reduce HIV incidence and mortality (96,97).Prior to these findings, PLWH were advised to begin cART as indicated by falling CD4 counts or comorbidities. However, PLWH who achieve undetectable viral loads with medication may experience comorbidities. This includes higher incidences of both HIV and non-HIV-related cancers (98,99), and increases in age-related pathologies, such as cardiovascular, bone renal disease (100–102).

1.3.5. HIV Prevention

Preventing acquisition of HIV in uninfected people is crucial in curbing the pandemic of HIV. Behavioural strategies to reduce onward transmission focus on the contact risk- sexual, percutaneous via needle-sharing or needlestick injuries, mother-to-child transmission and transmission via contaminated blood products. I shall briefly discuss prevention strategies targeting these populations.

1.3.5.1. Sexual transmission

Successful sexual transmission of HIV depends on multiple variables. These include the nature of sexual contact, viral load of the infected partner, and presence of additional sexually transmitted infections at the mucosal surface of contact. Early estimates of sexual transmissibility suggested infectivity rates of 0.001, 0.003, and 0.01 for female-to-male, male-to-female, and male-to-male, respectively (per contact transmission on logarithmic scale) (103). Consistent condom use reduces HIV transmission by 80% in heterosexual and 70% in anal intercourse (104,105), and can reduce HIV prevalence in commercial sex workers (106). However, condom success relies on consistent use, and uptake varies across risk groups. Barriers to condom use exist in communities. Regional barriers in heterosexual couples include condom availability, cultural beliefs, demonstration of fertility, and equality imbalances in sexual relationships (107). Condom use in MSM has decreased in recent years. Unprotected anal intercourse reported in a 12 months period in MSM rose from 48% in 2005 to 57% in 2011 (108). This trend was corroborated in a more recent study which reported reduced condom use in HIV-positive and negative MSM, and also in MSM of unknown serostatus (109). It is possible that increased community uptake of antiretroviral therapy and disclosure of serostatus by partners may contribute to this decrease, creating a perception of risk reduction for those engaging in condomless sexual intercourse (110).

Medication to prevent transmission has been gaining traction in recent years. In monogamous serodiscordant relationships, suppression of the seropositive partner's viral load prevents transmission to the seronegative partner. The seminal HPTN052 study from 2011 reported a 96% relative reduction in HIV transmission in serodiscordant heterosexual couples when seropositive partners began taking antiretroviral therapy, regardless of CD4 count (95). This concept was subsequently studied in the MSM population in the PARTNER2 study, which reported an HIV transmission rate of zero amongst serodiscordant couples when the viral load of the seropositive partner is suppressed with antiretroviral medication (111). Another advance in the arsenal against HIV transmission is the concept of prophylactic medication to prevent acquisition of HIV in sexually active

seronegative individuals with risk of HIV exposure. This is referred to as PrEP- pre-exposure prophylaxis and consists of self-administration of combined tenofovir disoproxil fumarate and emtricitabine. PrEP reduces HIV transmission in heterosexual and MSM couples, with relative reductions in HIV incidence of 75% and 86% respectively (112,113). PrEP can be taken regularly or on an event-based schedule, depending on levels of activity. Awareness of PrEP and availability make this an increasingly popular method of protection.

1.3.5.2. Percutaneous transmission

HIV transmission by percutaneous route from needle-sharing amongst intravenous drug users carries a probable infection risk of 0.0067 per exposure, which is slightly greater than the risk of transmission via occupational exposure via needlestick injury at 0.004 (114). Needlestick injuries can be avoided by training in safe management of sharps, but multidisciplinary methods are required to curb HIV transmission via needle sharing in intravenous drug users. One successful model is that employed by Portugal, in the decade from 1990 to 2000, the majority of Portuguese PLWH had acquired infection via needle sharing. In 1993, needle exchange programmes began operating, and in 2001, the decriminalization of all drugs held for personal use shifted the focus from persecution to public health and support for victims of drug use. Needle-sharing now accounts for just 1.5% of new HIV infections in Portugal (115).

However, new challenges for HIV prevention have arisen from the recent opioid epidemic in North America. The increasing use of oral opioids combined with aggressive marketing strategies by pharmacological companies has created a new swathe of opioid-addicted people who are turning to injectable forms of opioids to manage addiction (116). This practice in non-traditional drug user groups unfamiliar with safe injecting practices has led to increasing incidence of HIV as well as hepatitis B and C, and endovascular infections (117). In response, in 2018 the US Senate approved legislation for the Opioid Crisis Response Act which employs a variety of supportive and preventative strategies to curb the inappropriate prescribing and use of opioids. This tragic episode is a timely reminder of how

advancements in HIV prevention strategies must include community support efforts to maintain effectiveness.

1.3.5.3. Mother to child transmission

Prior to interventions aimed at reducing mother to child transmission, the rate of vertical transmissions was approximately 25%. With the introduction of widespread antenatal screening and use of combined antiretroviral therapy in nearly all women diagnosed HIV, transmission rates have fallen dramatically. If women receive their diagnosis of HIV prior to pregnancy and are taking effective antiretrovirals with a suppressed viral load at the time of delivery, the risk of vertical transmission is virtually zero (118). Postnatally, there is a risk of HIV transmission from breastfeeding, and current guidelines from the British HIV Association recommend use of formula milk to prevent perinatal HIV infection (119).

1.3.5.4. Contaminated blood product transmission

The use of blood products obtained from high risk sources began in the 1970s. The use of plasma derived factor concentrate for haemophiliacs was a cause of iatrogenically transmitted HIV and hepatitis C (120). In the UK this is currently the subject of a UK parliamentary enquiry into why product safety warnings were ignored, and imported products used, and why patient records relating to these cases may have been destroyed. At least 3891 people in the UK were infected with hepatitis C, of whom 1243 were coinfected with HIV. Of these, 1246 are known to have died, with estimates (121). Currently, NHS Blood Donation services screen for the following blood borne infections- HIV, hepatitis B,C and E, syphilis, and human T-lymphotropic virus (122).

1.3.5.5. Prevention summary

Considering these prevention strategies, HIV transmission remains prevalent worldwide. Knowing how universal testing and treatment combined with preventative strategies reduces transmission, other approaches to eradicate HIV must be considered. A position paper by the UNAIDS-Lancet Commission recommended that along with prevention measures and socio-political structures to support people and research, "…an effective vaccine and a cure remain priorities" (123).

1.3.6. Potential for a HIV vaccine

A vaccine to prevent HIV is highly desirable. Worldwide vaccination strategies have successfully curbed the spread of certain infectious diseases, such as smallpox and poliomyelitis, therefore an HIV vaccination program could significantly impact the epidemic. Yet despite multiple vaccination trials, only 6 HIV candidate vaccines have progressed to efficacy trials (see section 1.9). To understand the challenges facing development of a HIV vaccine, we must first consider the following; how HIV infects cells, innate and adaptive immune responses to HIV, and how HIV evades these defences to establish and maintain infection.

1.4. Humoral immunity

1.4.1. B cells

B cell discovery occurred following the discovery of antibodies. In 1938, electrophoresis of immune serum revealed presence of antibodies, and in 1948 plasma cells were proposed to be the source of antibodies (124). B cells take their name from their tissue of origin and were first identified in chickens in 1965, when cells from a lymphoid organ called the bursa of Fabricius (B cells) were shown to produce antibodies, whereas cells from the thymus (T cells) produced delayed hypersensitivity reactions (125). Cell surface marker technology was also in development at this time, and the study of B cells from normal people compared to those suffering from leukaemia and lymphoma paved the way for immunophenotyping to characterise B cells (126).

B cells begin life in bone marrow as haematopoietic stem cells. Here, these B cell precursor cells interact with local stromal cells to undergo rearrangement of their immunoglobulin genes and differentiate into multipotent progenitor cells, and then to common lymphoid progenitor cells. These cells are now pro-B cells. These cells undergo rearrangement and expression of the immunoglobulin genes. The heavy chain locus (V/D/J) rearranges and generates a heavy chain pre-B receptor which is expressed on the cell surface. This cell is now a large pre-B cell. The light chain locus (VJ) then rearranges and the cell becomes a small pre-B cell. The cell now assembles the light-chain gene and expresses a complete IgM molecule on its surface. This is an immature B cell and must now undergo

negative selection in the bone marrow. The cell is exposed to self-antigens, and any auto-reactive immature B cells are removed from the repertoire (127).

The immature B cells then exit the bone marrow and express IgD and cell surface markers CD21 and CD22 as well as IgM. These cells migrate to the spleen to become transitional cells, passing through two stages of transitional development, T1 and T2. These T2 cells may become follicular or marginal zone B cells and are now mature B cells, also referred to as "naïve" B cells. These cells migrate to peripheral lymphoid organs such as the gut associated lymphoid tissue, or lymphoid follicles of the spleen and lymph nodes. The development stages of B cells are mediated by signalling proteins and transcription factors.

Activation of mature B cells relies on stimulation by T helper cells. Antigen binds to the B cell surface receptor, is internalised and then presented as peptides to T helper cells. These T helper cells arise when naïve T cells interact with antigen presented by dendritic cells which activate $CD4^+$ T cells to produce T helper cells. The co-stimulation by bound antigen, T helper CD40 ligand and cytokines induces the B cell to proliferate and differentiate into antibody producing plasma cells. Mature B cells may also proceed to germinal centre reactions to undergo somatic hypermutation where B cells of increasing affinity are generated for memory B cell functions (127). The plasmablasts from follicles and mesenteric lymph nodes migrate to gut lamina propria and mesenteric surfaces, and those from lymph nodes or splenic follicles migrate to bone marrow at 2-3 weeks. Here, they differentiate to form plasma cells with a half-life of months-years, and bone marrow is now principle site of antibody production (127)

1.4.2. Antibody structure and function

Antibodies are the secreted forms of the B cell surface receptor. They are proteins which are present in the plasma and can effect a variety of functions. Figure 1.4-1 below depicts an antibody structure schematic.

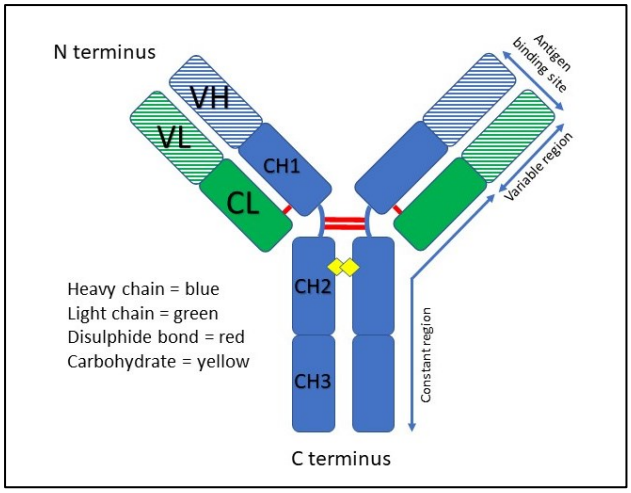


Figure 1.4-1 Schematic of antibody structure
This figure displays the heavy and light chains, disulphide bonds, carbohydrate. Also shown are the N (amino) and C (carboxy) termini, the variable and constant regions, the antigen binding sites. VH heavy chain variable region, VL light chain variable region, CH1,2,3 heavy chain constant regions 1,2,3, CL light chain constant region. Yellow diamonds indicate carbohydrate moiety, red lines indicate disulphide bonds. Original content.

Antibodies are Y-shaped and formed of three globular regions. Each antibody contains two heavy chains (H chain, approximately 50 kDa molecular weight) and two light chains (L chain, 25 kDa molecular weight). Light chains may be either lambda or kappa type. Heavy chains are joined to each other at the hinge region by disulphide bonds. Each heavy chain is joined to a corresponding light chain, and the antibody contains identical copies of both.

Antibody specificity begins with the germline rearrangement of the variable (V), joining (J) and diversity (D) gene segments. Heavy chains utilise variable (V_H), joining (V_J) and diversity (V_D) genes, while light chains use variable (V_L) and joining (V_J) genes. Immunoglobulin heavy-chain C-region genes are responsible for the various antibody isotypes- IgA, IgD, IgE, IgG and IgM. The corresponding C-region genes are Cα, Cδ, Cε, Cɣ and Cμ. The isotypes vary according to length of the Fc region, glycosylation, and ultimate distribution and function, but can all be produced as cell surface receptors or secreted as antibodies.

The antigen binding site is formed by the N terminus region of a heavy and light chain pairing and so each antibody has identical antigen binding sites. The antigen binding site is highly complex and is referred to as the variable region. Variable regions are responsible for the unique character of

antibody affinity. Each heavy and light chain contains a variable region, which is composed of two key structures- the framework region (FR) and the complementarity determining region (CDR). The framework region remains conserved across antibody groups, whereas the complementarity determining regions are hypervariable and lend unique antigen binding characteristics to each antibody. Of the three CDR, CDR3 is the most variable structure. The structures are regularly placed; four framework regions are interspersed by three complementarity determining regions as depicted in Figure 1.4-2 below.

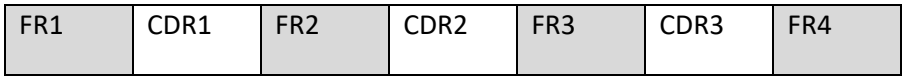


Figure 1.4-2 Schematic of variable region
Schematic shows framework regions 1-4 (FR) and complementarity determining regions 1-3 (CDR)

When the antibody molecule assumes a three dimensional structure, the antibody framework region beta-pleated sheets form a supportive scaffold for the hypervariable complementarity determining regions. The complementarity determining regions are then juxtaposed to create a highly variable site. Together the variable sites from each heavy and light chain (containing a total of six CDR) form the antibody's antigen binding site.

The C terminal is responsible for interaction with host cell molecules and effector cells. The heavy chain region distal to the hinge region is the Fc fragment (fragmentable crystallizable) as distinct from the Fab (fragment antigen binding) fragment. This Fc fragment is responsible for three key mechanisms of defence. It can bind Fc receptors on the surface of host immune cells to effect phagocytosis of pathogens. It can also activate the C1q complement cascade, and lastly can assist transport of antibodies to sites which may be difficult to access otherwise. Three key areas of Fc effector function are antibody dependent cellular cytotoxicity (ADCC), antibody dependent cellular phagocytosis (ADCP), and viral neutralisation.

ADCC occurs when specific Fc receptors (Fc gamma IIIa, FcɣRIIIa) bind the Fc region of IgG bound to viral antigens present on the surface of an infected cell. FcɣRIIIa are present on effector cells such as natural killer cells, monocytes and macrophages. The Fc/ FcɣRIIIa complex stimulates antiviral cytokine production and causes apoptosis of infected cells (128) .

ADCP also uses Fc receptor engagement. “Professional phagocyte” cells such as macrophages, monocytes, neutrophils and eosinophils are engaged either by antibody or antibody-fixed complement to engulf opsonised particles. Depending on the nature of the phagocytosing cell, other immune responses may be stimulated as a result (129).

Neutralising antibodies can act via several mechanisms including interception of free virus, inhibition of cell-to-cell viral spread, inhibition of viral transcytosis, or neutralisation of intracellular virus (130). I will discuss these activities in more detail as they relate to the host anti-HIV immune response later in this chapter.

1.5. Humoral responses in HIV infection

1.5.1. B cells in HIV infection

HIV causes abnormal immune activation including overproduction of serum immunoglobulin and autoantibodies, expansion of B cell populations in lymphoid tissue, and increased activation, proliferation and terminal differentiation of circulating B cells (131). Findings from DNA microarray studies show upregulation of specific genes in B cells of viraemic patients when compared to aviraemic and HIV negative individuals; these include interferon stimulated genes causing increased expression of apoptosis related cell surface marker CD-95, and terminal differentiation genes (132).

HIV causes disruption of B cell subsets resulting in altered populations of immature and mature cell populations. Immature/transitional B cells population in viraemic patients are expanded, exhibit lower levels of the B cell lymphoma cell 2 protein (promotes survival by inhibiting apoptosis), are prone to apoptosis, have an associated increased serum IL-7 level, and contribute to HIV-induced lymphopenia (133).

Activated memory and plasmablast cells in viraemic patients become large and activated, with increased expression of KI-67 and CD95 respectively, produce excess immunoglobulin, and arise due to HIV-induced immune activation (131).

Tissue-like memory B cells in viraemic patients are large and exhausted, express more inhibitory markers, have different levels of homing receptors compared with aviraemic and HIV negative patients, are less experienced in terms of replication history and somatic hypermutation, and are due to chronic viraemia (134).

Terminally differentiated B cells in HIV viraemic patients are phenotypically different from those seen in uninfected individuals, having lower expression of CD20 and CD21, and increased expression of CD27 and CD38. These changes are also thought to be responsible for increased incidence of B cell malignancies in the HIV population, and are directly caused by high levels of replicating virus (135). Sustained viraemia over many years leads to B (and T) cell exhaustion, characterised by the increased

expression of inhibitory receptors (136). Exhaustion is considered to be a defence against the harmful effects of a chronic hyperactive immune response (134).

Some of the B cell changes associated with HIV infection normalize with initiation of cART. Studies shown cART is associated with a reduction in circulating plasmablast numbers, decreased plasma immunoglobulin levels, restoration of the memory B cell compartment and an increase in total B cell numbers (137). Early initiation of therapy is more effective in quantitative restoration of memory B cell compartments, supporting the concept of early diagnosis and treatment to preserve health (138,139). However, qualitative function remains impaired, serving as a reminder that the repair is not absolute (140).

As well as B cell subsets, HIV also targets secondary lymphoid organs important for B cell maturation and development. Lymphadenopathy is caused by follicular hyperplasia and germinal centre B cells undergo hyperactive changes in response to viraemia. In mucosal tissues, viral-mediated suppression of antibody class switching results in defective production of mucosal IgA, and increased production of IgG (141).

T follicular helper cells are also targeted by HIV. These cells enable somatic hypermutation of B cells to produce high affinity antibodies (141).They are also a prime target for HIV as they display high levels of chemokine receptor type 5 (CCR5), are recognised as an early seeding site for the HIV viral reservoir resulting in reduced capacity to produce high affinity antibodies (142)

1.5.2. B cell responses to HIV infection

The initial B-cell response to HIV infection is polyclonal and sequential. Circulating immune complexes appear eight days post virus transmission (66). The first detectable antibody response occurs approximately two weeks after detectable viraemia, when anti-gp41 IgM antibodies appear and undergo class switching to IgG1 and IgG3. Antibodies targeting the p24, p55 and p17 epitopes appear over the following weeks(66). The first anti-gp120 antibodies appear four to six week post-viraemia and specifically target the V3 loop. These early responses do not control viral replication and fail to

neutralize virus in *in vitro* (143). The first antibodies with the capability to neutralise autologous virus appear at 13 weeks, preferentially targeting variable Env regions (144).

The initial humoral response to HIV is unable to control viral replication. As discussed in the introduction, the initial IgM anti-gp41 response is non neutralising (143). The first autologous neutralising antibodies appear several months following incident infection, and the inhibitory nature of this response results in replacement of the neutralisation-sensitive virus by a resistant viral population. Genetic analysis of this viral population shows occasional Env mutations and increased levels of N-glycosylation (145,146). PLWH develop these responses which have cross clade neutralising ability (147), and up to 30% develop antibodies with broadly neutralising properties appearing two to four years post infection (148). This is associated with increased viral load and lower CD4+ in early infection (149).

The production of neutralising antibodies is associated with Env structures of shorter V1-5 envelope lengths and fewer glycosylation sites at V1V2 (150). Identification of germline precursors and serial analysis of the maturing humoral response shows continual somatic hypermutation of antibody structures including the complementarity determining region 3 and occasionally framework regions (151,152). As viral escape mutations contribute to an altered progeny population, neutralising antibodies do not contribute to viral control in the host (153). However, *in vitro* studies with these antibodies show cross clade neutralisation (154,155), protection and reduction of infection in animal studies (156), and provide insights for immunogenic epitopes (157,158).

Viral mutations occur due to error-prone replication, resulting in an *env* gene product which contains new epitopes no longer susceptible to neutralising antibodies, characterised by changes in N-linked glycosylation. This evolving glycan shield provides mechanism of neutralisation resistance which does not affect receptor binding (145). Further viral mutation results in ongoing change in previously neutralising-susceptible epitopes (159). As plasma virus is continually replicating with mutations, the presence of altered epitopes results in concomitant antibody maturation (160) After 2-4 years of host immune pressure selecting viral mutants which evade control, and subsequent somatic

hypermutation to produce further antibodies, a polyclonal population of diverse antibodies has developed with the capacity to neutralise heterologous viral strains.

In summary, ongoing pressure from immune responses continually shapes drives viral mutation resulting in altered epitope targets and uncontrolled viraemia.

1.5.3. Control of viraemia in HIV-infected people

Long term control of HIV viraemia in the absence of cART is possible- and these long term non progressors (LTNP) have been described as having asymptomatic HIV infection for ten years post seroconversion and belonging to one of three groups. Viraemic non controllers maintain plasma HIV RNA levels greater than 2000 copies/ml for greater than 50% of all measurements; viraemic controllers maintain plasma HIV RNA levels less than 2000 copies/ml for at least 12 months, and elite controllers viraemic maintain plasma HIV RNA levels under threshold of detection for at least 12 months (161).

Characteristics of LTNP include innate mechanisms including possession of the HLAB57, HLAB27 and Bw4 alleles(162), and host expression of antiviral restriction factors including sterile alpha motif and histidine aspartate domain-containing protein 1 (SAMHD1), tetherin/bone marrow stromal antigen 2 (BST-2), tripartite motif 5 (TRIM-5α), and apolipoprotein B mRNA editing enzyme, catalytic polypeptide-like 3G (APOBEC3G) (163–166). Other features contributing to viral control are increased HIV-Gag-specific $CD4^+$ responses and virus-specific $CD8^+$ responses (167,168), or presence of broadly neutralising antibodies directed against known conserved epitopes including gp120, the CD4 binding site, the membrane proximal external region (169,170). LTNP may experience a decline in $CD4^+$ which is mirrored by brief elevations in HIV viral load (161)

Elite controllers represent approximately 1% of all PLWH. HIV-associated comorbidities may be greater in this population; a reminder of the chronic inflammatory characteristics of ongoing viral replication (171).

1.6. Broadly Neutralising Antibodies

In most PLWH, antibodies capable of neutralising autologous virus appear two to four years after initial infection (172). By screening large cohorts of PLWH, up to 50% of patient sera samples contain antibodies capable of neutralising 50% of a given viral panel (147), and approximately 1% of patient sera samples contain "elite neutralisation activity" capable of cross-clade neutralisation (173). Certain viral characteristics may influence the development of this response, as viral escape mutational changes can drive development of bnAb epitopes through generation of multiple epitope variants (174).

BnAb were initially isolated from HIV patient samples using phage-display. Advances in B cell technology including immortalisation, single B cell culture and screening, and antigen specific B cell sorting have led to the discovery of an increasing number of bnAb (175). The first bnAb isolated was b12 in 1994 and recognised an epitope on the CD4 binding site (176). Subsequent bnAb of increasing breadth and potency have since been discovered, and can be categorised according their Env target sites: 1. *N*-glycan: 2G12, 2. trimer apex/N-glycans V1V2 loops: PG9, PG16, CH01–04, PGT 141–145, 3. high mannose patch of gp120/N-glycans V3 loops: PGT121–123, PGT125–131, PGT135–137, 4. CD4 binding site: b12, HJ16, CH103–106, VRC01–03, VRC-PG04, 04b, VRC-CH30–34, 3BNC117, 3BNC60, NIH45–46, 12A12, 12A21, 8ANC131, 134, 1NC9, 1B2530, 5. *N*-glycan associated epitopes at the gp120-41 interface: 8ANC195, PGT151-PGT158, 6. the membrane proximal external region (MPER) 2F5, 4E10, M66.6, CAP206-CH12, 10E8, and 7. the "silent face" of gp120 (VRC-PG05) (49,130,175,177,178).

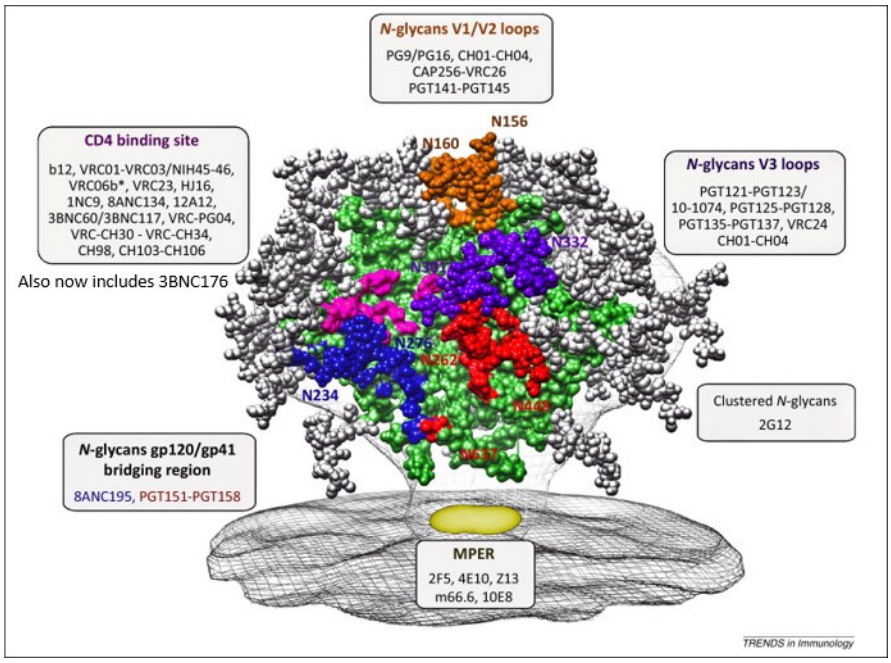


Figure 1.6-1 Sites of vulnerability on HIV-1 envelope glycoprotein

Figure 1.6-1 above shows an array of bnAb mapped to target epitopes (130).

As outlined, bnAb can be isolated from the HIV patient sera, but do not usually effect viraemic control in the host (157). Studies reviewing neutralisation of virus led to the question of bnAb ability to prevent infection. Passive administration of bnAb can protect from infection and induce viral-suppressing mechanisms in animal models, delay viral rebound after cART cessation in PLWH, and maintain viral suppression without development of resistance in PLWH (179). Therefore, bnAb represent desirable mechanisms for vaccine strategies.

BnAb development relies on responding to a continually evolving Env epitope. To illustrate, wild-type Env is not recognised by the germline precursors of bnAb PGT121, but sequential immunisation with Env trimers of step-wise epitope adjustment from original trimer towards eventual wild-type Env structure can stimulate development of germline precursors of bnAb (180). Some, but not all, bnAb have distinguishing properties, including multiple amino acid substitutions in heavy chains, unusually long HCDR3 regions to facilitate access to cryptic envelope epitopes, and somatic hypermutation in both complementarity and framework regions (130).

In summary, bnAb and the epitopes they bind represent promising areas for developing immune strategies to control HIV.

1.7. Non neutralising antibodies

In contrast to bnAb antibodies, non-neutralising antibodies (nnAb) appear during early HIV infection and employ several methods in an attempt to control viraemia (181). These include destruction of infected cells by antibody-dependent cellular cytotoxicity (ADCC) and antibody-dependent opsonisation and phagocytosis (ADCP). nnAb in HIV are mostly IgG and IgA and bind Fc receptors (FcɣR) present on the surface of effector cells, which include macrophages, dendritic cells, neutrophils, basophils, eosinophils, natural killer cells, B cells and platelets. FcɣR are coupled to stimulatory or inhibitory intracellular pathways (182).

In ADCC, natural killer cells are the predominant effector. Antibody Fab fragments bind viral antigen present on infected cell, and the Fc fragment binds the effector cell causing release of perforin and granzymes, resulting in infected cell death (128). The role of ADCC in HIV includes early control of viral replication (183), reduction of viral load in animal SHIV infection challenge (184), slower disease progression in PLWH (185), and a possible correlate of protection in the RV144 vaccination trial (186). ADCP has been associated with protection from infection in macaque models (187) and demonstrates *in vitro* enhancement of phagocytosis of gp120 coated cells (188). Antibody-dependent cell-mediated virus inhibition (ADCVI) has been elicited in macaque vaccination models, and is associated with lower rate of infection (189). Another feature of nnAb is ADE enhancement which was described seen in Dengue virus infection where sequential infection resulted in higher viral loads (190). This caused concern during initiation of early HIV vaccination trials, but ADE was not borne out in practice (191)

Other nnAb functions have been described in HIV including support for antigen presentation, complement deposition, and influence on anti-HIV antibody half-life and distribution.

An important consideration of nnAb is the complexity of their interactions, as suggested by the RV144 finding of decreased ADCC possibly blocked by IgA; “nnAb effects can be additive, synergistic, or antagonistic and should be considered as a whole” (191,192). This is illustrated by a subset of elite

controllers capable of maintaining viral control using a constellation of ADCC, ADCP and complement activation (193)

1.8. Anti-HIV responses in seronegative exposed individuals

Some individuals experience regular HIV exposure yet remain seronegative and are referred to as "highly exposed seronegative individuals", (HESN). Exposure to HIV in absence of infection was initially attributed to cytotoxic T lymphocyte (CTL) responses following identification of HIV-specific CTL in exposed seronegative HCW and infants of HIV positive mothers, and Env-specific CTL in seronegative HCW (194). Anti-Env T helper cell reactivity was reported in exposed seronegative HCW and MSM (195–197). The CTL responses corresponded to those known to control HIV viraemia and slow disease progression (198,199). A HESN commercial sex worker cohort was identified in Kenya. These HESN remained negative at 2-10 years follow-up despite increasing risk exposure (200). HESN individuals were also described in haemophiliacs exposed to HIV-contaminated blood products, and intravenous drug users who shared needles (201).

Observations of these groups prompted consideration of anti-HIV immune responses that develop in response to regular HIV exposure but in the absence of reported infection. However, these findings should be considered in the context of rare events occurring in unique subsets, and there has been some discussion as to the reliability of cohort follow-up.

1.8.1. Innate

The innate anti-viral immune response in HESN includes genetic and immune system components which may influence susceptibility and disease progression in HIV. The human leucocyte antigen family (HLA) bind antigenic epitopes and present them to T cells. HLA class I present to CD8 cells producing a cytotoxic response, and class II present to CD4 cells to produce a T helper cell and cytokine response (127). Certain class I HLA can influence the response to HIV. B27 and 57 alleles are associated with a slower disease progression in established HIV infection, and HLA-B51 is linked to resistance to infection (202). Other protective alleles include the class II HLA-DRB1*01 and the HLA cluster A2/6802 supertype, and reduced incidence of HIV in these populations suggest a protective mechanism involving CD4/CD8 responses related to HLA class I and II presentation (200,203).

Another innate mechanism of defence against HIV is a variation in the co-receptor required for viral entry. This is also discussed in section 1.10. Viral Env binds the CD4 binding in addition to chemokine receptor binding; the majority of infecting virus uses CCR5 ("R5 tropic"), as opposed to X4 viral strains ("R4 tropic") (56) . Deletion of a 32 base-pair region results in the genetic polymorphism CCR5-Δ32. Approximately 10-20% of European Caucasians are heterogenous for this allele; 1% are homozygous with a non-functional CCR5 receptor, and are effectively resistant to infection by R5 tropic HIV viruses (204,205).

Natural killer cells play a role in anti-viral defence and are activated and inhibited by cell surface receptors (206). The killer cell immunoglobulin-like receptor (KIR) family contains both activating and inhibitory loci- KIR3DL1 inhibitory allotypes and KIR3DS1 activating allotypes- and are specifically recognised by ligands from the HLA-B family, particularly the Bw4 subset, which contains the alleles B27 and B57, already noted to modulate the course of HIV infection. Therefore, the presence of the KIR receptors KIR3DL1 and KIR3DS1 could delay seroconversion to from HIV in HESN (207).

Homozygosity for KIR3DS1 has been shown to protect against HIV infection in a cohort of HESN when compared to people with primary HIV infection, regardless of HLA type (206). The combination of a homozygous KIR3DL1 receptor in combination with HLA-B57 allele was known to slow progression in established infection, but can also protect against HIV in HESN (208). Conversely, carriage of KIR3DS1 combined with the HLA-Bw4 member Bw4*801 does not delay time to infection in HESN (209).

The effector functions of natural killer cells may also explain the protective effect in HESN. Increased natural killer cell lytic and secretory activity was described in a Vietnamese intravenous drug using cohort. Additionally, HESN plasma levels of IFN-gamma, TNF-alpha and beta chemokines CCL3/4/5 were greater than those seen in unexposed participant samples (210). Moreover, *in vitro* stimulation studies of HESN natural killer cells, $CD3^{+}CD56^{+}$ and total T cells produced significantly greater amounts of intracellular IFN-gamma seen in control cells, suggesting the importance of NK cells in the mechanism of protection from HIV in HESN (211,212).

Other mechanisms of innate immune protection in HESN have been described. These include increased plasmacytoid dendritic cell function with higher maturation levels and decreased cell exhaustion (213), increased levels of secreted pro-inflammatory CC-chemokines in HESN MSM oral fluids (214) and increased levels of protective mucosal innate immune proteins in the cervico-vaginal fluids of HESN female sex workers (215). In summary, the innate immune response provides viable mechanisms for protection against HIV in HESN groups.

1.8.2. Adaptive immune response- cellular

The adaptive immune response to HIV exposure in HESN involves T cell mediated anti-HIV responses. HIV specific T cell responses were first described in HESN in 1989. T cells were stimulated in the presence of gp120, recombinant envelope and core proteins with 4 of 15 HESN showing a T cell response, demonstrating the immunogenic potential of HIV (216). Subsequent studies confirmed a T cell mediated response to HIV in HESN, demonstrating the expansion of CD4 cells expressing a common T cell receptor when PBMC samples were stimulated by HIV envelope protein gp120 (217). Functional T cell responses were then described by Mazzoli et al who stimulated HESN PBMC with HIV envelope peptides to produce IL-2, which is responsible for terminal differentiation of T cells into memory T cell and effector T cells. This demonstrated the role of HIV antigen exposure in producing a cellular immune response in the HESN population (218). Subsequent studies showed evidence of cellular immune responses to HIV exposure. Restrepo et al reported on expansion and activation of T cell subsets in serodiscordant couples (219). HIV-specific CD8 T cell IFN- gamma responses were reported in seronegative exposed commercial sex workers (220), and these responses were found to decrease over time if consistent exposure was not maintained. Kaul et al reported on the increase in HIV acquisition in previously protected commercial sex workers with less regular HIV exposure. This poses challenges for vaccine design, as repeated antigen exposure may be required to produce a durable CD8 response (221). The antigens responsible for protection in HESN include HIV envelope and other proteins. The first observational studies of healthcare workers exposed to HIV bodily fluids demonstrated cytotoxic T lymphocyte responses against envelope peptides, as evidenced by

increased IL-2 levels (194). These findings were further substantiated by Kuebler et al who demonstrated CD8 T-cell responses against the HIV envelope gp120 V2 epitope (222).

1.8.3. Adaptive immune response- humoral

Studies on the humoral response to HIV in HESN have primarily focused on mucosal and systemic HIV-specific IgA. By the definition of seronegative, these cohorts must be anti-HIV IgG negative, as confirmed by Western blot and HIV viral PCR negative. The initial discovery of anti-HIV mucosal IgA in the absence of IgG in genital secretions of HESN commercial sex workers prompted exploration of the antibody properties responsible for anti-HIV protection (Mazzoli et al., 1997). Since then, most HESN cohorts reporting mucosal exposure to HIV have evidence of HIV-specific IgA (201). Whereas initial studies on HESN protective mechanisms placed importance on anti-HIV T cell responses, the contribution of humoral factors has gained attention. A study by Nguyen et al showed a protective effect of anti-gp41 IgA gp41 anti-gp120 IgG in HESN (223).

The interest in mucosal IgA prompted investigation into their structure and function. Monoclonal expansion and analysis of IgA antibodies demonstrated inhibition of trancytosis and neutralisation of HIV infection *in vitro*. Structural antibody analysis revealed a gp41-membrane proximal external region (MPER) specific fragment with a long heavy-chain complementarity determining region (CDRH3), a feature of the two anti-gp41 broadly neutralising antibodies, 4E10 and 2F5. The extended length of the IgA complementarity determining region contained high levels of somatic hypermutations, which was attributed to affinity maturation processes driven by continuous antigen exposure (224). This process of ongoing antibody design and refinement was also proposed by Carrillo et al who found IgG and IgA in the plasma of HESN which recognized varied HIV envelope epitopes with no apparent virus neutralising capacity. They concluded that ongoing low-level HIV exposure prompts novel anti-HIV humoral responses (225).

Protection from HIV infection depends on the nature of exposure and may dictate the nature of resistance to future infection. A cohort of rhesus macaques who were frequently challenged with mucosal SIV infection remained seronegative, but acquired infection when the same viral challenge

was given intravenously (226). Therefore, anti-HIV protection mechanisms were thought to involve mucosal resistance in the absence of adaptive T cell responses.

1.8.4. Do HESN protective responses vary according to frequency of exposure?

As noted, HESN frequently exposed to regular sexual partners develop anti-HIV immune responses. But does the frequency of risk exposure influence the development of protective responses? A study from 2013 reviewed the magnitude of these responses and possible variation with levels of exposure. Anti-HIV humoral responses in plasma of HESN in relationships with known seropositive partners were compared to unexposed controls. HESN IgG and IgA recognised cell surface expressed HIV envelope protein more frequently than healthy controls, but no difference was seen when the two plasma groups were compared using Env-based ELISA assays. Moreover, levels of Env recognition did not correlate with estimated levels of HIV exposure in the HESN group. These results support the existence of humoral responses in HESN, but failed to find a correlation between the magnitude of response and levels of exposure (225).

Other studies reviewing T cell activation found support for the concept that risk exposure frequency influenced development of protective mechanisms. One study of serodiscordant couples found that HESN levels of CD4 activation as measured by CD38 expression varied in line with condom use with their positive partner (227). Another study of HESN MSM reviewed levels of T cell CD57 expression and levels of inflammation, finding that high risk MSM immune profiles were characterized by an increased levels of both (228).

1.9. Antibody responses in HIV vaccination trials

Immune responses to HIV are unable to control viral replication in the majority of those infected, with only a minority able to exert control of viral replication. Let us consider some challenges facing candidate vaccines. HIV replication is characterised by error-prone reverse transcriptase activity coupled with short generation times, creating genetic diversity at community and global levels. In addition, HIV conceals various immunogenic envelope epitope structures using glycan shields, frustrating the immune system's attempts to develop neutralising antibodies against these epitopes (145). In addition, HIV's ability to establish a latent reservoir in infection means antibody-mediated protection must be swift. Finally, there are no reports of sporadic clearance of HIV, meaning any mechanism for immune control of virus is not readily apparent (229). Which leads to the question: will HIV will ever be a vaccine preventable illness? There are reasons to think this is possible.

The RV144 vaccination trial remains the only trial to have demonstrated protection against HIV infection. Recipients were vaccinated with a combination of two vaccines; ALVAC (recombinant canarypox vector vCP1521 (Gag/Pol/Nef)) and recombinant gp120 AIDSVAX B/E. The investigators reported on two immune responses that correlated directly with infection. IgG1 and IgG3 subclass antibodies directed against the V1V2 region of gp120 mediated antibody-dependent cell-mediated cytotoxicity and were associated with protection against HIV-1 infection, whereas IgA envelope specific antibodies were associated with an increased risk of infection (186,230). Moreover, ADCC-mediating antibodies generated from study participant B cells targeted the C1 region and variable loop regions of gp120, suggesting protection could be mediated by non-neutralising mechanisms (231).

The RV144 trial used four priming doses of ALVAC recombinant canarypox vector and two of AIDSVAX B/E recombinant gp120 over a 6 month period. There was a 31.2% protection efficacy over in three years of follow-up in low-exposure risk vaccine recipients, with protection attributed these non-neutralising antibodies (nnAb) and antibody directed cellular cytotoxicity (ADCC) (232). HIV-specific antibody titres were low suggesting antibody functionality and quality is key for successful

immunisation (233). The modest success in the RV144 trial demonstrated protection, if only in lower risk individuals for a moderate duration (232).

Vaccination safety and efficacy were evaluated in the trials HVTN 097 and HVTN 100. HVTN 097 reviewed the immune correlates of protection reported in RV144. It used an ALVAC-HIV/AIDSVAX B/E vCP1521 (in conjunction with tetanus and hepatitis B vaccination) and took place in South Africa where clade C predominates. The study reported greater $CD4^+$ T cell responses, greater $CD4^+$ T cell Env-specific functionality scores, and greater Env-specific $CD40L^+CD4^+$ T cells. There were also greater IgG1 and IgG3 binding rates and response to gp120 vaccine and V1V2 antigen, and the study also reported on ADCC and ADCP functional responses (234)

HVTN 100 used a similar protocol to RV144 but with a booster against clade C virus at 12 months; ALVAC-HIV (vCP2438)/ bivalent subtype C gp120/MF59. HIV specific $CD4^+$ T cell and antibody (IgG1 and 3, ADCC, ADCP) responses were maintained throughout the vaccination schedule. The vaccination strategy was considered safe and produced durable immune response during the period of vaccination (235).

The vaccine efficacy was then studied in South Africa in HVTN 702. This study compared prevention of infection in recipients of either ALVAC-HIV (vCP2438)/bivalent Subtype C gp120/MF59 vs placebo. No difference seen between vaccine and placebo groups (infection count 129 vs. 123), and the trial was terminated in February 2020. Initial reasons for differences in vaccine efficacy between RV144 and HVTN705 included a possible higher rate of HIV incidence in the South African population studied (4%) compared with the Thai population vaccinated (0.3%) (236).

A comparison of RV144, HVTN 097 and HVTN 100 suggested the clade selected as adjuvant could have influenced the responses. HVTN 100 used a C-clade adjuvant, whereas a B-clade was used in the other two studies. HVTN 100 (C clade) showed low CD4+ T-cell and high anti-V1V2 IgG/IgG3 responses, and RV144 and HVTN 097 (B clade) showed broad responses to both. The authors of this study suggested the immune correlate analyses may have been limited by use of “vaccine-matched”, and that differences in responses between the regimens could have been due to antigens in the assays that did

not match the vaccine immunogens; in effect producing immune responses *in vitro* not matched *in vivo* (237). Another suggestion for variation in efficacy was antigen epitope variation between the boosters used in RV144 and HVTN 097/100; the former was a full length gp120 whereas the latter both used a truncated AIDSVAX gp120 variant (238).

In summary, HIV vaccines must generate antibodies capable of eliciting effector functional responses, coordinating these responses, and evolving to match the diversity of the HIV target epitopes. To date, very few vaccine trials have progressed to efficacy in human stage. These studies, the epitopes targeted, and immune responses generated are listed in Table 1.9-1.

Trial	Antigen	Description	Immune response	Vaccine efficacy
2005: VAX004 AIDSVAX B/B or B/E Phase III (239)	2 recombinant gp120 antigens	North America (B/E), Netherlands (B/B), Sexually active n= 5403, 94.3% male	Anti-gp120 CD4 blocking Neutralising	Not effective
2006: VAX003 AIDSVAX B/E Phase III (240)	Recombinant gp120 antigens Subtypes B/CRF01_AE	Thailand Injecting drug users n= 2546, 93.4% male	Anti-gp120 Non-neutralising antibody	Not effective
2008: STEP vaccine Phase III (241)	Adenovirus type 5 + clade B HIV Gag, Pol, Nef	Australia, Caribbean, North/South America Sexually active n= 2979 61.9% male	T-cell inducing	Not effective
2009: RV144 Phase III (232)	ALVAC- recombinant canarypox vector vCP1521 (Gag/Pol/Nef) + Recombinant gp120 AIDSVAX B/E	Thailand Sexually active N= 16,402, 61.4% male	Poorly T-cell inducing Non-neutralising antibody	31.2% of low risk individuals protected over medium term
2011: Phambili Phase III (242)	Internal viral proteins Capsid Gag, Pol, Nef	South Africa Sexually active N= 801, 55.0% male	T-cell inducing	Not effective
2019: HVTN 100 (236)	ALVAC-HIV (vCP2438)/ bivalent subtype C gp120/MF59	South Africa Sexually active N = 252	Non-neutralising antibody	Not effective

Table 1.9-1 Summary of HIV vaccine trials to date

Table shows trial name and year with references, vaccine antigen design, description of cohort studied, measured immune responses, and vaccine efficacy.

1.10. HIV eradication strategies

The mechanisms by which HIV incorporates itself into host DNA and tendency to establish latent infection mean that eradication on a cellular level is challenging. While cART medication has vastly improved health outlooks for PLWH, viral eradication and cure remain an important goal for disease management. Despite the seemingly insurmountable challenges presented by HIV, strategies have been developed which bring the possibility of viral eradication and cure a little bit closer.

Monoclonal antibodies have emerged as potential therapeutic agents. bnAb studies in animal models show prevention of infection and control of viraemia in established infection, and some have progressed to clinical trials in humans with modest reductions in plasma viral load (243). Non neutralising monoclonal antibodies such as A32 and 7B2 have also been studied in animal models and can reduce viral load but not prevent infection. Antibody engineering to enhance Fc-effector function or improve variable region affinity for HIV epitopes may improve performance of anti-HIV antibodies (243,244).

Compounds capable of reactivating provirus in resting cells known as “latency reversing agents” have generated interest in a “shock and kill” strategy to eradicate HIV provirus leading to a clearance of the reservoir (245,246). These agents act to reactivate the latent viral reservoir (“shock”) (247) which can then be attacked (“kill”) with a combination of host immune responses, immunotherapy, and cART (248).

Another area of research is the concept of gene editing to eradicate provirus, where the clustered regularly interspaced palindromic repeats (CRISPR)/Cas9 gene editing system uses a bacterial protective mechanism to excise DNA target. Various studies reviewing ability to excise integrated viral DNA are ongoing (249), and now include viral clearance in murine HIV reservoirs (250)

Much has been reported on patients “cured” of HIV. The first, known locally as “The Berlin Patient”, Timothy Ray Brown, was living with HIV and developed acute myeloid leukaemia. As part of treatment, he received a stem cell transplant from a donor homozygous for CCR5-Δ32. Following treatment, he discontinued cART and has not yet experienced viral rebound (251). A second patient known as “The

London Patient" underwent similar therapy and has also controlled viraemia in this fashion (252). These cases are rare and clinically challenging but suggest mechanisms for long term control of virus and possible eradication.

1.11. Anti-Env antibodies

I will now focus on the immune responses to Env which form the basis for this project.

1.11.1.The first responder

The initial responses to HIV infection are anti-gp41 IgM and IgG. This response is non-neutralising, and ineffective in controlling viraemia. As evidence of systemic immune activation appears shortly following detectable viraemia, and prior to immune complex development, the opportunity for an effective immune response to regain control of viral replication is very brief. bnAb directed against two gp41 epitopes have been found in PLWH and target the membrane proximal external region (MPER) and fusion protein, supporting the concept of gp41 as an immunogenic epitope (143).

MPER/gp41 directed antibodies can offer protection against HIV at mucosal sites and stimulate production of non-neutralising antibody responses. Examples of this include monoclonal antibodies directed against MPER linear epitopes, 2F5 and 4E10, which protect against simian-human immunodeficiency virus mucosal challenge in macaques (253). In addition, vaccination with virosomes containing neutralisation-directing gp41 trimeric subunits and an MPER analogue provided protection in macaques against repeated mucosal challenges (254). The anti-gp41 mAb 7B2 IgG1_AAA has been shown to limit the amount of virus transmission in macaques undergoing simian immunodeficiency virus (SIV) challenge (255).

bnAb which target the gp41 epitope fusion protein have also been identified. bnAb PGT151, N123-VRC34.01 and ACS202 target fusion protein and N88 glycan of gp120 (256), and ASC202 has cross-clade neutralisation properties (257). This has led to development of fusion protein as a HIV vaccine immunogen (258). Therefore, gp41 epitopes are of interest for vaccine design (255).

1.11.2.The second coming?

The origin of the gp41 response has gained interest due to recent studies. Initial exposure to pathogens and vaccination stimulates a diverse panel of precursor B cells, resulting in antibodies of low affinity and levels of somatic hypermutation. Secondary exposure results in a response predominantly from clonally expanded B cells which produce antibodies of greater affinity and maturation levels (127,259).

Liao et al compared mutation rates in antibodies isolated from early HIV infection with those from Env immunisation, and found lower unmutated antibodies after HIV-1 Env vaccination (30%) compared to levels of unmutated antibodies in acute HIV infection (10.4%) (260). This is described in greater detail in 3.8.4. The authors compared this to other secondary antibody responses, and commented on the increased frequency of mutated antibodies in the acute HIV response as compared to secondary post influenza vaccine (antibody mutation rate of 6.5%) (261)

Liao et al showed these anti-HIV (specifically gp41 directed) responses to be highly mutated and polyclonal, originating from pre-existing intestinal B cells, characteristic of a second exposure to a recognised antigen in a pre-primed host (260). By reviewing clonality and deriving reverted unmutated common ancestral antibodies, 8 of 11 MAb reacted with gut flora antigens. Anti-gp41 IgG1 antibodies were also isolated from plasma and ileal cells of patients uninfected with HIV and displayed similar gp41-binding affinities to that of HIV-infected patient serum.

The polyclonality has two possible origins. Firstly, it could be attributed to extensive proliferation and mutation of B cells during acute HIV infection. This is unlikely given the destruction of germinal centres, and data show a lack of diversity even at one month post transmission (40). An alternative hypothesis is the activation of a previously educated B cell pool.

Infectious agents are known to elicit cross-reactivity with host antigens; *Herpes simplex virus* and *Cytomegalovirus* share common structures with intestinal microbial antigens, and influenza reactive T cells can be stimulated by skin commensals (262).

This hypothesis was supported by a report demonstrating that 82% of HIV-infected patient ileal anti-HIV anti gp41 B-cell responses cross-react with intestinal microbial antigens (IMA), including *Escherichia coli* RNA polymerase (ERP), and bacterial protein pyruvate-flavodin oxidoreductase (PFO) (263). This activity was subsequently reviewed in the setting of immunisation with a recombinant adenovirus type 5 (rAd5) vaccine containing HIV *gag*, *pol*, and *nef* genes, and clade A, B, and C envelope gp140 genes with gp120 and gp41 antigens. The vaccine failed to show efficacy, and patient responses were interrogated. The results showed a predominantly gp41 focussed response, 10-fold that of the gp120 response. This gp41 response was non-neutralising, non-ADCC inducing, and the majority cross-reacted with host and intestinal microbial antigens (264). The authors concluded that pre-existing B-cell responses could divert B cell activity from creating a protective response to epitopes on HIV Env. Samples obtained prior to vaccination yielded antibodies cross reactive to vaccine-HIV-Env and IMA, supporting the theory of priming by existing host microbiota. One vaccine recipient was found to have a pre-vaccine IgM V_HDJ_H rearrangement which was clonally related to a post-vaccine gp41 reactive IgG1 antibody, again supporting the theory of a pre-primed B-cell pool stimulated to diversify by antigen exposure. Following these observations, it has been suggested vaccines should induce specific B-cell lineages but avoid pre-existing cross-reactivity (142).

Other considerations for vaccine administration include the following; overall “health” of intestinal microbiome, timing of vaccination, and presentation of multiple epitopes.

The microbiome may skew development of B cell responses. Varying gut populations of *Actinobacteria* and *Firmicutes* vs *Proteobacteria* and *Bacteroides* are positively and negatively associated with vaccination response respectively (265). “Healthy” gut flora profiles are associated with better responses to vaccination and improved B and T cell responses in infection (266). The microbiome influence on HIV vaccination showed increased microbiome diversity was associated with improved responses to gp140/41, p24 and V1V2 epitopes and CD 4 T cell responses (267).

Other causes of varying responses to vaccination have been attributed to physiological mechanisms. Circadian rhythms can influence response to vaccination, as influenza vaccination has been

demonstrated as more effective if given in the morning (268). In addition, vaccine candidate who exercise prior to administration of influenza vaccine produce better immunisation responses compared to more sedentary candidates (269).

Another consideration for vaccination strategies is the presentation of multiple epitopes within vaccines- are these problematic? To use the measles/mumps/rubella vaccination as an example- multiple epitopes are presented at one occasion, but should this be a concern for efficacy? Thankfully, no difference in efficacy is reported when multiple/combination vaccines given to children (270,271), and Public Health England recommend this strategy over singly administered vaccines in children (272). Other strategies now employing multi-epitope structures including vaccination against *Leishmania* (273) and *Helicobacter pylori* (274).

1.11.3.Significance of anti-Env response

The anti-gp41 immune response is swift and polyclonal but could this arise from a pre-educated B cell pool. And does this pre-exposure influence future immune responses and development of established infection?

1.12. Summary

In summary, I have discussed the following aspects of HIV; virus transmission and establishment of infection, the effect on B cells and the subsequent B cell response to HIV, the properties considered important for a vaccine, features of the immune response in highly exposed seronegative persons, and the presence of antibody responses against Env in seronegative individuals, with origins attributed due to viral or gut antigen exposure.

Some questions arise from these observations.

1. Does the presence of an anti Env response form the basis for any subsequent anti-Env response?
2. Does HIV-1 envelope recognition by the immune system influence the risk of future HIV-1 acquisition and/or progression of future infection?
3. Do HESN antibody responses vary according to the level of exposure to HIV?
4. Do HESN/seronegative responses to Env focus on similar epitopes?

To address these questions, I plan to evaluate the anti-Env response in seronegative participants and follow the development of the response through seroconversion events. Should anti-gp41 responses exist, I plan to evaluate their structure and function. Bringing these ideas together has stimulated the discussion for this project and forms the basis for the work intended.

1.14. Hypothesis

1.14.1. Anti-Env in HIV-uninfected people

Anti-HIV envelope (hereby referred to as Env) reactive antibodies in HIV-uninfected people have been described in two settings

1. Isolated from highly exposed seronegative people (HESN) (1,2).
2. Isolated from plasma and ileal cells of uninfected patients (3).

As described in the introduction chapter, anti-Env antibodies are present in uninfected people (4). Their origin may arise from a pool of B cells previously educated by exposure to intestinal microbial antigens resulting in an antibody response with affinity for the Env antigen (5). It has also been demonstrated that when candidates are vaccinated with the r-Ad-5 construct, the pre-vaccination anti-Env antibody ancestor can be clonally related to the post-vaccination-component (3).

1.14.2. Origin of anti-Env antibodies in HIV pathogenesis

I wish to explore the role of the anti-envelope immune response in individual participants. As shown in the immunisation setting, pre-existing anti-Env antibodies could evolve in a similar fashion on encountering HIV epitopes in the setting of HIV infection *in vivo*.

1.14.3. Role of anti-Env antibodies in HIV disease and progression

As described, the early antibody response in HIV acts predominantly through non-neutralising functions. This Fc mediated antiviral activity dominates acute infection, subsides at six months, and is replaced by autologous neutralising antibodies. Moreover, Fc functionality in acute infection mediated via Env-directed antibodies has been shown to provide varying levels of protection both in human and non-human models (described in section 1.7).

Humoral responses to vaccination with certain HIV Env vaccine structures produces anti-Env responses the function of which is unclear and may divert B-cell activity from developing effective control of viral replication. This was shown by Williams et al who reviewed the efficacy of HIV-1 DNA rAd5 boost vaccine with *gag, pol, nef* and *gp140 Env* genes. The vaccine responses were mainly towards gp41 and were non-protective and mirrored by low frequencies of gp120-memory B-cells in

these patients; 0.05% population were gp120-specific memory B-cells vs 0.28% gp140-specific memory B-cells. As other studies using Env gp120 immunogens had shown memory B-cell populations of 0.73%, this suggested Env gp120 does produce a B-cell response and the reduction seen could not be attributed to inability to produce a serum antibody response. The authors then searched for the unmutated common ancestor B-cells from the pre-vaccine samples with V_HDJ_H rearrangements matching those of the Env-specific memory B-cells to identify a clonal lineage and produced the corresponding mAb.

They found that post vaccine mAb (post-mAb) reacted with gp41 and IMA, pre-vaccine mAb IgM (pre-mAb) reacted with vaccine Env, MN gp41 and IMA; with greater binding to IMA of pre-mAb vs post-mAb, and greater binding to Env of post-mAb vs pre-mAb. The authors concluded suggesting Env vaccination induced a polyreactive non-neutralising anti-gp41 responses from pre-existing B-cells, and this response could cross react with IMA (Williams et al., 2015).

For this work, the previously referenced study suggests anti-Env antibodies in HESN who subsequently seroconvert precede the expected anti-Env antibody response in acute HIV infection and may influence the future antibody response.

1.14.4.Hypothesis

I wish to determine the following

1. Do pre-existing anti-Env antibodies exist in HESN, either from exposure to virus in the absence of infection, or from cross reactivity with intestinal microbial antigens?
2. Does the frequency of anti-Env antibodies vary according to presumed levels of exposure to HIV infection?
3. Do pre-existing anti-Env responses in HESN target similar epitopes as those found in acute HIV infection?
4. Do pre-existing anti-Env antibodies influence the course of HIV infection via Fc-mediated processes?
5. Does the presence of anti-Env antibodies in seronegative populations bind/block HIV epitopes *in* vitro, or influence future infection?

In response to these questions I hypothesize

1. Anti-Env antibodies are present in seronegative individuals
2. Anti-Env antibody frequency and epitope targets may be influenced by HIV exposure
3. Anti-Env antibodies present in seronegative people may act as primer epitopes for the B cell response, with recognition of similar epitope in the course of subsequent infection acting as a prime and boost response, similar to that employed in vaccination strategies
4. Anti-Env antibodies may influence the future disease course, either protectively via Fc-mediated functions, or could divert the acute immune response away from producing an effective neutralising response and facilitate HIV infection.
5. Anti-Env antibody may be associated with increased risk of HIV infection if this is demonstrated *in vitro* assays

Depending on the outcomes proposed above, future work could review the inclusion of Env epitopes in vaccine development. I believe the anti-Env antibody response represents an important component of the anti-HIV acute immune response and should be explored in greater detail.

1.15. Objectives

1.15.1.Cohort

To establish a cohort of HESN men who have sex with men, collect baseline demographic information, serological and peripheral blood mononuclear cell (PBMC) samples, and sequential samples in the event of HIV seroconversion.

1.15.2.Analysis

To employ serial sampling and analysis to assess the presence or absence of anti-Env responses antibodies in this cohort. The initial focus is initially seronegative MSM, and then to review anti-Env responses in HESN MSM who later acquire HIV infection. I will track the anti-Env response in early and later HIV infection, and will review cross-reactivity with intestinal microbial antigens, interrogate early HIV responses to identify immunogenic regions of Env, and the relationship to subsequent disease progression.

1.15.3.Function

To determine anti-Env functionality by generating monoclonal antibodies and using these in assays to review Fc effector function. These assays will include antibody dependent cellular cytotoxicity (ADCC), and neutralisation capabilities.

Chapter 2
Materials and methods

Chapter 2 Materials and Methods

2.1. Project details

2.1.1. Project design

The protocol for this project was written by Katie McFaul and Peter Kelleher. All project documents including the patient information leaflet, patient consent forms and case report form (CRF) were written by Katie McFaul and Peter Kelleher (Appendix 1).

2.2. Ethical approval

An application was submitted to the Fulham NHS Research Ethics Committee via the UK integrated Research System (IRAS- https://www.myresearchproject.org.uk/). The study REC reference number was 14/LO/2058 and the review was held in the Fulham REC. Following minor amendments, approval was granted on 17th December 2014. There were four major amendments submitted after the original application, and these were approved on 29th June 2015. (Appendix 1).

2.2.1. Local Biosafety approval

A Biosafety application was submitted to Imperial College London Biosafety Officer which was approved. Local laboratory was sought approval and clearance was granted in March 2015. This covered all laboratory preparatory work, including gain of yeast surface display technology, single cell fluorescence-activated cell sorting, B cell cloning, and monoclonal antibody production.

2.3. Cohort details

A cohort of study participants was established to review adaptive immune responses stimulated by exposure to HIV envelope antigens. A busy inner city sexual health clinic was selected as the study site. This study coincided with a larger initiative to establish an immunological study group at that site.

Prior to formation of these cohorts, advice was sought from clinicians, patient representation groups and study leads on how best to approach and manage trial participants. All seronegative patients were approached to participate during routine sexual health assessments. Seropositive patients were approached during routine HIV clinic visits. All consent procedures and tissue samples were obtained at that time. The resulting recruitment drive was successful, and approximately 300 individuals were recruited to study groups. The data and tissue samples obtained are now in use in multiple immune based studies within our department and also in national collaborations with other academic institutions.

Participants were recruited from 56 Dean Street, Chelsea and Westminster NHS Foundation Trust. At the time of recruitment, this clinic diagnosed one in four UK HIV cases in men who have sex with men, equating to 350-400 new diagnoses per year (275). Clinic attendees disclose details of sexual activity and HIV acquisition risk factors, which allowed identification and recruitment of individuals at increased risk of HIV infection. This provided an opportunity to recruit individuals prior to and post seroconversion to HIV.

Participants were recruited from three clinical areas. The first, Dean Street Express, is a walk-in sexual health clinic in the heart of Soho, London. At time of recruitment, approximately 300 people attended for sexual health screening, with a large proportion of men who have sex with men (MSM). The second clinical recruitment site was the weekly CODE clinic. This clinic is attended by MSM involved in recreational drug use (colloquially referred to as “chemsex”) and aims for reduce high risk behaviour associated with increased HIV acquisition.

High risk HIV negative MSM were identified from their clinic registration details and reported risk factors identified within the past year. Suitable study candidates were approached and asked to participate in the study. These participants were recruited to group A and this visit was their initial visit where they completed questionnaires and had blood drawn for serum, plasma and PBMC sampling.

The third clinical area were HIV outpatient clinics attended by known HIV positive individuals. Potential candidates were approached and asked to participate in the study. Depending on their time since diagnosis and antiretroviral status, participants were recruited to groups C/D/E. The final study group was B, which contained individuals from Group A who underwent seroconversion to HIV seropositivity. Overall, participant experience and feedback has been positive to date.

2.3.1. Cohort characteristics

The study design included five separate cohorts for the work intended. As previously described, these were recruited from the clinic at 56 Dean Street, Chelsea and Westminster NHS Foundation Trust, Soho, London.

2.3.1.1. Group A

238 seronegative MSM with a background history of any unprotected anal intercourse were recruited into group A, a seronegative group. All participants were informed of the nature of the study and had the opportunity to decline participation.

Serostatus was confirmed by a negative point of care HIV test (INSTI HIV-1/HIV-2 Antibody Test, Biolytical Laboratories, Washington State, USA) if previous unprotected sexual intercourse had been six weeks or greater, or blood serology (Abbott Architect Combo p24/ HIV 1and 2, Abbott Laboratories UK) test if previous unprotected sexual intercourse had been four weeks or greater.

These testing methods report sensitivities of >99% and 100%, and specificities of >99% and >99% respectively when used at the recommended interval time since last unprotected sexual intercourse (276,277). All patients were recorded on an Excel database.

All participants completed baseline case report forms and had sixty millilitres of blood drawn for PBMC, serum and plasma banking. All participants also had a “study participant” notification attached to their clinical notes. Participants were given signed copies of their consent forms and a patient information leaflet to take away for future references.

One hundred individuals were selected from this group; fifty “high risk” and fifty “low risk”. We defined risk of HIV acquisition according to criteria derived from the PROUD UK trial. This identified two significant baseline characteristics for development of HIV infection; the presence of a sexually transmitted rectal infection (STRI), and a greater number of sexual partners reported in the past ninety days (113). These risks were associated with an incidence rate of 9.1 new HIV infections per 100-person years.

Accordingly, fifty participants were classified as low risk (medium number of six sexual partners, only one participant with a confirmed episode of a sexually transmitted rectal infection in the previous twelve months) and fifty participant as high risk (medium number of thirty sexual partners and all with a confirmed episode of a sexually transmitted rectal infection in the previous twelve months).

In order to assess true negative serostatus at the initial visit, all participants selected for analysis were cross referenced in two ways. Participant hospital numbers were cross referenced against all patients newly diagnosed with HIV attending any of the trust’s sites- this also served the purpose of locating participants who had seroconverted and were eligible for Group B participation. In addition, all patients had evidence of at least one routine sexual health assessment at least one month following initial recruitment.

2.3.1.2. Group B

This group consisted of individuals from Group A who underwent seroconversion to HIV positive status. As stated in 2.3.1.1, all individuals from Group A were followed longitudinally. All new positive HIV diagnoses from the study site were cross referenced against the Group A participant registry. Staff members working at the study site were advised to inform the study investigators in the event of a seroconversion in a study participant. Individuals attending the study centre are encouraged to present for sexual health screening at least yearly, or every three months if having unprotected sex with new or casual partners as per national guidelines (86)

If an individual was identified from Group A who was now seropositive for HIV, they were invited to participate in this part of the study, and if agreeable, longitudinal follow-up was organised. This consisted of monthly blood test for the first six months of their involvement with Group B, and blood tests six monthly thereafter.

2.3.1.3. Group C and D

Group C participants were patients with known HIV infection who were not taking antiretroviral medication. The aim was to recruit men who have sex with men, diagnosed with HIV for more than three years, who had never taken HIV medication. Only two patients were recruited into this arm of the study, as international guidelines advise all patients diagnosed with HIV should be offered antiretroviral medication at diagnosis (87,94).

Group D participants were patients with known HIV infection who were taking antiretroviral medication and had achieved an undetectable viral load. Eleven patients were recruited to this arm of the study. As the work focused on immunological responses in seronegative and recently seroconverted individuals, statistical and molecular analysis was not performed in this group.

These two groups were recruited as part of the overall immunology cohort but were not part of this study. They have been discussed here to explain the group allocation and will not be mentioned again.

2.3.1.4. Group E

Group E participants were those recently diagnosed with HIV infection who had yet to begin antiretroviral medication. All patients newly diagnosed with HIV attending clinic for initial review were screened and asked to participate. All blood samples were obtained prior to initiation of medication. A total of nineteen patients were recruited to this group. Group E samples were used as positive control samples for work done on seronegative (group A) and seroconverter (group B) samples.

2.3.2. Cohort management

Maintenance of patient demographics involved manual entry of data into an Excel document (Microsoft) and data analysis of demographics and PBMC was done using IBM SPSS Statistics (Version 23). Initial feedback from study participants has been positive, with many commenting on the ongoing interest in immunological studies and HIV. Feedback from colleagues at the recruitment centre was positive as it stimulated discussion on multiple aspects of immune responses to HIV.

2.4. Experimental techniques

The following techniques were used to assess the anti-gp41 response- construction of a yeast display system to assess serological responses to HIV envelope epitopes, B cell baiting to extract candidate B cells of interest using selected yeast epitopes, and monoclonal antibody generation for future functional experiments.

SCHEMATIC OF YEAST SURFACE DISPLAY TECHNOLOGY

Figure 2.4-1 below outlines the process of constructing the yeast library

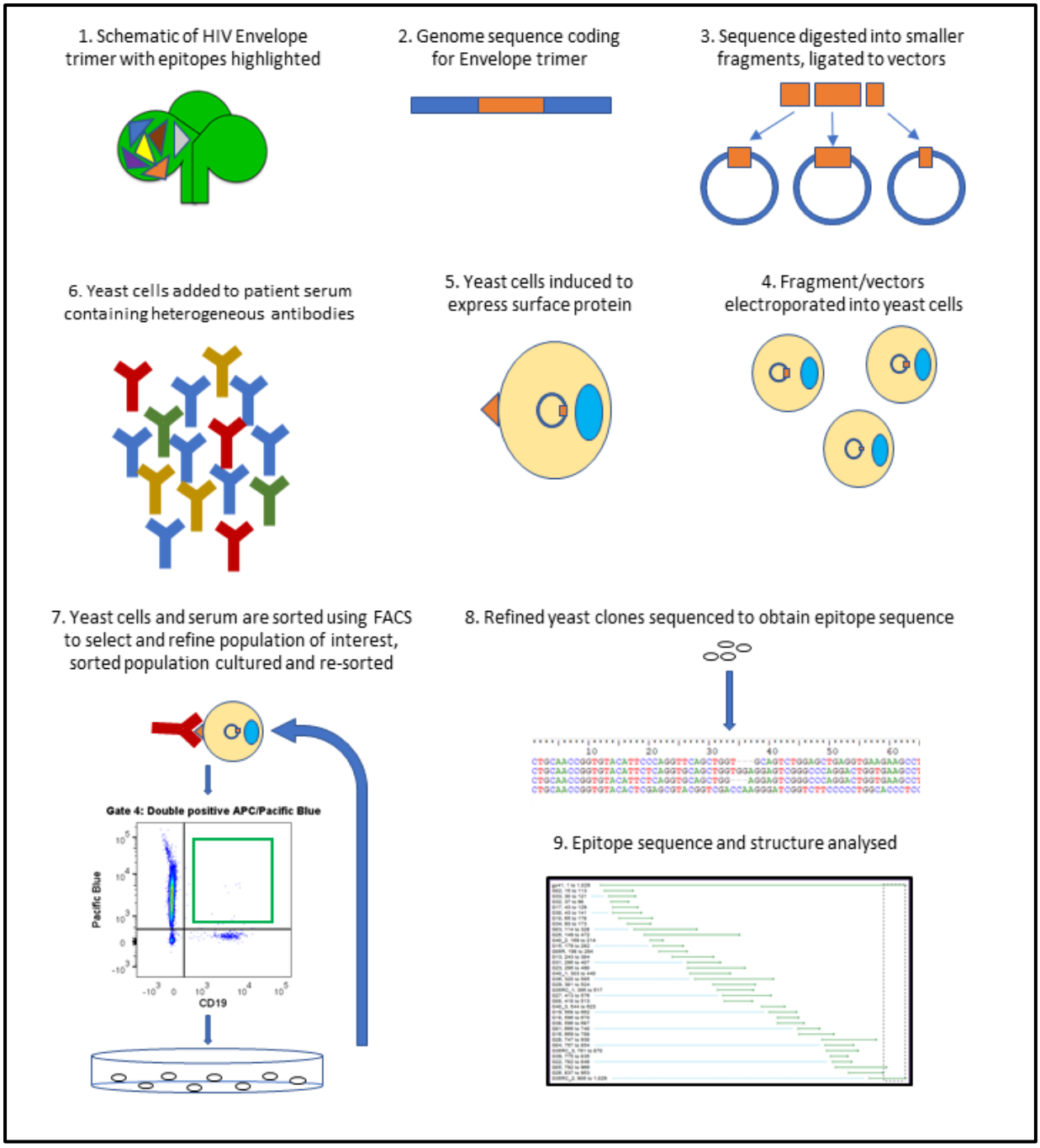


Figure 2.4-1 Schematic of yeast surface display technology

Nine steps showing steps of methods used to create the yeast surface display library.

2.5. Yeast Display System construction

A novel yeast surface display (YSD) system was used to generate a combinatorial unbiased antigen library from the HIV envelope gp160 (gp 120/41) genomic region. Major antigenic determinants of the anti-HIV-1 anti-envelope gp160 response were subsequently determined by identifying any areas under the curve with a peak amino acid frequency of greater than five residues. This method was described by Wittrup et al and has been widely used for display of recombinant proteins on the yeast cell surface (278,279) and more recently for directed evolution of a high-affinity gp140 envelope protein (280). This method was used to screen participant serum for antibodies with affinity for gp160 epitopes.

2.6. Genomic sequence

The template for the HIV Envelope library was a HIV-1 B clade insert (donated by Prof. Xiao-Ning Xu, Imperial College London) named BJOX35. The donor of this sample had viral load of 11,600 and the sample was obtained at Feibig stage I/II. Plasmid samples were made into a 1:100 working solution with RNase free water and stored at -20°C. The working sequence, BJOX35, was a 4687 base pair long genomic fragment spanning the HIV envelope region. The sequence was uploaded to the HIV sequence database at Los Alamos National Laboratory and given the GenBank accession number KY076491 (HIV LANL, https://www.hiv.lanl.gov/content/sequence/HIV/mainpage.html).

2.6.1. Primers

Primers were designed to target HIV envelope gp160 (Env) and gp41 (gp41) glycoproteins using the National Center for Biotechnology's Basic Local Alignment Search Tool (NCBI primer blast; https://www.ncbi.nlm.nih.gov/tools/primer-blast/). Two pairs were designed for each target. Each pair was designed to target the 2750 base pair (bp) HIV-1 envelope sequence (bp 6045- 8795). Primers were constructed by Sigma Aldrich (Sigma-Aldrich Company Ltd, Dorset, United Kingdom). RNase free water was added to make 100umol stock solution and made working aliquots a 1:10 solution. The primers are shown in Table 2.6-1.

Primer sequences		
HIV envelope/gp160 library 2750 base pair (bp) sequence (bp 6045-8795)	Pair 1	Forward primer: AGAAGACAGATGGAACAAGCCCC Reverse primer: GCACTCAAGGCAAGCTTTATTGA
	Pair 2	Forward primer: ATGAGAGTGAAGGGGATCAG Reverse primer: CTACCAAATCTTTGTATTCCTTC
HIV gp41 library 1037 base pair (bp) sequence (bp 7758-8795)	Pair 1	Forward primer: AACATGTGGCAGAAGGTAGG Reverse primer: CAGGTCGACCCAGATAATTGCTA
	Pair 2	Forward primer: AAACATGTGGCAGAAGGTAGGA Reverse primer: AGGTCGACCCAGATAATTGC

Table 2.6-1 Primer sequences used for HIV gp160 envelope PCR
This table shows the two pairs of primers designed to target the envelope glycoproteins gp160 and gp41

2.6.1.1. Polymerase Chain Reaction (PCR) optimisation for HIV envelope

A polymerase chain reaction was used to identify and amplify the desired region of interest- HIV-1 envelope. I used Phusion® High-Fidelity DNA Polymerase (New England Biolabs) for amplification of the HIV-1 envelope region of interest. Products were analysed using a 1% concentration Tris-borate EDTA (TBE) with SYBR® Safe DNA Gel Stain (Thermo Scientific). A 5µl aliquot of PCR product was mixed with 1-2µl of 6X gel loading dye (New England Biolabs). Electrophoresis was conducted at 400milliAmp, 60volts for 60 minutes to allow identification and confirmation of the desired fragments; 2740 bp HIV envelope and 1037 bp gp41 PCR product. Primer pair two was selected for HIV envelope sequencing as it produced a more prominent band on the PCR gel. This is shown in Figure 2.6-1 TBE gel electrophoresis of HIV envelope PCR target products

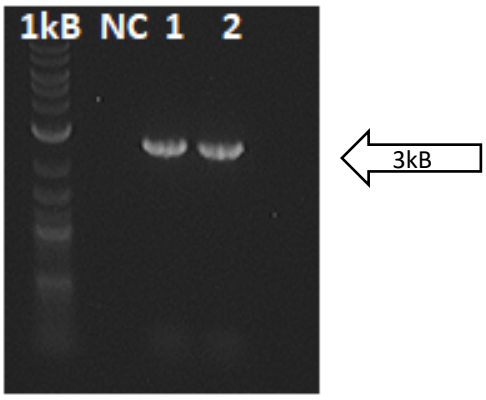


Figure 2.6-1 TBE gel electrophoresis of HIV envelope PCR target products
Gel displaying 1 kB 1 kilobase DNA reference ladder, NC negative control (no template), P1 primer pair 1, P2 primer pair 2. The two PCR products were in the 3-4kb region as expected for the HIV envelope size. Primer pair two resulted in a more prominent band and was selected for further use. The negative control channel remained blank.

PCR annealing conditions were optimised using temperature gradient PCR to eliminate non-specific bands. A negative control was used- PCR mix with absence of the plasmid template. The final reaction conditions were as follows: denaturation at 98°C for 30 seconds, 35 cycles of: a) 98°C denaturation for 10 seconds, b) annealing at 61°C for 82 seconds, and c) elongation at 72°C for 77 seconds, an extension at 72°C for ten minutes, and a final hold at 4°C. PCR products were purified with the QIAquick PCR Purification Kit (Qiagen, UK) to give 50µl solution. This is shown in Figure 2.6-2.

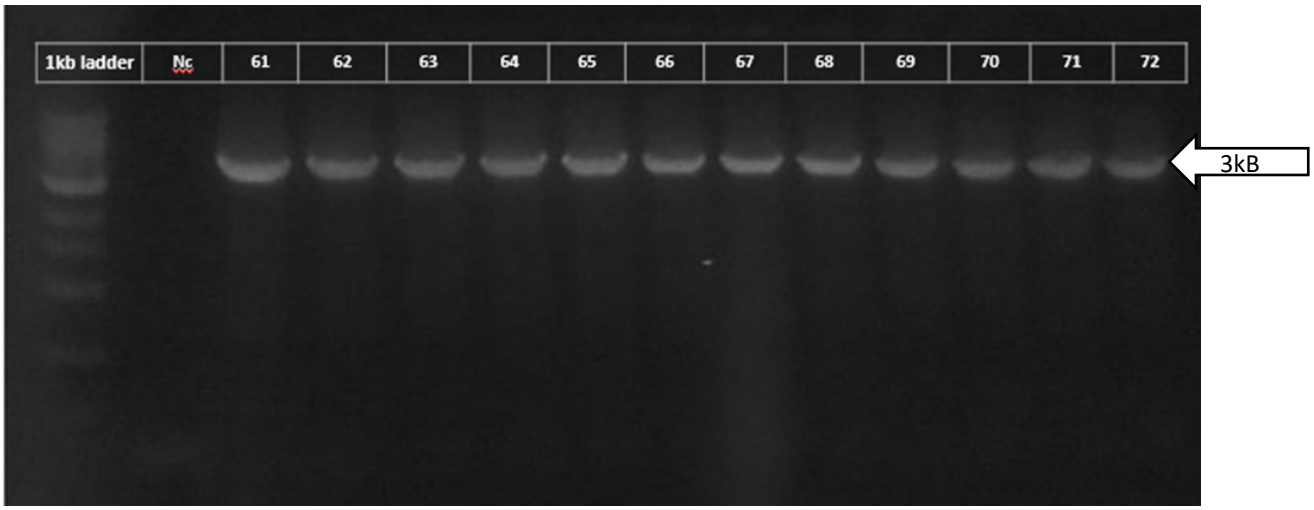


Figure 2.6-2 Temperature gradient PCR optimisation
Gel electrophoresis showing PCR performed at increasing temperatures; samples analysed at 1°C intervals from 61°C to 72°C. An annealing temperature of 61°C gave the most prominent band with no nonspecific bands visible and was selected for use. 1 kB: 1 kilobase DNA reference ladder, Nc: negative control (no template), 61-72°C is temperature of each annealing step.

2.6.1.2. Polymerase Chain Reaction (PCR) optimisation for HIV gp41

The following reaction conditions were used for optimisation of the gp41 PCR reaction: denaturation at 98°C for 30 seconds, 35 cycles of: a) 98°C denaturation for 10 seconds, b) annealing at 64°C for 31 seconds, and c) elongation at 72°C for 77 seconds, an extension at 72°C for 10 minutes, and a final hold at 4°C. PCR products were purified with the QIAquick PCR Purification Kit to give 50µl solution. An aliquot containing all PCR components except the plasmid template was used as a negative control. Figure 2.6-3 below shows the PCR products. As no non-specific bands were seen, no gradient temperature experiment was needed. Primer pair 2 was selected for all future experiments. Products were analysed using the NanoDrop 1000 Spectrophotometer (Thermo Scientific) and yielded the results shown in Table 2.6-2. When not in use, all samples were stored at -20°C.

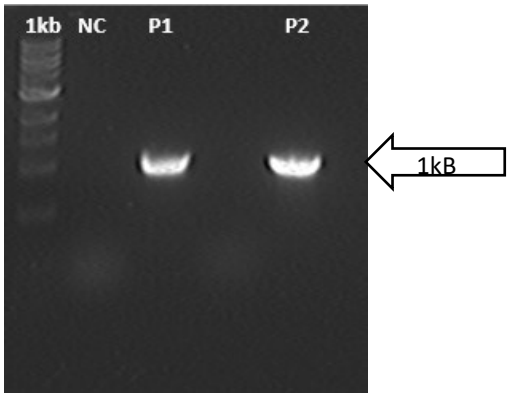


Figure 2.6-3 TBE gel electrophoresis of gp41 envelope PCR target products
Gel displaying 1 kB 1 kilobase DNA reference ladder, NC negative control (no template), P1 primer pair 1, P2 primer pair 2. The two PCR products were in the 1kb region as expected for the HIV gp41 size. Primer pair two resulted in a more prominent band and was selected for further use. The negative control channel remained blank. 1 kB: 1 kilobase DNA reference ladder, Neg C negative control (no template), P1 sample 1, P2 sample 2

	Volume (µl)	Conc (ng/µl)	260/280 ratio	260/230 ratio	Total (ng)
HIV Env	50	186.1	1.91	2.38	9305
HIV gp41	50	132.1	1.90	2.41	6605

Table 2.6-2 HIV Envelope and gp41 primer optimisation products
Each purification stage yielded 50ul of PCR product. DNA concentration was calculated by spectral absorbance. The 260/280 ratio represents the ratio of absorbance at these wavelengths; 1.8 generally considered as pure for DNA. 260/230 ratio is a secondary measure of DNA purity; 2.2 generally considered as pure indicating absence of contaminants.

2.6.1.3. Random digestion

HIV envelope and gp41 PCR products underwent random digestion using increasing concentrations of DNAse I (New England Biolabs). The following reaction conditions were used: DNA approximately 4µg, 2.5µl of 1M Tris-Cl, PH7.5, 10µl of 50mM MnCl2 (freshly made), and total reaction volume made up to 48µl with RNase-free water. The DNase I (2U/µl) was diluted with 50 mM Tris-Cl (pH7.5) to an initial concentration of 0.1U/µl (20- fold dilution), and subsequently to 0.067U/µl. The higher concentration 0.1 unit/µl DNase I solution was used to create the small fragment library, and the lower concentration 0.067 unit/µl Dnase I to create the large fragment library. An aliquot of 2µl diluted of each DNase I solution (0.1 or 0.067 U/ µl) was added to the bottom of each reaction vessel to make 50µl of reaction mixture. This was mixed by pipetting 2-3 times and the digestion reaction time was four minutes. The reaction was terminated by adding 10µl of 0.5M EDTA (in 1M Tris-Cl, pH7.5) to each reaction vessel. These were subsequently immersed in liquid nitrogen for 3-5 minutes.

The reaction vessels were placed in a PCR block at 90°C for ten minutes to denature the DNase I enzyme and products were identified using gel electrophoresis. Figure 2.6-4 below shows the two HIV envelope DNA product "libraries" with different length of fragments. The small library fragments were 100-300bp in length, and the big library fragments were 100-500bp in length. The digested fragment products were purified in 50µl solution and the concentrations were analysed using the Nanodrop spectrophotometer and recorded in Table 2.6-3.

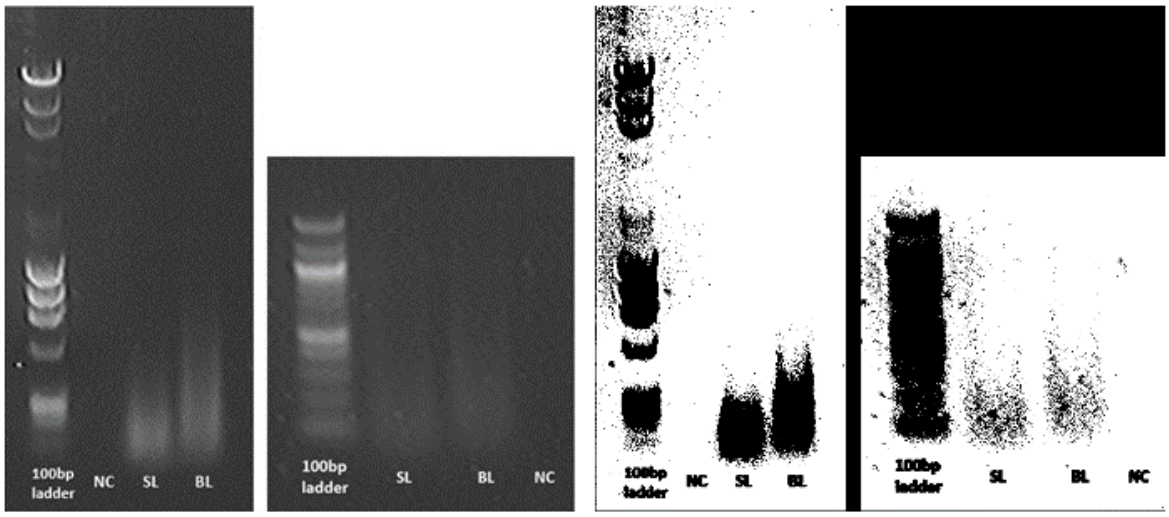


Figure 2.6-4 Gel electrophoresis of digested HIV envelope and gp41

Figure showing digested PCR products: left HIV envelope, right gp41 products. Second image shows inverted colour selection and hyper saturation of black and white tones to enable visualisation. Both images display a "smear" of products, characteristic of multiple small fragment sizes of 50-300bp length. Also shown is 100 bp DNA reference ladder, NC negative control (no template); SL small library, BL big library.

	Volume (µl)	Conc (ng/µl)	Total (ng)
HIV Env small library	50	55.8	2790
HIV Env big library	50	68.4	3420
gp41 small library	50	25.7	1285
gp41 big library	50	30.6	1530

Table 2.6-3 Digested library product concentrations

Envelope and gp41 big and small library post digest product concentration and total product

2.6.1.4. A-tailing of PCR-reassembled fragments

Taq DNA polymerase (NEB) was used to add non-template nucleotides to the blunt ends of library fragments (A-tailing). This facilitated ligation of fragments into cut vector. The reaction vessel contained: 0.25µl of Taq, 1µl of 10mM deoxynucleotide (dNTP) mixture, 5µl of 10X reaction buffer (supplied with Taq DNA polymerase), and approximately 2µg of the blunt-ended DNA, made up to 50µl with RNase free water. The reaction vessel was incubated at 72°C for 20 minutes and cooled on ice for four minutes. The library products were purified with the QIAquick PCR Purification Kit (Qiagen, UK) to give 50µl solution. The concentrations were recorded as shown in Table 2.6-4.

	Volume (µl)	Conc (ng/µl)	Total (ng)
HIV Env small library	50	36.6	1830
HIV Env big library	50	64.5	3225
gp41 small library	50	22.9	1145
gp41 big library	50	30.6	1300

Table 2.6-4 A-tailed PCR library fragments
Envelope and gp41 big and small library product concentration and total product post A tailing

2.6.1.5. Preparation of pCTCON2-T vector

An *E. coli* vector containing the pCTCON2-T plasmid (kindly donated by Jia Guo, Centre for Immunology and Vaccinology, Imperial College London) was used for this section of work. Plasmid-containing *E. coli* were grown overnight at 37°C on lysogeny broth (LB) with 1% ampicillin plates and harvested. Plasmids were prepared from *E. coli* using a commercial kit (Qiagen Plasmid Midi Kit, Qiagen, UK) and digested using the restriction endonuclease XcmI (NEB), reaction conditions as follows: 10µg plasmid DNA, 10µl of 10X buffer (provided with enzyme), 2µl XcmI enzyme, and made up to 100µl total volume with RNase free water. The reaction vessel was incubated in a water bath at 37°C for six hours. The products were purified and analysed with gel electrophoresis (Figure 2.6-5), and the 6kB band product excised from the gel (3.56g weight) with a scalpel. The DNA was extracted using a commercial gel extraction kit (QIAquick Gel Extraction Kit, Qiagen, UK) and the resulting product purified into a low salt solution yielding the concentrations shown in Table 2.6-5.

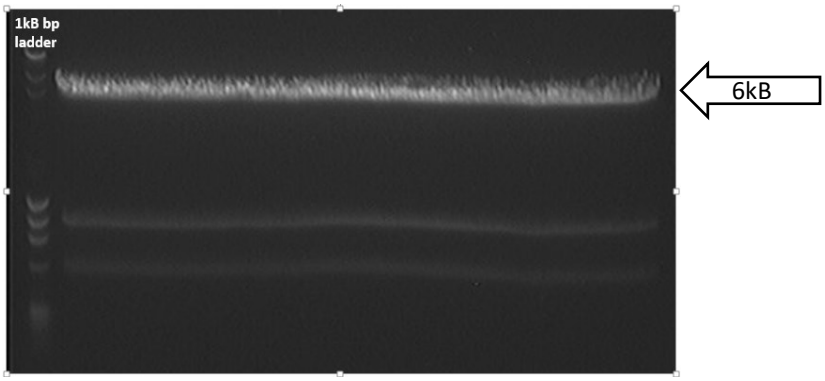


Figure 2.6-5 Digested pCTCON2-T vector
Gel showing digested pCTCON2-T vector with 1kB bp ladder. The thick band at the top is the 6kB digested vector

	Volume (µl)	Conc (ng/µl)	Total (ng)
pCTCON2-T	25	273.0	8190

Table 2.6-5 pCTCON2-T vector digest concentration
Table shows the final vector product concentration and total product available following digestion

2.6.1.6. Ligation of random fragments to pCTCON2-T vector

Library fragments were inserted into the cut pCTCON2-T vector using a DNA ligase enzyme, T4 (Thermo Scientific). Ideal reaction conditions involve a DNA ratio of gene and vector of 3:1 - 6:1. As an example: if DNA fragments are approximately 500bp, use 2µg with 4µg vector. If DNA fragments are approximately 300bp, use with 1.2µg with 4µg vector.

Reaction conditions were as follows: small library DNA 1.2µg/ big library DNA 2.0µg, pCTCON2-T vector 4µg, 10X T4 ligase buffer (supplied with enzyme) 20µl, T4 ligase 10 µl, and the final reaction mixture was made up to 200µl total volume with RNase free water. The reaction was incubated at 22°C for two hours. I purified the resulting product to yield the results displayed in Table 2.6-6.

	Volume (µl)	Conc	Total (ng)
HIV Env small library +	50	85.4	4270
HIV Env big library + vector	50	99.3	4965
gp41 small library + vector	50	65.7	3285
gp41 big library + vector	50	69.1	3455

Table 2.6-6 Ligated fragment/vector yield
Table shows the final library/fragment product concentration and amount following ligation

2.6.1.7. Bacterial transformation (electroporation)

The library and vector ligation products were transformed into electrocompetent DH10B™ *E. coli* cells (ThermoFisher Scientific) with the Gene Pulser XcellTM Electroporation system (Bio-Rad, UK) and the following setting: manual, 2500 volts, with a 0.2cm cuvette. The reaction components of purified DNA ligation product, competent cells and cuvettes were chilled on ice. A 50µl aliquot of competent electrocompetent DH10B™ *E. coli* cells were mixed with 2-5µl (~500ng-1µg)/tube of purified library and vector ligation products in a 1.5ml Eppendorf tube and chilled on ice for three minutes.

This aliquot was transferred this to the pre-chilled electroporation cuvettes; four Eppendorf tube contents were accommodated in one 0.2cm cuvette. The cuvettes were tapped to remove bubbles and dried the external cuvette surfaces to prevent poor electrical contact. The electroporator discharged a pulse duration of approximately 0.4 milliseconds. Following this, 1ml of room temperature super optimal broth with glucose (SOC) recovery medium was added to the cuvette and re-suspended this in a 15ml centrifuge tube with 1ml of pre-warmed SOC. This was then placed in a shaker incubator for at one hour at 37°C to allow expression of the antibiotic resistance gene.

The post electroporation reaction mixture was plated onto pre-warmed LB + 1% ampicillin agar plates as follows: ten standard culture plates and two dilution plates to assess efficacy of electroporation. Standard culture plates contained approximately 200 µl of the transformation reaction mixture. Dilution plates consisted of 200µl of culture medium diluted to 1:1000 and 1:10000 concentration. All plates were incubated overnight at 37°C.

2.6.1.8. Bacterial transformation efficacy

The colonies were selected from culture plates and added to 3ml of LB+1% ampicillin medium and placed these in a shaking incubator at 37°C, 225 RPM for one hour. The mixture was decanted into a 50ml centrifuge tube, centrifuged at 1000g for 20 minutes to pellet, and stored at -20°C. Table 2.6-7 shows transformation colony yield.

	No. colonies from 200µl/1000 solution
HIV Env SL dilution plate 1:10000	325
HIV Env BL dilution plate 1:10000	960
gp41 SL dilution plate 1:10000	306
gp41 BL dilution plate 1:10000	259

Table 2.6-7 Bacterial transformation efficacy
Number of bacterial colonies from each transformation. The number of colonies grown on each plate was counted at the time of harvesting, and the HIV envelope big library produced the most colonies. Env envelope, SL small library, BL big library.

2.6.1.9. Assessment of library coverage

The individual colonies from dilution culture plates were selected for analysis of the library coverage. The 10µl pipette tips were used to pick approximately of 48 colonies from each plate. This amount had been advised by the protocol and by colleagues familiar with this technology. The tips were placed in individual 3ml LB culture medium in 15ml culture tubes, and incubated for 12 hours at 37°C, 225 RPM. The tubes were retrieved, centrifuged at 1000g for 15 minutes, supernatant poured off and the resulting pellet frozen. The colony pellets were sent (HIV envelope SL + BL, gp41 SL + BL) to the MRC Protein Phosphorylation and Ubiquitylation Unit (DNA Sequencing and Services, Medical Sciences Institute, School of Life Sciences, University of Dundee, Dundee, DD1 5EH) for plasmid extraction and sequencing analysis.

2.6.1.10. Sequencing Results

Bioedit v7.2.51 (281) and Sequencher v4.92 (Genecodes Corporation) were used to analyse the returned sequences. Briefly, vector terminal sequences were used to identify the library fragment of interest. The fragments were collectively aligned to parent sequence strand to assess library coverage. The libraries are shown in the figures below (Figure 2.6-6, Figure 2.6-7, Figure 2.6-8) and presented as follows: HIV small and big libraries combined, gp41 small and big libraries presented separately. These analyses show how the library capacity spans that of the parent nucleotide sequence. The figures show adequate fragment coverage across the parent sequence with minor gaps at C2, C3 and C4 loop in HIV envelope library.

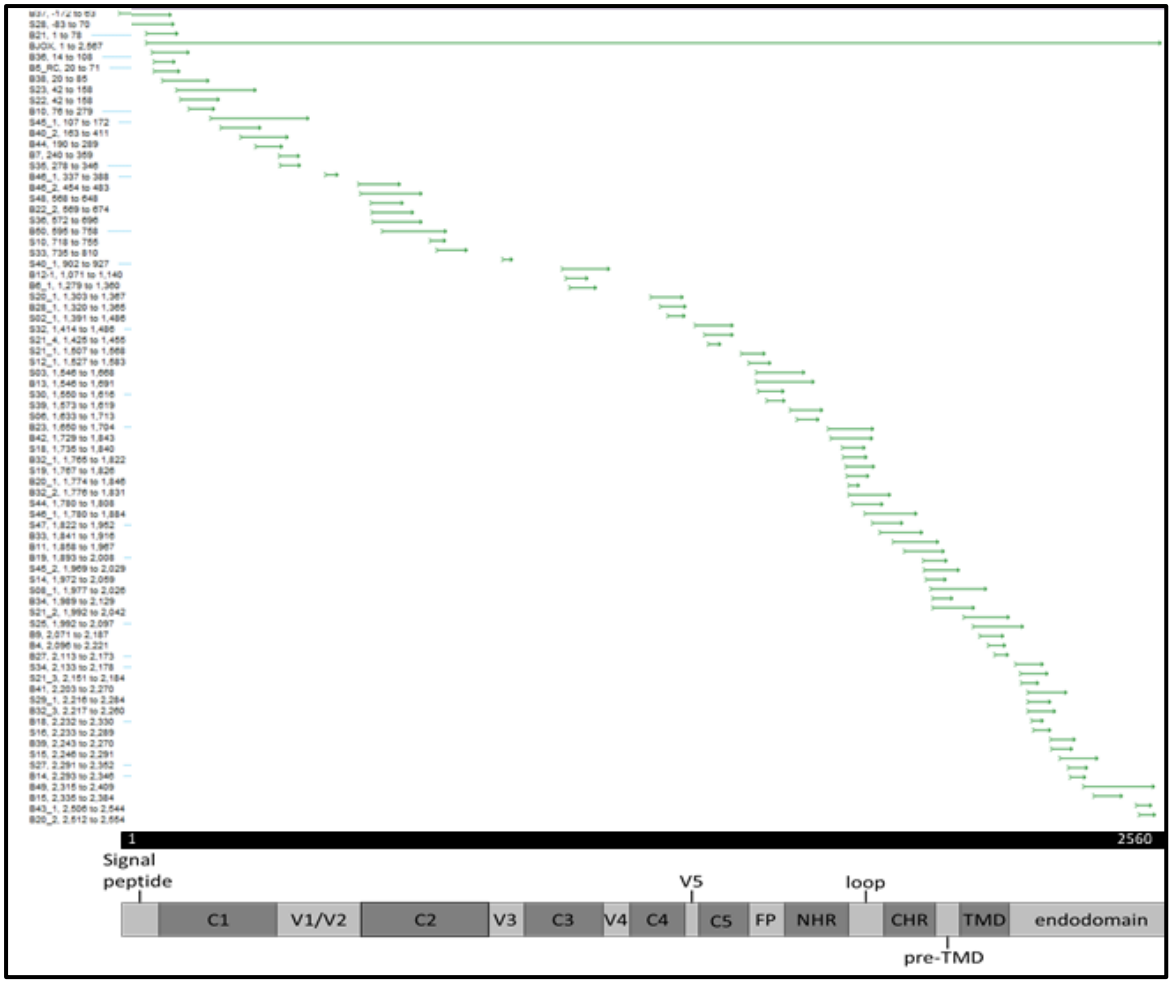


Figure 2.6-6 HIV envelope library coverage

HIV envelope small and large library sequence fragments combined and aligned to HIV envelope parent sequence. 74 out of a possible 96 fragments aligned in total. X axis- HIV envelope sequence 1-2560 base pairs, envelope schematic shown for reference. Y axis shows fragment names. Parent reference sequence BJOX/HXB2 indicated by solid green fragment line at top of figure, length 1 to 2567.Fragment lengths described in base pairs (bp): minimum: 19, maximum: 410, medium: 96, average: 109.7.

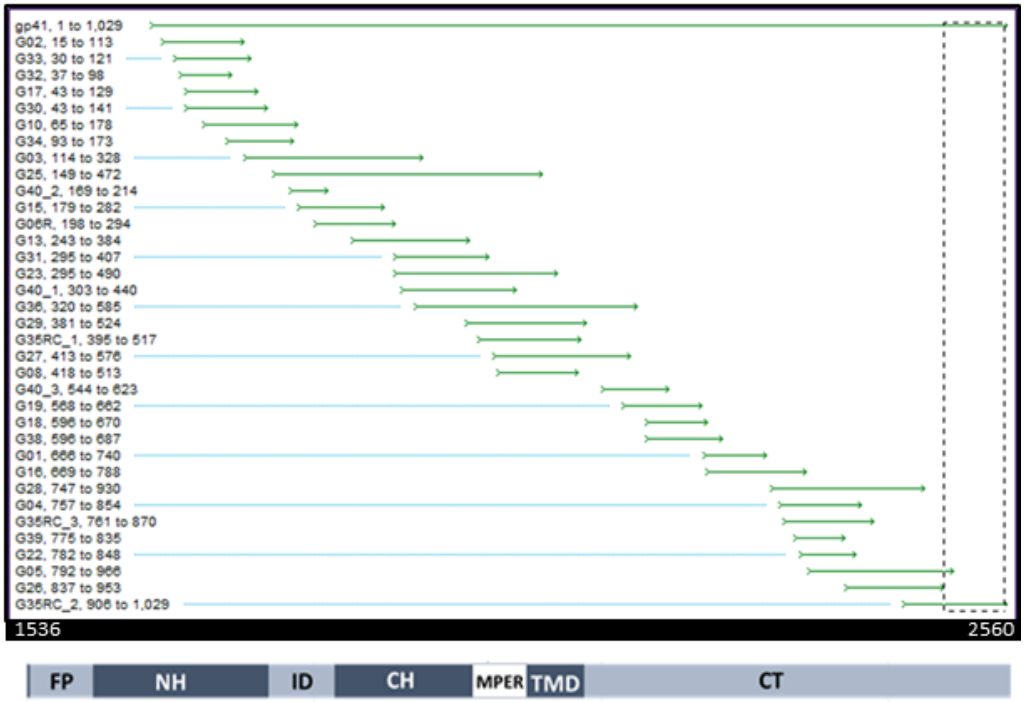


Figure 2.6-7 HIV gp41 small library coverage

HIV gp41 small library sequence fragments aligned to HIV gp41 parent sequence. 35 out of a possible 48 fragments aligned in total. X axis- HIV gp41 sequence 1536-2560 base pairs, gp41 schematic shown for reference. Y axis shows fragment names. Parent reference sequence gp41 portion of HXB2 indicated by first listed fragment- gp41, 1 to 1029. Fragment lengths (bp): minimum: 45, maximum: 323, medium: 94.5, average: 121.1.

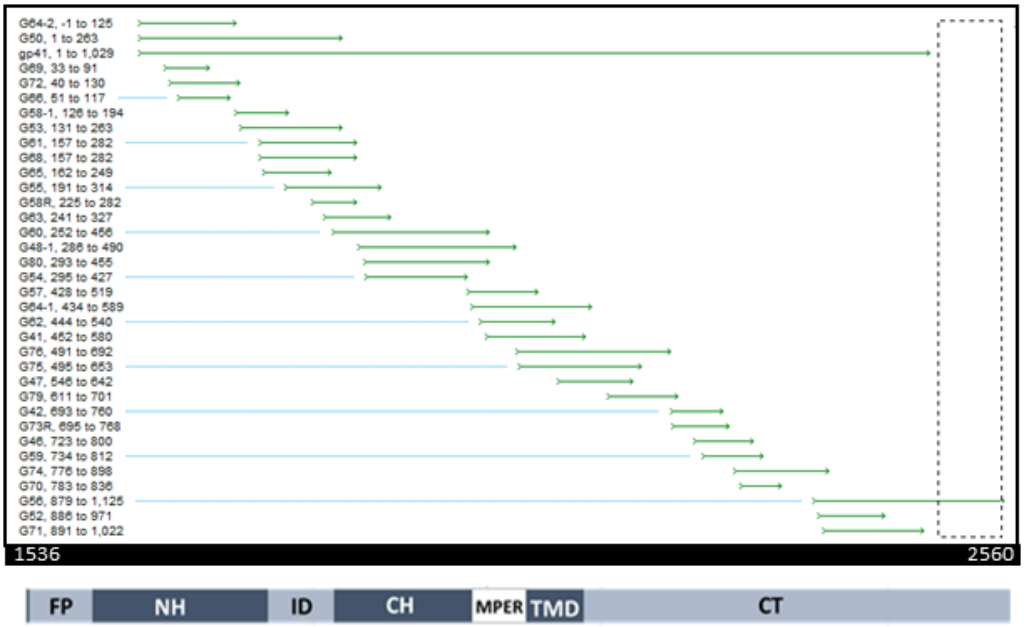


Figure 2.6-8 HIV gp41 big library coverage

HIV gp41 big library sequence fragments aligned to HIV gp41 parent sequence. 34 out of a possible 48 fragments aligned in total. X axis- HIV gp41 sequence 1536-2560 base pairs, gp41 schematic shown for reference. Y axis shows fragment names. Parent reference sequence gp41 portion of HXB2 indicated by first listed fragment- gp41, 1 to 1029. Fragment lengths (bp): minimum: 53, maximum: 262, medium: 122, average: 120.7.

Plasmid extraction was performed on the parent bacterial pellets using a commercial kit (Qiagen Plasmid Midi Kit, Qiagen, UK), purified the products, and measured concentration and amount (Table 2.6-8).

	Volume (µl)	Conc (ng/µl)	Total (ng)
HIV Env small library plasmid	500	962.6	481300
HIV Env big library plasmid	500	1175.7	587850
gp41 small library plasmid	500	856.3	428150
gp41 big library plasmid	500	894.5	447250

Table 2.6-8 Library fragment plasmids
DNA concentrations and amounts of library sequence fragments

2.6.1.11. Yeast preparation

Saccharomyces cerevisiae EBY100 yeast cells (Invitrogen) were retrieved from frozen glycerol stocks. A freshly streaked inoculum was plated onto a yeast extract peptone dextrose (YPD) agar plate and incubated at 30°C for 48 hours. I selected a single colony and placed this in a 1litre conical flask with 50ml of liquid YPD medium and incubated for 12 hours, at 30°C and 30g. The culture was diluted to an optical density at 600nm wavelength (OD600) of 0.4 (liquid YPD medium used for zero reference). A 25ml aliquot of the overnight yeast culture medium mixture was added to 180ml YPD to reach an OD600 of 0.4 and incubated at 30°C and 30g. As yeast doubling time was 90 minutes, the cultures reached an OD600 of 1.6 after three hours.

A 50ml aliquot of the OD600/1.6 yeast culture was decanted into a 50ml centrifuge tube, washed twice with 4°C double distilled water and centrifuged at 2500g for three minutes. The resulting pellet was washed once with 4°C electroporation buffer (EP buffer: 1M sorbitol + 1mM calcium chloride) and centrifuged at 2500g for three minutes. The pellet was resuspended in 20ml of 0.1M lithium acetate (LiAc) and 200µl of 10mM dithiothreitol (DTT) and decanted into a 250ml conical flask and incubated for 30 minutes at 30°C at 30g. The culture was pelleted by centrifugation at 2500g for three minutes, washed twice with 50ml 4°C EP buffer, and resuspended with 250µl of EP on ice in a 1.5ml Eppendorf tube. This provided 1ml of electrocompetent EBY100 cells, corresponding to approximately 1.6x109 cells/ml.

2.6.1.12. Yeast electroporation

The yeast and library products were transformed using electroporation with settings as follows: manual, 2000 volts with a 0.1cm cuvette. A ratio of 1ml of yeast cells to 40µg of library DNA products was used. The reaction components- DNA ligation product, yeast cells and cuvettes- were pre-chilled on ice. Cuvette capacity was 350µl and multiple cuvettes were used per 1ml transformation reaction. The electroporator discharged a pulse duration of approximately 0.4 milliseconds. The post electroporated yeast cells were resuspended in a 1:1 aliquot of 1M sorbitol and YPD medium and incubated at 30°C for 1h without shaking. Following this, 1:100 and 1:1000 dilution preparations of each yeast library culture were prepared. A 150µl aliquot of each dilution was plated onto yeast minimal medium agar plates (SDCAA- dextrose, nitrogen, amino acid with buffer salts) and incubated at 30°C for 48 hours, with colony yields displayed in Table 2.6-9

	No. colonies from 150µl/1000 solution
HIV Env SL dilution plate 1:10000	1600
HIV Env BL dilution plate 1:10000	1550
gp41 SL dilution plate 1:10000	1440
gp41 BL dilution plate 1:10000	1480

Table 2.6-9 Yeast transformation efficacy
Efficacy measured as colonies counted on SDCAA culture plate from 150ul culture solution

2.6.1.13. Yeast library culture and storage

The remainder of the electroporation yeast culture was added to 200ml of SDCAA liquid medium and incubated for 36 hours at 30°C, and 30g. The yeast culture was decanted into 4x50ml tubes and pelleted by centrifugation at 2500g for three minutes and all pellets resuspended together in 40mls of 15% glycerol in SDCAA. Individual aliquots of 1ml yeast library/glycerol/SDCAA were prepared and stored in -80°C for future use.

2.6.1.14. Growth and induction of proteins on yeast cell surface

A scraping from a frozen glycerol yeast aliquot was streaked onto an SDCAA plate and incubated at 30° C for 24-48 hours. A single colony was selected and placed in 5ml of SDCAA liquid medium and incubated at 30°C, 30g for 24-48 hours. The yeast growth was assessed by measurement of the optical density of the culture, using a spectrophotometer to measure light absorbance of 600nm wavelength, referred to as the OD600. The OD600 measurement of the aliquot was used to identify the yeast cells at exponential growth phase, reflected by an OD of 0.5-1.0. The OD600 value also enabled counting of yeast cells present in aliquots, as an OD600 value of 1.0 *Saccharomyces cerevisiae* contains approximately $1x10^7$ cells/ml.

The SDCAA culture optical density was regularly measured during the incubation phase. When the OD600 reached 0.5-1 (measured as a 10-fold dilution), the yeast aliquot was retrieved and centrifuged at 2000g for one minute and the supernatant discarded. The yeast cells were now at exponential growth phase and ready for transfer to SGCAA medium to stimulate expression of the yeast surface display epitope. A 300µl aliquot of SDCAA yeast cell culture was resuspended in 2700 µl liquid SGCAA medium in a flask volume of at least five times that of the solution and incubated at 20°C and 30g for 36hrs. The incubation in SGCAA medium promoted expression of cell surface protein, and the library was ready for use.

2.6.1.15. Single clone sequence analysis of yeast populations

Following flow cytometric sorting of yeast using patient serum, single clone analysis was used to determine the proportion of yeast clones recognised by the patient sera. This process reviewed the "fidelity" of participant serum samples from a representative population of yeast clones from post sort "parent" SDCAA plates.

Sorted yeast cells were captured in liquid SDCAA medium and incubated at 30°C, 30g for 24-48 hours. A 200µl aliquot of medium was plated onto SDCAA plates and incubated at 30°C for 24-48 hours. The resulting growth displayed single colonies. Approximately 10 to 20 of these colonies were transferred to 1ml of SDCAA aliquots in individual wells of a 96-well plate, incubated at 30°C, 30g for 24-48 hours. A 100µl aliquot of each culture was transferred to a 900µl aliquot of SGCAA medium and incubated at 20°C and 30g for 36-48hrs. These individual cultures were analysed using patient sera aliquots to assess the proportion of single clones recognised by patient sera. The yeast cell populations with a high proportion of PE positivity were selected for sequence analysis.

These yeast clones were submitted for sequence analysis to identify recognised epitopes. The DNA extraction from 1ml SDCAA yeast culture aliquots was performed using a commercial kit (YeaStar Genomic DNA Kit, Zymo Research Labs). This DNA was used to transform chemically competent *E. coli* cells (DH5α competent cells). A standard pUC-17 control was used to check efficiency of transformations. A 5µl aliquot of DNA was added to 50µl of cells thawed on wet ice, incubated on wet ice for 30 minutes, heat shocked in a 37-40°C waterbath, and incubated on wet ice for a further two minutes. Following this, a 200µl aliquot of room temperature LB or SOC medium was added and the mixture incubated for one hour at 37°C and 30g to allow expression of the ampicillin resistance phenotype.

The post transformation aliquot was placed on LB with 1% ampicillin agar plates and incubated at 37°C for 12 hours. Transformation was successful when plates grew colonies. An individual colony from each single clone plate was picked using a 10µl pipette tip, added to 2ml of liquid LB-Amp medium in a 15ml culture tube, and incubated for 12 hours at 30°C and 30g. The culture was pelleted at 2500g for 15 minutes and the supernatant poured off to yield a solid pellet which was stored at -20°C. Pellet containers were placed in a sealed container and shipped on dry ice to a sequencing facility (MRC Protein Phosphorylation and Ubiquitylation Unit as previously noted) for plasmid preparation and sequencing analysis. The resulting sequences were accessed at the MRC Protein Phosphorylation and Ubiquitylation Unit's online portal (https://www.dnaseq.co.uk/) as compressed files and analysed using methods previously described.

2.6.1.16. Parent culture sequence analysis

The yeast culture sequences were analysed in a similar fashion; when single clone analysis demonstrated affinity of these yeast clones for patient sera, the sorted population was analysed. The SDCAA liquid culture from sorted yeast was centrifuged as previously described to produce a pellet, the DNA extracted (2.6.1.15) and used to transform chemically competent DH5alpha *E. coli* cells which were then plated onto LB agar. Approximately 30-40 individual colonies were selected, placed in 2ml LB aliquots and incubated overnight at 37°C for 18 hours at 30g. The resulting cultures were pelleted and submitted for sequence analysis.

The yeast parent and single clones which demonstrated affinity for patient serum underwent sequence analysis. The parent yeast family DNA sequences indicated the distribution of serum antibody epitope responses; an overall recognition of gp160 by serum. The single clone sequences identified discrete epitopes of HIV envelope gp160 specifically selected by the patient serum samples and led to development of antibodies targeted against these regions.

2.6.1.17. Algorithm to assess amino acid frequency in obtained DNA sequences

A computational algorithm was used to analyse potential antigenic domains from the sequence fragments. This was first described by Zuo et al (282). Briefly, original fragment sequences were translated into amino acid sequences and aligned to the full-length HIV amino acid sequence. A sliding window of ten amino acids scanned the alignment from N to C terminus. The positive criteria for an antigenic domain was defined as per the following conditions: if the window encountered a fragment sequence containing at least five amino acids, or an amino acid sequence with greater than 50% matching residues compared to the parent sequence, the position of that window was scored based on the number of fragment sequences identified. A window containing the greatest amount of fragment sequences was termed an antigenic domain.

The amino acid frequency was plotted against at each amino acid residue position to yield a histogram (6). The area under the curve (AUC) was calculated for each group of sequences and reflected a quantitative probability of a reactive antigenic region or domain at any part of the reference sequence. The core stretch of amino acid residues at the midpoint of the antigenic domain was referred to as the "major antigenic domain" and was usually 11-29 residues in length.

2.6.2. Preparation of patient samples- plasma and serum

Participants in all cohort groups A-E were requested to donate blood for analysis. This project used samples from groups A, B, and E. Eleven tubes of blood were drawn from each participant at each study visit; two EDTA tubes for blood plasma collection (4ml each, K2-EDTA tubes, BD Vacutainer), two serum tubes for blood serum collection (6ml each, BD Vacutainer™ SST™ II Advance Tubes UK) and seven lithium heparin tubes (6ml, BD VacutainerTM plasma tubes) for peripheral blood mononuclear cell (PBMC) collection. Total blood draw at each study visit was 62 millilitres. Patient samples were transported from the study site to the research laboratory by commercial courier. The EDTA plasma and SST tubes were centrifuged at 1200G for ten minutes and the supernatant plasma and serum harvested from the top layer. Plasma and serum were stored in 1ml cryovials and frozen at -80°C.

2.6.3. Preparation of patient samples - PBMC

Each participant's PBMC preparation was performed in either CL2 or CL3 facility depending on serostatus. All PBMC samples were centrifuged at 500g for ten minutes. At this point, supernatant plasma was drawn from the top layer, placed in 2ml cryovials and stored with the participant's other plasma samples. The remaining cells were then transferred to a 50ml Falcon tube and diluted to a total volume of 50ml with PBS. Two more 50ml tubes containing 15ml of room temperature Histopaque were prepared.

A 25ml aliquot of the PBMC -PBS mixture was carefully layered over each Histopaque layer using a 50ml pipette. The two 50ml Histopaque/PBMC-PBS tubes underwent density gradient centrifugation at 800g for twenty minutes with the braking set to zero. The tubes were retrieved and the PBMC layer carefully aspirated from each using a 20ml pipette. The collected cell layer was placed in a 50ml tube and made up to 50ml with PBS for a wash stage. The tube was centrifuged at 500G for ten minutes with the brake set to nine, producing a cell pellet at the bottom of the tube. The supernatant was poured off and the pellet resuspended in a known volume of PBS for cell counting.

2.6.4. PBMC counting

Cell counting was performed by microscopy using a 3x3 grid haemocytometer. From the resuspended cell pellet, 10ul was added to 10ul of Trypan Blue dye (Sigma Aldrich, UK). This 20ul volume was placed in the haemocytometer and viewed. The total cell number from three squares was counted and used to determine the overall cell number. The formula for cell calculation was as follows: average of the following populations (no. cells in square A, no. cells in square B, no. cells in square C), the average divided by two to account for Trypan Blue dilution, then multiplied by 10,000 to account for cell dilution, resulting in the total number of PBMC in PBS suspension.

2.6.5. PBMC freezing and storage

The PBMCs were stored in cryovials at a cell density of approximately $1x10^6$ cells/ml. This was achieved by centrifuging cells at 500G for ten minutes and resuspending the cell pellet in the desired volume of freezing medium. Freezing medium consisted of 90% FBS and 10% DMSO and was made freshly for each batch of processed PBMCs. The freezing medium was added dropwise to the cell pellet to create a cell concentration of $1x10^6$ cells/ml. These 1ml aliquots of the cell suspension were transferred to cryovials and placed in Mr. Frosty™ freezing containers for a cooling rate of approximately -1°C/minute. The containers were placed in -80°C overnight and transferred to -140°C liquid nitrogen storage the following day.

2.6.6. Tissue bank depository

All plasma, serum and PBMC sample storage location was documented in a central catalogue and updated on each new submission. Any requests to use any of the stored samples was subject to approval by all study leads.

2.6.7. CD20 adsorption of patient serum pools

Prior to analysis with flow cytometry, patient serum sample underwent adsorption with CD20 expressing yeast to remove non-specific anti-yeast antibodies which may have affect downstream yeast-serum antibody binding. The original sequence of the yeast expression vector pCTCON2 contained an irrelevant gene CD20 of approximately 60 amino acids which served the purpose of a negative yeast control to remove non-specific yeast-antibody binding (283). For this project, CD20 was an irrelevant antigen, and were not expected to impact HIV specific antibody binding.

The CD20 yeast cultures were produced in a similar fashion to the yeast library generation. Scrapings of CD20 *Saccharomyces cerevisiae* EBY100 yeast cells (Invitrogen, Carlsbad, CA) were obtained from frozen glycerol stocks, streaked an inoculum onto selective growth yeast medium with dextrose (SDCAA) agar plate and incubated at 30°C for 48 hours. A single colony was selected and placed in 5ml of liquid SDCAA medium and incubated at 30°C, 30g for 24-48 hours. When the OD600 reached 0.5-1.0 (at a 10-fold dilution, liquid SDCAA medium used for zero reference), the culture was centrifuged and resuspended at a 1:10 dilution in liquid selective growth yeast medium and galactose (SGCAA) and incubated at 20°C, 30g for 36hrs.

A 10mls aliquot of SGCAA CD20 culture was used for each adsorption step. Each 10ml SGCAA CD20 aliquot at was centrifuged as previously described to produce a pellet of CD20 cells and washed twice with PBS. The patient sera pools were diluted to 1:100 with PBS to create a 1ml volume aliquot, added to the CD20 pellet and placed in a rotator for two hours at 4°C, and centrifuged as previously described to produce a pellet. The supernatant containing participant pooled sera was removed using a 1000µl pipette tip and added to a second CD20 cell pellet, placed in a rotator for one hour at 4°C, and centrifuged as previously described. This supernatant was collected and stored at -20°C pending further use.

2.6.8. Flow cytometry

2.6.8.1. Preparation of yeast library for use with flow cytometry

The frozen HIV Env gp160 and gp41 yeast library aliquots were thawed at room temperature, washed twice with PBS to remove traces of glycerol, and the resulting pellet placed in 3ml of SDCAA medium in a 15ml culture tube and incubated for 48 hours at 30°C, and 30g. The OD600 was checked and compared to liquid SDCAA or SGCAA (baseline for measurement) to identify the exponential growth phase.

A $1x10^7$ aliquot of induced yeast cells was used for initial analysis using the OD600 value to calculate the volume of culture required. An OD600 of 1 is approximately $1x10^7$ cells/ml. At OD600 of 0.5-1.0 (at a tenfold dilution), a 300µl aliquot of this culture was added to 2700ul of SGCAA induction medium to create a 10-fold dilution and incubated at 20°C and 30g for 36hrs. This step stimulated expression of the Aga-2 linked surface protein (in this case HIV-envelope antigens gp160 and gp41).

The SGCAA culture OD600 was measured to calculate the volume required for $5x10^7$ cells. This volume was washed twice with 4°C PBS and resuspended with 1ml of PBS in a 1.5ml Eppendorf tube in preparation for addition to the patient serum samples.

2.6.8.2. Flow cytometry sample labelling

The primary antibody source was participant serum. For the primary antibody labelling and incubation, a 1000µl aliquot of each serum sample (at a dilution of 1:100 post CD20 adsorption) was added to 1ml/$5x10^7$ washed prepared gp160 yeast library cells and incubated at 4°C for one hour in a rotating rack. This allowed patient antibody to bind yeast-mounted HIV-gp160 epitopes. The samples were then washed twice with 4°C PBS and resuspended in 500µl PBS.

The secondary antibody source was Fc gamma-specific anti-human IgG labelled with R-phycoerythrin (referred to from here onwards as PE, Affymetrix eBiosciences, ThermoFisher). For the secondary incubation, samples were labelled with 0.1µg of PE and incubated at 4°C for 40 minutes in a rotating rack, washed twice with 4°C PBS and resuspended in 1ml of flow buffer (BSA/NaN3/EDTA- see materials and methods) in standard glass flow cytometry tubes.

2.6.8.3. Flow cytometry buffer

A flow cytometry buffer was prepared as follows: -490ml of PBS, ten ml of 1% fetal bovine serum, 0.25 g of NaN3 (sodium azide) and 2ml of 0.5 M ethylenediaminetetraacetic acid (EDTA) at a pH of 8.0, to give 500ml of buffer. This gave a mixture of 2% (vol/vol) FBS, 0.05% (wt/vol) sodium azide (NaN3) and 2mM EDTA in PBS.

2.6.8.4. Yeast library sorted by patient serum flow sorting and enrichment

Approximately $5x10^7$ yeast library cells were prepared for each patient serum sort. The collection tubes for positive sorted yeast cells were prepared with 1ml of SDCAA medium and 1% penicillin/streptomycin solution. Between 50,000-100,000 positive yeast cells were sorted per experiment. Post-sorting, the 1ml cell/SDCAA + penicillin/streptomycin aliquot containing sorted yeast cells was transferred to a 15ml culture tube with 1ml of SDCAA with 1% penstrep solution and incubated for one hour at 30°C and 30g.

After a one-hour post sorting rest period, a 150µl aliquot of each yeast cell culture was plated on solid SDCAA agar and incubated at 30°C for 48-72 hours. These plates were used to identify individual yeast clones. The remainder of the post sort yeast cell culture was left to incubate for 48 hours at 30°C and 30g to promote growth of the sorted yeast cell culture population. A 300µl aliquot of this culture was added to a 10-fold dilution of SGCAA induction medium and incubated for 48 hours at 20°C and 30g. The resulting yeast growth was labelled and submitted for flow analysis, as previously described. This was the standard protocol for each successive round of flow cytometry enrichment.

2.6.8.5. Flow cytometry panel

Primary and secondary antibody staining formed the basis for the flow cytometry work. The flow cytometry panel was set up with the following control samples shown in Table 2.6-10

	Yeast cells	Primary antibody	Secondary Ab
Autofluorescence	Yeast	None	None
Unstained yeast	Yeast	None	PE
Fluorescence minus one	Yeast	Lab/healthy control sera	None
Lab/healthy control	Yeast	Lab/healthy control sera	PE
Positive control	Yeast	Positive control sera	PE
Participant serum	Yeast	Participant serum	PE

Table 2.6-10 Flow cytometry panel setup

Table shows all flow cytometry controls. Three experimental controls (autofluoresence, unstained yeast and fluorescence minus one), biological controls (seronegative "laboratory" control consisting of sera from healthy seronegative low exposure laboratory controls), positive control (serum from known HIV positive individual from Group E) and participant serum sample of interest.

2.6.8.6. Flow cytometry equipment

A BD LSR II was used for initial flow cytometry analysis of seronegative patient samples in a containment level two (CL2) area of the laboratory. All flow cytometry sorting experiments were performed on a FACS Aria III machine housed in a biological safety cabinet within a containment level three (CL3) laboratory. All sorting experiments were done under the supervision of a trained flow cytometry facility manager. All experimental sample flow tubes were stored at 4°C wrapped in foil until use, when they were briefly vortexed and placed in the cell sorter entry port.

2.6.8.7. Flow cytometry gating strategy

The following gating strategy was designed to select and sort a double positive population of yeast cells bound to fluorophore labelled patient antibody. The first three gates are described below in Table 2.6-11 and Figure 2.6-9. Both flow cytometers had FACS DIVA software which was used to harvest data, and files were stored as FSC files and analysed with FlowJo software (FlowJo LLC, version 10.1).

Gate	x axis	y axis	Represents
1	Forward scatter (FSC) area	Side scatter (SSC) area	Yeast cells
2	Forward scatter (FSC) area	Forward scatter (FSC) width/height	Single yeast cells
3	Fluorochrome of interest	Side scatter (SSC) area	PE serum bound to selected yeast clones

Table 2.6-11 Flow cytometry gating strategies
Table shows each gate number, x axis property, y axis property and population gated by this selection.

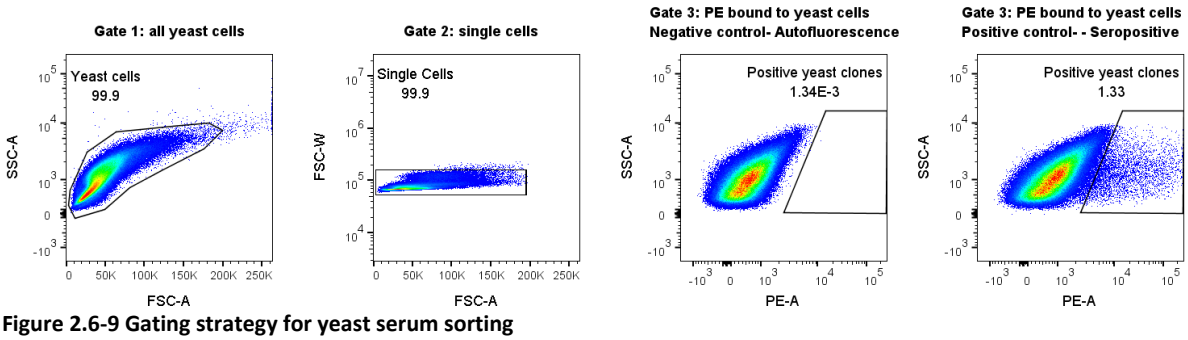


Figure 2.6-9 Gating strategy for yeast serum sorting
Gates 1, 2 and 3. Gate 3 shows populations for a technical negative control (autofluorescence) and a positive control (seropositive) sample

2.6.9. Monoclonal antibody work

2.6.9.1. Introduction

This section describes the process used to extract B cells of interest and produce monoclonal antibodies to explore properties and function.

2.6.9.2. Identification of B-cell repertoire

A category level three (CL3) fluorescence assisted cell sorter (FACS Aria III) was used to identify and select anti gp41/120 antibody secreting memory B cells (CD3-CD19+). Our department has a category three cell sorter, and the expertise of a senior flow cytometry manager. Fluorochrome Pacific Blue (BV421) was added to yeast clones bearing known epitopes to create HIV envelope fragment baits. As patient serum samples selected yeast clones of interest, the B cells which produced the antibodies would bear B cell receptors autologous to the paratope which retrieved the original yeast clone. These B cell surface receptors would have affinity for the surface bound epitopes subsequently and form an antigen-antibody bond. The anti-human CD19 antibody fluorochrome allophycocyanin (APC, Thermo Fisher Scientific UK) was selected to identify B cell population.

The double positive Pacific Blue/APC population represented yeast cell/B cell doublets. This double positive population was sorted into appropriate medium, lysed, and subjected to PCR amplification and next generation sequencing for isolation of variable region immunoglobulin (Ig) heavy- and light-chain genes (VH, VK/L). These insert sequences were used to transfect candidate cell lines and produce monoclonal antibodies.

The antibody structural and functional properties of pre HIV infection envelope specific memory B cells were analysed, with and clonal lineage members identified, supporting the hypothesis of evolution of an anti-gp41 response from the pre-existing B cell pool.

2.6.10. Protocol for yeast antigen baiting

2.6.10.1. Selection of samples

Work from the chapter describing seroconverter responses informed the selection of samples for this part of the project. The aim was to analyse seronegative antibody responses to HIV envelope epitopes, particularly gp41. As will become apparent, participant B003 displayed pre-infection serum affinity for HIV gp41 epitopes and was selected for B cell baiting work.

2.6.10.2. Preparation of specific yeast clones

The yeast clones were selected based on affinity for patient serum- those with greatest affinity were stored as frozen glycerol stocks and retrieved when required. From experiment results, yeast clones were identified by B003 pre infection samples. A scraping from a frozen yeast clone glycerol stock aliquot was streaked onto an SDCAA culture plate, incubated at 30°C for 24-48 hours to produce single colonies. One single colony was placed in liquid SDCAA medium, incubated at 30°C, 30g for 24-48 hours to stimulate growth. The exponential growth phase was identified using an OD600 reading of 0.5-1 and removed from incubation. A 5ml aliquot of this culture was transferred to a 45ml aliquot of SGCAA medium and incubated at 20°C and 225rpm for 36-48hrs to stimulate expression of membrane bound epitope. This culture was pelleted at 2000g for one minute and the OD600 measured to determine cell number in preparation for yeast cell dyeing. Approximately $20x10^6$ yeast cells in 1ml were prepared for each experiment.

2.6.10.3. Selection of yeast dye

There were two dyes considered for yeast dyeing- eFluor450 (Pacific Blue, ThermoFisher UK) with emission wavelength of 450 nm, and allophycocyanin (APC, ThermoFisher Scientific) with emission wavelength of 670nm. These were analysed in the presence of PBMC cell surface markers; as APC CD19 was used as a PBMC cell surface marker, Pacific Blue was selected for yeast dyeing to avoid spectral overlap.

2.6.10.4. Pacific Blue yeast (Y450) preparation

The dyed yeast cells were prepared to allow for sorting a double positive population when combined with stained PBMCs. A 20uM (2x) Pacific Blue staining solution aliquot was made by adding 2µl 10mM stock to 998µl of PBS and added to 1ml of cells at a concentration of $20x10^6$ cells/ml, to make a final concentration of $10x10^6$ dyed yeast cells/ml. The solution was then mixed well and placed in a 12ml tube, wrapped in foil and incubated at 37°C for ten mins.

Meanwhile, the following was prepared: an ice container, 10% FBS solution (10% FBS + 90% PBS). Following the initial yeast/dye incubation, dye labelling was terminated by adding 2mls of cold neat serum per 20M cells and incubated on ice for five minutes before centrifuging at 1000g for three minutes. All medium was aspirated with a pipette tip and yeast cells resuspended in 4-5 times the original solution volume with 10% FBS. This process was repeated twice, and the final yeast cell pellet resuspended in 1ml PBS, foil wrapped, and stored at 4°C. The solution was washed with PBS prior to use in subsequent assays.

2.6.10.5. PBMC isolation

PBMC harvest and isolation was performed as previously described. Cells were stored in recorded aliquots of $1x10^6$ cells/ml in a central liquid nitrogen repository, and retrieved on dry ice, thawed in a 37°C waterbath, with gentle shaking to encourage transition until a few ice crystals remained visible. Cold RPMI medium was added dropwise to thawed vials and gently aspirated to retrieve cells. The cell solution was placed in a 15ml tube and made up to a total volume of 12ml with R10 solution (500ml RPMI medium supplemented with: 55ml of foetal bovine serum (10%), 5ml penicillin-streptomycin (1%, 10,000 IU penicillin and 10mg/ml streptomycin solution), 5ml L-glutamine (1% 200mM solution) and 5ml 4-2-hydroxyethyl-1-piperazineethanesulfonic acid (HEPES, Sigma Aldrich UK) buffer). This mixture was centrifuged at 300g for eight mins. The supernatant was poured off and cells resuspended in 5ml R10 medium. A 10µl aliquot was then mixed with Trypan Blue for cell counting using a haemocytometer and microscope as previously described. Cells were washed with R10 medium and the cell pellet resuspended as 1 million cells/ml.

2.6.10.6. PBMC staining

Cells were prepared for staining as follows: control and experimental aliquots of cells with $0.5x10^6$ and $0.5x10^6$ cells respectively. Fluorescence activated cell sorting (FACS) buffer was prepared with 2.5% FBS and 97.5% PBS. Cells were placed in prelabelled 5ml standard glass flow cytometry tubes. and washed with FACS buffer, centrifuged at 300g for five minutes, supernatant removed, and cells resuspended by gentle flicking. PBMCs were stained with cell surface markers in the quantities specified (Table 2.6-12):

Marker	Stain	Fluorochrome	Quantity per million PBMC (µl)
CD3	FITC	V500	1.25
CD14	FITC	V500	1.25
CD16	FITC	V500	1.25
CD19	BV421	BV650	2.5

Table 2.6-12 PBMC cell surface markers
Markers with stain name, fluorochrome and volume

A master mix of dyes was prepared to facilitate bulk labelling of cells. This included all cell surface markers multiplied by n+1 (where n = number of cell aliquots in use per experiment) to allow for pipetting errors. The cells were subjected to the following conditions. FACS tubes were vortexed and incubated at 4°C in the dark for 20 minutes, washed with 1ml sterile PBS, centrifuged at 300g for five mins, supernatant poured off and re-suspended in 1500µl FACS buffer. This mixture was stored in the fridge until next step.

2.6.10.7. PBMC plus yeast

The stained PBMCs were mixed with stained yeast cells, wrapped in foil and incubated at 4°C for 40 minutes, washed twice with PBS and resuspended in FACS buffer, passed through a mesh strainer cap to reduce cell clumping and placed in a FACS tube in preparation for sorting. Table 2.6-13 shows the controls and experimental samples used in each experiment.

Name in experiment	Components	Purpose
PBMC alone	PBMC with no surface markers	Identify unstained PBMC
USY	Unstained yeast	Identify unstained yeast
450Y	Yeast stained with dye	Identify stained yeast
USY + Y450	Unstained and stained yeast	Delineates between stained and unstained yeast populations
USY + SM	Unstained yeast with all lymphocyte cell surface markers	To assess for non-specific binding of cell surface markers to unstained yeast
450Y + SM	Stained yeast with all lymphocyte cell surface markers	To assess for non-specific binding of cell surface markers to stained yeast
PBMC + CD19 APC	PBMC with CD19 B cell surface marker	Identifies B cell PBMC
PBMC + CD3/14/16 FITC	PBMC with CD3/14/16 surface markers	Identifies non-B cell PBMC
PBMC + all markers	PBMC with all lymphocyte cell surface markers	Identifies non-specific cell surface marker binding to PBMC
PBMC + USY	PBMC with all lymphocyte cell surface markers and unstained yeast	Non-specific yeast binding
PBMC + 450Y	PBMC with all lymphocyte cell surface markers and stained yeast	Specific B cell surface receptor bound to epitope of interest on the yeast membrane

Table 2.6-13 Flow sorting experiment samples
All controls and samples listed in table. Name of sample (control or experimental), components therein, and population and purpose served by each sample

2.6.10.8. Fluorescence Activated Cell sorting of yeast and PBMC cells

All sorting was performed in a containment level three laboratory (CL3) with a trained FACS operator, using the BD FACS Aria III sorter. Prior to all sorting sessions, the machine was calibrated as per standard protocol and voltages checked for each population. Approximately 50,000 cells were sorted per experiment.

The purpose of sorting was to end up with one cell/yeast dyad in each well of a 96-well plate. By using the index sorting feature of the FACS device, it was possible to trace the origin of each cell that is sorted into each well. Downstream PCR processing also revealed success of single cell sorting, where each PCR readout should only contain either a kappa or a lambda chain.

2.6.10.9. Gating strategy

The gating strategy was selected to identify the double positive population of interest, informed by work carried out on yeast cell sorting. The gates, axes and populations of interest along with a diagram of the gates is shown in Table 2.6-14 and Figure 2.6-10

Gate	x-axis	y-axis	Population of interest
1	Forward scatter area (FSC-A)	Side scatter area (SSC-A)	Lymphocytes and yeast cells
2	Forward scatter area (FSC-A)	Forward scatter height (FSC-W)	Single events
3	FITC (CD 3/14/16)	Side scatter area (SSC-A)	FITC low (CD19 cells)
4	APC	Pacific Blue	Double positive APC/Pacific Blue (CD19/yeast)

Table 2.6-14 Gating strategy for yeast sorting of B cells
All gates 1,2,3 and axes displayed along with population identified by gate.

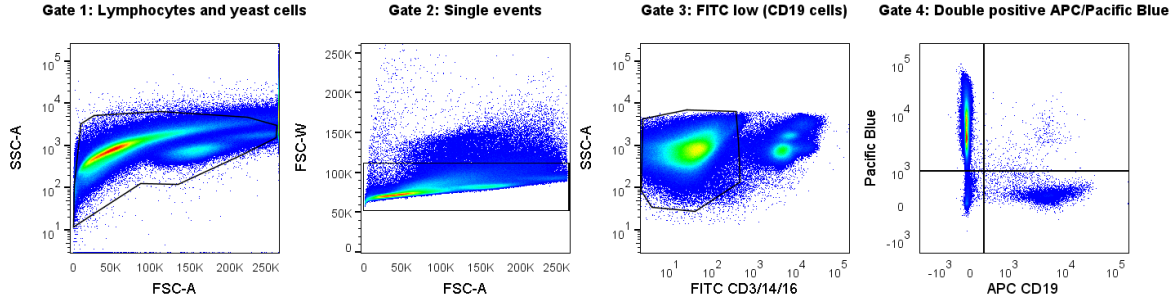


Figure 2.6-10 Gating strategy for B cell baiting using yeast library
Gates 1 lymphocytes and yeast cells, 2 single events, 3 FITC low (CD19 cells), 4 double positive APC/Pacific Blue (CD19/yeast)

2.6.10.10. Bulk sorting

A selection of wells of the sort plate were used to assess efficacy of "bulk sorting". This was suggested by the laboratory sorting supervisor to increase yield from sorting and decrease sorting time. A large APC high (the CD19 marker of interest) population was sorted into a collection tube. This tube's contents were subsequently sorted to select the APC high/Pacific Blue high population from the initial sort population. However, the subsequent cultures of these five samples became contaminated more easily despite the presence of penicillin/streptomycin in the SDCAA culture. Following discussion with the laboratory sorting supervisor, this extra step was considered unnecessary and future bulk sorting was abandoned.

2.6.10.11. Post sort procedure

The double positive sorted population was sorted onto 9six-well trays. Single cells were sorted into 96-well PCR plates containing 10µl of RNase-inhibiting RT-PCR catch buffer. The catch buffer was a hypertonic solution which causes immediate cell lysis in preparation for freezing at -80°C. The buffer was composed of RNase-free water (9.6 µl), 1M Tris pH 8.0 (0.09 µl) and RNase OUT (0.24 µl) per well and was made up in bulk for each plate. The first seven rows of each plate (A-G) were reserved for experimental samples, and row H contained catch buffer only to allow for subsequent PCR negative controls.

Following buffer placement, the plates were centrifuged at 120g for one minute and frozen until required. For sorting, plates were retrieved from cold storage and immediately placed into the sort chamber. Following sorting, plates were immediately sealed with foil, centrifuged at 120g for one minute, placed in a plastic bag and labelled. The plates were kept on dry ice until transferred to a-80°C freezer.

2.6.10.12. Schematic of process

Figure 2.6-11 outlines the components of B cell baiting and how they relate to each other.

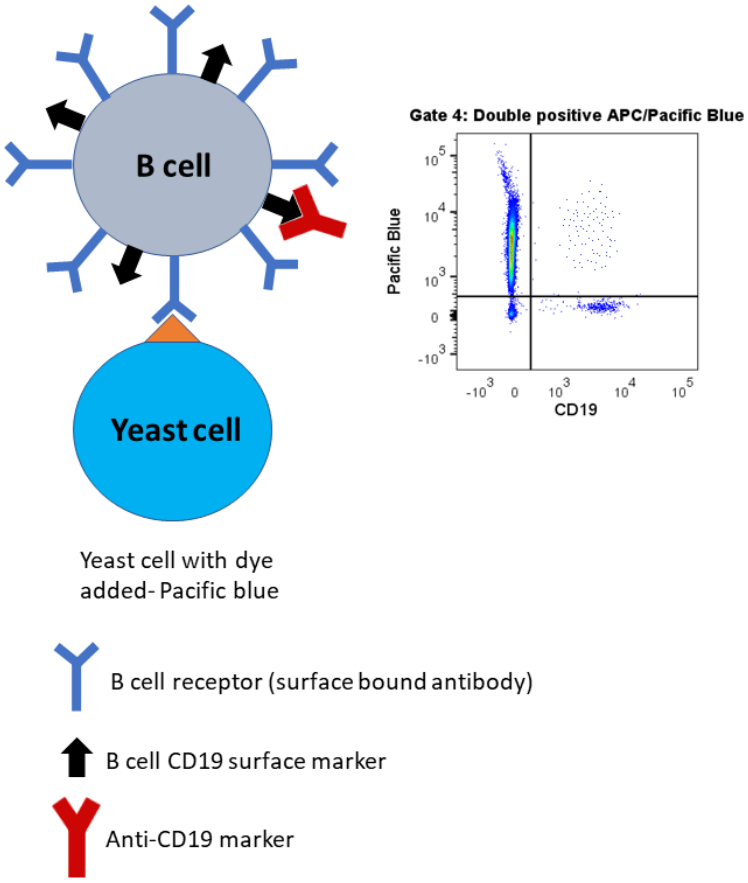


Figure 2.6-11 Yeast B cell baiting schematic

PBMCs bearing cell surface markers, CD19 bind Pacific Blue dyed yeast clones bearing epitopes of interest. The double positive CD19/Pacific Blue population is selected using FACS and sorted for further analysis.

2.6.11. Monoclonal antibody production

The aim of this work was to extract B cell heavy and light chain DNA sequences and transfer to competent cell lines for large volume production and was based on a published protocol where antibodies specific to a vaccinating antigen were produced in a four-week period (284)

Briefly, sequences were extracted from sorted B cell population and amplified by PCR. The sequences were ligated to expression vectors containing constant region sequences and used to transform chemically competent cells, colonies harvested and incubated to produce large volume cultures and DNA purified. Verified heavy and light chain pairs were then used to transfect a HEK293 cell line. The cell line was cultured over one week to produce an antibody-rich supernatant which was harvested, and antibodies purified for use. The steps are described below in detail.

2.6.11.1. Single cell reverse transcriptase polymerase chain reaction (RT-PCR).

RT-PCR was used to extract sequences from the sorted B cells. All PCR work was carried out in a designated PCR safety cabinet within a CL2 laboratory. The 96-well sorted plates were retrieved from -80°C and thawed at room temperature before undergoing a brief centrifugation at 120g for one minute to ensure all well contents were at the well base. The wells contained lysed PBMC and yeast cells and the purpose of this stage was to amplify any heavy or light chain DNA sequences therein.

A commercial One-Step RT PCR kit (Qiagen) which contained enzyme, kit buffer, deoxynucleoside triphosphates (dNTP) and sterile water was used to create a master mix containing sixteen 5’ prime and four 3’ primers using the specific primers as previously published (284–286) and gently vortexed before use. All primers are listed in Figure 2.6-12. The primer cocktail was designed to account for variations in B cell chain sequence. All primers were manufactured to order (Oligo Design Tools, Thermo Fisher Scientific UK) and were made up to 10µM stock solutions.

Name (5 prime)	Sequence 5' - 3'
5' L VH1	ACAGGTGCCCACTCCCAGGTGCAG
5' L VH2	GACCATCCCTTCATCAGATCACC
5' L VH3	AAGGTGTCCAGTGTGARGTGCAG
5' L VH4/6	CCCAGATGGGTCCTGTCCCAGGTGCAG
5' L VH5	CAAGGAGTCTGTTCCGAGGTGCAG
5' L VH7	GGCAGCAGCAACAGCAGGTGCAGC
5' L VK1/2	ATGAGGSTCCCYGCTCAGCTGCTGG
5' L VK3	CTCTTCCTCCTGCTACTCTGGCTCCCAG
5' L VK4	ATTTCTCTGTTGCTCTGGATCTCTG
5' L Vλ1	GGTCCTGGGCCCAGTCTGTGCTG
5' L Vλ2	GGTCCTGGGCCCAGTCTGCCCTG
5' L Vλ3	GCTCTGTGACCTCCTATGAGCTG
5' L Vλ4/5	GGTCTCTCTCSCAGCYTGTGCTG
5' L Vλ6	GTTCTTGGGCCAATTTTATGCTG
5' L Vλ7	GGTCCAATTCYCAGGCTGTGGTG
5' L Vλ8	GAGTGGATTCTCAGACTGTGGTG
Name (3’ prime)	
3' Cγ CH1	GGAAGGTGTGCACGCCGCTGGTC
3’ Cμ CH1	GGGAATTCTCACAGGAGACGA
3' CK 543	GTTTCTCGTAGTCTGCTTTGCTCA
3' Cλ	CACCAGTGTGGCCTTGTTGGCTTG

Figure 2.6-12 Reverse transcriptase PCR primers
Primers as referenced in main body of text

All reagents were thawed at room temperature prior to use and made up into a master mix according to the number of wells undergoing RT-PCR. The plate foil lid was carefully removed, and reagents added to each well before each was sealed with a dome cap (Table 2.6-15). The plate was placed on a PCR thermal cycler and the following cycle was used: 30 minutes at 50°C, 15 minutes at 95°C and 50 cycles of the following: 30 seconds at 94°C, 30 seconds at 58°C and one minute at 72°C. The reaction was then heated to 72°C for ten minutes to complete before being stored at 4°C. The 96-well plate was centrifuged at 120g for one minute to settle all contents to the base of the well and the plate frozen at -20°C until the next step.

Reagent	**Per well (µl)**	**Per plate (µl)**
Forward Primer	0.5	50
Reverse Primer	0.5	50
dNTPs	0.5	50
5x buffer	5	500
HotStarTaq enzyme	0.5	50
Nuclease free H2O	8	800
Total volume per well	15	1500

Table 2.6-15 Reagents and volumes for RT-PCR reaction
All components listed placed in master mix

2.6.11.2. Nested PCR of kappa chains

The kappa RT-PCR product underwent nested PCR to amplify DNA prior to sequencing. The primer sequences are listed below in Table 2.6-16. Kappa sequencing was necessary to select gene family specific primers for subsequent cloning PCR. These two primers are designed to span the whole variable region, with 5’ Pan VK forward primer recognising a sequence at the start of the variable region and 3’ CK reverse primer recognising a sequence at the start of the constant region

Name	**Sequence 5' - 3'**	**Translation**
5' Pan VK	ATGACCCAGWCTCCABYCWCCCTG	MTQXPXXL
3' CK 494	GTGCTGTCCTTGCTGTCCTGCTC	EQDSKDS

Table 2.6-16 Nested kappa PCR primers
Primers as described in literature referenced

The following reaction volumes were scaled up according to the volume desired (Table 2.6-17). The work was performed in a designated CL2 PCR workspace with 1st round PCR product added last and centrifuged briefly. The 96-well plate was placed onto a thermal cycler this program was used: 30 minutes at 50°C, 15 minutes at 95°C and 50 cycles of the following: 30 seconds at 94°C, 30 seconds at 58°C and 45 seconds at 72°C. The reaction was then heated to 72°C for ten minutes to complete before being stored at 4°C. The 96-well plate was centrifuged at 120g for one minute to settle all contents to the base of the well and stored at -20°C until the next step.

Reagent	**Per well (µl)**	**Per plate (100)**
Forward Primer	0.5	50
Reverse Primer	0.5	50
dNTPs	0.5	50
10x buffer	2.5	250
HotStarTaq enz	0.125	12.5
Nuclease free H2O	18.875	1888
1st round PCR product	2	
Total	25	23µl reagents per well

Table 2.6-17 Nested kappa chain variable region PCR
Reaction volumes for all components listed.

2.6.11.3. TBE gel electrophoresis

The efficacy of the RT-PCR and nested kappa PCR stages was assessed with Tris/Borate/EDTA (TBE) gel electrophoresis to review all products. A 1X working stock solution of TBE was prepared from 100ml 10X TBE (Sigma Aldrich) and 900ml of distilled water. A 1g amount of agarose was added per 100ml of TBE and microwaved for three minutes at full power until dissolved, creating a 1% TBE gel solution. Once cooled, SYBR Safe DNA gel stain was added to the solution to give a final concentration of 1:10000 (25µl per 250ml).

The gel wells were created by inserting combs into the liquid TBE/agarose which was then cooled until solid. The gel rig was then filled with 1X TBE solution to the maximum fill level and the gel was ready to use. A 100bp reference DNA ladder was loaded into the first well to identify fragments. A 5 µl aliquot of each reaction product was added to 1µl of 6X loading buffer and then loaded into the preformed gel wells and the sample loading pattern documented.

A 12-channel multichannel pipette was used to load product onto the gel. To account for inequality between pipette channel and TBW gel well distribution, a sample key was designed to locate the correct products. The TBE/agarose gel and samples ran at a rate of at 120 volts for 30 mins using a BioRad powerpack. The final gel was viewed using a UV lightbox while wearing all necessary personal protective equipment and eyewear and gel images digitally captured using the Gel Doc XR+ imager system. Bands present at the following locations were consistent with useful PCR product- heavy (380bp), lambda (405bp) and kappa (540bp). Any positive band results indicated the presence of useable PCR product and the corresponding plate well was purified. Figure 2.6-13 shows the TBE gels and bands present.

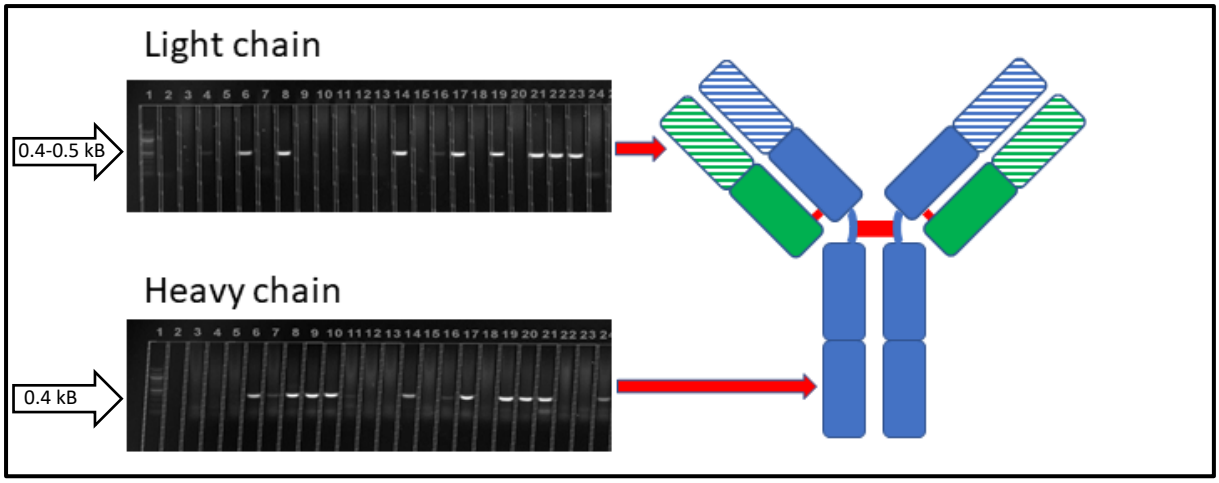


Figure 2.6-13 TBE gel electrophoresis of RT-PCR sorted chain inserts

Chain inserts include heavy and light chain (either kappa or lambda) inserts. A DNA reference ladder of 1KB was used to gauge the PCR products. Bands present at the correct position according to the DNA reference ladder (bp = base pairs) indicated success of the sorting and RT-PCR stages (heavy bands at 380bp, lambda bands at 405bp, and kappa bands at 540bp).

2.6.11.4. Cloning PCR of heavy and light (lambda and kappa) chains

To use the correct primers for kappa chain cloning, chain insert PCR products were sent to an external laboratory for sequencing (Genewiz UK Ltd). The primer Ck 493-516 was used for all sequencing reactions. The sequencing results, were analysed using BioEdit and uploaded to the online database of the international ImMunoGeneTics information system® (IMGT® http://www.imgt.org/IMGT_vquest/vquest?livret=0&Option=humanIg) which holds a database of antibody sequences, allowing users to determine primers for kappa gene family cloning PCR.

The cloning PCR reactions were performed on three separate 96-well plates to allow for consistency in tracking results. One heavy, one lambda and one kappa plate were organised per original RT-PCR plate. This step was to allow for the insertion of restriction sites. An AgeI restriction site was placed at the 5' end of each chain sequence. The 3' ends had the following restriction sites attached: SalI (heavy), XhoI (lambda) and BsiWi (kappa). These sites facilitated digestion and insertion into the relevant vectors.

Master mixes were created for each chain family using the primers listed in Table 2.6-18Table 2.6-19Table 2.6-20.Each master mix facilitated bulk loading onto each plate using multichannel pipettes. The first round PCR products (heavy, lambda, nested kappa) were added to plates last and mixed briefly before placing onto the PCR thermal cycler and the following program used: 15 minutes at 95°C and 50 cycles of the following: 30 seconds at 94°C, 30 seconds at 58°C and 45 seconds at 72°C. The reaction was heated to 72°C for ten minutes before being stored at 4°C. Each plate was centrifuged, and products were applied onto 1% TBE gel to check for the presence of bands at the relevant positions (heavy at 380bp, lambda at 405bp and kappa at 540bp).

2.6.11.5. Cloning chain primers

Direction	Name	Sequence 5' - 3'
Forward primer	5' AgeI VH1/5	CTGCAACCGGTGTACATTCCGAGGTGCAGCTGGTGCAG
	5' AgeI VH3	CTGCAACCGGTGTACATTCTGAGGTGCAGCTGGTGGAG
	5' AgeI VH4	CTGCAACCGGTGTACATTCCCAGGTGCAGCTGCAGGAG
	5' AgeI VH3-23	CTGCAACCGGTGTACATTCTGAGGTGCAGCTGTTGGAG
	5' AgeI VH4-34	CTGCAACCGGTGTACATTCCCAGGTGCAGCTACAGCAGTG
	5' AgeI VH 1–18	CTGCAACCGGTGTACATTCCCAGGTTCAGCTGGTGCAG
	5' AgeI VH 1–24	CTGCAACCGGTGTACATTCCCAGGTCCAGCTGGTACAG
	5' AgeI VH 3–9/30/33	CTGCAACCGGTGTACATTCTGAAGTGCAGCTGGTGGAG
	5' AgeI VH 6–1	CTGCAACCGGTGTACATTCCCAGGTACAGCTGCAGCAG
	5′ AgeI VH4–39	CTGCAACCGGTGTACATTCCCAGCTGCAGCTGCAGGAG
	5′ AgeI VH1	CTGCAACCGGTGTACATTCCCAGGTGCAGCTGGTGCAG
	5′ AgeI VH3–33	CTGCAACCGGTGTACATTCTCAGGTGCAGCTGGTGGAG
Reverse primer	3' SalI JH1/2/4/5	TGCGAAGTCGACGCTGAGGAGACGGTGACCAG
	3' SalI JH3	TGCGAAGTCGACGCTGAAGAGACGGTGACCATTG
	3' SalI JH6	TGCGAAGTCGACGCTGAGGAGACGGTGACCGTG

Table 2.6-18 Heavy chain cloning PCR primers

Direction	Name	Sequence 5' - 3'
Forward primer	5' AgeI Vλ1	CTGCTACCGGTTCCTGGGCCCAGTCTGTGCTGACKCAG
	5' AgeI Vλ2	CTGCTACCGGTTCCTGGGCCCAGTCTGCCCTGACTCAG
	5' AgeI Vλ3	CTGCTACCGGTTCTGTGACCTCCTATGAGCTGACWCAG
	5' AgeI Vλ4/5	CTGCTACCGGTTCTCTCTCSCAGCYTGTGCTGACTCA
	5' AgeI Vλ6	CTGCTACCGGTTCTTGGGCCAATTTTATGCTGACTCAG
	5' AgeI Vλ7/8	CTGCTACCGGTTCCAATTCYCAGRCTGTGGTGACYCAG
Reverse primer	3' XhoI Cλ	CTCCTCACTCGAGGGYGGGAACAGAGTG

Table 2.6-19 Lambda chain cloning PCR primers

Direction	Name	Sequence 5' - 3'
Forward primer	5' AgeI VK1-5	CTGCAACCGGTGTACATTCTGACATCCAGATGACCCAGTC
	5' AgeI VK1-9	TTGTGCTGCAACCGGTGTACATTCAGACATCCAGTTGACCCAGTCT
	5' AgeI VK1D-43	CTGCAACCGGTGTACATTGTGCCATCCGGATGACCCAGTC
	5' AgeI VK2-24	CTGCAACCGGTGTACATGGGGATATTGTGATGACCCAGAC
	5' AgeI VK2-28	CTGCAACCGGTGTACATGGGGATATTGTGATGACTCAGTC
	5' AgeI VK3-11	TTGTGCTGCAACCGGTGTACATTCAGAAATTGTGTTGACACAGTC
	5' AgeI VK3-15	CTGCAACCGGTGTACATTCAGAAATAGTGATGACGCAGTC
	5' AgeI VK3-20	TTGTGCTGCAACCGGTGTACATTCAGAAATTGTGTTGACGCAGTCT
	5' AgeI VK4-1	CTGCAACCGGTGTACATTCGGACATCGTGATGACCCAGTC
Reverse primer	3' BsiWI JK1/2/4	GCCACCGTACGTTTGATYTCCACCTTGGTC
	3' BsiWI JK3	GCCACCGTACGTTTGATATCCACTTTGGTC
	3' BsiWI JK5	GCCACCGTACGTTTAATCTCCAGTCGTGTC

Table 2.6-20 Kappa chain cloning PCR primers

2.6.11.6. PCR purification

When bands had confirmed presence of respective cloned PCR product, positive wells were purified using QIAquick PCR Purification kit to yield 20µl of DNA product. The kit reagents were added to PCR products and loaded onto specialised filter columns, placed columns in a table-top vacuum manifold to draw off buffers and then transferred to collection vials and elution buffer added. The final product concentrations were measured using the Nanodrop system and stored products at -20°C until the next stage.

2.6.11.7. Vector preparation and digestion

The individual vectors were prepared according to heavy, lambda or kappa chain type using cultures from frozen glycerol aliquots as previously described for standard bacterial culture, and pellets processed by miniprep. Vector restriction sites corresponded to those carried by heavy/lambda/kappa chain inserts. Vectors were digested to open these sites in preparation for ligation of chain inserts. The kappa vector required two rounds of digestion with the first-round product purified prior to use. Table 2.6-21 below shows the reagents and volumes used. The reaction vessels were placed on the thermal cycler for one hour at 37°C, and then heated to 65°C for 15 minutes to inactivate the enzymes. A 1% TBE gel tray was prepared with a 9-tooth comb to allow wider channels for the vector loading. A 1KB DNA ladder was used as reference, and the gel run at 120V for 30-90 minutes using a powerpack. Vectors were identified by the presence of a band at the 5.2Kb ladder rung and the gel placed on a UV lightbox to identify successfully digested vectors.

	Heavy	**Lambda**	**Kappa 1**	**Kappa 2**
DNA	10ug	10ug	10ug	Kappa 1 (30µl)
AgeI-HF	1µl	1µl	1µl	-
SalI-HF	5µl	-	-	-
XhoI	-	1.5µl	-	-
BsiWi	-	-	-	0.5µl
BsiWi	-	-	-	0.5µl
Nuclease Free H20	Up to 100µl	Up to 100µl	Up to 1000µl	Up to 100µl
TOTAL	100µl	100µl	100µl	100µl

Table 2.6-21 Vector digestion components

2.6.11.8. Variable chain insert digestion

The purified PCR products were digested with the same enzymes used for vector digestion. The digestion was performed from 8-12 hours for optimal results. The kappa chain inserts underwent two rounds of digestion. A master mix of the reagents was prepared as per Table 2.6-22 and briefly vortexed before the addition of enzyme. The digestion was performed at 37°C, and the second kappa digestion at 55°C. A 1% TBE gel tray was prepared with the narrow comb to allow for sample loading using a multichannel pipette. A 100bp ladder was used as reference and the gel run at 120V for 30-60 minutes. The gel was placed on a UV the lightbox to identify the digested chain insert regions, and a digital image captured as previously.

	Heavy	**Lambda**	**Kappa 1**	**Kappa 2**
DNA	10ug	10ug	10ug	Kappa 1 (30µl)
AgeI-HF	1µl	1µl	1µl	-
SalI-HF	5µl	-	-	-
XhoI	-	1.5µl	-	-
BsiWi	-	-	-	0.5µl
BsiWi	-	-	-	0.5µl
Nuclease Free H20	Up to 100µl	Up to 100µl	Up to 1000µl	Up to 100µl
TOTAL	100µl	100µl	100µl	100µl

Table 2.6-22 Variable chain insert digestion product concentration
Components including enzymes vary according to chain insert

2.6.11.9. Digested vector and variable chain insert purification

The gels were placed on a UV lightbox, relevant bands identified, and the images digitalised using the Gel Doc XR+ system. A scalpel was used to dissect bands of interest, which were then were placed in labelled Eppendorf tubes in preparation for extraction and stored at -20°C.

A gel extraction kit was used to obtain DNA fragments from the gel. This contained gel dissolving solutions and buffers to trap the DNA in a resin within a specialised filter column. The columns were placed in a vacuum manifold as previously, buffers drawn off, and transferred to collection vials and elution buffers added. Final product concentrations were measured using the Nanodrop system and products stored at -20°C until the next stage.

2.6.11.10. Ligation of vector and variable chain inserts

Vector and insert fragments were ligated at a 3:1 ratio. Concentrations of all vector and insert solutions were noted and the following equation used to calculate ligation reaction mixtures. Vol (I) volume insert, C(V) concentration of vector, Mw(V) molecular weight of vector, Mw(I) molecular weight of insert, C(I) concentration of insert. The vector and inserts molecular weights were as shown in Table 2.6-23.

$$Vol(I) = [\frac{C(V)}{Mw(V)} \times Mw(I) \times 3] \div C(I)$$

The necessary volume of each insert was calculated and added to 1µl of vector in a 200µl PCR tube, and the other components added as described in Table 2.6-24. The aliquots were incubated on a thermal block at 65°C for five minutes and a kit used for the ligation reaction with the following T4 ligase (New England Biolabs). The ligation reactions were incubated at room temperature for 16 hours and underwent PCR purification using a kit as previously described.

Chain	Vector Molecular Weight	Region Insert
Heavy	5.7kb	0.38kb
Lambda	5kb	0.4kb
Kappa	5kb	0.54kb

Table 2.6-23 Vector insert molecular weight

Component	20 µl reaction
T4 DNA Ligase Buffer (10X)	2 µl
Vector DNA	50 ng (0.020 pmol)
Insert DNA	37.5 ng (0.060 pmol)
Nuclease-free water	to 20 µl
T4 DNA Ligase	1 µl

Table 2.6-24 Ligation reaction components

2.6.11.11. Transformation of DH5 alpha cells with ligated insert/vector

The ligated purified DNA product was used to transform DH5 alpha cells to provide ample quantities of DNA for subsequent transfection of mammalian cell lines for monoclonal antibody production. Cells were purchased from a commercial supplier and stored at -80°C until use. The cells arrived in vials of 500µl which were thawed on ice before dividing into aliquots of 25µl for transformation. All aliquots were stored on ice until use.

LB agar plates were prepared by adding 250ml of distilled water to 8.75g of LB agarose powder and autoclaving. The liquid agar was cooled to 50°C in a waterbath and transferred to a sterile hood, 250µl of ampicillin added to produce a concentration of 1:1000 (100mg/L) and poured onto plates which cooled in a sterile hood. Each 250ml water/8.75g LB agarose/250µl ampicillin batch produced approximately 20 plates. Once cooled and solid, plate lids were replaced and stored at 4°C until use. All plates were removed from refrigeration and allowed to come to room temperature prior to bacterial work.

Each transformation used a 1.5ml Eppendorf tube containing 3µl of each ligation reaction placed on wet ice to which 25µl of DH5 alpha cells were added, tapped gently to mix, and incubated on ice for 30 minutes. At the end of this incubation, each tube was placed in a 42°C waterbath to heat shock for 35 seconds and transferred back to the ice to incubate for two minutes. Following this process, 950µl of warmed LB broth was added to each tube and incubated at 30g and 37°C for one hour.

The reaction tubes were centrifuged at 1500g for ten minutes and the supernatant aspirated to leave a pellet and 200µl of LB broth; this was gently resuspended by pipetting up and down, transferred to solid LB agar plates and evenly distributed, and incubated at 37°C overnight. The following day, all plates were assessed for the presence of bacterial colonies, representing successful transformation of DH5 alpha cells containing the desired inserts.

2.6.11.12. Preparation of glycerol stocks

A 96-deep-well-plate was prepared for glycerol stocks for each vector-insert sequence by adding 1.2ml of Terrific Broth to each well. A single colony from each bacterial transformation plate was added to the well, the plate sealed and incubated overnight at 30g and 37°C. The following day, the culture was retrieved and made up glycerol stocks in 1:1 ratio, and stored in cryovials at -80°C.

2.6.11.13. Preparation of plate stocks

Plate stocks consisted of three LB agar plates to store individual colonies for quick retrieval. A grid was drawn on the base of the plate and numbered according to the chain being stored. A single colony from each transformation was placed in the corresponding square of the grid and stored at 4°C.

2.6.11.14. Harvesting amplified vector/insert sequences

After single colonies had been selected for glycerol and plate stocks, the remaining colonies were harvested from the plates. 1ml of LB broth was added to each plate and the colonies gently scraped from the agar surface. The broth and colonies were pipetted into a 1.5ml Eppendorf tube and centrifuged at 1500g for one minute. The supernatant was discarded, and the pellet resuspended by vortexing.

A kit (QuickLyse Miniprep Kit, Qiagen) was used to purify vector plasmid DNA according to the manufacturer's instructions. Preparation of kit buffers included addition of RNAse A solution to Buffer P1, and addition of 96% ethanol to Buffer PE. LyseBlue reagent was added to Buffer P1 which aided with identification of successful bacterial cell lysis. A 250µl aliquot of Buffer P1 was added to the bacterial pellet and the mixture transferred to a microcentrifuge tube. A 250µl aliquot of Buffer P2 was added, the tube inverted five times and the reaction mixture turned blue. 350µl of Buffer was N3 added, the tube inverted five times and the mixture turned clear.

The tube was centrifuged at 1500g for ten minutes the supernatant added to a column provided by the kit. The column was placed in a vacuum manifold and the supernatant drawn through. A 0.5ml aliquot of Buffer PB was added to the column and the vacuum reapplied, followed by 0.75ml of Buffer PE and the vacuum reapplied.

The column was transferred to a collection tube, centrifuged for one minute, and transferred to a labelled microcentrifuge tube and a 50µl aliquot of RNA/DNAase free water applied to the centre of the membrane. After allowing to rest rested for one minute, this was then centrifuged at 1500g for one minute to elute the miniprepped DNA into the microcentrifuge tube. All collected samples were stored at -20°C until further use.

2.6.11.15. Minidigest to assess for the presence of vector and insert

A minidigest was performed to ensure all steps of the reaction had been performed adequately and the inserts were present within the vectors. The same enzymes were used as previously for digestion of both insert and vectors; heavy with EcoRI and SalI, lambda with AgeI, and kappa with XhoI. 3µl of each vector/insert DNA sample was assessed here. The reagent components and volumes were as listed in Table 2.6-25

	Heavy chain vector	**Lambda chain vector**	**Kappa chain vector**
Miniprep DNA	3	3	3
EcoRI	0.2	-	0.2
SalI	0.2	-	-
AgeI	-	0.125	-
XhoI	-	0.2	-
HindIII	-	-	0.2
Cutsmart buffer	2	2	2
Nuclease free H20	14.6	14.675	14.6
Total	20	20	20

Table 2.6-25 Minidigest reagent list and volumes
All measurements in microlitres (µl) to assess for the presence of ligated inserts.

The product was mixed with 6X loading dye and placed in a 1% TBE gel. DNA ladders of 1kb and 100bp were loaded into the first two wells to allow measurement of the fragment molecular weight. The gel was run at 120V for 30 minutes to visualise the digested insert for the heavy, lambda and kappa chains. Viable samples were those with two bands visible on the gel- one at 5-6kb representing the vector, and one at 500bp representing the insert. This is shown in Figure 5.6-2.

2.6.11.16. Sequencing of verified insert samples

If the gel showed the presence of an insert of the correct molecular weight, two miniprepped samples were sent to an external laboratory (Genewiz laboratories UK) for sequencing. A 15µl aliquot of each sample at a concentration of 100ng/µl was sent either in 1.5ml Eppendorf tubes or batched on a 96-well plate, along with the relevant AbVec primer (GCTTCGTTAGAACGCGGCTAC). The sequencing results were downloaded from the Genewiz online portal and analysed sequences using BioEdit. If there was consensus between two sequences, these were noted as suitable for transfection and monoclonal antibody generation.

2.6.11.17. Assessment of insert character

All available heavy and light chain inserts were analysed using the online IMGT database for insert gene family usage, complementarity-determining region length. This allowed comparison of the monoclonal antibody properties.

2.6.11.18. Preparation of mammalian HEK293A cells in preparation for transfection

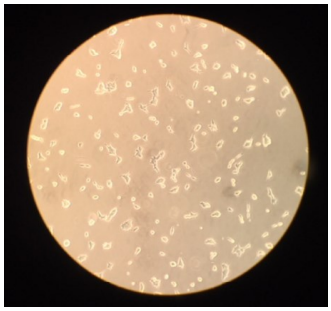
The human embryonic kidney cells (HEK) were selected for vector and insert transfection, as this cell line grows well in culture and facilitates transfection. The cell line was created by the addition of adenovirus 5 DNA to foetal embryonic kidney cells (287). The cells were obtained commercially (Invitrogen UK) and stored at -80°C until required. For this part of the project, all cells were thawed as described previously.

All work was done in a sterile hood in a containment level two facility. Vials of $1.1x10^7$ cells were retrieved from storage and kept on dry ice, placed in a 37°C water bath and thawed until a few ice crystals remained. The cells were transferred to a 4°C cooled 15ml conical tube, 5ml cold DMEM added dropwise and gently mixed. A 6ml aliquot of RPMI was added to bring the total volume to 12ml and the tube was centrifuged at 300g for eight minutes.

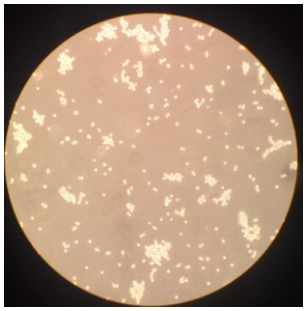
The supernatant fluid was poured off and the pellet resuspended in 12ml of DMEM and centrifuged for five minutes at 300g. The supernatant was again poured off and the cell pellet resuspended in 10ml of R10 for counting. Usual viability of thawed HEK293A cells was 70-85% of fresh cell amount. The cells were transferred to T75 (75cm2) tissue culture flasks and placed supine in a 37°C and 5% CO2 incubator to encourage adherence of cells to the flask surface. The flask lids were left loosely open to allow for gas exchange.

The cells were reviewed daily using a light microscope until a 70-80% confluency had been reached, at which stage they were ready for passaging. This level of confluency represents a cell density of $>5x10^5$ cells/ml according to the manufacturer. Figure 2.6-14 below shows the appearance of each cell growth stage.

Day 0: cells placed in T75 flask



Day 1: cells growing and adherent to flask surface



Day 5: cells now covering 70-80% of the visible flask surface and ready for passaging



Figure 2.6-14 HEK293A cell growth
HEK293A cells were placed in T75 flasks. Day 0 shows cells. Daily checks reveal progressive growth and adherence to flask surface. By day 5, confluency is achieved, and cells are ready to passage

2.6.11.19. Passaging HEK293A cells

When cells achieved 70-80% confluency, they were reseeded into new T75 flasks at a 1:10 split. The manufacturer recommended a cell seeding density of 2-5x10^4 viable cells/cm^2. Cell passaging was performed twice weekly, with a minimum of 3-5 passages recommended before being ready for transfection. Passage of cells was done in a sterile hood in a containment level two laboratory. All aspirated medium and PBS were disposed of in Virkon unless otherwise stated.

Complete medium was used for passaging cells and made up as follows: 450ml of high glucose Dulbecco's Modified Eagle Medium (D-MEM), 50ml of FBS, 5ml of L-glutamine (2mM), 5ml of non-essential amino acids (NEAA, 10mM), 5ml of sodium pyruvate (10mM) and 1% penicillin/streptomycin. This was filter sterilised using a 0.45µm filter and stored at 4°C. Prior to use, aliquots were placed in a 37°C waterbath.

Flasks were opened and a sterile 10-20ml pipette used to aspirate off old medium. A fresh 10ml pipettes was used to introduce 10ml of PBS to the cells the flask rocked gently back and forth to remove any remaining medium and wash cells, ensuring no medium or serum remained which could inhibit the action of trypsin. The PBS was removed and disposed of, and 1-2ml of Trypsin/Versene (EDTA) solution added to the flask. The flask was incubated at room temperature for five minutes to allow detachment of cells from the flask surface.

The flask was checked microscopically to ensure all cells had detached. A 9ml aliquot of complete medium was added to the flask and this cell suspension used to seed the required number of flasks required for cell growth. Each flask received 1ml of this cell suspension and 19ml of either complete or D10 medium to create the 1:10 cell split used for each cell passage. All freshly seeded flasks were labelled with date, passage number and cell line name before placing in the 37°C and 5% CO2 incubator. All further cell incubations were performed in this incubator unless otherwise specified.

2.6.11.20. Seeding HEK293A cells in preparation for transfection

2.6.11.20.1.1. 6 well plates

A six well plate was used for initial small-scale transfection work. Each well required a concentration of $4x10^5$ cells/ml. Each well was 2ml capacity, each plate contained six wells, meaning $4.8x10^6$ cells were needed per plate. From the T75 flasks, the total cell number was calculated and divided by $4.8x10^6$ to give the number of plates available for transfection. Number of plates was multiplied by 12 to give the total volume for resuspension of the cells. D10 was used as the resuspension medium.

The six well plates were seeded with 2ml of the D10 cell suspension and rocked backwards and forwards to evenly disperse the cells. Plates were labelled and dated and checked with a microscope to ensure the presence of cells in each well, lids replaced, and placed in the incubator overnight. The following day, plates were checked microscopically to ensure 70-80% cell confluence. Once this level was achieved, the cells were ready for seeding.

2.6.11.20.1.2. 15 cm diameter plates

A 15cm plate was used for large scale transfections to produce a greater volume of antibody, with each plate having a surface area of 148 cm2. The cell concentration required per plate was $5.5x10^5$ cells/ml. This meant a total cell number of $11x10^6$, with a 20ml volume of cell suspension. The plates were rocked as previously described to ensure even dispersion of cells, checked microscopically and placed in the incubator until transfection the following day.

2.6.11.21. Transfection of HEK293A cells

Once cells were considered viable for transfection, they were removed from the incubator and placed in a sterile hood. One hour prior to the transfection, D10 medium was removed from each well. The plate was carefully tilted and a 20ml sterile pipette used to carefully aspirate the old medium taking care not to dislodge the adherent cell layer. Fresh D10 medium was added to each well and returned plates to the incubator for one hour.

After one hour in the incubator, the plates were returned to the sterile hood in preparation for addition of heavy and light chain DNA. The exact amount of DNA per well was 1µg of each heavy and light chain, giving 2µg in total. The correct volume of miniprepped DNA was calculated by dividing 1µg by concentration of each miniprepped sample (ng/µl).

Polyethylenimine (PEI) was used to enhance transfection as it condenses DNA into positively charged particles more easily endocytosed intracellularly by mammalian cells. A stock solution of PEI was created by dissolving 50mg in 1ml nuclease-free water. The solution was then diluted to give a working stock solution of 1mg/ml, filter sterilised with a 0.22µm filter and divided into 500µl aliquots and stored at -20°C until required.

Six well plates: 1µg each of heavy and light chain DNA was added to 250µl of DMEM in a 1.5ml Eppendorf tube and vortexed. A 9µl aliquot of polyethylenimine (PEI) was added to the tube and the mixture left to sit at room temperature for 15 minutes.

15cm diameter plates: 15µg each of heavy and light chain DNA was added to 2ml of DMEM in a 12ml tube and vortexed. A 100µl aliquot of polyethylenimine (PEI) was added to the tube and the mixture left to sit at room temperature for 15 minutes.

Each well of the six-well HEK293A plates and each 15cm plate corresponded to an antibody heavy and light chain pairing and was labelled accordingly. The correct heavy and light chain/DMEM/PEI mixture was carefully added dropwise to the corresponding well/plate before returning to the incubator for 6-18 hours.

2.6.11.22. Addition of protein free medium

The following day, old DMEM medium was removed, the cells washed with DMEM, and the appropriate volume of Ultra-DOMA protein-free medium added; 2ml for the six-well plate and 20ml for the large plates. The plates were rocked gently back and forth and returned to the incubator for 4-5 days to allow growth and secretion of the monoclonal antibody.

2.6.11.23. Antibody harvesting

After 4-5 days incubation, plates were examined microscopically to ensure cells remained adherent to the well/plate surface. For six-well plates, 1000µl pipette tips were used to aspirate supernatant into pre-labelled 2ml microcentrifuge tubes. For the 15cm plates, a 20ml sterile pipette was used to collect supernatant and stored in a pre-labelled 50ml centrifuge tube. The remaining plates were doused with Virkon and disposed of appropriately. All harvested supernatant was stored at 4°C.

2.6.12. IgG enzyme-linked immunosorbent assay (ELISA) to test for the presence of antibody

A commercial ELISA kit (Human IgG total Ready-SET-Go! ELISA kit ThermoFisher, UK) was used to screen for the presence of antibody in each transfection supernatant sample. All preparation and experimental steps were performed as per the manufacturer's instructions.

2.6.12.1. ELISA plate coating

The day before the planned ELISA experiment, test plates were coated with capture antibody. The coating buffer (1X) was prepared by making a 1:10 dilution of PBS (1ml) with deionised water (9ml). A 1:250 dilution of capture antibody was made by adding 40µl capture antibody to 9960µl coating buffer. This buffer/antibody coating mixture was poured into a 25ml reservoir and mixed gently. A multichannel pipette was used to dispense 100µl to each well of the 96-well plate, sealed with film and incubated overnight at 4°C.

2.6.12.2. ELISA wash stages

On the day of the ELISA experiment, a wash buffer was prepared by adding 250µl of Tween-20 (Sigma Aldrich) to 500ml of PBS to give 0.05% Tween-20, hereafter referred to as PBS-T. The wash stages were performed by pipetting 250µl of wash buffer into each well of the 96-well plate using a multichannel pipette. As per the manufacturer's instructions, the wash stages differed.

The initial two wash stages included two washes, and all washes following this required four washes. The first two wash steps involved aspirating all liquid from the 96-well plate wells using a multichannel pipette, followed by addition of wash buffer. This process was repeated and the wash complete. All subsequent washes were performed as follows: the 96-well plate was rapidly inverted to "flick" off all buffer from the wells. A 250µl aliquot of PBS-T was added to each well using the multichannel pipette and left to soak for one minute to increase effectiveness of the wash. The wash was then flicked off again and the plate blotted on absorbent paper to remove residual wash buffer. This process was repeated three times.

2.6.12.3. ELISA blocking stage

The ELISA plate was washed as per the two-wash stage process. A blocking buffer was prepared with a 1:10 dilution of Assay Buffer A (2.5ml) concentrate (20X) in deionised water (22.5ml). The tube containing the buffer was inverted several times to mix, placed in a 25ml reservoir and 250µl dispensed into each well of the 96-well plate using a multichannel pipette. An adhesive seal was applied to the plate and the sealed plate incubated at room temperature for two hours.

2.6.12.4. ELISA Standard Preparation

As per the manufacturer's instructions, the recombinant IgG standard provided with the kit required a reconstitution time of 30 minutes before being added to the plate. The ELISA kit contained the standard as powder for reconstitution with deionised water, intended for immediate use once reconstituted. These steps were performed at room temperature to create a final concentration of 200ng/ml.

2.6.12.5. ELISA testing of supernatants- primary antibody

Following the blocking step, plates were washed twice with PBS-T and all residual wash buffer removed by blotting on absorbent paper. Each well was allocated to one of the supernatants prepared from the transfection steps and the standards as described below. Columns 1 and 2 were allocated for the IgG standard. Each well was filled with 100µl of 1X Assay Buffer A. 100µl of IgG standard was then added to wells A1 and A2 and mixed well using a pipette. This gave a standard concentration of 100ng/ml. 100µl from A1 and A2 was then transferred to wells B1 and B2, the wells mixed using a pipette and this procedure repeated for all subsequent wells to G1 and G2 to give two-fold serial dilutions. The final two wells of H1 and H2 were left blank.

For the experimental wells, 100µl of undiluted transfection supernatant was added to each referring to a plate layout prepared beforehand (Figure 2.6-15). A clear adhesive plate seal applied, and the plate incubated at room temperature for two hours. The transfection supernatants contained monoclonal antibodies and fulfilled the role of the primary antibody for the purposes of ELISA. Each transfection supernatant was assessed in triplicate to allow more accurate estimations of concentration.

	1	**2**	**3**	**4**	**5**	**6**	**7**	**8**	**9**	**10**	**11**	**12**
A	Std 1	Std 2	1	1	1	4	4	4	7	7	7	
B	Std 1:2	Std 1:2	2	2	2	5	5	5	8	8	8	
C	Std 1:4	Std 1:4	3	3	3	6	6	6	9	9	9	
D	Std 1:8	Std 1:8	10	10	10							
E	Std 1:16	Std	11	11	11							
F	Std 1:32	Std	12	12	12							
G	Std 1:64	Std										
H	0	0										

Figure 2.6-15 ELISA plate layout
Columns 1 and 2 contain the standard in an increasing dilution of 1:2, and rows 3-12 contain transfection supernatant experimental samples

2.6.12.6. ELISA testing of supernatants- Secondary Antibody

Following incubation, the ELISA plate underwent a four-step wash as described above. A secondary or "detection" antibody was provided in the kit. This was an enzyme probe consisting of an IgG antibody conjugated to a horseradish peroxidase (HRP) enzyme. In the following steps this enzyme reacts with 3,3',5,5'-Tetramethylbenzidine (TMB) to produce a visible colour change within the plate wells, indicating the presence of antibody. The conjugated secondary antibody (IgG/HRP) was prepared by diluting the provided antibody 1:250 in 1x assay buffer A and 0.5ml of 1X assay buffer A added to 9.5ml of deionised water in a 12ml tube. A 40µl aliquot of this solution was removed to leave 9600µl, and a 40µl aliquot of the provided IgG/HRP solution was added to create the required 1:250 dilution. The tube was inverted five times and the solution poured into a reservoir. A multichannel pipette was used to place 100µl of IgG/HRP solution into each well, the plate resealed and incubated at room temperature for one hour.

2.6.12.7. ELISA substrate and stop solution

Following the one-hour incubation, the plate underwent a four-step washing process as previously described. The kit contained the TMB substrate described above. On addition of TMB to the HRP enzyme, a blue pigment is produced. When the stop solution was added, the solution changed to a yellow colour. The TMB solution was contained in the kit and a 100µl aliquot was added to each well using a multichannel pipette. The plate was resealed, wrapped in foil, and incubated at room temperature for fifteen minutes. A stop solution containing sulphuric acid (H_2SO_4) was prepared by diluting 2ml of 10N sulphuric acid with 8ml of deionised water. I added 100µl of this solution to each well of the ELISA plate.

2.6.12.8. ELISA plate interpretation

A plate reader was used to review the optical density of each well of the ELISA plate. This machine detects absorbance of solution within the wells when light of wavelength 450nm passes through the sample. Each well is measured in this fashion and a readout of figures is displayed. All results are compared to the standard absorbances in columns 1 and 2 to assess for the presence of antibody within the supernatant samples. The lowest standard results determined the cut-off value indicating the presence of antibody. This is a semi-quantitative assay as concentrations can also be estimated.

The results from the standard absorbance and were recorded and used to plot a calibration curve in Microsoft Excel. The purpose of two standards per dilution increased the accuracy of the calculations. The x-axis was the concentration of the standard and y-axis was level of absorbance. The equation for the line was calculated using the standard formula y=mx+c. A linear regression analysis was performed to give the coefficient of determination- R2, where R is the correlation coefficient. Ideally, R2 was 0.95 or greater to indicate a robust correlation curve. As the supernatant sample absorbance values of were known, the concentration for each sample could be calculated. Any sample with a concentration greater than the lowest value for the standard was deemed to contain antibody.

2.6.13. Polyacrylamide gel electrophoresis (PAGE) to assess antibody molecular weight

2.6.13.1. PAGE set-up

The molecular weights of antibodies present within the supernatant were determined using SDS-PAGE gel electrophoresis. This used sodium dodecyl sulphate (SDS) to denature the three-dimensional structure of protein, allowing transit of the protein to be determined purely by molecular weight. The denatured protein was placed in a polyacrylamide gel and subjected to an electrical current. The protein moved through the gel, and its progress compared to a kit standard, and molecular weight determined.

A Mini-PROTEAN TGX was used kit for this step. As per the manufacturer's instructions, a 1X strength running buffer was created by diluting 100ml of 10X stock with 900ml of deionised water. The electrophoresis cell was assembled, and gels prepared by removing combs and tape. The inner and outer chambers of the electrophoresis cell were filled with the appropriate amount of running buffer. The inner chamber buffer volume was 200ml, and the outer chamber buffer volume varied according to the amount of gels being run at any one time. Care was taken to ensure all chambers were sealed appropriately.

I prepared the supernatant samples for electrophoresis; 5µl of each sample was added to 4.75µl of Laemmli sample buffer (provided by the kit manufacturer, Sigma-Aldrich) and 0.25µl of β-mercaptoethanol in a 200µl microcentrifuge tube. The samples were placed in a heat block at 95°C for five minutes before being loaded onto the gel carefully using a 20µl pipette tip. The electrophoresis chamber was connected to a powerpack and the experiment performed at 200V for 40 minutes and following this the gel was removed from the chamber by opening the gel cassette and floating it off in water.

2.6.13.2. Coomassie dye staining of SDS-PAGE gel product

Coomassie dye binds to basic and hydrophilic protein residues, undergoing a colour transformation from brown to blue in the presence of protein. The PAGE gel was washed several times in fresh water before it was loaded into a container. The stain 0.25% Coomassie Blue R-250 was added to the container and placed on a rocker for 2-4 hours to allow the stain acquisition by the gel. Excess dye was drained away, the gel rinsed twice with water and a de-staining solution of 5% methanol, 7.5% acetic acid and 87.5% water added to the container. This was returned to the rocker for 4-20 hours or until the gel background had shed the blue colour. A Gel-Doc XR reader was used to read and digitise the image.

2.6.14. Screening supernatant antibodies for HIV specific responses

An assay was designed to assess the affinity of recovered antibodies for HIV specificity. This was a flow cytometry based assay in which target CEM.NKr cells were coated with HIV envelope proteins, and then mixed with the transfection supernatant which acted as the primary antibody.

Following this, a fluorescent conjugated anti-human IgG antibody was added as the secondary antibody. When these cells were analysed by flow cytometry, any fluorophore positive populations represented HIV specific antibodies bound to CEM.NKr membrane bound HIV envelope protein and confirmed the presence of HIV-specific antibodies within the transfection supernatant.

2.6.14.1. CEM.NKr cell preparation

The CEM.NKr cell line was used for this experiment. These cells are derived from T-lymphoblasts and are resistant to natural killer-mediated cell lysis. The CEM.NKr cells were obtained commercially and stored in cryovials in liquid nitrogen. Cell vials were thawed and counted as described for the HEK293A cell line. The thawed cells were resuspended in R10 medium and placed in a T25 culture flask. This flask was labelled and placed in a 37°C temperature and 5% CO2 incubator and cell growth monitored. The cells were transferred to a T75 flask and passaged twice weekly, as they grew optimally in suspension with a doubling time of 24 hours. Post passage cell resuspension amounts were usually $1x10^7$ cells per flask.

For this assay, the CEM.NKr cells were transferred from the T75 flask into a 50ml centrifuge tube and made up to 50ml with R10 medium. The tube was centrifuged at 350g for five minutes, the supernatant poured off, and the pellet resuspended in 10ml of R10. The cells were counted by mixing 10µl of cell suspension with 10µl of Trypan Blue, this aliquot transferred to a haemocytometer chamber and counted with a microscope. $2.5x10^6$ cells were required for each assay. The calculated volume of cell suspension was aliquoted into a FACS tube, centrifuged at 350g for five minutes, the supernatant removed with a 1000µl pipette tip and the pellet resuspended in 50µl of R10 medium.

2.6.14.2. CEM.NKr cell coating with HIVgp140

The HIV gp140 surface protein was selected for cell coating. Frozen aliquots of this were thawed and available in a 1mg/ml concentration. A 10µl aliquot of HIV gp140 was mixed with 90µl of R10 and 50µl was added to each CEM.NKr cell aliquot. The FACS tube was briefly vortexed and incubated at 37°C for one hour. Following this incubation, cell aliquots were washed twice with R10 medium and centrifuged at 350g for five minutes. The cells were counted and resuspended at a concentration of $6.5x10^5$ cells/ml.

2.6.14.3. Addition of supernatant to the coated CEM.NKr cells- primary antibody

Approximately 65,000 cells or 100µl of resuspended cells were placed in each well of a 96-well plate. All control and experimental samples were performed in triplicate. The selection of experimental controls was as previously described. The biological controls included one negative control (IgG) and one positive control (HIVIG). IgG1 is a stock preparation of pooled IgG from confirmed HIV negative donors (288). Anti-HIV Immune Globulin (HIVIG) is a solution of polyclonal anti-HIV antibodies prepared from donor sera of asymptomatic HIV antibody positive donors with CD4 counts above 400 and confirmed negative for hepatitis B and C (289). The experiment was set out as shown in Figure 2.6-16 below.

	1	2	3	4	5	6	7	8	9	10	11	12
A	AF			US			FMO					
B	IgG			A32			HIVIG					
C	Supernatant sample			Supernatant sample			Supernatant sample			Supernatant sample		
D	Supernatant sample			Supernatant sample			Supernatant sample			Supernatant sample		
E												
F												
G												
H												

Figure 2.6-16 96-well plate for supernatant screening
Plate layout as shown in the figure, AF autofluorescence, US unstained, FMO fluorescence minus one, IgG pooled HIV negative IgG, HIVIG anti-HIV immune globulin. Supernatant samples allocated as required.

For control wells, the following were prepared cells: autofluorescence (cells only). unstained (cells with supernatant only), fluorescence minus one (cells with secondary antibody only), IgG1 (negative control, 100µl of a 1:500 dilution of 2µl IgG1 + 998µl PBS), A32 (positive control): 100µl of 1:500 dilution (2µl A32 + 998µl PBS), HIVIG (positive control, 100µl of a 1:500 dilution of 2µl HIVIG + 998µl PBS). For experimental wells, 100µl of neat supernatant was added to each well in triplicate and the plate incubated at 37°C for one hour.

2.6.14.4. Addition of secondary antibody

The plate was retrieved, washed twice with of 200µl of PBS in each well and centrifuged at 350g for five minutes. The plate was vortexed after the second wash. I prepared a secondary antibody solution of an anti-human IgG- FITC conjugated antibody and diluted to 1:100 solution. I added 100µl of 1% IgG-FITC to experimental sample well and the FMO control well. I wrapped the plate in foil and incubated at room temperature for 30 minutes. I washed twice with PBS, removed supernatant, vortexed and added 100µl of BD Cytofix to each well to ensure stability of the fluorophore labelled cells. I prepared microtubes on a 96-well rack in accordance with the plate set up. I transferred the well contents were to the microtubes and the samples were then ready for flow cytometry analysis.

2.6.15.Identification of cross-reactivity with gut microbiota

In relation to previously published work suggesting intestinal microbiota may provide a template for antibodies which cross react with gp41 antigens (264), reactive epitopes were reviewed against *E coli* RNA. Any reactive sequences were compared to the RNA molecules described in the literature by using BioEdit software (previously described) and the online NCBI basic local alignment software tool (BLAST; https://blast.ncbi.nlm.nih.gov/Blast.cgi) to review sequence alignment.

2.6.16.Functional assessments

A rapid fluorometric assessment of antibody dependent cell-mediated cytotoxicity was used to assess monoclonal antibody function. This was adapted from the protocol described by Gómez-Román et al (290) and optimised by colleagues working in our laboratory.

The target cells were double stained with two dyes; one membrane dye (PKH red fluorescent cell linker, PKH-26, Sigma Aldrich UK) and a viability dye (5(6)-Carboxyfluorescein diacetate N-succinimidyl ester, CFSE, Invitrogen).

Briefly, CEM.NKr cells were used as target cells and PBMC from healthy controls were used as effector cells. CEM.NKr cells were cultured as previously described and stained using a PKH-26 dye staining kit, washed twice, counted and resuspended in 10ml of complete R10 medium. A 5mM stock solution of CFSE dye was diluted 1:5 with PBS and used to stain the CEM.NKr cells at a concentration of 1µl per $1x10^6$ cells. These were washed twice and resuspended in 10ml R10 complete medium. The cells were then coated using HIV-1 gp140 as previously described.

Doubly stained CEM.NKr cells were resuspended at $2x10^5$ cells per ml and 50µl/$1x10^5$ placed in each well of a 96-well plate. Effector PBMCs were prepared as previously described and added at a 1:1 ratio with 50µl/$1x10^5$ cells added to each well. Each experiment was done in triplicate and the wells allocated as follows; negative control IgG (A1-3), positive control HIVIG (A4-6) and experimental monoclonal antibody thereafter. A 100µl aliquot of monoclonal antibody was added to experimental wells.

The plate was centrifuged for three minutes to gather cells at the base of each well and then incubated for four hours at 37°C. Following incubation, wells were washed twice with PBS before adding 100µl of BD Cytofix to each well and transferring contents to FACS microtubes, which were wrapped in foil and chilled at 4°C.

FACS analysis was performed using the BD LSRII and data analysed using FlowJo software. ADCC was assessed by identifying the percentage of target CEM.NKr cells which retained PKH-26 membrane dye but lose intracellular CFSE dye indicated lysis of this population. Gating using negative and positive controls identified the quadrant of interest. This is shown below in Figure 2.6-17.

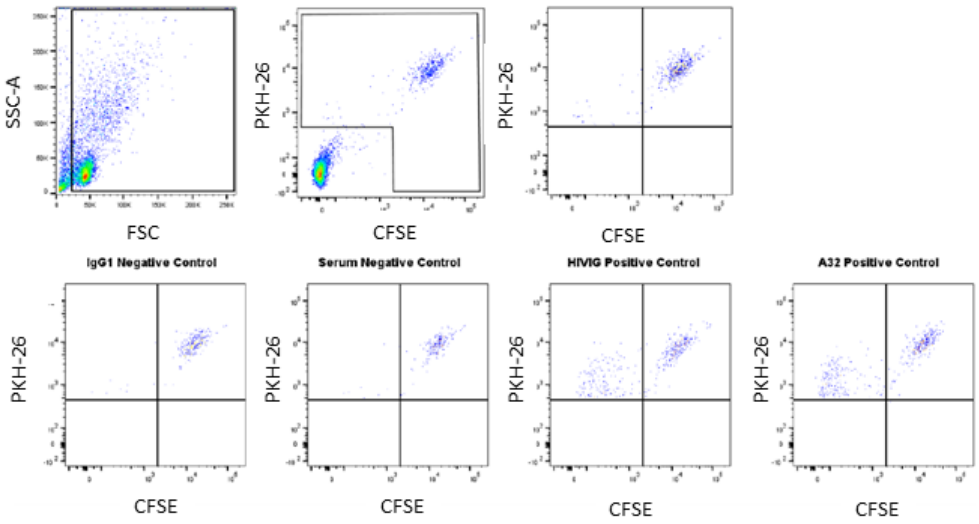


Figure 2.6-17 RFADCC assay- courtesy Dr Scarlett Turner
First row gating strategy. The first gate selects live PBMC and target cells; x axis forward scatter area, y axis side scatter area. Second and third gates x axis CFSE, y axis PKH-26; positive and negative controls are used to select the CFSE high, PKH-26 high, and CFSE/PKH-26 double high populations. Cells which are CFSE low/PKH-26 high have lost intracellular dye but retain membrane dye and indicate the percentage ADCC population.

Second row negative controls, positive controls HIVIG and A32. X axis CFSE, y axis PKH-26

Chapter 3
Seronegative Cohort

Chapter 3 Seronegative cohort

3.1. Introduction

Humoral responses against the HIV envelope protein subunit gp41 include non-neutralising IgG and IgA, and mucosal IgA which can inhibit trancytosis and effect neutralisation of HIV infection *in vitro* (224,225). There is also evidence to support the origin of anti-gp41 responses as a result of immune priming by previous exposure to other epitopes such as intestinal microbial antigens (264).

The purpose of this part of the study was to review participant serum responses to HIV envelope antigens. The initial part of my work concerns the development of anti-HIV immune responses in a seronegative population and asks if levels of exposure to potential HIV infection can influence this response.

Low level viraemic challenges are of interest. The group A population of seronegative individuals reported regular unprotected sexual intercourse, but it has been suggested to consider the possibility of “silent infection” described in MSM with negative ELISA and Western blot but HIV cultured from PBMC (291). This event was not described in other cohorts which specifically reviewed high-risk exposures in haemophiliacs exposed to contaminated blood products (292) and antibody negative heterosexual females with HIV positive haemophiliac male partners where it was not possible to identify viral RNA PCR from PBMC status (293,294). These data suggest the absence of HIV infection in humans with persistently negative HIV antibody testing. The initial “silent infections” may be due to assay sensitivity may vary between studies; some used denatured as opposed to conformational epitopes which may not capture anti-HIV humoral responses to *in vivo* epitopes (295,296).

Conversely, low level viraemic challenges in animal models have shown the following. Transient viraemia in macaques resulted in cytotoxic T-lymphocyte responses to SIV, with tissue samples positive for proviral DNA and SIV gag RNA, suggesting latent or low level production of virus (297). Data from macaque models using repeated low dose SIV exposure caused SIV-specific cytotoxic T-lymphocyte responses in absence of anti-SIV antibody, and were found to be non-protective, as

subsequent larger dose challenges eventually causing seroconversion and disease progression, suggesting repeated low dose challenges with SIV may create subclinical infection with proviral DNA detectable in tissue/PBMC in absence of seroconversion, (298). There is minimal data to support low dose viral challenges can cause protective effects in animals (299).

The cohort of MSM in group A reported HIV exposure but did not display seroconversion. Returning to animal models, repeated intrarectal SIV challenges did not produce infection in five of 18 macaques but no antigen specific cellular or humoral correlates of infection identified, suggesting other possibly innate mechanisms provided protection (226). In addition, not all sexual exposure results in transmission- consider "highest risk" practice of receptive anal sex.

In the pre cART era, HIV infection was associated with 5 – 30 per 1000 receptive anal exposures in from partners of unknown serostatus (300). Knowledge of partner serostatus altered the per contact risk of acquiring HIV; 0.82% if partner was known HIV infected (viral load unquantified), and 0.27% if the partner serostatus was unknown (301). In the cART era, the per contact risk of acquiring HIV is 0.65-1.43% per contact, depending on ejaculation occurring extra/intrarectally (302). Therefore exposure to HIV in the absence of seroconversion/infection can occur.

The group A study cohort was made up of HIV-negative men who have sex with men who reported unprotected receptive anal intercourse within the previous three months. Given the levels of potential exposure to HIV as suggested by the above paragraph and the PROUD-UK criteria (113), the hypothesis was that some study participants could develop anti-HIV antibody responses in the absence of infection. As outlined in chapter 2, all group A participants were followed longitudinally to confirm seronegative status and assess for seroconversion events.

This study used a yeast surface display system (YSD) to interrogate participant serum. This system produces a combinatorial library of HIV-gp160 envelope fragments on the surface of yeast cells. The advantage of this method over traditional phage-based systems is the presentation of antigen as a

conformational rather than linear epitope due to yeast protein processing and display, and more akin to *in vivo* HIV Env. Also, as YSD contains a variety of antigen fragments, it allows a more in-depth analysis of antigenic determinants. Yeast surface display has been used to analyse humoral responses in HIV (280), simian immunodeficiency virus, and in hepatitis C (280,282,283,303).

The interest in exploring HIV Env protein serum responses was to identify immunogenic epitopes in HESN. Germline precursors of anti-Env antibodies have minimal affinity for Env (304), therefore it may be useful to explore Env structures which present stable epitopes to screen for antibodies.

YSD has been used previously in HIV protein engineering to construct mutated of Env including versions of gp120 to identify variants with enhanced binding for CD4bs antibodies (305), versions of gp140 to screen for anti-CD4bs antibodies (280).

YSD glycosylation is similar but not identical to mammalian cell procedure. Glycosylation serves several functions in protein production; chaperoning through endoplasmic reticulum, allows correct folding of proteins by creating stearic hindrance, and transporting functions including signalling and homing (306). In YSD, core *N*-glycosylation is similar, but mammalian proteins undergo post translational processing to complex and high mannose forms whereas yeast cells perform glycosylation in a step-wise fashion (307). Attempts to engineer in additional glycosylation steps to more closely match mammalian cell processing results in detrimental effects on yeast cell culture. Post culture enzymatic alteration of glycosylation affects antibody binding and the complexity was beyond the scope of this project (308)

YSD has been compared with HEK293 cellular-based display assays; yeast display achieved better binding for 2G12, VRC01, PGT121 which may have reflected mAb specificity for mammalian glycan processing; MPER-specific MAbs 2F5, 4E10 and 10E8 preferentially bound yeast epitope, suggesting yeast bound gp41 is better accessed on a yeast than mammalian structure (308).

It was decided to evaluate fragment/epitope recognition as opposed to intact Env trimer structure, as the purpose was to review epitopes of interest. In hindsight, constructing display system of intact Env trimers might have allowed for swifter processing of samples by identifying a population of trimer-specific antibodies. But as YSD might bias towards gp41/MPER specific antibodies, gp120 may have been presented in a more accessible fashion.

An important consideration is antibody recognition of fragments or denatured epitopes, as this is the feature of this assay. Western blots use denatured fragments, and sera from HIV-infected people can recognise Env structures (295). Yeast surface display sequences of greater than 100 base pairs displays conformational epitopes as opposed to the linear epitopes displayed by fragments less than 100 base pairs (282).

In summary, YSD was considered preferable to mammalian cell lines due to reasons outlined, ease of use, robustness in storage/culture and scalable in order to review the expected volume of samples to be assayed.

3.2. Aims

My aims with this study were as follows

- To identify serum responses to HIV envelope antigens serum of HIV negative individuals using a yeast surface display system

- To describe the antigenic determinants of this response

- To make a preliminary assessment of the frequency and character of this response as regards risk of HIV exposure

3.3. Baseline demographics

I used samples from group A (seronegative) and group E (seropositive) in this chapter of work.

3.3.1. Group A seronegative

Baseline demographics and PBMC parameters for group A participants are shown in Table 3.3-1. The two groups were similar across apart from number of sexual partners number and presence of a sexually transmitted rectal infection. The median number of partners for all participants in group A was 6 partners in previous 6 months and this was selected as the threshold between high and low-risk.

	Low-risk (n = 50)	**High-risk (n = 50)**	***P* value**
Age mean (Std dev)	36.4	32.9	
Ethnicity			
White	80.0%	90.0%	
Non-white	20.0%	10.0%	
Median partners in 6/12 (IQR)	6 (2.75 – 9.35)	30 (5 – 55)	**<0.05**
Median regular partners	1	1	
Median casual partners	4.5	20	
Presence of GCr/CTr/syphilis	1	fifty	**<0.05**
CD3 % median (IQR)	80.5 (75.4-85.6)	80.5 (77.6 -83.5)	0.342
Cells/uL (IQR) (300-2000)	2910.0 (2535.0- 3285.0)	1803.0 (1403.5 - 2202.5)	0.427
CD4 % median (IQR)	39.6 (33.1 - 46.1)	41.3 (36.0 - 46.6)	0.384
CD4 cells/uL (IQR) (300 - 1400)	1431.0 (1246.0 - 1616.0)	930.0 (723.5 - 1136.5)	0.384
CD8 % % median (IQR)	40.2 (32.7 - 47.7)	31.0 (27.2 - 34.8)	0.411
CD8 cells/uL (IQR) (190 - 900)	1453.0 (1239.5 - 1666.5)	694.0 (485.0 - 903.0)	0.427
CD56 % median (IQR)	12.5 (8.3 - 16.7)	11.6 (9.7 - 13.6)	0.427
CD56 cells/uL (IQR) (90-600)	443.0 (358.0 - 528.0)	252.0 (163.5 - 340.5)	0.382
CD19 % median (IQR)	8.2 (6.6 - 9.8)	8.9 (6.7 - 11.1)	0.471
CD19 cells/uL (IQR) (100 - 1fifty)	291.0 (239.0 - 343.0)	214.0 (1fifty.5 - 277.5)	0.426
CD4:CD8 ratio	1.0 (0.6 - 1.5)	1.3 (1.1 - 1.6)	0.525

Table 3.3-1 1 Group A details
Seronegative population Baseline demographics and peripheral blood mononucleated cell characteristics of Group A. The groups have no differences except for median number of partners in 6 months and presence of a rectal sexually transmitted infection ($p<0.05$ for both)

3.3.2. Group E seropositive

Group E samples were used as the positive control. Group E participants were individuals diagnosed with HIV infection who had yet to begin taking cART. These individuals were approached at the time of first medical visit to ensure samples were drawn in the absence of cART. Details of this group are displayed in Table 3.3-2

	Median (range)
Age (years)	31.7 (24.7-50.0)
Log viral load (copies/ml)	5.4 (2.7-6.9)
No. partners last 6/12	6 (1-150)
Regular	0 (0-2)
Casual	6 (0-149)
CD3 %	82.8 (70.9-96.2)
CD3 cells (700-2100)	1512 (948-4378)
CD4 %	26.2 (12.0-36.8)
CD4 cells/µL (300 - 1400)	461 (275-915)
CD8 %	53.5 (37.8-61062.0
CD8 cells/µL (190 - 900)	965 (488-3868)
CD56 %	7.0 (2.0-21.1)
CD56 cells/µL (90-600)	161 (59-368)
CD19 B cells %	6.9 (1.1 19.8)
CD19 B cells/µL (100 - 150)	132 (52-409)
CD4:CD8 ratio	0.5 (0.1-0.8)

Table 3.3-2 Group E details
Baseline demographics and PBMC parameters for seropositive group E participants

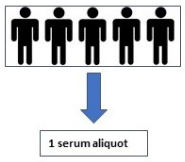
3.4. Selection of participant serum samples

For this part of the study, two groups of seronegative participants were created and divided according to risk of HIV exposure. The risk stratification followed on from findings in the Pre-exposure Option for reducing HIV in the UK: immediate or Deferred (PROUD-UK) trial (9).

3.5. Serum aliquot allocation

Each group of fifty participants was randomly allocated into groups of five participants. These groups would form the basis for batched serum aliquots. Ten low-risk and ten high-risk serum aliquot pools were created.

I combined five 200µl serum samples into one 1ml aliquot, and created ten aliquots for each risk status, as shown in Figure 3.5-1 below. Batching of serum samples allowed screening of a large number of participants thought to represent the risk groups of interest. Exploration of individual serum-yeast binding was assessed by single clone analysis (see sections 3.6.5, 3.7.4) for cultures displaying viable levels of enrichment.



Low risk	High risk
L01	H01
L02	H02
L03	H03
L04	H04
L05	H05
L06	H06
L07	H07
L08	H08
L09	H09
L10	H10

Figure 3.5-1 Schematic of seronegative aliquot creation
Five individual serum aliquots samples are randomly combined to form one pooled seronegative aliquot

3.6. HIV gp160 library analysis of seronegative serum aliquots

The combined large and small fragment HIV gp160 yeast surface display library were used to investigate the serum immune responses to HIV in this seronegative cohort. As the yeast surface display system expresses a protein composition more akin to that produced *in vivo*, this was considered this a more accurate way of reviewing antigen recognition by these participant samples.

Alternative mechanisms considered to screen for antigen recognition include pooled peptide epitope mapping to identify T-cell epitope specificities (309,310), phage-displayed peptide libraries to screen patient sera for epitope-specific antibodies (311) or mammalian cell lines. YSD epitope presentation on yeast cell surface is preferable to phage (as discussed previously in view of eukaryotic nature of cell); and proteins are displayed as constructs fused to Aga2p proteins are projected away from cell surface, which minimises obstruction of epitopes (278)

For this study, as intention was to produce a screening tool to identify B cell responses and then subsequently sort B cell populations of interest, yeast surface display was selected due to the ability to identify cultures bearing fragments of interest.

A schematic of the HIV envelope protein is displayed here for reference purposes below in Figure 3.6-1.

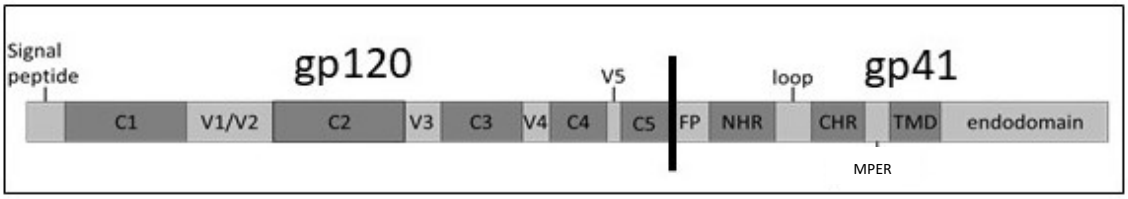


Figure 3.6-1 HIV envelope gp160 schematic
gp120: signal peptide C1-C5 conserved regions, V1-V5 variable regions. gp41: FP fusion peptide, NHR N-helix, loop, CHR c-helix, MPER membrane proximal external region TMD transmembrane domain, endodomain including cytoplasmic tail

3.6.1. Preparation of the patient serum samples

Serum aliquots were retrieved and underwent CD20 adsorption as previously described. Each serum aliquot was diluted by a factor of 1:100 with PBS and prior to adsorption with CD20-bearing yeast. This removed anti-yeast antibodies which could have caused non-specific yeast binding irrespective of HIV-gp160 antigen recognition. All serum processing was done in a containment level 2 laboratory.

The twenty patient serum sample aliquots (each aliquot = pooled serum of five participants, ten low-risk and ten high-risk) were analysed alongside experimental and biological controls. The three experimental controls were: autofluorescence, unstained and fluorescence minus one, produced as described previously. The two biological controls were lab(laboratory)/healthy control (LC) and positive control (PC). LC were from healthy HIV-negative heterosexual volunteers with minimal reported exposure to HIV infection ("healthy control") to account for background anti-HIV-1 envelope reactivity. PC were group E participants; patients with early HIV infection who had yet to begin antiretroviral medication at the time blood samples were drawn.

3.6.2. Sample preparation for HIV Envelope library analysis of seronegative aliquots

Fluorescence-activated cell sorting was used to analyse the participant serum anti-envelope response by selecting a PE high population representing yeast cells expressing surface antigen which bound serum antibodies, and all experimental analysis performed as described in the previous chapter. All samples were prepared as described in materials and methods.

The yeast library construct contained a C-terminal c-myc tag which allowed for screening of library cells to assess success of transformation and assess for differences in fragment expression; this has been demonstrated in our lab and by others (279)

Another consideration was optimal transformation of yeast cells, and how to ensure one transformant per yeast cell and not multiple. Optimal transformation conditions have been reviewed and suggest a ratio of 100µl yeast culture at OD600 of 1 with 1µg of vector DNA to give an electroporation cell density of 1.6 x 10^9 cells/ml, resulting in transformation efficacy of 3x10^7transformants, or

approximately 2%. A 1:1.5 vector/yeast cell ratio ensures efficient transformation (312). The protocol in our laboratory has been previously evaluated by selecting two colonies for sequencing to ensure results match each other; rate of sequence multiplicity was approximately 10-15%.

To set up the flow cytometry work, initial analysis was performed on seronegative samples on a BD LSRII cytometer in a CL2 laboratory. Seropositive samples were analysed on the FACS ARIA III in a CL3 laboratory.

Samples were labelled as described in 2.6.8.2. These included the three technical experimental controls (autofluoresence, unstained yeast and fluorescence minus one), biological controls (laboratory control and positive control) experimental samples of the participant sera aliquot. The gating strategy was as discussed in 2.6.8.7.

3.6.3. Initial FACS gp160 screening of serum aliquots

All twenty serum aliquots (10 low-risk, 10 high-risk) were screened by FACS using the HIV envelope gp160 yeast library and approximately 50000 cells were sorted per sample. Any serum aliquot groups with a PE positive population greater than that of the LC were considered reactive and selected for further analysis.

Results were displayed as % PE population rather than mean fluorescence intensity (MFI). MFI measures expression level of antigen and hence antibody binding, and this project reviewed all antigen/antibody and did not discriminate based on level of binding- which may have biased towards expression of surface displayed protein by yeast.

The positive control showed a large population of PE high yeast cells, in keeping with the known serostatus of that sample, shown in Figure 3.6-2. Low-risk and high-risk aliquot screening plots are shown in Figure 3.6-3, with the size of the PE high population shown above the gate. All PE high population percentages were documented as shown in Table 3.6-1, Figure 3.6-4 and

Table 3.6-2.

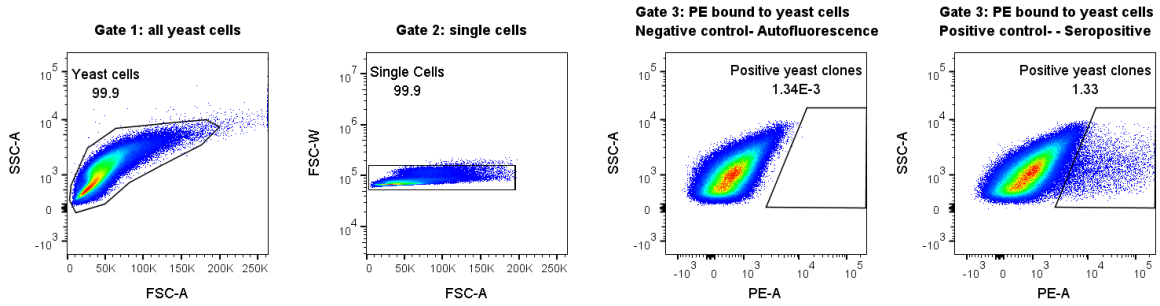


Figure 3.6-2 Controls for seronegative FACS analysis
Gate three shows technical negative control (autofluorescence) and second gate three shows positive control (seropositive serum)

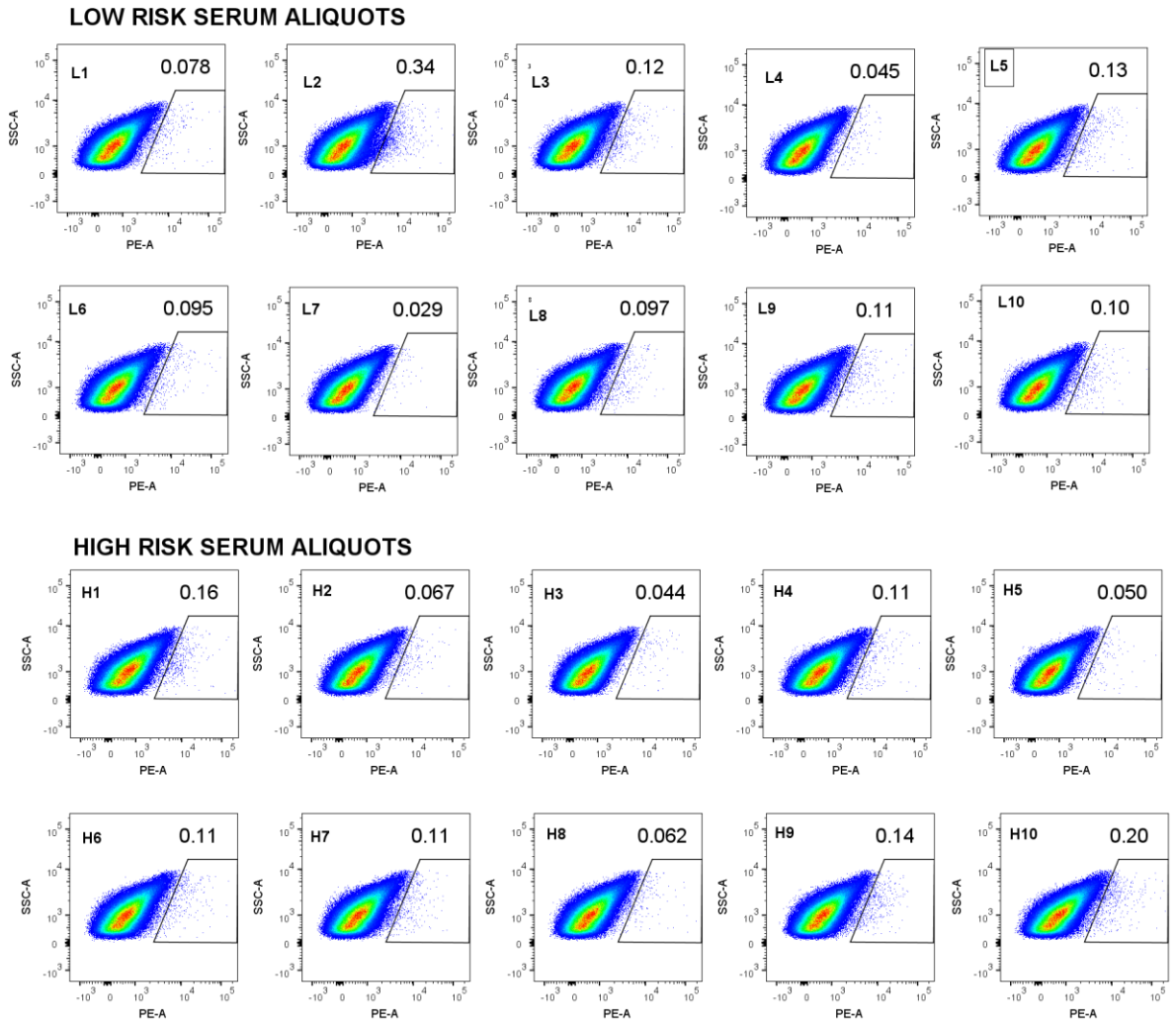


Figure 3.6-3 3 Representative flow cytometry dot plots of low and high-risk MSM sera sorted with gp160 yeast library
X axis PE, y axis side scatter area. Gate shows the PE high population and number represents size of population as percentage of total. The negative controls were autofluorescence, unstained yeast, fluorescence minus one and laboratory/healthy control (not shown here), and the positive control was seropositive serum (shown above). The low-risk serum aliquots were L1-L10, and high-risk H1-10.

Sample	PE high yeast population	Sample	PE high yeast population
Healthy control	0.00	Positive control	1.33
L1	0.08	H1	0.16
L2	0.33	H2	0.07
L3	0.12	H3	0.04
L4*	0.05	H4	0.11
L5	0.13	H5	0.05
L6	0.10	H6	0.11
L7	0.03	H7	0.11
L8	0.10	H8	0.06
L9	0.11	H9	0.14
L10	0.10	H10	0.20

Table 3.6-1 Proportion of low and high-risk MSM sera which react with gp160 yeast expressing clones
All values represent PE high percentage of total yeast population, PE high yeast population rounded to 2 decimal places

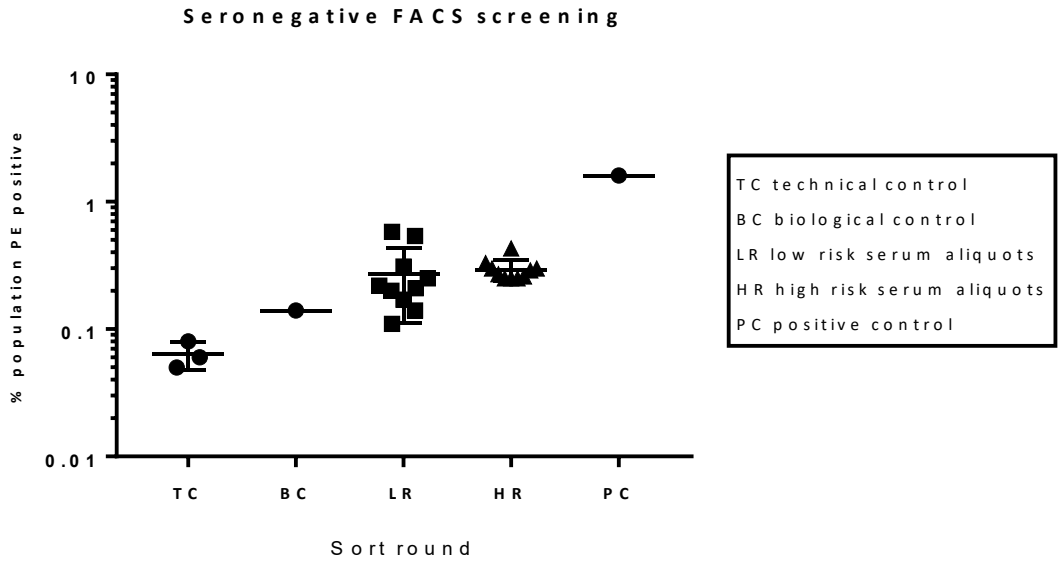


Figure 3.6-4 Mean and standard deviation (SD) of percentage of total yeast population expressing gp160 envelope library recognized by low and high-risk MSM sera
Samples grouped as follows: TC technical controls (autofluorescence, fluorescence minus one, unstained), BC biological control (lab/healthy control), LR low-risk serum aliquots L1-L10, HR high-risk serum aliquots H1- H10, and PC positive control

NB: Results displayed as PE population rather than mean fluorescence intensity (MFI). MFI measures expression level of antigen and hence antibody binding, and for this project I wished to review all antigen/antibody and not discriminate based on level of binding- which may have biased towards expression of surface displayed protein by yeast. This follows for all subsequent similar analyses.

	Mean	Standard Deviation	Number samples
Technical control	0.06	0.02	3
Biological control	0.14	NA	1
Low-risk	0.27	0.16	10
High-risk	0.29	0.06	10
Positive control	1.61	NA	1

Table 3.6-2 Mean and standard deviation (SD) of percentage of total yeast population expressing gp160 envelope library recognized by low and high-risk MSM sera
Analysis showing mean and standard deviation for PE positive populations across groups of serum samples. NA Not analysed

3.6.4. Sequential enrichment

The yield of PE high populations was assessed following each sort and the numerical value of the PE positive population recorded. Serum aliquot/yeast clone pairings with PE high populations greater than that of the technical and biological experimental controls were selected for successive rounds of flow sorting analysis. Eleven serum aliquot/yeast clones successfully enriched post first sort, five post second sort, and four post third sort. The sorted yeast populations were a refined selection of epitopes recognised by the serum aliquots, as the aim of sorting was to sort yeast clones displaying epitopes most strongly recognised by patient sera. Data from the flow cytometry analysis was plotted as percentage positive PE population per sort.

Two samples from each of the high-risk and low-risk groups enriched to yield viable populations- L6, L9, H5, and H9. The negative and positive control samples were also selected. Another sample H3 initially demonstrated a positive PE population but failed to enrich on subsequent rounds of enrichment.

These results are shown below in plots in Figure 3.6-5 and Figure 3.6-6, and the amounts plotted as a graph with PE high/positive population expressed as a percentage of the total yeast population in Figure 3.6-6. Figure 3.6-6 Mean and standard deviation (SD) of percentage of total yeast population expressing gp160 envelope library recognized by low and high-risk sera

The FACS analysis negative control was autofluorescence, and the positive control is as previously described, participant serum aliquots L1-10, and H1-10. The plots focus on those serum aliquot/yeast clone pairings with successively enriched.

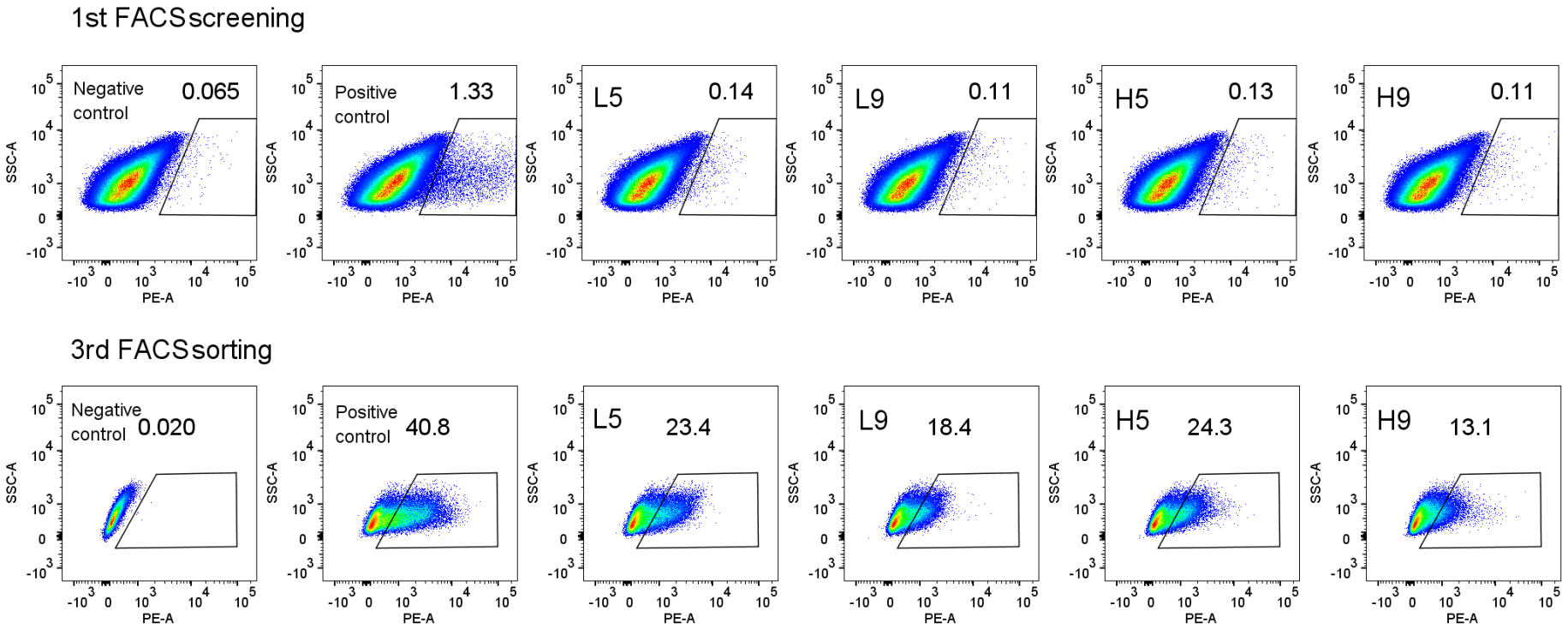


Figure 3.6-5 Serial enrichment of seronegative serum binding to the yeast gp160 envelope library following sequential FACS sorting

FACS plots showing serial enrichment of yeast library with seronegative aliquots. Negative control used is autofluorescence, positive control is seropositive patient sera. First row is FACS plot of screening sort, and second row is following two successive rounds of enrichment. The yeast is now a more refined population and better recognised by patient sera.

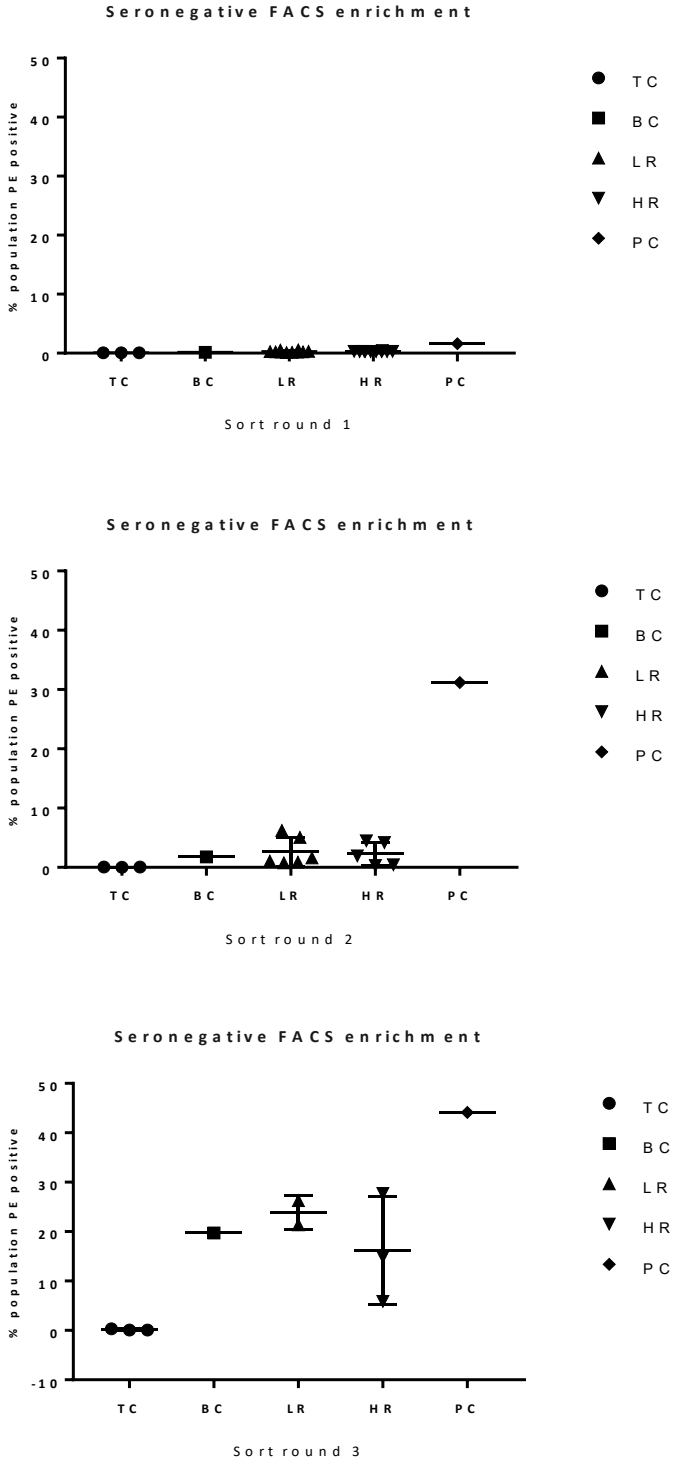


Figure 3.6-6 Mean and standard deviation (SD) of percentage of total yeast population expressing gp160 envelope library recognized by low and high-risk sera

FACS plots showing serial enrichment from initial screening analysis through successive rounds of flow sorting. TC technical controls (autofluorescence, fluorescence minus one, unstained), BC biological control (lab/healthy control), LR low-risk serum aliquots L1-L10, HR high-risk serum aliquots H1- H10, and PC positive control. X axis shows sample groups, y axis shows p population which is PE positive. Not all sorted yeast enriched and so number of aliquots sorted decreased with each sort; initial screening sort round 1 (10 LR and 10 HR), sort round 2 (6 LR and 5 HR) and sort round 3 (2 LR and 3 HR).

3.6.5. Single clone analysis

The selected sorted yeast clones underwent single clone analysis (as described in materials and methods) with the respective participant sera by flow cytometry in order to verify affinity of selected yeast populations and patient serum samples.

As described in materials and methods, the yeast library display system possesses a large number of fragments. The estimated library size is $1x10^{7-9}$. This has been estimated previously in the literature by using a selection process using FACS and polyreactive single chain variable fragments whereby reactive clones are eliminated from a positive population and the total library size estimated based on the remaining population (313).

By mixing the library with patient serum samples, it allows antibody-epitope binding, and selection of only those yeast cells to which antibody has attached. Sequence analysis of the selected population suggests which antigenic domain is recognised by patient antibodies.

Single yeast clones were selected from a post sort SDCAA plate to obtain a population of homogenous yeast cells bearing a common epitope of the HIV envelope protein. These populations were then used for analysis with the respective patient serum. By using approximately sixteen individual clones from each patient group, the aim was to produce a diverse group of epitopes to review antigenic regions responsible for the serum recognition and to determine discrete epitopes in addition to the major antigenic domain (MAD) revealed by overall family sequence analysis.

Sorted yeast clones underwent single clone analysis (as described in materials and methods) with their respective patient serum samples by flow cytometry. A 96-well plate was used to facilitate bulk analysis. Sixteen individual clones were picked from each sorted yeast SDCAA plates and cultured in liquid SDCAA and SGCAA as previously described.

Single clone population histograms were defined as positive if the peak population was greater than that of negative/healthy controls, indicating the serum had selected epitopes of interest greater than

that of background interest. Any clones identified as positive in this fashion were selected for downstream DNA extraction and sequence analysis to identify epitopes of interest. The following groups underwent single clone analysis- L6, L9, H5, H9. Sixteen individual clones were picked from each sorted yeast SDCAA plates. They were cultured in liquid SDCAA and SGCAA as previously described in a deep well 96 well plate as shown in Figure 3.6-7.

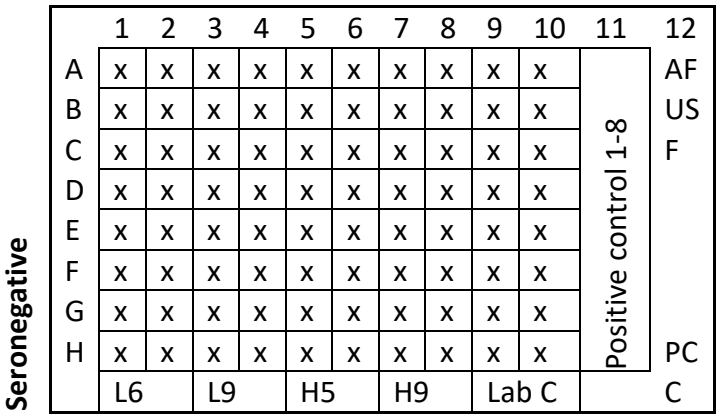


Figure 3.6-7 FACS plate analysis
96 well plate with selected yeast clones for analysis by flow cytometry

The gating strategy for the single clone analysis was as previously described and is shown in Figure 3.6-8. Also shown are negative and positive controls, and the third sorting gate depicted both as plot and histogram. For the experiment setup, the three technical controls were used (autofluorescence, unstained, fluorescence minus one) and a biological control (negative healthy/laboratory control, positive control Group E early HIV infection).

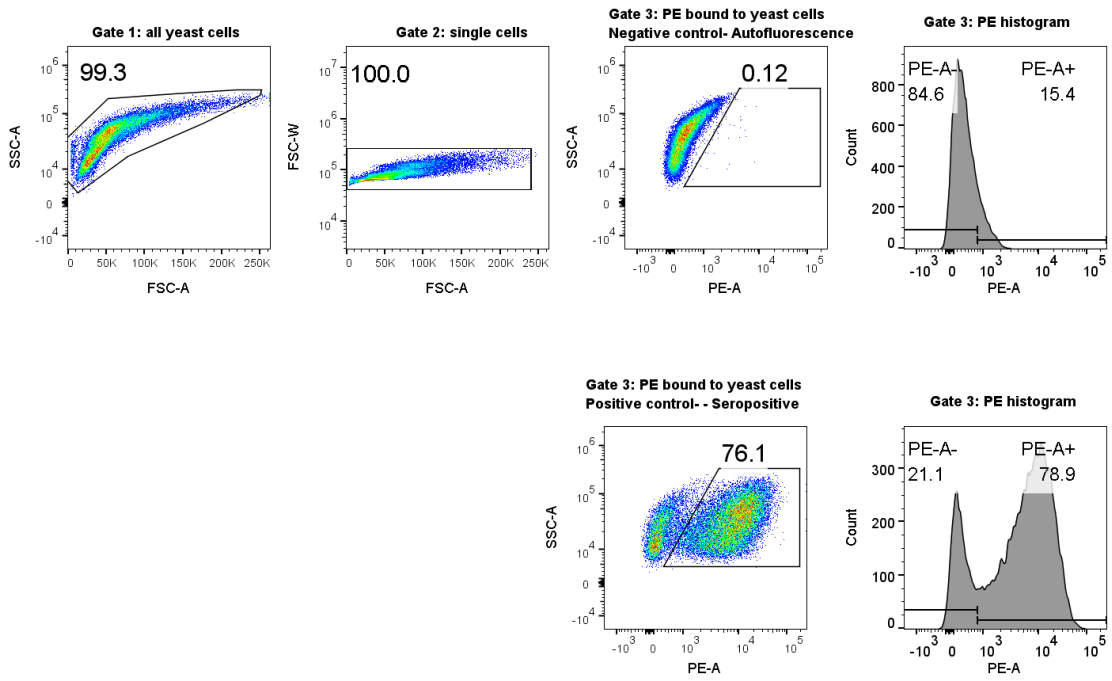


Figure 3.6-8 Flow cytometric analysis of single yeast clones
Gating strategy and histograms showing selection of positive single clones as compared to negative and seropositive controls

The histograms for the single clone analysis indicated affinity of various yeast and serum combinations for the yeast library. The peak shifting towards the right axis indicates increasing amount of yeast-bound PE tagged serum antibody and hence affinity of epitope bearing yeast for patient serum antibodies. Any single clones with PE positive populations greater than that of the laboratory controls were selected for further analysis.

L6, L9, H9 and the positive control sample (see Table 3.6-3 below) serum aliquot/yeast clone pairings showed PE high populations greater than the healthy control serum. The histograms for this section are shown in Figure 3.6-9. Those with PE high populations greater than the technical control were selected for DNA extraction and sequencing as previously described.

The positive population in the healthy lab control was thought to represent epitope recognition by antibodies which recognise some Env structures, perhaps by molecular mimicry and exposure to other non-HIV structurally similar epitopes, as suggested in previously published literature (260,263).

Sample	No. samples with a PE yeast population greater than technical control	Selected for sequence analysis
BC	8/16	Yes
PC	10/13	Yes
L6	13/16	Yes
L9	11/16	Yes
H5	6/16	No
H9	9/16	Yes

Table 3.6-3 Number of single clones which bind to yeast gp160 envelope library
Samples with a PE yeast population greater than negative controls and which ones were selected for further sequence analysis. BC biological control- lab/healthy control, PC seropositive control

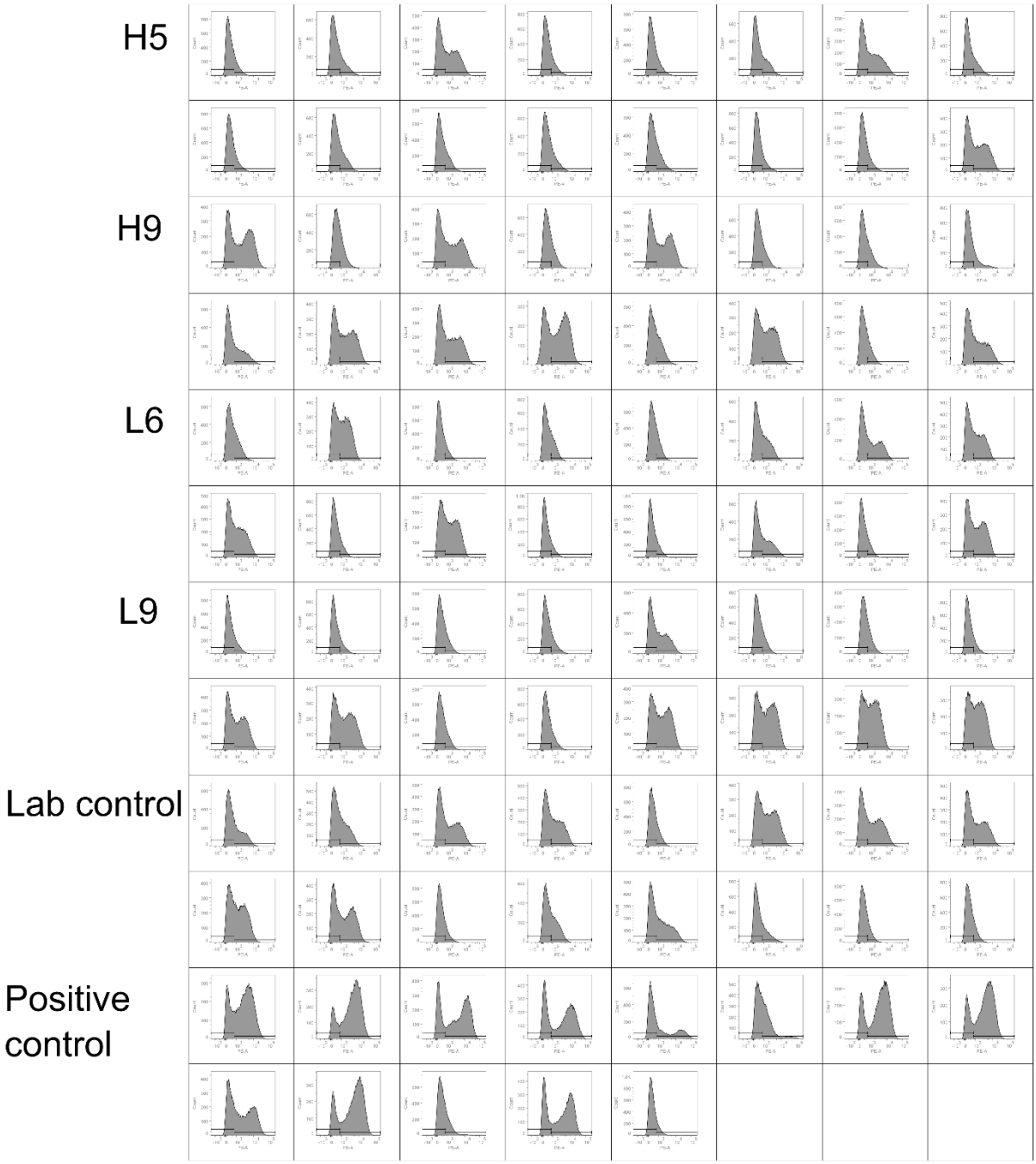


Figure 3.6-9 Histograms of single yeast clones which bind to the gp160 envelope library
Histograms showing PE positive populations of H5, H9, L6, L9 and biological (lab) and positive controls with gp160 refined yeast clone population. 16 plots shown for each member (13 shown for positive control). X axis- PE, y-axis count (1000)

3.6.6. Sequential enrichment summary

The purpose of selectively culturing the sorted yeast population chosen by serum antibodies was to create a refined yeast population bearing a specific set of antigens, and interrogate this yeast population to characterise any major antigenic determinants selected by patient serum.

Low-risk: samples with a yeast PE high population greater than the laboratory control were selected from low-risk flow cytometry plots. A degree of non-specific yeast antibody binding was expected despite the CD20 yeast adsorption of serum and so the biological control attempts to account for this. The following samples qualified and were prepared for a second round of enrichment: L3, L4, L6, L7, L9 and L10. The laboratory and positive control samples were also selected for enrichment.

From second round sorting, the laboratory control yeast PE high population was again chosen as the baseline for comparison for serum aliquots considered to respond to yeast displayed antigen. The samples with a greater yeast PE population were L6 and L9. Again, laboratory and positive controls were also selected for culture and enrichment. All four samples underwent enrichment. For the experimental serum aliquots, this yielded a yeast high PE population of 21-27% of the total.

High-risk: a similar strategy to that described above was used for selecting positive yeast populations from high-risk flow cytometry plots. The following samples qualified and were prepared for a second round of yeast culture and analysis: H3, H5, H6, H8, H9. Control samples were again selected for enrichment.

From second round sorting, the samples with a yeast high PE population were H3, H5, H9. Laboratory and positive control were also selected for enrichment. All five samples underwent another round of culture and sorting, and all but H3 enriched successfully. Experimental serum aliquots yielded a positive population of 14-28% of the whole yeast population. In summary, five candidate serum aliquots enriched with subsequent rounds of flow cytometry- L6, L9, H3, H5, H9 as shown in Table 3.6-4.

Sample		Sort			Single clone analysis
		1	2	3	
Control	AF	0.06%	0.05%	0.05%	
	US	0.08%	0.07%	0.33%	
	FMO	0.05%	0.02%	0.05%	
	LC	0.14%	1.77%	**19.70%**	**50.0%**
	PC	1.61%	31.20%	**44.10%**	**76.9%**
Seronegative participant group = pool of 5 participants	L1	0.11%			
	L2*	0.58%			
	L3	0.25%	1.07%		
	L4	0.22%	0.90%		
	L5	0.14%			
	L6	0.21%	5.05%	**26.30%**	**56.25%**
	L7	0.31%	1.59%		
	L8	0.17%			
	L9	0.20%	6.23%	**21.40%**	**56.25%**
	L10	0.54%	0.75%		
	H1	0.25%			
	H2	0.25%			
	H3	0.33%	1.93%	**5.87%**	
	H4	0.27%			
	H5	0.43%	4.18%	**27.70%**	**25.00%**
	H6	0.29%	0.31%		
	H7	0.26%			
	H8	0.30%	0.42%		
	H9	0.30%	4.47%	**14.90%**	**43.75%**
	H10	0.25%			

Table 3.6-4 Summary sequential FACS sorting and single yeast clone analysis
Table shows successive enrichments of HIV envelope yeast library by serum aliquot pools. Controls LC biological control, PC seropositive control. * L2 sample not viable for further analysis after first round of enrichment. Threshold for selection based on each sample's ability to enrich, all samples considered.

3.6.7. Sequence analysis plots

Positive yeast populations were selected for further analysis. Following post sort cell resting, yeast cultures were cultured on SDCAA agar plates (for single clone selection) and liquid SDCAA culture for DNA extraction and sequencing. DNA was used to transform chemically competent Dh5 alpha cells Chemically competent Dh5 alpha cells were transformed with yeast DNA and the cell line was cultured and selected as per materials and methods. Sequences were obtained from the reference laboratory and analysed using Sequencher v4.92 (Genecodes Corporation) as described in materials and methods.

Figure 3.6-10 below shows returned yeast clone DNA sequences aligned to the parent gp160 sequence. Approximately 50 clones post culture were selected for sequencing for each of the four analysed experimental serum aliquot/yeast clone pairings along with clones from the positive control. The yield of interpretable sequences was 30-40 per group, with the remainder unreadable or corrupted. As mentioned, H5 failed to enrich as was not sent for sequence analysis. This left L6, L9, H9, and positive control sequences available for review. All three experimental samples sequences demonstrated recognition of HIV-gp160 epitope as demonstrated below in the figures showing sequences aligned to gp160.

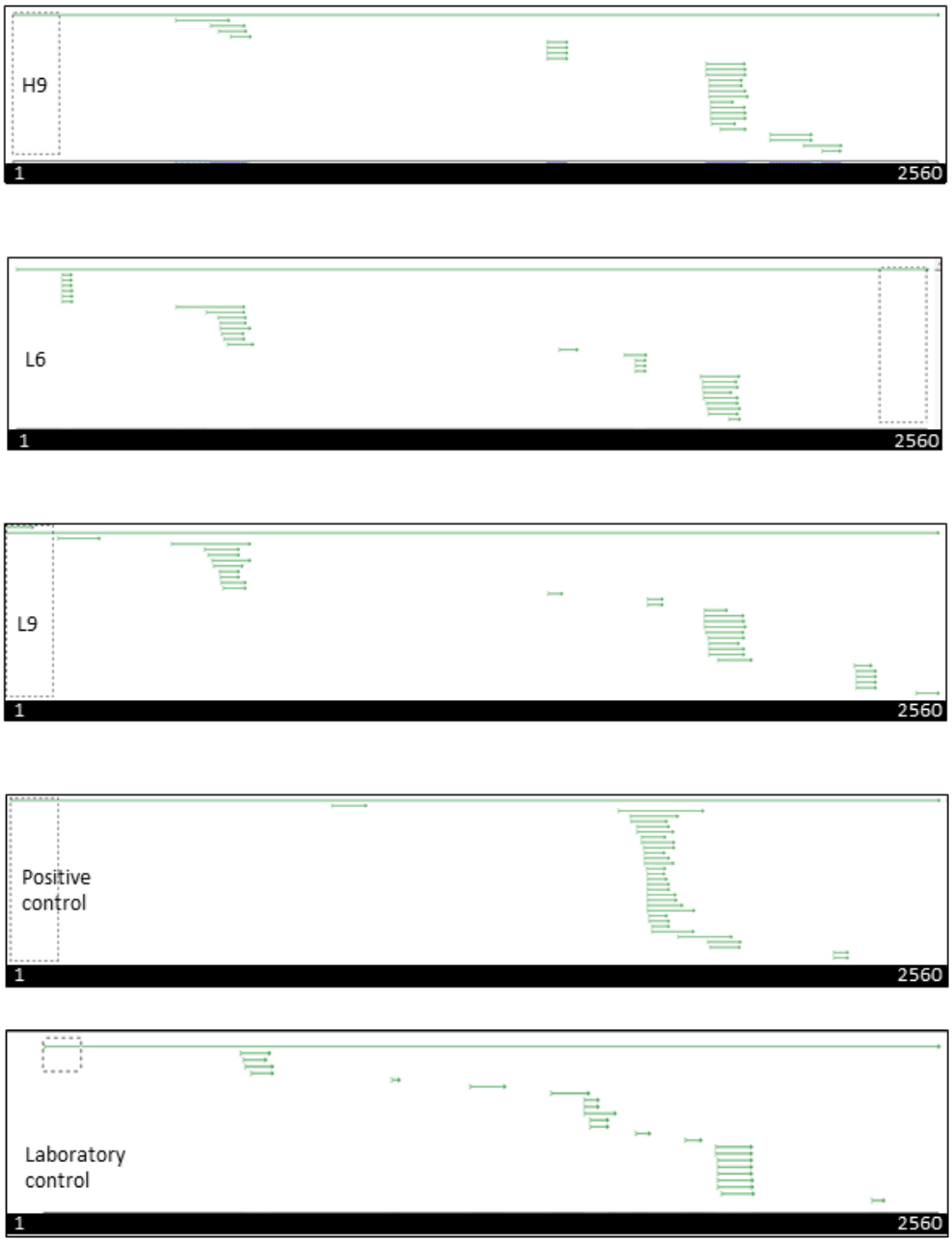
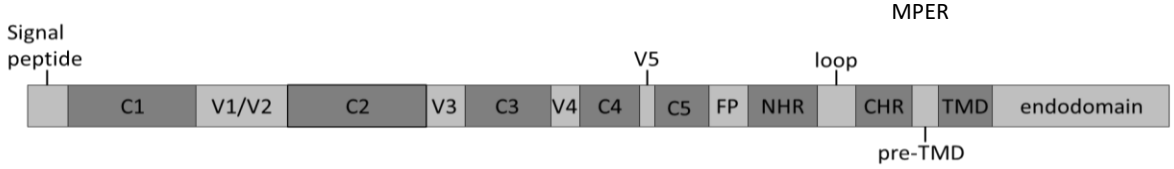


Figure 3.6-10 Sequences aligned to gp160 parent sequence



L6, L9, H9 and positive control yeast clone DNA sequences Analysed fragments in green, black strip 1-2560 represents gp160 reference sequence (HXB2, www.hiv.lanl.gov as previously). HIV gp160 schematic shown underneath x axis for reference purposes. HIV envelope sequence with initial gp120 components: signal peptide C1-C5 conserved regions, V1-V5 variable region. gp41 components: FP fusion peptide, NHR N-helix, loop, CHR c-helix, MPER membrane proximal external region, TMD transmembrane domain, endodomain

3.6.8. Sequence analysis histograms

Returned sequences were aligned to the parent HIV-1 envelope sequence. An algorithm was used to determine frequency of amino acid residues recognised by serum aliquots (282) and the results plotted as a histogram for healthy and positive controls, low-risk and high-risk.

The curve produced by the histogram was considered significant for epitope recognition if distributed in a Gaussian fashion. Therefore, an epitope was defined as any cluster of residues where the peak amino acid frequency was greater than or equal to five, distributed in a Gaussian fashion.

Once identified, the AUC of this region was calculated as a proportion of the total AUC for the histogram (representing all fragments identified). The proportion of the AUC for each cluster/epitope was calculated as a percentage of total number of cluster/epitopes recognized in low and high-risk sera.

3.6.8.1. Discrete epitope recognition

The positive control group seropositive serum recognised one discrete epitope gp41, in keeping with known early anti-HIV antibody responses. Healthy control serum recognised two epitopes in gp41, with other non-significant areas in gp120.

Low-risk L6 group serum recognised regions of two regions of gp120 and one in gp41. For epitope 2, only the Gaussian curve portion of the AUC frequency was considered, and the left sided tail omitted from calculations. L9 group serum recognised regions of both gp120 and gp41.

High-risk H9 group seronegative serum recognised two regions; one in gp120 and one in gp41.

The patterns of the high and low-risk serum were similar but different to the patient or healthy control. This may have been due to low level exposure to HIV epitopes which has not resulted in infection. This differed from the positive control samples from known early HIV infected patients, with a predominantly gp41-directed antibody response. There was some overlap between the LR/HR samples and the healthy control, suggesting similarity across the three seronegative groups. This is

shown in figure 3.6.12 where all seronegative samples recognise the similar gp120 and gp41 epitopes- aa151-224 (V1V2, C2 regions) and aa640-694 (C-helical region, MPER).

These findings are shown in Figure 3.6-11 and Figure 3.6-11, and the relevant findings for epitopes summarised in Table 3.6-5. For summary analysis, the two low-risk samples were analysed together. This is shown along with the other control and experimental samples in Figure 3.6-12.

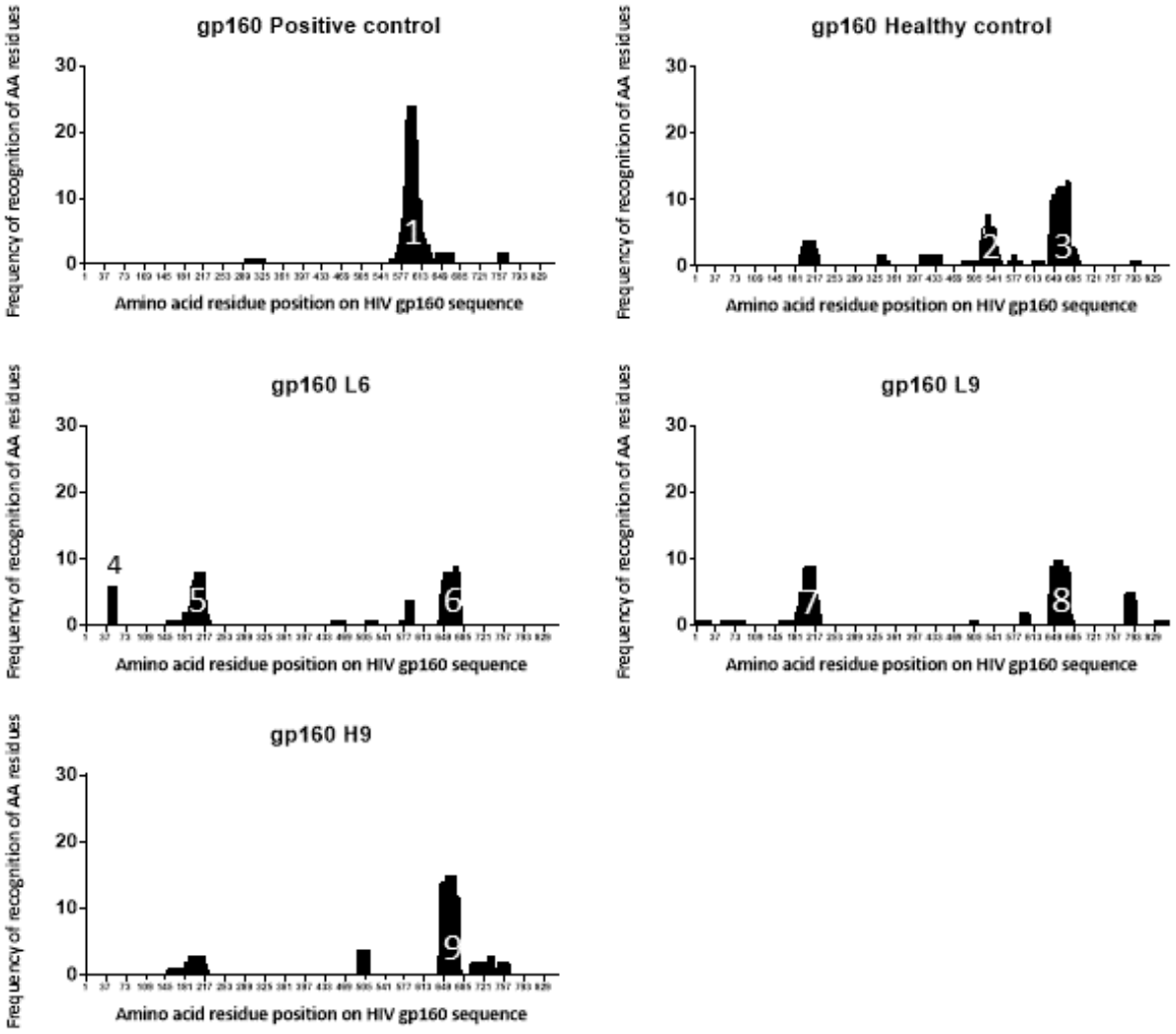


Figure 3.6-11 Histograms of gp160 library sorted by serum samples:
Histogram showing amino acid frequency at each position on the HIV-1 gp160 parent sequence as recognised by positive control, healthy control, low-risk serum aliquots L6 and L9, and high-risk serum aliquot H9. X axis is amino acid residue position on HIV gp160 sequence, y axis is frequency of recognition of amino acid residue. Epitopes denoted by figures on histogram. Regions of the histogram considered significant for epitope if residue frequency greater than five

	Epitope	Total residues	Location	Start	Finish	Length of sequence in (AA residues)	AUC (total AA in epitope)	AUC as % of total fragment residues	Epitopes	Sequence
PC	1	817	gp41	559	637	79	695	85.1%	N helical region, Loop, C-helical region (gp41)	DQQLLGIWGCSGKLICTTAVPWNASWSNKSLEQIWNHTT WMEWDREINNYTSLIHSLIEESQNQQEKNEQELLELDKWA
HC	2	885	gp120 gp41	485	551	67	197	22.3%	C5 (gp120) Fusion protein, N helical region (gp41)	IGALFLGFLGAAGSTMGAASMTLTVQARQLLSGIVQQQN NLLRAIEAQQHLLQLTVWGIKQLQARIL
	3	885	gp41	641	694	54	432	48.8%	C-helical region (gp41) Membrane proximal external region,	NWFNITNWLWYIKLFIMIVGGLVGLRIVFAVLSIVNRVRQG YSPLSFQTHLPTP
L6	4	668	gp120	44	53	10	60	9.0%	C1 (gp120)	CVPTDPNPQE
	5	668	gp120	151	223	73	251	37.6%	V1V2, C2 (gp120)	IIPIDNDTTSYKLTSCNTSVITQACPKVSFEPIPIHYCAPAGFAI LKCNNKTFNGTGPCTNVSTVQCTHGIRP
	6	668	gp41	641	678	38	266	39.8%	C helical region Membrane proximal external region (gp41)	NWFNITNWLWYIKLFIMIVGGLVGLRIVFAVLSIVNRV
L9	7	835	gp120	152	224	73	282	33.8%	V1V2, C2 (gp120)	IPIDNDTTSYKLTSCNTSVITQACPKVSFEPIPIHYCAPAGFAI LKCNNKTFNGTGPCTNVSTVQCTHGIRPV
	8	835	gp41	640	683	44	332	39.8%	C helical region Membrane proximal external region (gp41)	WNWFNITNWLWYIKLFIMIVGGLVGLRIVFAVLSIVNRVR QGYS
H9	9	814	gp41	640	678	39	470	57.7%	C helical region Membrane proximal external region (gp41)	WNWFNITNWLWYIKLFIMIVGGLVGLRIVFAVLSIVNRV

Table 3.6-5 5 Summary of findings for gp160 envelope epitopes detected in LR and HR sera

Epitopes as numbered in previous diagram, total residues of all retrieved sequence fragments, location of epitope as AA position on HIV gp160 parent sequence, start and finish of epitope, length of sequence (AA residues), AUC (area under the curve) total AA content for each epitope, AUC as % of total fragment residues, epitopes described as recognised location on gp160 parent sequence. PC positive control, HC healthy control.

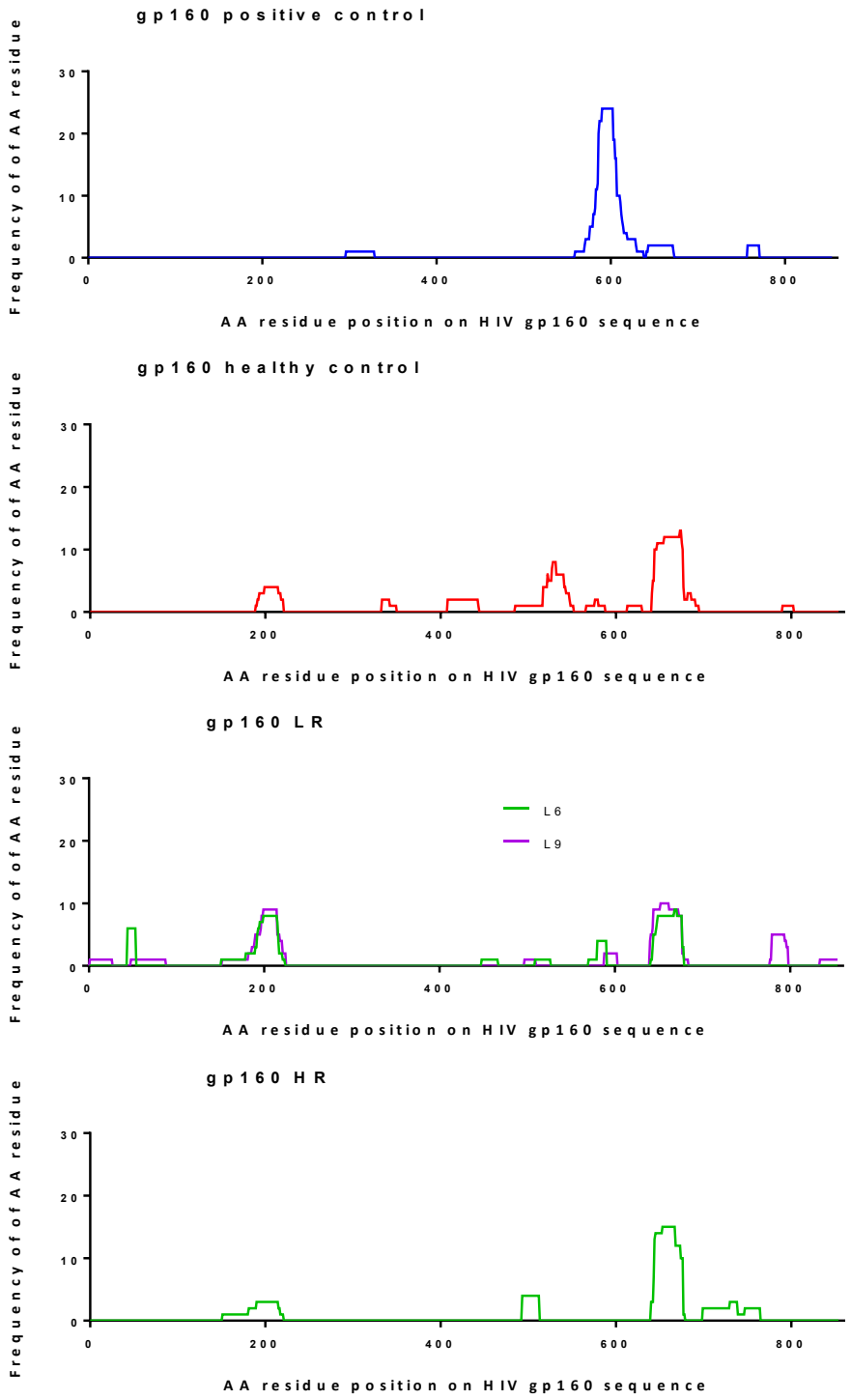


Figure 3.6-12 HIV gp160 library sorted by seronegative serum samples

On closer inspection, there are two key features of epitope recognition in gp120 and gp41. By overlaying all seronegative histogram curves and comparing to the positive control in Figure 3.6-13 below, there are epitopes recognised by all seronegative samples- laboratory control, L6, L9 and H9.

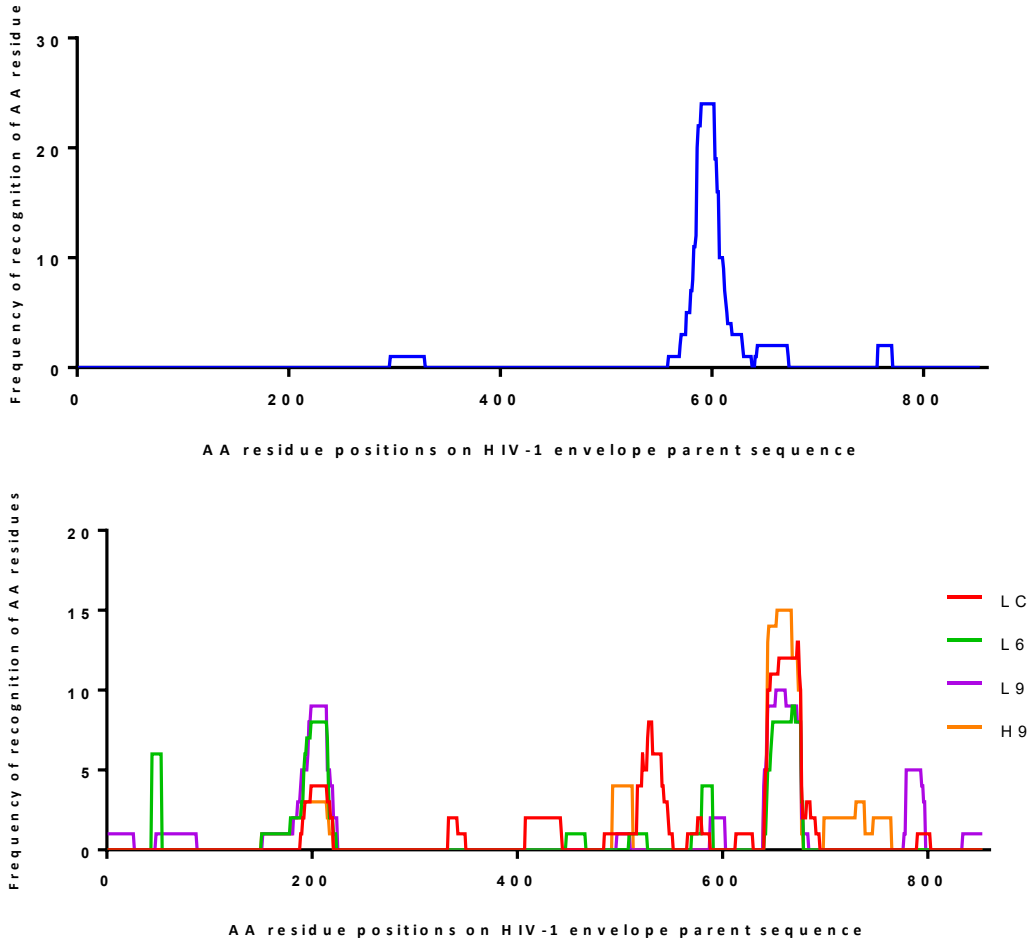


Figure 3.6-13 Overlay of HIV-1 amino acid sequences detected in HSEN and laboratory control
X axis shows residue position on gp160, y axis shows frequency of recognition at that position. PC positive control, LC laboratory or healthy control. Experimental samples L6, L9 and H9.

The gp120 region recognised by all seronegative samples spans the residue positions 151-223. This region corresponds to a portion of the V1V2 epitope (69 AA, 127 – 195) and the C2 epitope (104 AA, 196 – 299).

The gp41 region recognised by all seronegative samples spans three epitopes from position 640 to 694. These are the C-helical region (42 AA, positions 622 to 663), the Membrane proximal external region (20 AA, position 664 – 683) and the transmembrane domain (40 AA, 684 – 723).

3.6.9. Single clone analysis of individual participant serum

In order to review the validity of this epitope recognition, selected gp160 yeast clones were reviewed with individual patient serum aliquots. Recalling that each aliquot consisted of five individual participant serum samples, these individual serum samples were retrieved from storage and prepared them with yeast adsorption as previously described. Yeast clones which produced greatest PE high populations during single clone analysis were selected and analysed with individual patient serum samples using FACS as previously described using the same gating and controls.

As all yeast clones had their sequence DNA extracted and sent for analysis, which enabled identification of antigen sites selected by the individual participant serum samples.

For low-risk serum analysis, the aliquot L9 with the individual serum samples from participants A0170, A0173, A0182, A0183, A0188 was selected. The low-risk yeast clones L9-05 and L9-06 were selected for analysis. These clones both spanned the gp120 amino acid sequence 182-214, representing gp120 V1V2 and the C2 region. Low-risk serum samples recognised L9-05 most frequently, with all five demonstrating a PE high population greater than the control (5/5). Only 2 of the 5 serum samples recognised L9-06. What was the difference between L9 05 and L9 06

L9-05 was recognised by the first four serum aliquots (A0170, A0173, A0182, A0183) with minimal recognition by the fifth group member (A0188).

For the high-risk MSM serum analysis, the aliquot H9 was selected from individual participant serum samples from A0163, A0166, A0180, A0181, A0190. Two high-risk yeast clones H9-01 and H9-16 were selected. H9-01 spanned the amino acid sequence 653-676, and H9-16 aa644–676, both corresponding to the gp41 C-helix and membrane proximal external region. High-risk serum samples recognised both H9-01 and H9-16, with all five aliquot members demonstrating a PE high population greater than the control (5/5) for both clones.

The FACS plots and histograms for these analyses are shown in Figure 3.6-14 and Figure 3.6-15.

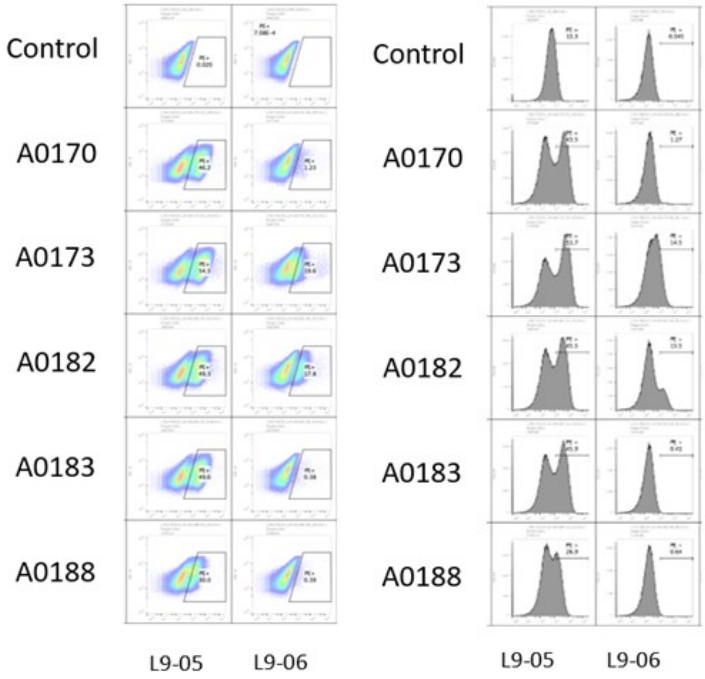


Figure 3.6-14 FACS plot and histograms individual serum from low-risk gp160 single clone analysis- low-risk
Control is technical control autofluorescence, five individual serum samples analysed with low-risk clones L9-05 and L9-06, represent gp120 epitopes V1V2 and the C2 region. FACS plot X axis is PE population, y axis is SSC-A. Histogram X axis is PE population, y axis is count (1000)

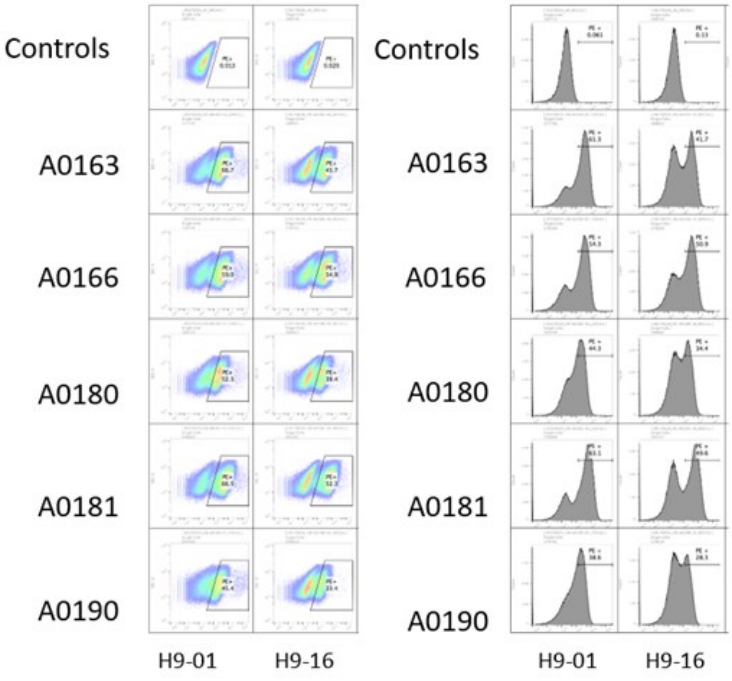


Figure 3.6-15 FACS plot and histograms individual gp160 single clone analysis- high-risk
Control is technical control autofluorescence, five individual serum samples analysed with low-risk clones H9-01 and H9-16, represent gp41 C-helix and membrane proximal external region. FACS plot X axis is PE population, y axis is SSC-A. Histogram X axis is PE population, y axis is count (1000)

3.6.10.Summary of HIV gp160 epitope recognition

All control and experimental samples recognised epitopes on gp160.

3.6.10.1. Histogram review- individual

Healthy controls showed low levels of HIV envelope recognition across the whole sequence (sequence histograms Figure 3.6-11, flow data not shown). Positive control serum sample demonstrated a strong recognition of the gp160 epitope sequence, predominantly the gp41 sequence as would be expected in early infection.

Low-risk serum analysis (L6 and L9) demonstrated recognition of epitopes across the entire HIV envelope sequence (sequence histograms Figure 3.6-11, flow data not shown). The L6 serum aliquot recognised two epitopes, one in gp41 and two in gp120. The L9 serum aliquot recognised two epitopes, one in gp120 and one in gp41.

High-risk serum analysis (H9) showed one major peak on the histogram of sequences at gp41, and low level recognition of gp120 which did not meet significance for classification as an epitope. The second high-risk sample H5 did not successfully enrich and was not available for further analysis.

3.6.10.2. Histogram review- overlaid

When the sequence histograms are overlaid, there was consistent recognition of gp120 and gp41 epitopes- C2 region and C-helical, membrane proximal external region and transmembrane domain respectively.

3.6.10.3. Individual serum single clone analysis

Analysis of individual serum responses confirmed seronegative serum recognition of the epitopes identified by grouped aliquots. Low-risk individual serum identified V1V2 and C2 region of gp120, and high-risk serum identified the C helical region and membrane proximal external region of gp41.

The single clone analysis used yeast clones which had produced greatest PE populations during successive sorting rounds. The reasons for this selection were to try and ensure selected clones would

be recognised by the patient sera responsible for their enrichment, and to validate the yeast/serum pairings by demonstrating binding of serum to yeast clones.

For the low-risk samples, all five patient serum samples were assessed with the yeast clones L9-05 and L9-06, both mapping to an amino acid sequence 182-214 representing V1V2 and C2 region. From the low-risk samples, A0170, A0173, A0182, A0183, and to a lesser extent A0188 serum showed binding to yeast clone L9-05. When L9-06 was assessed, only A0173 and A0182 showed significant binding to this clone. This suggests poorer quality epitope display by L9-06. It also raises the possibility that individual patient serum samples in one batched aliquot could influence that aliquot's binding to yeast epitopes, and overrepresent the significance of the result for this aliquot.

High-risk patient serum samples were assessed for binding to yeast clones H9-01 and H9-16 (aa653-676 and aa644-676 respectively), both mapping to gp41 C-helical region and MPER regions. All five serum samples showed binding to both H9-01 and H9-16, suggesting reliable epitope display in both yeast clones, and presence of antibody-recognised epitopes was demonstrated to occur on individual as well as batched level. As all HR patient serum samples bound yeast clones, it suggests the HR epitope recognition is due to all aliquot members rather than individuals influencing results.

3.6.10.4. Conclusion

From this data, humoral responses to Env epitopes were present in participant sera, and seen in healthy unexposed, low and high HESN. These findings would not be expected to influence standard HIV serology testing, as HIV serology tests use a standard combination of denatured epitopes, including gp120 and 41, but also a variety of other HIV proteins which were not reviewed here (314).

3.6.10.5. Low-risk vs high-risk serum immune responses

For this section of analysis, the AUC of fragment sequences located in either gp120 or gp41 was calculated for each of the low and high-risk collated histograms. The proportion of discrete regions identified by the low and high-risk serum aliquot pools was reviewed.

The proportions of selected fragments were compared and demonstrated a greater recognition of the HIV-Env gp41 epitope by healthy control serum, high-risk participant sera and positive control serum. The proportion of either gp120 or gp41 fragments recognised by low-risk serum was similar. This is shown below in Table 3.6-6 and Figure 3.6-16.

	gp120	gp41
Healthy control	25.6%	74.4%
Positive control	4.0%	96.0%
Low-risk MSM	49.8%	50.2%
High-risk MSM	25.4%	74.6%

Table 3.6-6 Proportions of fragments recognising discrete region of HIV-1 envelope
Table shows the proportions of fragments from the control and experimental samples. Low-risk MSM analysis from two aliquots, high-risk MSM analysis from one aliquot

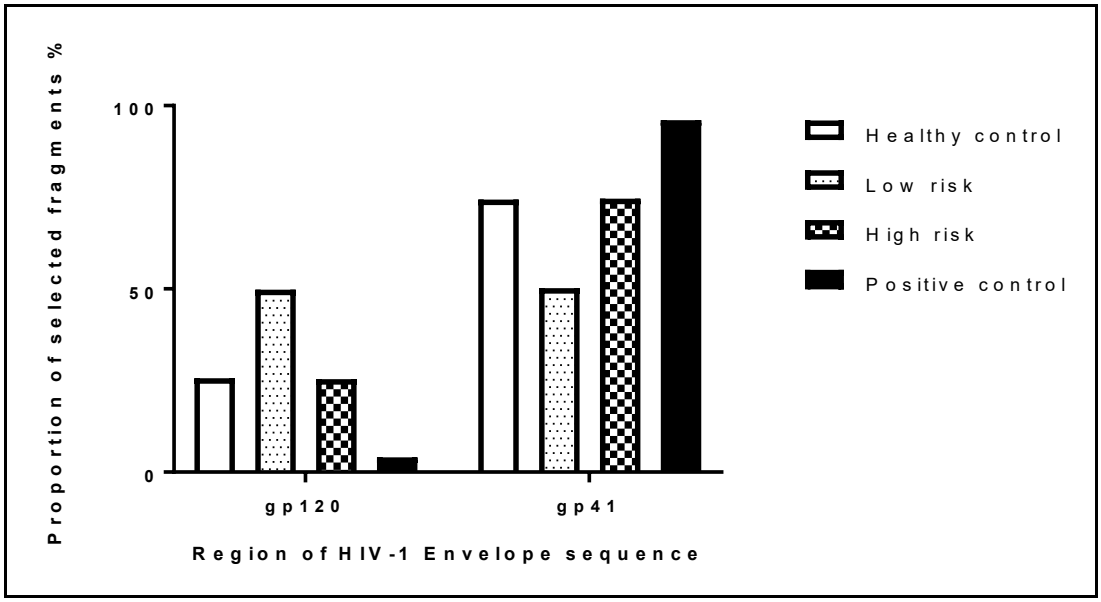


Figure 3.6-16 Figure 3.6 16 Proportions of fragments recognising discrete region of HIV-1 envelope
Frequency displayed as discrete area on parent sequence. Proportions of each area recognised expressed as percentage of total fragments. Gp41 to 120

The next part of this chapter describes analysis of the gp41 epitope recognition in greater detail. The focus on gp41 epitope recognition was because results from gp160 library screening suggested overall greater recognition of gp41 epitopes as compared to gp120 by all seronegative samples, and previously published data on pre-existing anti-HIV humoral responses suggested cross reactivity of gp41 and host intestinal microbiota (264).

3.7. HIV gp41 library analysis of seronegative serum aliquots

As described in the introduction to this section, anti-envelope responses have been reported in HIV exposed seronegative persons. From the initial work in this part of the study, a greater proportion of fragments from high-risk participants recognised gp41 antigens, whereas for low-risk participants there was no difference in frequency of recognition of gp120 versus gp41 epitopes. To further explore the role of gp41, the participant serum aliquots were reanalysed with a gp41 yeast surface display library (combined big and small libraries), to further evaluate the serum immune response to gp41

3.7.1. Aims

1. Review the role of the gp41 HIV envelope antigen in highly exposed seronegative immune responses

2. Characterise this response in terms of epitopes

3. Review any variations in anti-gp41 responses between low and high-risk participants.

Responses to HIV-1 envelope protein gp41 subunit in low and high-risk MSM serum aliquots were reviewed. The same serum aliquots were used (low-risk 1-10, high-risk 1-10) and the gp41 yeast library construct was used for analysis.

Figure 3.7-1 below shows a schematic of the HIV gp41 genome structure with regions of interest.

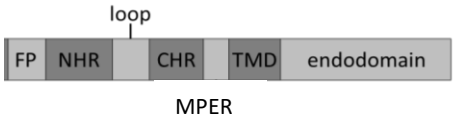


Figure 3.7-1 HIV gp41 sequence schematic
FP fusion peptide, NHR N-helix, loop, CHR c-helix, MPER (membrane proximal external region), TMD transmembrane domain, endodomain. Numbers 0/100/200/300 indicate amino acid residue position

3.7.2. Sample preparation for HIV gp41 library analysis of seronegative serum aliquots

FACS analysis was used to explore participant serum anti-gp41 responses in a similar fashion to that described for anti-HIV envelope responses by selecting a PE high yeast population.

Participant serum aliquots were prepared with the HIV gp41 yeast library construct as described. All seronegative samples were initially analysed on the BD LSRII in the CL2 laboratory, and seropositive samples analysed on the FACS ARIA III in a CL3 laboratory. Flow controls consisted of three technical experimental and two biological control samples. The gating strategy was designed to select yeast cells bound to patient serum and was the same as described previously. All twenty serum aliquots (10 low-risk, 10 high-risk) were again screened by flow cytometry for PE-high populations. Approximately 50000 cells were sorted per sample.

3.7.3. Initial FACS gp41 screening of serum aliquots

All twenty serum aliquots (10 low-risk, 10 high-risk) were screened and all showed a PE positive population. Approximately 50,000 yeast cells were sorted by the BD FACS Aria into SDCAA and pen/strep collection media. All samples were rested in an incubator for one hour post sorting before transfer to SDCAA plates and liquid media for culture as previously described.

Double positive yeast and PE population proportions were reviewed, and serum aliquot groups with a PE high yeast population greater than healthy negative controls were considered reactive and selected for further analysis. The positive control showed a large population of PE high yeast cells, in keeping with the known serostatus of that sample.

Low-risk and high-risk aliquot screening plots are shown in Figure 3.7-2 with the size of the PE high population shown above the gate. All PE high population percentages were documented as shown in Table 3.7-1, Figure 3.7-3, and Table 3.7-2.

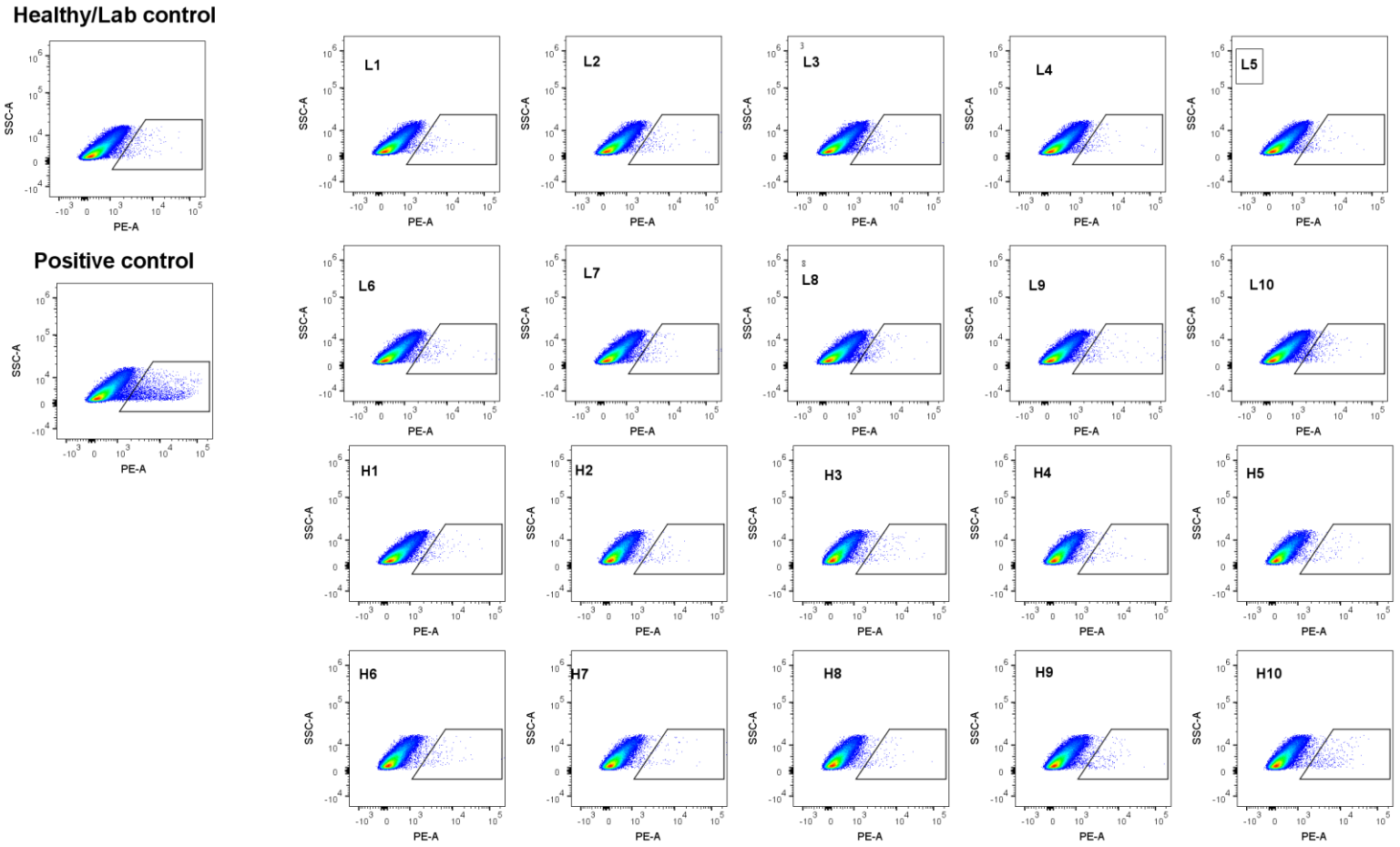


Figure 3.7-2 Representative flow cytometry dot plots of low and high-risk MSM sera sorted with gp160 yeast library

X axis PE, y axis side scatter area. Gate shows the PE high population and number represents size of population as percentage of total. The negative controls were autofluorescence, unstained yeast, fluorescence minus one (not shown here) and laboratory/healthy control (shown here), and the positive control was seropositive serum (shown above). The low-risk serum aliquots were L1-L10, and high-risk H1-10.

Sample	PE high yeast population	Sample	PE high yeast population
Healthy control	0.13%	Positive control	1.89%
L1	0.20%	H1	0.30%
L2	0.60%	H2	0.20%
L3	0.70%	H3	0.40%
L4*	0.40%	H4	0.20%
L5	0.30%	H5	0.70%
L6	0.60%	H6	0.30%
L7	0.30%	H7	0.20%
L8	0.80%	H8	0.20%
L9	0.30%	H9	0.30%
L10	0.70%	H10	0.30%

Table 3.7-1 Proportion of low and high-risk MSM sera which react with gp41 yeast expressing clones
All values represent PE high percentage of total yeast population, PE high yeast population rounded to 2 decimal places

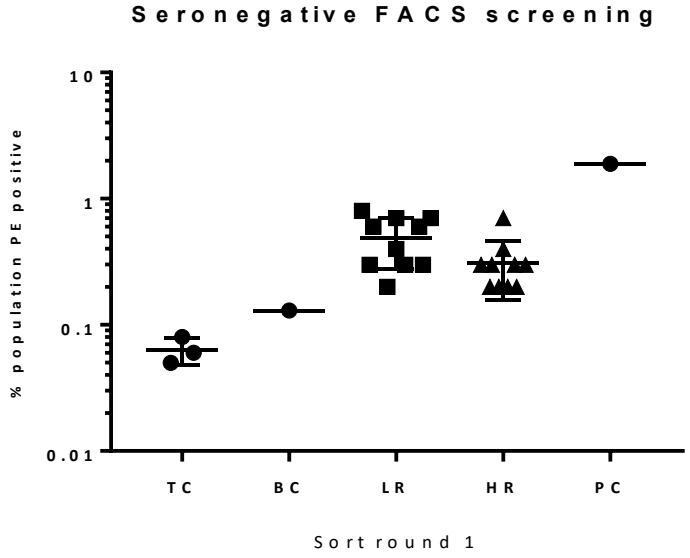


Figure 3.7-3 Mean and standard deviation (SD) of percentage of total yeast population expressing gp41 envelope library recognized by low and high-risk MSM sera
Analysis showing PE positive populations of samples. Samples grouped as follows: TC technical controls (autofluorescence, fluorescence minus one, unstained), BC biological control (lab/healthy control), LR low-risk serum aliquots L1-L10, HR high-risk serum aliquots H1- H10, and PC positive control

	Mean	Standard Deviation	Number samples
Technical control	0.06	0.01	3.00
Biological control	0.00	NA	1.00
Low-risk	0.11	0.08	10.00
High-risk	0.11	0.05	10.00
Positive control	1.33	NA	1.00

Table 3.7-2 Mean and standard deviation (SD) of percentage of total yeast population expressing gp41 envelope library recognized by low and high-risk MSM sera
Analysis showing mean and standard deviation for PE positive populations across groups of serum samples. NA Not analysed Sequential enrichment

Yield of the PE high populations was assessed following each sort and the numerical value of the PE positive population recorded. Any aliquots with PE high populations greater than that of the experimental controls were selected for further flow analysis and enrichment. This involved two further rounds of flow cytometry sorting and subsequent culture of sorted yeast cells. For each round of yeast culture, approximately 5 x 10^7 yeast cells were prepared. The cell number was estimated using the OD600 reading from the healthy control yeast culture and applied to all samples.

Flow plots for each enrichment event were reviewed and showed an increasingly PE high population Successive rounds of flow sorting produced four enriched yeast cell populations. Two samples from each of the high-risk and low-risk groups yielded viable populations- L6, L10, H5, and H9. The healthy control (LC) and positive control (PC) samples were also selected.

Data from the flow cytometry analysis was plotted as PE high population as a percentage of total yeast cells. The plots and data are shown in Figure 3.7-4 and Figure 3.7-5.

The healthy control was seen to enrich as much as that seen in L6, and possible reasons include to assay technique, in that same epitopes selected by same serum samples, leading to increasing positive population, or support findings that seronegative serum can bind Env epitopes as shown in previous section.

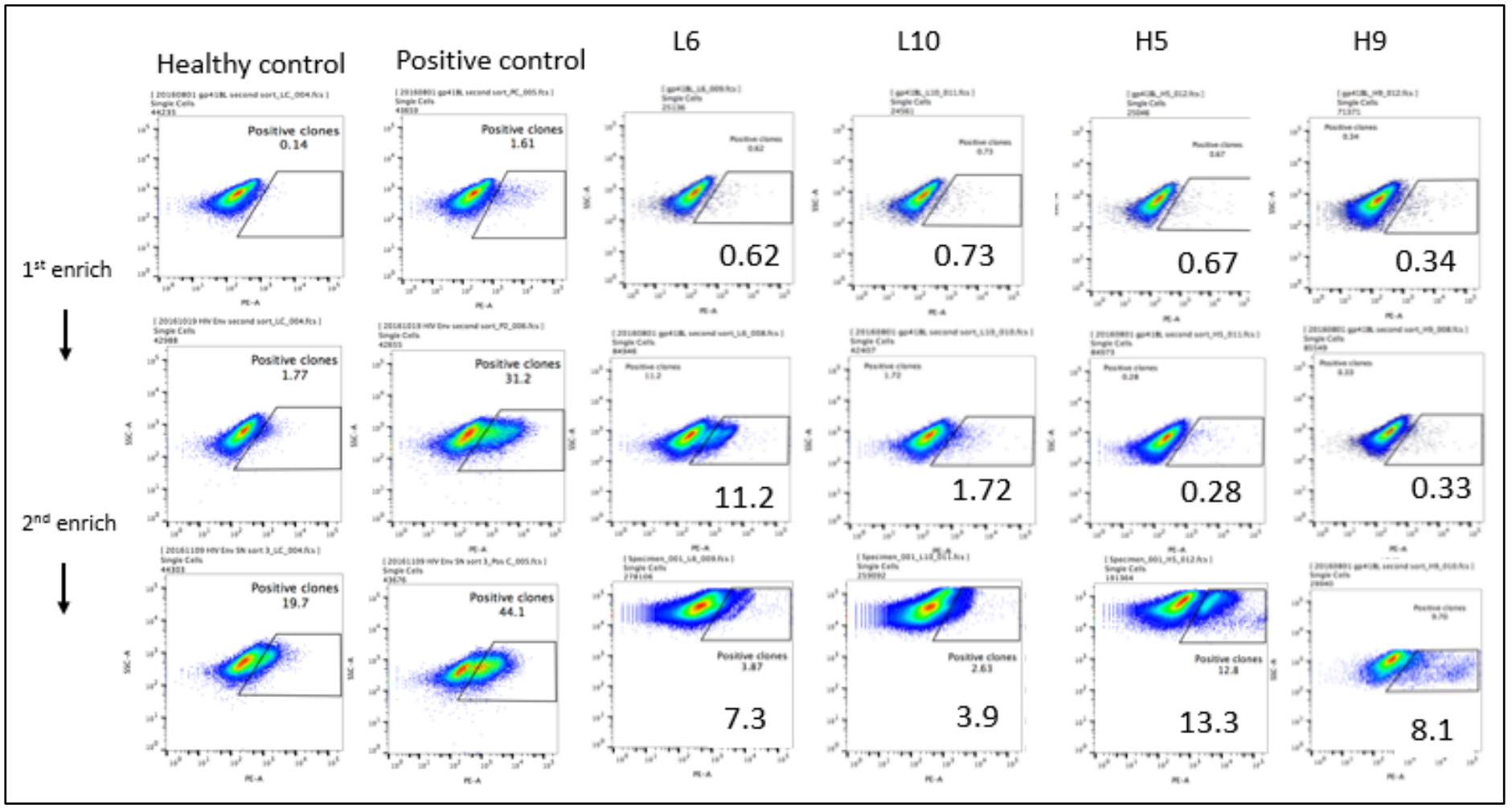


Figure 3.7-4 Serial enrichment of seronegative serum binding to the yeast gp41 envelope library following sequential FACS sorting

FACS plots showing serial enrichment of yeast library with seronegative aliquots. Negative control used is biological healthy control, positive control is seropositive patient sera. First row is FACS plot of screening sort, and second row is following two successive rounds of enrichment. The yeast is now a more refined population and better recognised by patient sera

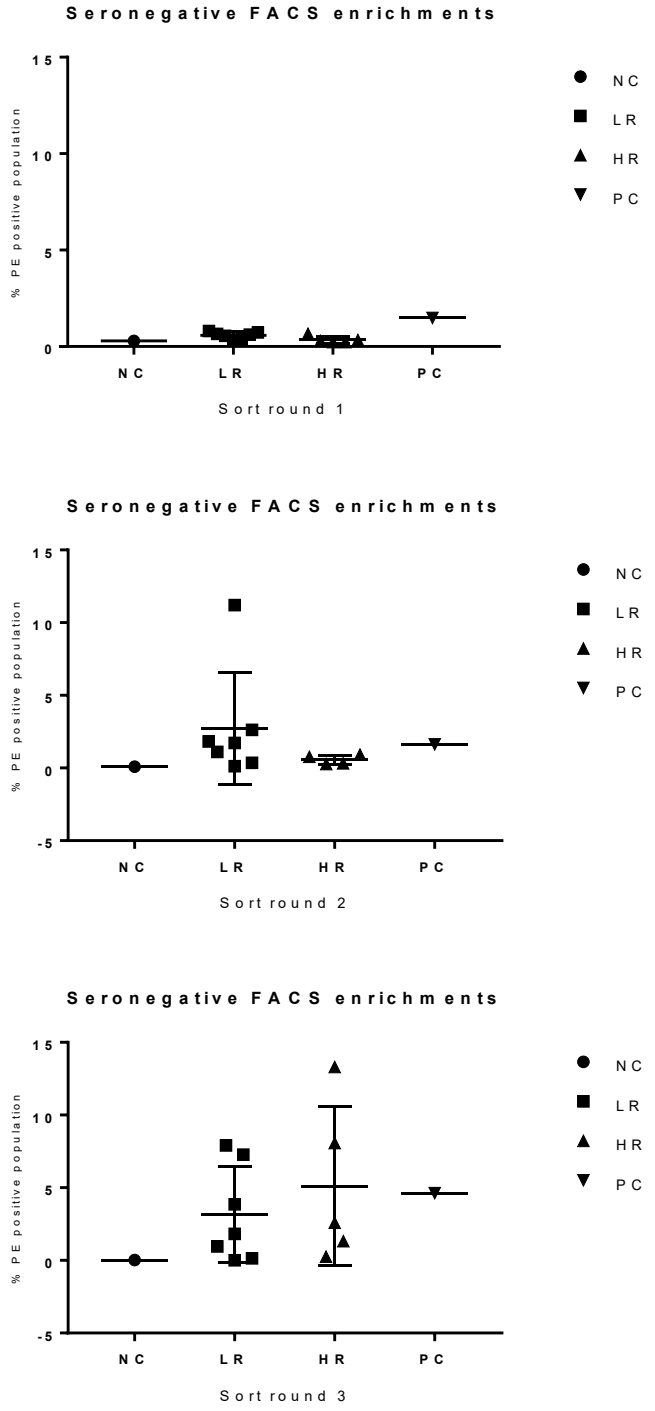


Figure 3.7-5 Mean and standard deviation (SD) of percentage of total yeast population expressing gp41 envelope library recognized by low and high-risk sera

FACS plots showing serial enrichment from initial screening analysis through successive rounds of flow sorting. NC biological control (lab/healthy control), LR low-risk serum aliquots L1-L10, HR high-risk serum aliquots H1- H10, and PC positive control. X axis shows sample groups, y axis shows p population which is PE positive. Not all sorted yeast enriched and so number of aliquots sorted decreased with each sort; initial screening sort round 1 (10 LR and 10 HR), sort round 2 (7 LR and 4 HR) and sort round 3 (7 LR and 4 HR).

3.7.4. Single clone analysis

As in the gp160 section, single yeast clones were selected from the following post sort SDCAA culture plates L6, L10, H5, H9. Sixteen individual clones were picked from each plate and cultured in liquid SDCAA and SGCAA for growth and surface protein expression as previously described. The resulting yeast cultures were then analysed with participant serum by flow cytometry. A 96 well plate was used to facilitate bulk analysis (Figure 3.7-6). Gating strategy and controls were as described in gp160 work (Figure 3.7-7). A summary diagram of the single clone analysis plots is shown in Figure 3.7-8.

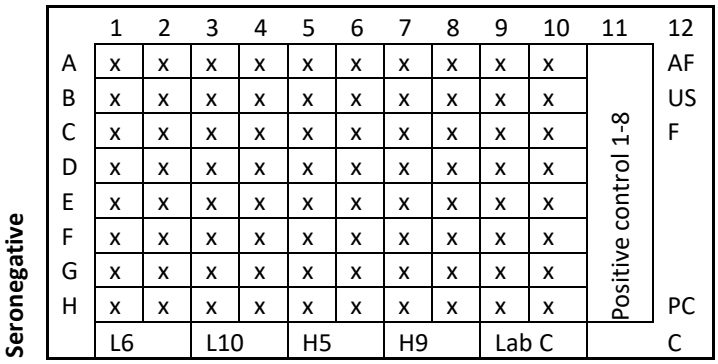


Figure 3.7-6 96 well plate with selected yeast clones for analysis by flow cytometry

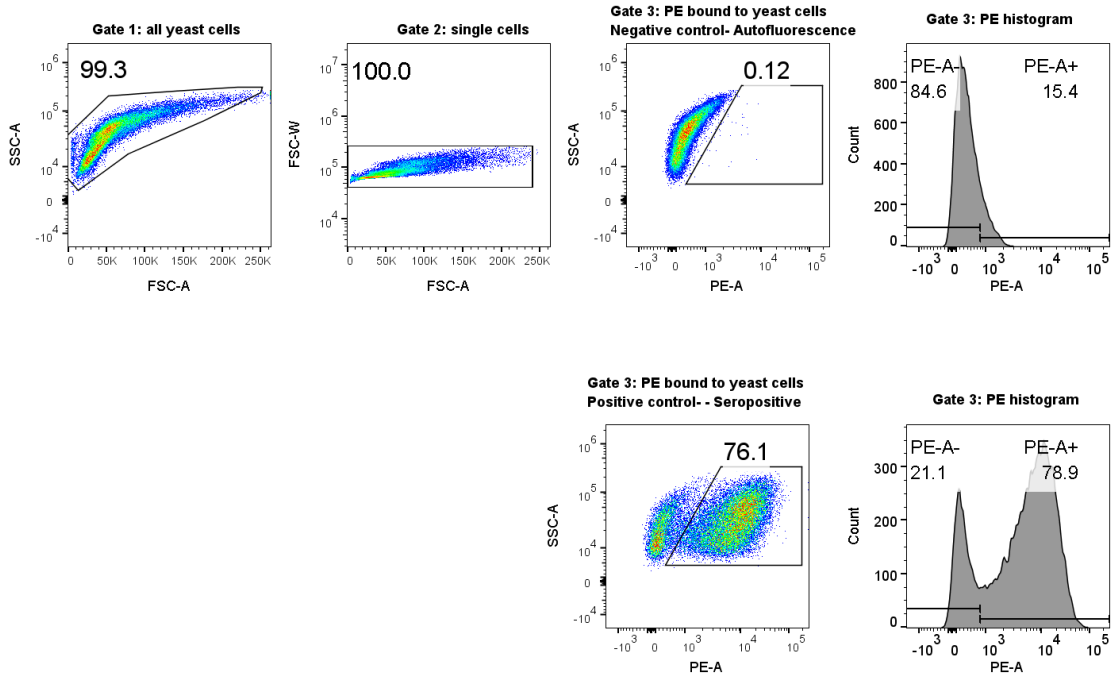


Figure 3.7-7 Flow cytometric analysis of single yeast clones
Gating strategy and histograms showing selection of positive single clones as compared to negative and seropositive controls

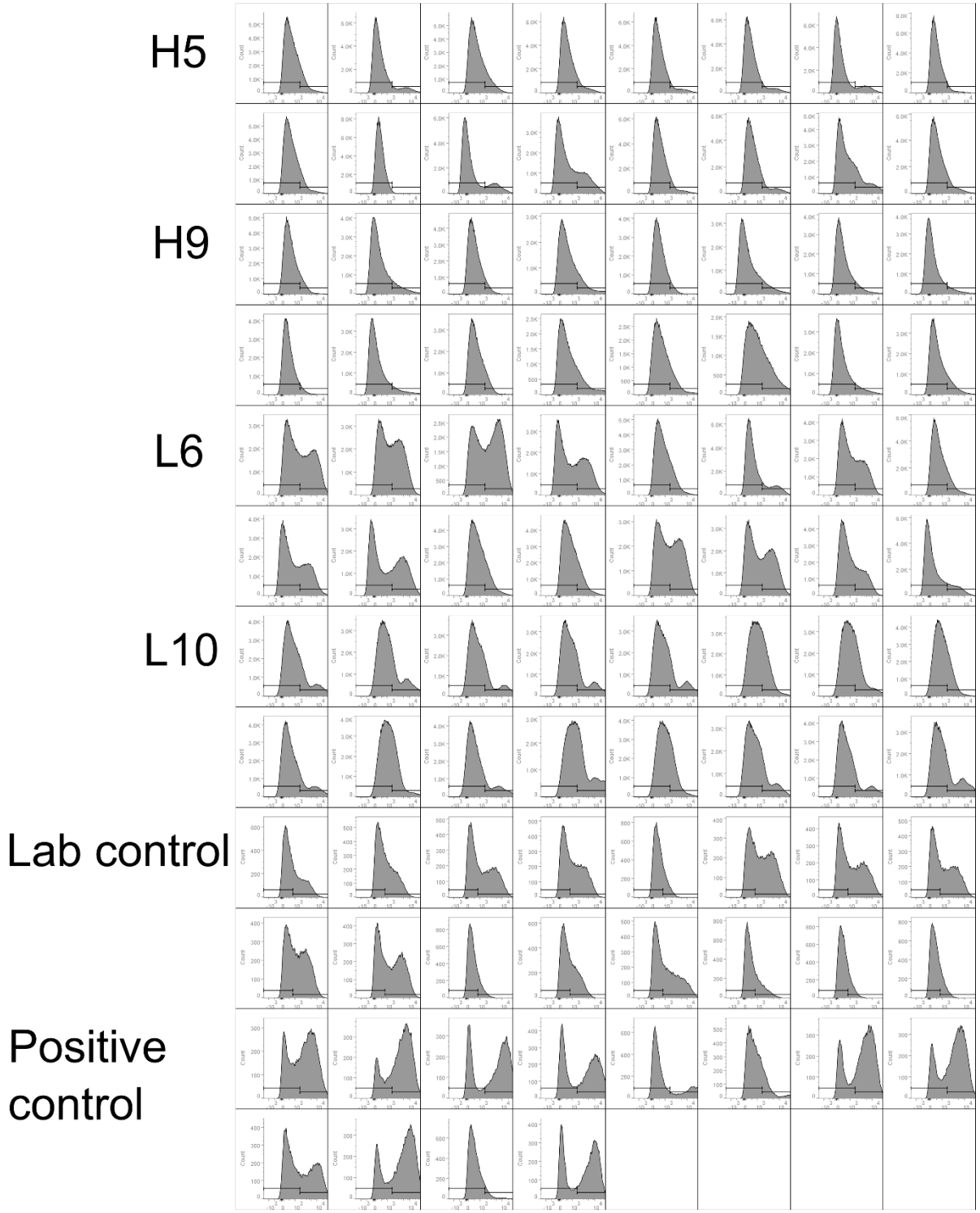


Figure 3.7-8 Histograms for single clone analysis
H5, H9, L6, L10 and lab and positive controls with gp41 refined yeast clone population. 16 plots shown for each member. X axis- PE, y-axis count (1000)

3.7.5. Sequential enrichment summary

As in the first part of this chapter, yeast sorting by participant sera creates a refined yeast population bearing a specific set of antigens which may then be interrogated to characterise major antigenic determinants selected the humoral immune response. All samples underwent baseline screening by flow cytometry, and all samples underwent one round of flow sorting and culture enrichment. This differed from the prior gp160 sorting, where only the samples with greatest PE positive yeast populations were selected.

Participant sera sorted PE positive yeast populations were again compared to the laboratory controls. The purpose of this control was to account for any remaining non-specific yeast antibody binding. Both laboratory and positive controls were selected for all rounds of culture and enrichment.

Following the first round of enrichment, all samples were again submitted for flow analysis and sorting, and the two best performing samples were selected from the low and high-risk groups. This was done for two reasons. Firstly, to ensure consistency of methods to those used for the gp160 library screening, and secondly in the interests of time as each stage demanded one week of culture and preparation.

Low-risk: samples with a PE positive yeast population greater than the laboratory control were selected; these were L6 and L10. L4 demonstrated a positive PE yeast population but unfortunately developed bacterial contamination and was not suitable for further analysis. The experimental serum aliquots yielded a positive population of 3.9-7.3% of the whole yeast population.

High-risk: From second round sorting, the samples with a greater yeast PE population were H1, H2, H5, H9, with the latter two samples having the greatest PE positive population. Experimental serum aliquots yielded a positive population of 8.1-13.3% of the whole yeast population.

These results are summarised in Table 3.7-3.

Sample		1st	2nd	3rd	Single clone analysis (% of 16)
Controls	AF	0.3%	0.1%	0.0%	
	US	0.3%	0.2%		
	FMO	0.3%	0.1%	0.0%	
	Lab C	**0.6%**	**1.8%**	**19.7%**	
	Pos C	**1.5%**	**31.2%**	**44.1%**	
Seronegative participant group = pool of 5 participants	L1	0.2%	0.3%		
	L2	0.6%	0.4%	0.1%	
	L3	0.7%	1.8%	0.0%	
	L4*	0.4%	0.1%	7.9%	
	L5	0.3%	1.1%	1.0%	
	L6	**0.6%**	**11.2%**	**7.3%**	**68.8%**
	L7	0.3%	0.4%		
	L8	0.8%	2.6%	1.8%	
	L9	0.3%	0.4%		
	L10	**0.7%**	**1.7%**	**3.9%**	**62.5%**
	H1	0.3%	0.1%	2.6%	
	H2	0.2%	0.8%	1.3%	
	H3	0.4	0.3%		
	H4	0.2%	0.1%		
	H5	**0.7%**	**0.3%**	**13.3%**	**43.8%**
	H6	0.3%	0.2%		
	H7	0.2%	0.9%	0.3%	
	H8	0.2%	0.2%		
	H9	**0.3%**	**0.3%**	**8.1%**	**0.0%**
	H10	0.3%	0.2%		

Table 3.7-3 Summary sequential FACS sorting and single yeast clone analysis
Table shows successive enrichments of HIV envelope yeast library by serum aliquot pools. Controls LC biological control, PC seropositive control. Threshold for selection based on each sample's ability to enrich, all samples considered.

* sample contaminated, and no further analysis performed

3.7.6. Sequence analysis plots

The positive experimental yeast populations were selected for further analysis. Following post sort cell resting, yeast cultures were cultured on SDCAA agar plates (for single clone selection) and liquid SDCAA culture for DNA extraction and sequencing. Forty-eight clones were selected. in total from each group. This amount was determined by the capacity of culture incubators and reasonable yield expected per experiment. Sequences obtained from the reference laboratory and analysed using Sequencher v4.92 (Genecodes Corporation) as described in materials and methods and aligned to the parent HIV-1 gp41 sequence as previously described.

Figure 3.7-9 below shows the experimental and positive control sequence fragments aligned.

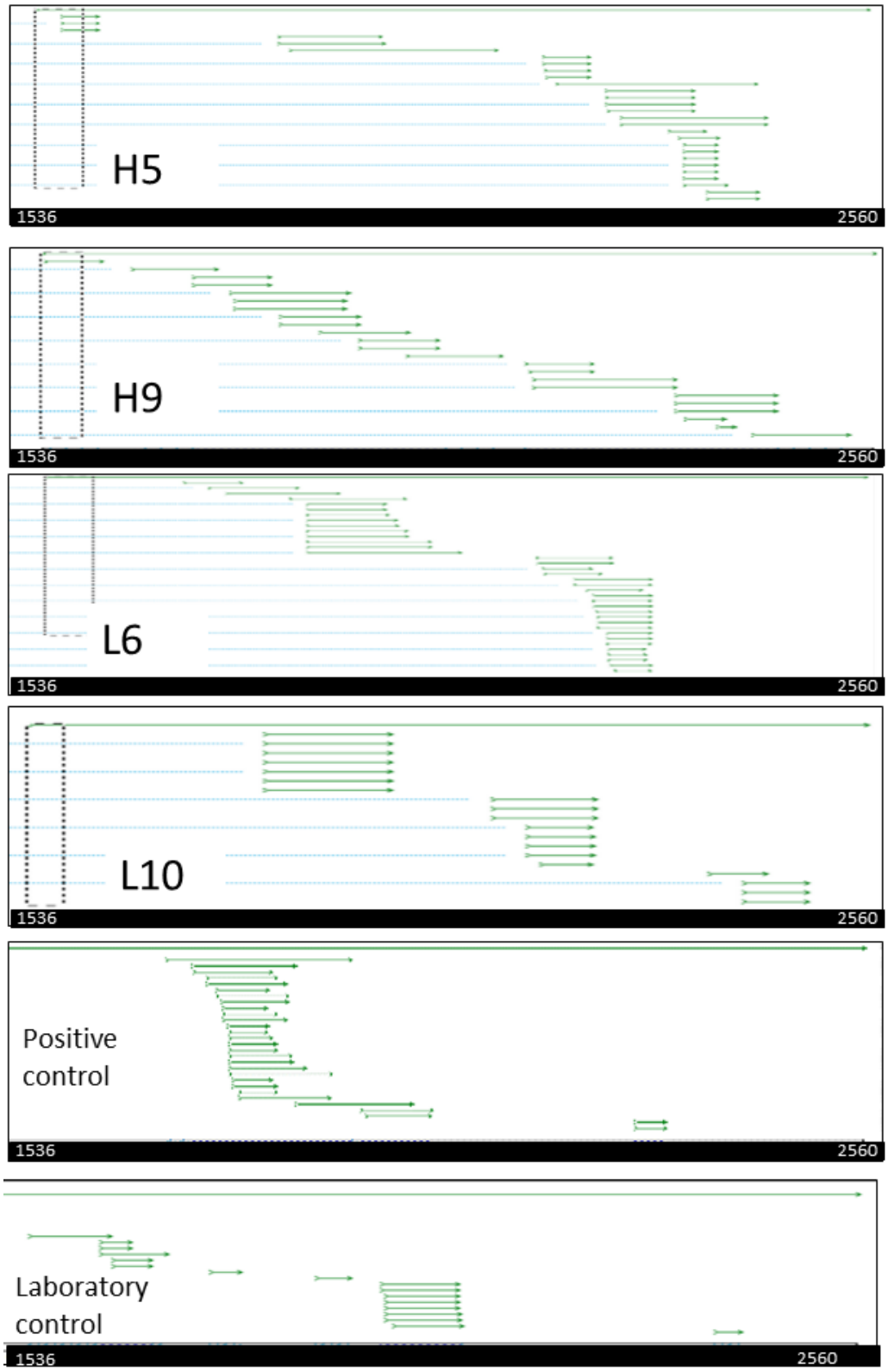


Figure 3.7-9 Yeast clone sequence fragment analysis of H5, H9, L6, L10 and positive control
Black strip 1536-2560 at bottom of figure represents gp41 DNA sequence (starting point on HIV envelope sequence) nucleotide positions, green strips represent sequence fragments aligned

3.7.7. Sequence analysis histogram

Sequences were aligned to the parent HIV-1 gp41 sequence as previously described. A variety of HIV-gp41 epitopes were recognised by participant serum aliquots and the results plotted as a histogram for healthy and positive controls, low-risk and high-risk samples. An algorithm was used to determine frequency of amino acid residues at each position on the gp41 sequence (283).

As previously, the area under the curve (AUC) was calculated if amino acid amino acid frequency exceeded five residues, representing an epitope. The AUC for each residue cluster/epitope was calculated as described previously in 3.6.8. Epitope recognition was considered significant if distributed in a Gaussian fashion. All gp41 x axes begin at 512 as per the position of gp41 relative to HIV envelope sequence.

Positive control serum recognised one epitope of gp41, in keeping with known early anti-HIV antibody responses. Healthy control serum recognised two regions of gp41 (data shown in Figure 3.7-10 and Table 3.7-4); the first mapping to the fusion protein and N helical region epitopes (aa512-551), and the second mapping to the C-helical region, MPER, and transmembrane domain epitopes (aa641-694).

L6 serum recognised two epitopes of gp41, and L10 serum recognised three epitopes of gp41, but only one reached a residue frequency of five. H5 serum recognised two epitopes of gp41. H9 serum recognised three regions of gp41, but only two qualified as epitopes according to the prespecified criteria- this was an overlapping region.

These findings are shown in the histograms in Figure 3.7-10 and Table 3.7-4.

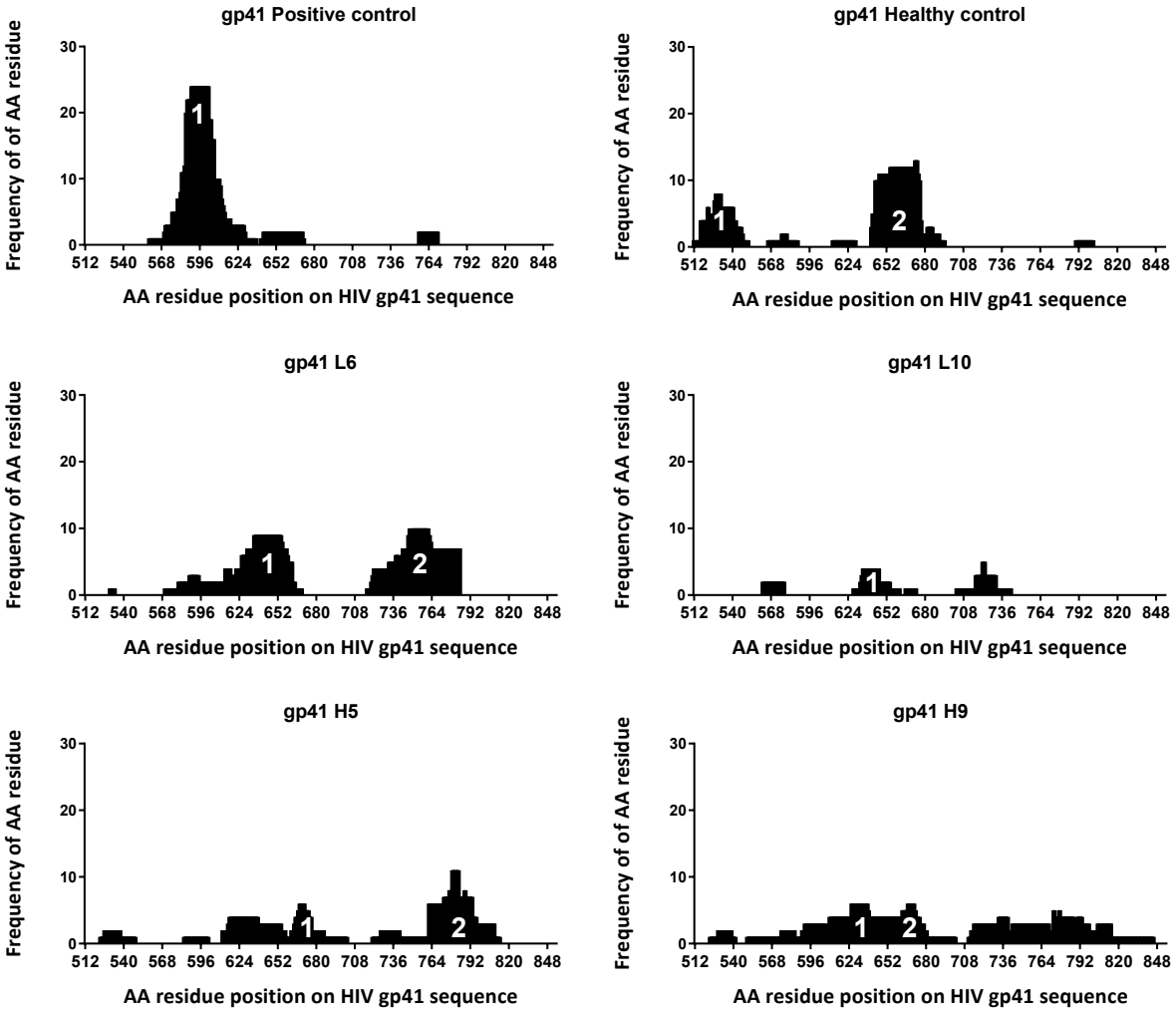


Figure 3.7-10 Histograms of gp41 library sorted by serum samples

Histogram showing amino acid frequency at each position on the HIV-1 gp41 parent sequence as recognised by positive control, healthy control, low-risk serum aliquots L6 and L10, and high-risk serum aliquots H5 and H9. X axis is amino acid residue position on HIV gp41 sequence (begins at AA position 512 according to HIV envelope), y axis is frequency of recognition of amino acid residue. Epitopes denoted by figures on histogram. Regions of the histogram considered significant for epitope if residue frequency greater than five.

	Epitope	Total residues	Start	Finish	Length of sequence in (AA residues)	AUC (total AA in epitope)	AUC as % of total fragment residues	Epitope	Sequence
Positive control	1	784	559	637	79	695	88.6%	N helical region C helical region Loop	DQQLLGIWGCSGKLICTTAVPWNASWSNKSLEQIWNHTTWMEWDREINNYTSLIHSLIEESQNQQEKNEQELLELDKW
Healthy control	1	658	512	551	40	170	25.8%	Fusion protein N helical region	RQLLSGIVQQQNNLLRAIEAQQHLLQLTVWGIKQLQARIL
	2	658	641	694	54	432	65.7%	C-helical region MPER Transmembrane domain	NWFNITNWLWYIKLFIMIVGGLVGLRIVFAVLSIVNRVRQGYSPLSFQTHLPTP
L6	1	864	570	669	100	427	49.4%	N helical region C helical region	GKLICTTAVPWNASWSNKSLEQIWNHTTWMEWDREINNYTSLIHSLIEESQNQQEKNEQELLELDKWASLWNWFNITNWLWYIKLFIMIVGGLVGLRIVF
	2	864	717	784	68	443	51.3%	Endodomain	RLVNGSLALIWDDLRSLCLFSYHRLRDLLLIVTRIVELLGRRGWEALKYWWNLLQYWSQELKNSAVSL
L10	1	195	703	742	40	74	37.9%	Transmembrane domain Endodomain	IEEEGGERDRDRSIRLVNGSLALIWDDLRSLCLFSYHRLR
H5	1	660	661	702	42	103	15.6%	MPER Transmembrane domain	GLVGLRIVFAVLSIVNRVRQGYSPLSFQTHLPTPRGPDRPEG
	2	660	761	813	53	292	44.2%	Endodomain	EALKYWWNLLQYWSQELKNSAVSLLNATAIAVAEGTDRVIEVVQGACRAIRHI
H9	1	826	607	650	44	196	23.7%	C-helical region	NYTSLIHSLIEESQNQQEKNEQELLELDKWASLWNWFNITNWLW
	2	826	651	701	51	149	18.0%	MPER Transmembrane domain	YIKLFIMIVGGLVGLRIVFAVLSIVNRVRQGYSPLSFQTHLPTPRGPDRPE

Table 3.7-4 Summary table of epitope recognition and sequences for gp41 yeast library sorting
Table shows information on all epitopes considered significant in gp41 analysis.

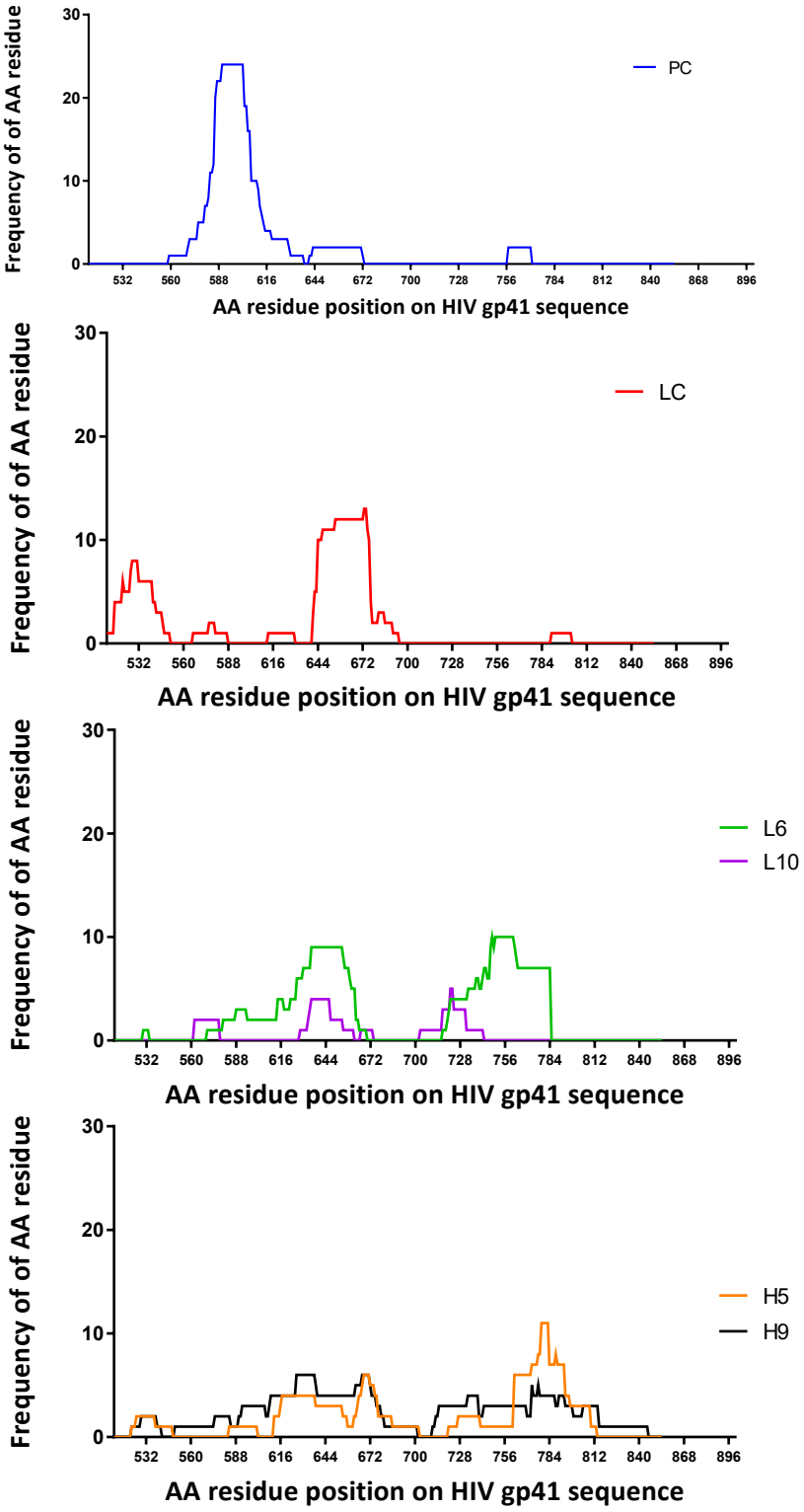


Figure 3.7-11 HIV gp41 library sorted by seronegative serum samples
Histograms of gp41 library sorted by serum samples

As in the gp160 histogram analysis, all histogram curves were overlaid as shown below in Figure 3.6-12. As expected, positive control serum showed prominent recognition of gp41 epitope, but otherwise there were no patterns of common epitope recognition by all seronegative samples.

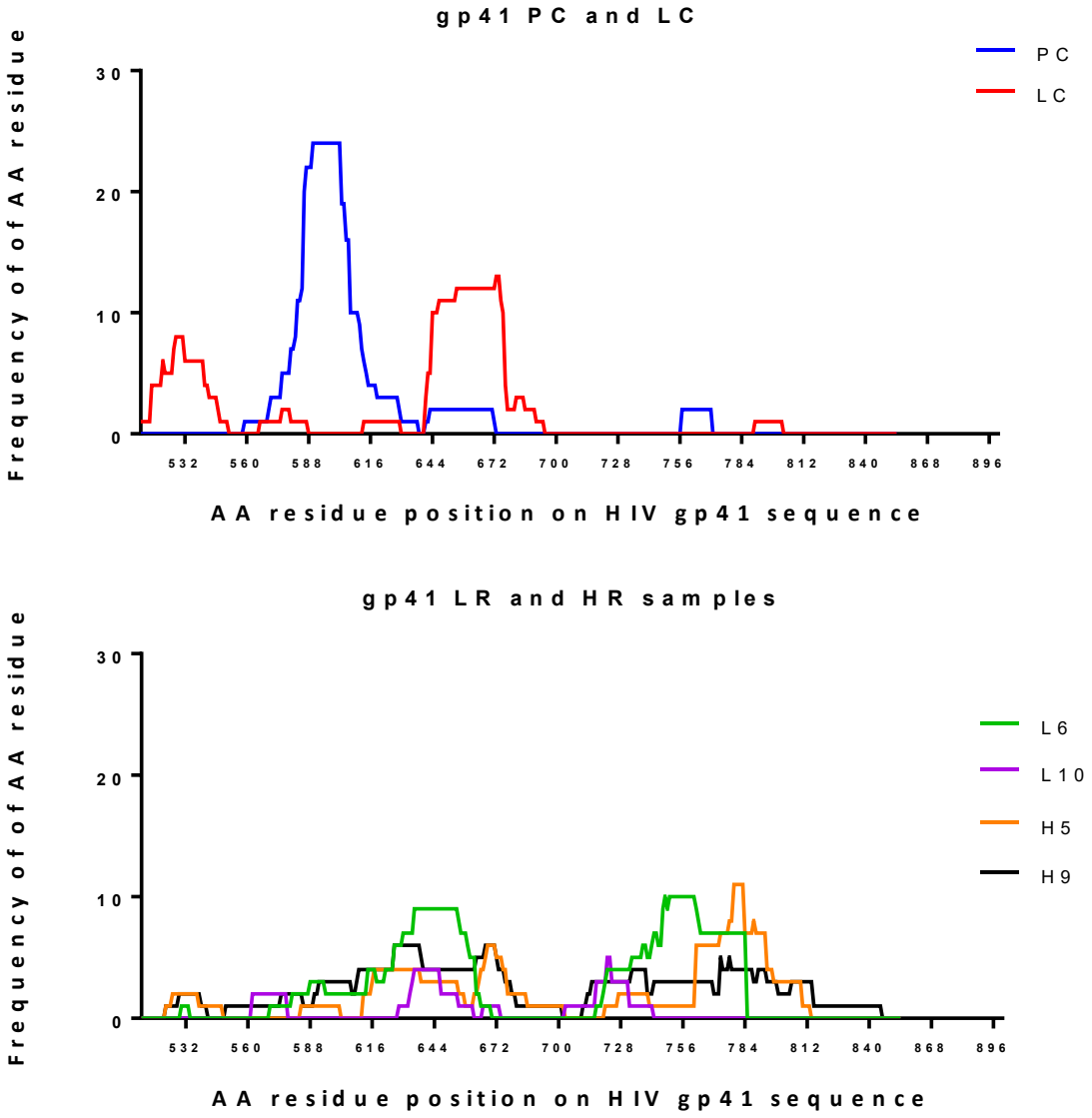


Figure 3.7-12 Overlay of HIV-1 gp41 amino acid sequences detected in HESN and controls
X axis shows residue position on gp41, y axis shows frequency of recognition at that position. PC positive control, LC laboratory or healthy control. Experimental samples L6, L10, H5 and H9.

In addition, histograms of all samples; lab control and positive control, and low and high-risk samples combined were overlaid, but there was no discernible pattern in seronegative sample recognition. See Figure 3.7-13 below.

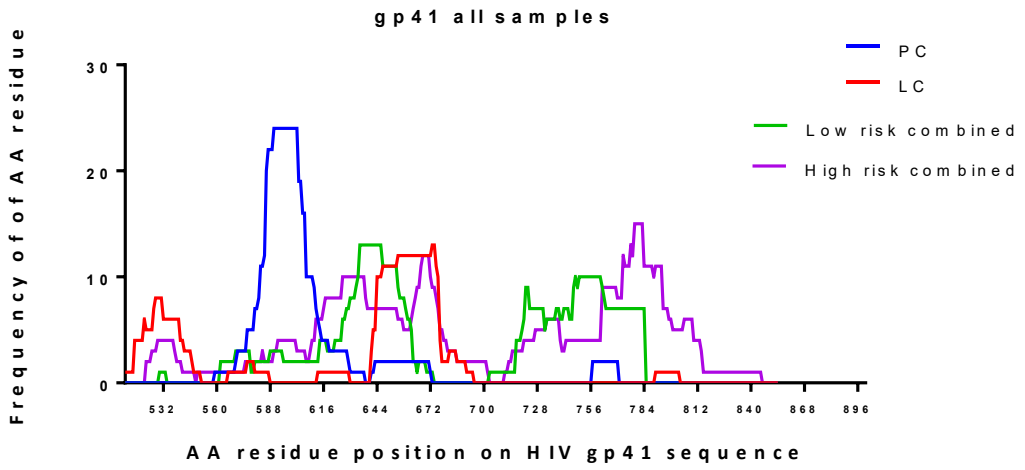


Figure 3.7-13 All HIV-gp41 amino acid sequences detected in all samples
X axis shows residue position on gp41, y axis shows frequency of recognition at that position. PC positive control, LC laboratory or healthy control. Experimental samples L6, L10, H5 and H9.

3.8. HIV-1 gp41 epitope recognition in low-risk vs high-risk serum aliquots

The next step of the project looked at variation in the recognition of gp41 epitopes based on exposure to HIV.

3.8.1. Overall gp41 sequence recognition

Low-risk and high-risk amino acid residue frequencies were combined to compare recognition of gp41 sequences by low and high-risk serum. This is shown below in Figure 3.8-1.

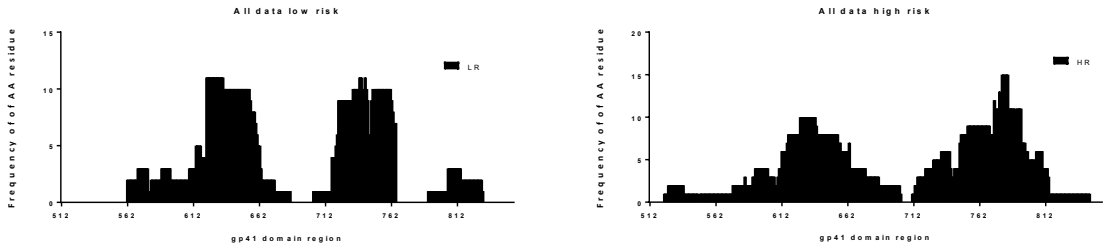


Figure 3.8-1 Low and high-risk sequences combined
Combined frequency of amino acid residue recognition by serum relative to HIV-1 gp41 sequence

Top row: line graphs showing frequency of amino acid residues (y axis) at position on gp41 sequence (x axis). Low-risk aliquots L6 and H10 in left panel, high-risk aliquots H5 and H9 on right panel. Second row: combined histograms showing frequency of amino acid residues (y axis) at position on gp41 sequence (x axis). Low-risk aliquots L6 and H10 in left panel (LR), high-risk aliquots H5 and H9 on right panel (HR). Amino acid residue frequencies from each risk group added together.

3.8.2. Proportion of gp41 sequences recognised by fragments from each risk group.

For reference here, the total length of the gp41 sequence was 342 amino acids. When sequence fragment histograms AUC totals were combined, low-risk serum fragments recognised 57.9% (198/342) of all amino acid positions. The total area under the curve was 1069 amino acids. Combined high-risk serum fragments recognised 91.8% (314 of 342) of all amino acid positions. The total area under the curve was 1486 amino acids.

The proportions were analysed using 2 tailed unpaired t-test where significance was determined by $p<0.05$. There was a significant difference in the frequency of amino acid residues recognised by the two participant serum aliquots, with greater recognition of gp41 in high-risk groups as compared to low-risk groups. The combined high-risk serum aliquots identified a greater proportion of the sequence than low-risk serum (75.75 ± 7.494) compared to the low-risk serum aliquots (35.1 ± 7.081). This difference was significant with a P value 0.0076. This is shown in Figure 3.8-2.

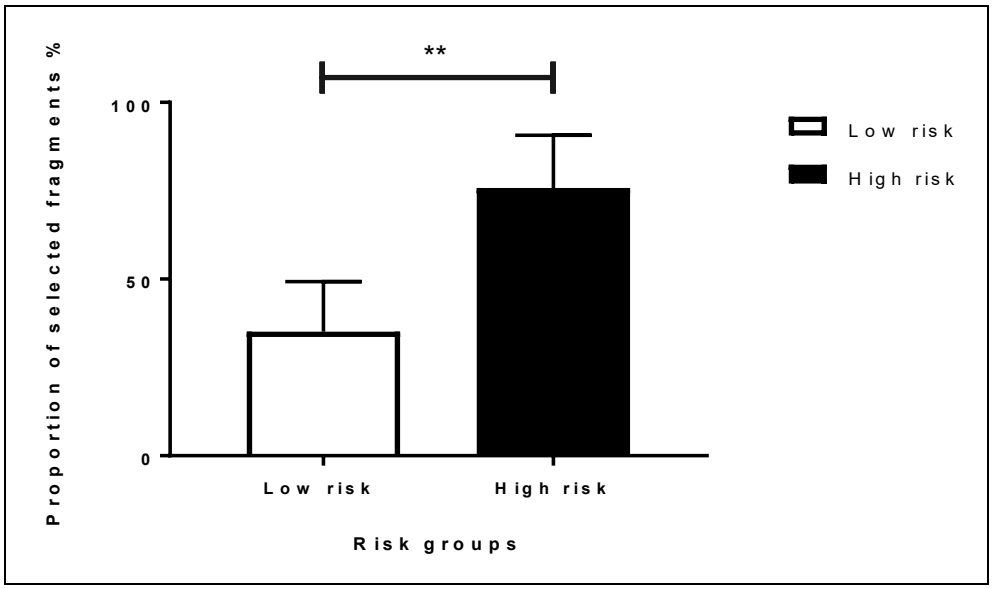


Figure 3.8-2 Proportion of gp41 epitope identified by low and high-risk MSM serum aliquots
X axis- low or high-risk serum aliquots, y axis proportion of selected fragments as percentage of total fragments, P value 0.0076.

3.8.3. HIV-1 gp41 epitope recognition in low-risk vs high-risk serum aliquots

The proportions of discrete gp41 epitopes recognition by low-risk as compared to high-risk participant samples were analysed by calculating the AUC for each epitope as a proportion of the total AUC for all fragments. Both low and high-risk MSM sera displayed responses to gp41 epitopes. Overall numbers for the AUC proportions were documented. High-risk serum aliquots had greater recognition of fusion protein, loop, membrane proximal external region, and endodomain. Low-risk serum aliquots had greater recognition of N helical region, C helical region and the transmembrane domain. This is shown below in Table 3.8-1 and Figure 3.8-3.

Gp41 region	LR		HR	
	L6 gp41	L10 gp41	H5 gp41	H9 gp41
FP	0.50%	0.00%	4.50%	3.40%
NHR	4.70%	16.40%	2.60%	7.00%
loop	8.20%	0.00%	6.10%	11.70%
CHR	34.30%	41.50%	18.90%	22.40%
MPER	1.60%	4.10%	12.30%	10.50%
TMD	1.80%	20.00%	3.60%	6.20%
Endodomain	48.90%	17.90%	52.00%	38.70%

Table 3.8-1 Seronegative sera recognition of discrete gp41 epitope
All amounts measured as percentage of total fragments

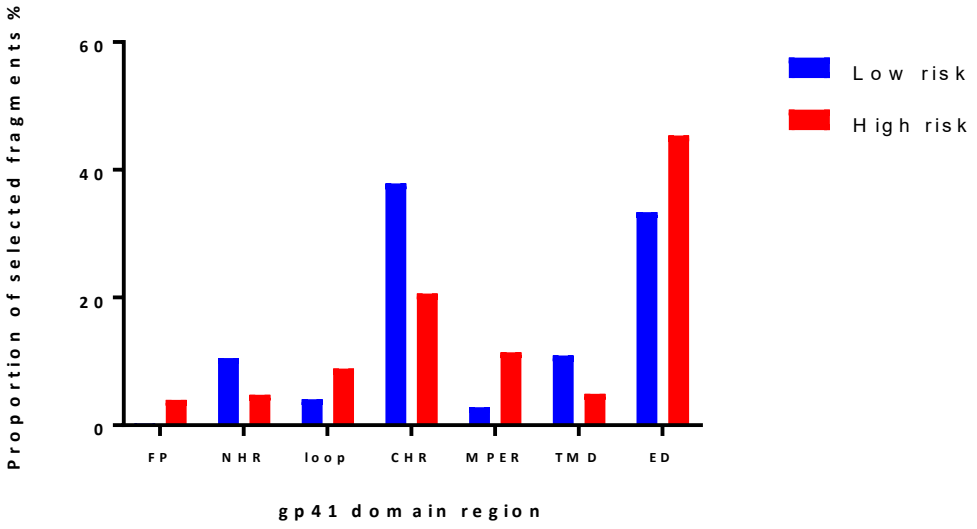


Figure 3.8-3 Seronegative sera recognition of discrete gp41 epitope
Recognition measured as percentage of total fragments. Frequency of selected fragments from low and high-risk individuals displayed as discrete genes on parent sequence, with proportions of each area recognised expressed as percentage of total fragments reviewed. FP fusion peptide, NHR N-helix, loop, CHR c-helical region, MPER membrane proximal external region, TMD transmembrane domain, ED endodomain

3.9. Discussion

3.9.1. Summary

The aims of this chapter were to identify B cell responses to HIV envelope antigens present in the serum of HIV negative individuals, describe the antigenic determinants of this response, and assess if the frequency and character of this response varies with the risk of HIV exposure.

3.9.2. Cohort recruitment

A total of 238 participants were recruited to group A. Baseline demographics, behavioural risk information and tissue samples were obtained from all. Participants were stratified according to history of confirmed rectal sexually transmitted STI, history of unprotected receptive anal intercourse, and number of sexual partners in the preceding three months.This was based on information from the PROUD-UK study, which identified key behavioural risks for HIV infection, including presence of a rectal sexually transmitted infection (STI) in previous 12 months, and 2 or more sexual partners in the previous 90 days. Other features including recreational drug use during sex ("chemsex"), use of anti-HIV medication post sexual HIV exposure ("PEP", post exposure prophylaxis), and relationship status did not affect HIV incidence (113).

These criteria allowed random selection of fifty low-risk and fifty high-risk participants according to history of sexually transmitted infections and number of sexual partners in the previous three months. These formed the low and high-risk cohorts studied in this chapter.

3.9.3. HIV gp160 library analysis of seronegative serum aliquots

In the initial part of this chapter, humoral immune responses to gp160 were reviewed. Seronegative individuals may have had anti-gp160 responses from previous exposure to HIV virus in the absence of infection (201,212) or pre education of the immune system by cross reactivity with intestinal microbiota (264).

The initial focused was on serum responses to gp160. FACS screening of patient serum aliquots produced PE high populations of <1% total yeast population, but two low-risk (L6, L9) and one high-

risk (H9) yeast clone demonstrated increasingly PE high populations with successive enrichment. These yeast/sera pairings were further interrogated with single clone analysis and review of gp160 regions identified.

3.9.3.1. Seronegative gp160 recognition

There were two key regions in gp160 recognised by all seronegative serum samples. The gp120 region spanning 151 to 223 was recognised by all seronegative aliquots (healthy control, low and high-risk) and corresponds to a portion of the V1V2 epitope and the C2 epitope. Single clone analyses of individual participant serum and yeast clones revealed high affinity between serum and mapped epitopes, supporting group aliquot findings on individual serum sample level.

The V1V2 epitope recognised by seronegative aliquots was located at aa167–171, which was also the region selected by the seronegative fragments.

The V1V2 epitope is a recognised antibody target. It is structurally diverse across strains, but approximately 75% of the residues are conserved, probably due to its role in viral entry, although V1V2 is not essential for viral replication (315). Multiple bnAb targeting the V1V2 loops have identified including PG9/PG16, CH01-04, CAP256-VRC26, PGT141-PGT145 (130,316), and immunisation strategies involving V1V2 epitopes can induce antibodies capable of neutralising a variety of HIV subtypes (317–319).

V1V2 can evade neutralisation by varying sequence and glycosylation to produce a “glycan shield” (320). Immunisation of animal models with Env trimer BG505 SOSIP.664 induces antibodies directed against residue which is a hole in the glycan shield (321). As many wild type viruses have glycan holes and only up-glycosylate in more infection, this suggests glycan shield holes are targets for antibodies with neutralising capabilities.

Anti-V2 ADCC-mediating IgG1 and IgG3 antibodies were associated with reduced infection in the RV144 vaccine trial (232). As outlined in the introduction, the correlates of immune protection in

RV144 were also seen in the follow-up HVTN 097 and 100 trials, however these failed to protect against HIV infection, which raises the question of which immune responses correlate with durable immunisation (234,237)(236).

The C2 epitope is a poorly accessed site. Interrogation of this site by monoclonal antibodies is more successful when gp120 is presented in a monomeric form, suggesting this epitope is cryptic *in vivo* presentation. A feature of the yeast display technology is presentation of epitope fragments; despite best efforts, it may not mimic *in vivo* protein conformation, especially if sequence fragments are shortened.

The gp41 region recognised by all seronegative samples spanned three epitopes from position 640 to 699, corresponding to the C-helical region (42 AA, positions 622 to 663), the membrane proximal external region (20 AA, position 664 – 683) and the transmembrane domain (40 AA, 684 – 723). This region has been identified in HESN previously by Tudor et al, who showed monoclonal mucosal IgA can block epithelial transcytosis and neutralise infection (224).

When comparing the gp41 epitopes identified by the gp160 and gp41 libraries, commonly identified epitopes were the C helical region, and MPER. The gp41 library also identified the fusion protein, N helical region, C-helical region, MPER, transmembrane domain, and endodomain epitopes. This could be explained by more in depth analysis of these epitopes by the gp41 library.

While the regions identified by these sera groups did not meet significance for epitopes (peaks <5 residue frequency, major antigenic determinant (as defined in materials and methods section 2.5), the pattern of recognition by all seronegative samples is of interest. But what is the significance of anti-envelope responses in seronegative individuals? There are reports of anti-HIV gp120/41 IgA in vaginal secretions of highly exposed females, and IgG in plasma samples of HESN (218,225), and a study by Nguyen et al showed a protective effect of anti-gp120 IgG in HESN (223). As described in the introduction chapter, most HESN cohorts reporting mucosal exposure to HIV have evidence of HIV-

specific IgA (201). This analysis follows those findings, with additional insight into the presence of anti-envelope plasma IgG in seronegative individuals, and targets selected by seronegative serum.

3.9.3.2. Seronegative gp160 differential recognition by low and high-risk serum

The proportions of selected fragments were compared and greater recognition of the HIV-Env gp41 epitope was seen in healthy control, high-risk participant and positive control sera. Low-risk sera had similar proportions of gp120 or gp41 fragment recognition.

The division of envelope protein into two regions may appear a simplistic arrangement, but Env *in vivo* is a 3-dimensional structure of a trimer with the two glycoproteins occupying different spatial regions (50). Moreover, broadly neutralising antibodies discovered in HIV infected patients target immunogenic epitopes in distinct regions of gp120 or gp41 (130). With this in mind, proportions of fragments recognised by each of the groups relative to gp120 and gp41 areas of the HIV-1 envelope parent sequence were compared. In the gp160 seronegative sera and positive control fragment analysis there was a clear distinction of recognised epitopes in the two glycoprotein regions. There was a variation in frequency of recognition of gp41 fragments in high versus low-risk patients and this was further explored.

3.9.4. HIV gp41 library analysis of seronegative serum aliquots

There was variation in serum responses to gp41 according to presumed level of HIV risk exposure. Combined high-risk serum aliquots sequence recognition frequency was greater than twice that recognised by low-risk serum (HR MSM 75.75% ± 7.494 versus LR MSM 35.1 ± 7.081, p value 0076), suggesting highly exposed persons have greater breadth and magnitude of immunologic responses, possibly due to increased exposure.

To confirm the gp41 response differences attributed to HIV risk exposure, the gp160 library data for high-risk and low-risk sera responses was reviewed.

For the gp41 library analysis there were two groups of each of high-risk and low-risk results (L6, L10, H5, H9) which allowed a 2-tailed unpaired t-test for comparison of the area under the curve (AUC) for each group. In the gp160 library screening, there was only one high-risk aliquot to compare the AUC of the different risk groups. By duplicating the data from H9 and performing a 2-tailed unpaired t-test, the proportion of the AUC covering the gp41 epitope is significantly greater in high-risk (74.57 ± 0) than low-risk groups (53.46 ± 3.31), P value 0.0237. This supports the finding of greater recognition of gp41 by high-risk sera samples as seen in the gp41 library analysis. This data is shown in Table 3.9-1 and Figure 3.9-1.

	L6	L9	H9	H9 (duplicate)
gp120	49.85%	43.23%	25.43%	25.43%
gp41	50.15%	56.77%	74.57%	74.57%

Table 3.9-1 Proportions of total AUC found in each region of gp160 as per aliquot.
L6, L6, H9, with H9 figures duplicated for comparison purposes. Total AUC

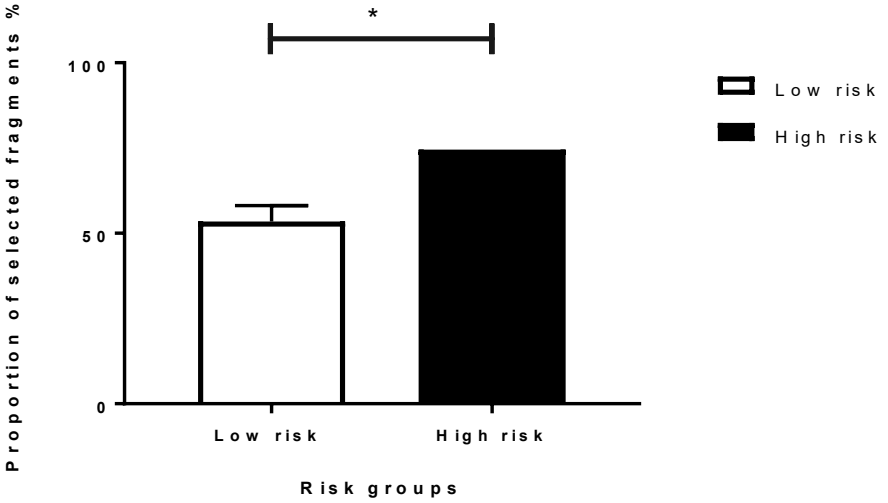


Figure 3.9-1 Proportions of total AUC found in each region of gp160
Low-risk samples L6 and L9, and high-risk sample H9 duplicated

3.9.5. HIV-1 gp41 epitope recognition in low-risk vs high-risk serum aliquots

Previous work by Carrillo et al (225) suggested a variation in HIV-envelope binding IgG according to exposure risk. The work shown here in chapter three stratified risk groups with measured HIV exposure risks and batched serum aliquots to increase the likelihood of this effect being assessed.

The Carillo paper reviewed serodiscordant monogamous partnerships and reported IgG and IgA recognition of cell-surface expressed Env in 85% of HESN. These findings were not borne out in ELISA based methods, nor did they correlate with reported risk exposures. This chapter suggests a variation in anti-Env IgG responses based on clearly defined risk exposure groups, which may explain the differences reported here as compared to the previous study (225). The "dose" of HIV involved in exposure for each risk group is difficult to quantify, as many factors influence viral transmission e.g. pre-existing genital mucosal ulceration caused by infection, viral load of partner (39).

High-risk serum aliquots had greater recognition of fusion protein, C helical region and membrane proximal external regions compared to low-risk serum, but these differences were small and not tested for statistical significance.

3.9.6. Limitations of work

Assessment of the gp160 library revealed gaps in library coverage spanning individual regions of C2, C3, and C4. However, these regions were still identified by fragments. Library coverage was assessed by randomly selecting 48 clones from the original bacterial transfection plate. Assessment of coverage could be improved by selecting a greater number. Also, small fragments were identified in these regions, suggesting the library coverage is broader than suggested.

It must be considered here that the findings could be due to chance. Perhaps presentation of antigens influenced epitope recognition, with better expression of certain clones due to more successful yeast culture. Also, previously discussed, yeast and mammalian glycosylation are not identical therefore recognition of glycan-dependent epitopes may have been missed.

YSD epitope presentation may have also displayed typically cryptic regions. *In vivo*, the endodomain epitope is concealed in the viral membrane. In addition, YSD may have artificially increased sensitivity for usually glycan shielded epitopes e.g. V1V2 *in vivo*. Perhaps any epitope recognition here is a

function of the assay as opposed to truly immunogenic but could also due to abortive infection and release of non-intact virus in the setting of apoptosis/pyroptosis (see section in discussion page 309).

On reflection, constructing one library of whole trimers might have allowed for swifter processing of samples, as this would have identified a population of trimer-specific antibodies. One approach could have been to screen for initial anti-Env responses using whole displayed trimers, and then reviewing discrete epitopes. However, the intention of this project was to review epitopes of interest, and as yeast surface display could bias towards gp41/MPER specific antibodies, it may have been better to review fragments as the gp120 epitopes were presented in a more accessible fashion.

Biological controls were prepared (laboratory/healthy control) from individual serum aliquots as compared to the aliquots which were made from five samples. This could contribute to better epitope recognition due to a more concentrated sample. Conversely, high levels of binding to epitope by one patient serum member of an aliquot could skew the whole aliquot response; single clone analysis work in the gp160 analysis supported the technical validation that data from batched aliquots can be applied to individual samples.

CD20 adsorption of serum samples by yeast was performed as the original pCTCON2 vector contained a CD20 gene which was expressed as part of the yeast surface display. This step removed anti-CD20 antibodies from experiment sample serum to reduce nonspecific antigen/yeast-antibody binding which would give a falsely high readout. Ideally an empty vector with no CD20 or other foreign genes would have been used. For this, CD20 was an irrelevant antigen, as genuine HIV specific antibodies would not be removed by CD20-yeast adsorption.

Another limitation of this chapter is the individual single clone analyses were only performed with gp160 clones. However, the epitope targets were from gp120 and gp41, supporting the proposal that batched aliquots reflect individual participant serum responses.

Variation in the quality of epitope displayed by the yeast cells may have contributed to the fluctuations in serum responses, however the PE high populations are maintained throughout the groups, suggesting serum affinity for the surface displayed protein is maintained. YSD quality of some clones was also compromised by bacterial contamination, another risk when using this assay.

This assay would probably not be suitable for screening seronegative populations, due to the presence of anti-Env responses in our "healthy" control population. However, only a small number of healthy controls were used (n=5) compared to fifty of each low and high-risk group, and perhaps results were skewed by dominant responses of one healthy control volunteer. Also, healthy controls were colleagues, and might not have been comfortable disclosing all details of sexual activity.

Another limitation is the inability to quantify dose expsosure per sexual act. As discussed in the introduction, risk exposure based on the PROUD-UK study allowing stratification of participants into low and high risk groups. Multiple factors can influence transmission risk e.g. pre-existing genital mucosal ulceration caused by infection, viral load of partner (38,39).

3.9.7. Future Work

With more time, exploration of individual participant serum single clone responses to gp41 library epitopes could show more discrete levels of epitope recognition by individuals. Another project would be to explore the HIV envelope response in a cohort of HESN in receipt of PrEP, to review sera responses in the context of ongoing exposure and likely abortive attempts by virus to establish infection.

3.10. Conclusion

The aims of the chapter were to identify serum responses to HIV envelope antigens in HIV negative individuals, describe antigenic determinants of this response, and review variations in response in association with risk exposure to HIV in MSM.

This chapter suggests that seronegative individuals have humoral responses to Env protein epitopes presented on yeast surface display. This can be shown in “healthy” controls as well as HIV exposed seronegative people, and findings may be over-emphasised due to enrichment by successive rounds of yeast sorting and culture. There is a difference in frequency epitope recognition of gp41 as compared to gp120 between self-reported low and high-risk participant sera; this was shown in both gp160 and gp41 specific libraries, suggesting the level of risk exposure to HIV increases Env antibody recognition.

Chapter 4
Seroconverter cohort

Chapter 4 Seroconverter cohort

4.1. Introduction

The first chapter of results indicated immune responses exist towards HIV in highly exposed seronegative persons. Based on this, initial serum antibody responses could shape the developing response to HIV, and that selected epitopes may be responsible for ongoing immune response in incident infection.

This chapter describes longitudinal antibody responses in HIV infection according to HIV-1 envelope (Env) epitope recognition, attempts to characterise the serum antibody response at pre-infection, early infection and late infection, and to examine if prior exposure to HIV can influence the development of anti-HIV antibody response.

To recap, antibody responses in HIV infection can be categorised into Fiebig stages using plasma markers of HIV including HIV viral RNA, p24 antigen, HIV enzyme immunoassay (EIA) and HIV Western blot. Fiebig Stage III HIV infection is the first evidence of a humoral response and with the emergence of a sensitive HIV EIA at approximately 13.5 days (43). This part of the study aimed to evaluate the evolution of this antibody response and to explore if HIV-1 epitope recognition played a part in this development, and if epitope recognition persisted throughout the course of infection.

As discussed in the introduction chapter, humoral responses to HIV are impaired by direct and indirect effects on B-cell function and antibody production (131). Direct effects include complement bound HIV binding to the B-cell surface complement receptor CD21 to cause apoptosis. This causes B-cell depletion and further viral dissemination. HIV gp120 binds to B cells and causes secretion of inflammatory cytokines tumour necrosis factor (TNF) and interleukin (IL)-6. HIV-Nef suppresses B-cell class switching, reducing diversity of antibody production. Over the longer term, B-cell exhaustion appears. This phenotypical change in B-cell functionality is characterised by loss of CD21 cell surface marker.

Indirect effects on B-cell function include the following. B-cell hyperactivation by HIV induced immune cell activation, caused by increased serum levels of lipopolysaccharide (bacterial from leaky gut in early HIV), B-cell activating factor (BAFF), TNF, interferon alpha INF-α), IL-6 and IL-10. Depletion of T_{FH} CD4 T cells causes an increase in number of immature transitional B cells (131). Depletion of the antibody response also permits to spread of HIV from cell to cell.

The initial humoral response to HIV is unable to control viral replication. As discussed in the introduction, the initial IgM anti-gp41 response is non neutralising (143). The first autologous neutralising antibodies appear several months following incident infection, and the inhibitory nature of this response results in replacement of the neutralisation-sensitive virus by a resistant viral population. Genetic analysis of this viral population shows occasional Env mutations and increased levels of N-glycosylation (145,146). The majority of PLWH develop these responses which have cross clade neutralising ability and up to 30% develop antibodies with broadly neutralising properties appearing two to four years post infection (148). This is associated with increased viral load and lower CD4+ in early infection (149) The production of neutralising antibodies is associated with Env structures of shorter V1-5 envelope lengths and fewer glycosylation sites at V1V2 (150). Identification of germline precursors and serial analysis of the maturing humoral response shows continual somatic hypermutation of antibody structures including the complementarity determining region 3 and occasionally framework regions (152,231). As viral escape mutations contribute to an altered progeny population, neutralising antibodies do not contribute to viral control in the host (153).

However, *in vitro* studies with these antibodies show cross clade neutralisation (154,155), protection and reduction of infection in animal studies, and provide insights for immunogenic epitopes (156–158).

In summary, HIV creates a multi-level attack on the immune system's humoral response to HIV infection by direct action on B cells, and indirect actions on B-cell stimulatory pathways and T cell activation.

4.2. Aims

The key aims for this part of the project were

1. Characterise the serum antibody responses/antigen recognition in HIV envelope protein for pre-infection, early infection and late infection

2. Characterise antigen recognition by host immune response

3. Identity common antigen recognition

As in the previous chapter, the HIV gp160 yeast surface display library was used to investigate the serum immune responses to HIV in this seronegative cohort. Again, the aim was to review immune responses to conformational as opposed to linear epitopes. A schematic of the HIV envelope protein is displayed below in Figure 4.2-1 for reference purposes.

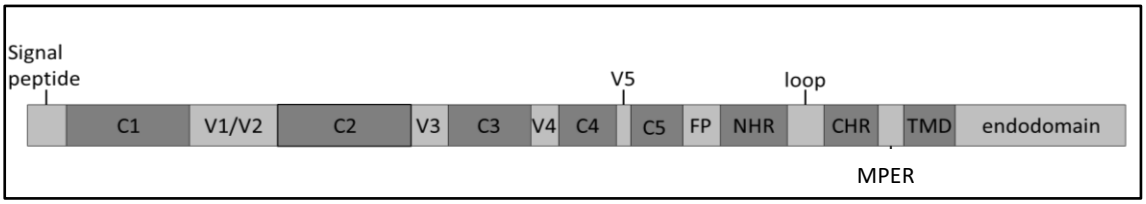


Figure 4.2-1 HIV gp160 envelope sequence schematic
Figure shows HIV envelope sequence with initial gp120 components: signal peptide C1-C5 conserved regions, V1-V5 variable region. gp41 components: FP fusion peptide, NHR N-helix, loop, CHR c-helix, MPER membrane proximal external region, TMD transmembrane domain, endodomain

4.3. Group B cohort

4.3.1. Identification of candidate samples

I undertook longitudinal follow-up of all new HIV infections at the study site and identified nine individuals in Group A who seroconverted from HIV negative to positive during the study period from 2015-2017. The rate of seroconversions in this cohort was impacted by significant developments in HIV prevention and care and will be discussed in the final chapter. Hence, group B numbers are modest.

I approached all nine seroconverter patients and asked them to participate in longitudinal follow up visits which would include regular blood sampling and demographic information. This would be done in parallel with standard HIV care but did not replace routine clinical care. Participants were offered travel expenses. To improve compliance with return visits, study visits were scheduled concurrently with routine clinical follow-up where possible.

4.3.2. Baseline demographics group B

Nine individuals in Group A were identified as having seroconverted during the study period from 2015-2017. Five individuals agreed to participate in longitudinal follow-up with blood sampling. These patients were coded B001, B002, B003, B004 and B005. The baseline demographics and peripheral blood mononucleated cell and baseline patient characteristics shown in Table 4.3-1 and Table 4.3-2. The median age of the five patients was 34.0 years (29.8 - 37.8). As numbers were small, no statistical analysis was attempted to determine association of risk factors and disease incidence.

Study No.	B0001	B0002	B0003	B0004	B0005
Consent Date	04/02/2016	05/02/2016	10/03/2015	31/03/2016	23/04/2015
DOB	18/04/1979	15/04/1978	24/01/1983	02/06/1986	17/04/1981
Age at consent date (years)	36.8	37.8	32.1	29.8	34.0
Gender 1 = male	1	1	1	1	1
No. partners last 6/12	4	50	30	6	18
No. regular	1	0	1	0	1
No. casual	3	50	29	6	17
STI in last year (1= yes, 0=no)	1	1	1	1	1
CD3 cells %	82.3	78.8	81.5	82.5	89.3
CD3 cells/µl (700-2100)	1736.0	1577.0	1622.0	1686.0	2486.0
CD4 %	21.5	20.4	41.9	25.3	24.0
CD4 cells/µl (300 - 1400)	456.0	403.0	827.0	519.0	657.0
CD8 %	58.0	55.7	36.8	56.3	64.7
CD8 cells/µl (190 - 900)	1228.0	1099.0	727.0	1153.0	1774.0
CD56 %	9.4	15.2	14.0	12.5	5.0
CD56 cells/µl (90-600)	198.0	308.0	281.0	254.0	142.0
CD19 cells %	8.1	5.7	4.5	43.4	6.1
CD19 cells/µl (100 - 150)	170.0	116.0	91.0	89.0	174.0
CD4:CD8 ratio	0.4	0.4	1.1	0.5	0.4

Table 4.3-1 Group B baseline information

Baseline demographics and peripheral blood mononucleated cell characteristics of seroconverter population

Characteristics	Median	Min	Max
No. partners last 6/12	18	4	50
No. regular	1	0	1
No. casual	17	3	50
CD3 cells %	82.3	78.8	89.3
CD3 cells/µl (700-2100)	1686.0	1577.0	2486.0
CD4 %	24.0	20.4	41.9
CD4 cells/µl (300 - 1400)	519.0	403.0	827.0
CD8 %	56.3	36.8	64.7
CD8 cells/µl (190 - 900)	1153.0	727.0	1774.0
CD56 %	12.5	5.0	15.2
CD56 cells/µl (90-600)	254.0	142.0	308.0
CD19 cells %	6.1	4.5	43.4
CD19 cells/µl (100 - 150)	116.0	89.0	174.0
CD4:CD8 ratio	0.4	0.4	1.1

Table 4.3-2 Distribution of baseline patient characteristics

Baseline partner and lymphocyte subset information of Group B participants

4.3.3. Group B visits

Group B participants attended for blood sampling according to the following schedule: monthly for the first six months following diagnosis and subsequent visits at 12, 18 and 24 months to complete 2 years of follow-up. Not all patients were able to attend for each monthly follow-up. Total visit number ranged from 3-9 visits, with the maximum number of study visits achieved by B004.

Blood samples were obtained at each visit at the study site, transported to the research laboratory and processed and stored as previously described. Follow-up blood sampling was not possible beyond December 2016 due to time limitations and the need to focus on the following part of the project

4.3.4. HIV seroconversion assessment

Several key factors were sought regarding group B individual's diagnosis of HIV including estimated date of seroconversion, the assurance that any seronegative samples were obtained prior to HIV infection, and assurance that samples obtained during the period considered seronegative had no evidence of HIV infection.

I reviewed two pieces of information for each group B participant pertaining to their HIV diagnosis.

Recent Infection Testing Algorithm: In 2009 Public Health England introduced the recent infection testing algorithm (RITA)(322). This is a serology test which measures anti-HIV antibodies using the AxSym avidity assay (Abbott Laboratories). Other disease parameters, including CD4 count (low count being less than 200 cells/mm^3), and presence of an AIDS-defining illness are also considered when applying the test. An avidity of <0.8 indicates HIV infection acquired in the previous 4 to 6 months. All patients diagnosed with HIV undergo RITA testing to estimate the timing of infection. On a population level this offers information on the profile of newly diagnosed HIV infections. All but one of our patients had a RITA test available for analysis.

Last negative HIV test: All group B participants had their records reviewed for the most recent previous negative HIV screening test.

Using both RITA and documented evidence of previous HIV testing, the more recent test was used as confirmation of the individual's HIV negative status at the point of blood sampling when termed "seronegative".

4.3.4.1. Ensuring seronegative samples were obtained prior to HIV infection

For all group B participants, samples termed "seronegative" were checked to ensure they were drawn prior to date of HIV diagnosis.

4.3.4.2. Ensuring samples termed seronegative had no evidence of HIV infection

I confirmed the seronegative status of group B participant pre-infection samples by Western Blot assay. This detects antibodies to HIV proteins (p) and glycoproteins (gp) p17, p24, p55, p31, p66, gp41, gp120, gp160 and gp36 (specifically HIV-2) (314). 200ul aliquots of pre-infection plasma samples were sent to the National Infection Service at Public Health England Colindale and underwent Western Blot analysis. All five patient samples were confirmed negative on Western Blot analysis as listed in Table 4.3-3. B001 sample was described as indeterminate due to a trace reactivity against p17 but all other antibodies were negative, and PHE laboratory confirmed this as a negative result.

Group B participant	Anti-HIV-1 and 2
B001	Indeterminate*
B002	Negative
B003	Negative
B004	Negative
B005	Negative

Table 4.3-3 Western blot analysis of Group B participants
Group B participant Western blot analysis of pre-infection plasma samples

4.3.4.3. Estimating date of HIV seroconversion and subsequent sampling

I estimated the date of HIV seroconversion based on either the RITA or previous negative HIV test and considered this would provide the most conservative estimate of the date of seroconversion. Ideally, infection would have described according to Fiebig acute HIV infection (AHI) staging system (43) but this data was not available for each group B member.

Samples were grouped into "early" and "late" infection. The dates were based on the greatest interval of time possible since incident HIV infection. The group B participants occasionally volunteered possible dates for infection based on a personal risk assessment of sexual contacts, but for consistency of data the time estimation was maintained as discussed above. Early infection samples were estimated to have been taken on average 18.8 to 123.4 days post-infection, and late infection samples taken 177.6 to 282.2 days post-infection.

The following tables Table 4.3-4 and Table 4.3-5 document the chronology of HIV infection- the estimated date of seroconversion based on the above details, and the schedule of follow-up visit attended by the group B participants.

	Estimated last date HIV negative by RITA	Last HIV negative test	HIV negative	HIV diagnosis date	Early sample date	Possible maximum days since infection	Days since diagnosis	Late sample	Date	Days since infection	Days since diagnosis
B001	23/09/2015	15/10/2015	15/10/2015	21/01/2016	04/02/2016	112	14	VISIT 6	18/07/2016	277	179
B002	21/08/2015	03/09/2015	03/09/2015	19/12/2015	05/01/2016	124	17	VISIT 4	16/06/2016	287	180
B003	11/08/2015	17/09/2015	17/09/2015	09/12/2015	07/01/2016	112	29	VISIT 4	04/07/2016	291	208
B004	24/11/2015	08/09/2015	24/11/2015	23/03/2016	07/04/2016	135	15	VISIT 5	01/09/2016	282	162
B005		29/12/2015	29/12/2015	22/04/2016	11/05/2016	134	19	VISIT 3	28/09/2016	274	159
					MEAN	123.4	18.8			282.2	177.6

Table 4.3-4 Chronology of Group B HIV infection

Estimated date of HIV infection, known date HIV diagnosis, and the dates that early and late blood samples obtained

Study No.	Date of HIV diagnosis	Date started ARV	Visit 1	Visit 2	Visit 3	Visit 4	Visit 5	Visit 6	Visit 7	Visit 8	Total visits
B001	21/01/2016	04/02/2016	✓	✓	✓	✓	✓	✓	✓		8
B002	19/12/2015	05/01/2016	✓	✓	✓	✓	✓	DNA	DNA		6
B003	09/12/2015	07/01/2016	✓	✓	✓	✓	✓	✓	DNA		7
B004	23/03/2016	07/04/2016	✓	✓	✓	✓	✓	✓	✓	✓	9
B005	22/04/2016	11/05/2016	✓	✓	DNA	✓	DNA	DNA			4
B006	17/05/2016	09/06/2016	✓	✓	✓	✓	DNA	DNA			5
B007	29/07/2016	01/08/2016	✓	✓	DNA	DNA	DNA	DNA			3

Table 4.3-5 Group B longitudinal follow-up schedule

ARV antiretroviral therapy, ✓ indicates visit complete, DNA patient Did Not Attend for scheduled visit

All patients agreeing to follow-up post diagnosis entered a care structure. At the study centre, it is standard practice for all patients diagnosed with HIV to attend a review with a health counsellor on the day of diagnosis. This appointment includes discussion about HIV medication and the patients are offered literature to review prior to their initial clinical visit with a HIV specialist doctor. At the first clinical visit with a HIV specialist, all patients are offered standard HIV medication as per current guidelines (323).

4.3.5. Group B antiretroviral therapy

All five group B patients began antiretroviral therapy within one month of diagnosis. The median time to initiation of medication was 17 days with a range of 3-29 days as shown below in Table 4.3-6. This is in keeping with standard practice at the study centre, as on the day of diagnosis multiple blood testing samples are obtained to inform choice of medication. These tests include measurement of viral load, a baseline viral resistance assay to check for the presence of viral mutations which could impact efficacy of antiretroviral medication, viral tropism, and other biochemical and haematological assays relevant to patient care. It takes 7-10 days for all results to be made available, and initial clinical visits were scheduled to allow for these results to return.

Study No.	Date dx	Started medication	Days
B001	21/01/2016	04/02/2016	14
B002	19/12/2015	05/01/2016	17
B003	09/12/2015	07/01/2016	29
B004	23/03/2016	07/04/2016	15
B005	22/04/2016	11/05/2016	19
B006	17/05/2016	09/06/2016	23
B007	29/07/2016	01/08/2016	3
		Median	17 (3-29)
		Minimum	3
		Maximum	29

Table 4.3-6 Details of antiretroviral initiation
Table shows details of cART for group B participants B001-B005

4.3.6. Group B baseline HIV characteristics

Patient viral load ranged from 5-6 log copies RNA per ml. This is in keeping with early HIV-1 infection, where a high viral load emerges in concert with typical symptoms and signs of "seroconversion". This viraemia usually drops within 3 months of incident infection, albeit more rapidly with use of antiretroviral medication.

Patient HIV subtype/clade was documented. This information is captured at the time of diagnosis. All viral load samples are interrogated to retrieve the genomic sequence of the protease (PR) and reverse transcriptase (RT) regions. The majority sequence (expressed as a percentage) is then applied as that strain's subtype.

The most frequently seen HIV-1 variety was subtype B. This subtype is most widely distributed across western Europe, north America and Australia, and in keeping with the demographics of this group. One participant, B002, acquired HIV-1 subtype F. This subtype is usually seen in west Africa along with subtypes G, H, J, K, CRF01 (Circulating Recombinant Forms). Both subtype B and F are members of the HIV-1 M (major) group which is the most widespread circulating viral group globally (324).

These findings are summarized in Table 4.3-7.

Study No.	Viral load at diagnosis (copies RNA/ml)	Subtype/clade info
B001	24924	1. PR: B (95.6%) 2. RT: B (92.9%)
B002	421909	1. PR: F (93.3%) 2. RT: F (93.5%)
B003	1134266	1. PR: B (95.6%) 2. RT: B (94.7%)
B004	528964	1. PR: B (95.6%) 2. RT: B (94.3%)
B005	140726	1. PR: B (94.6%) 2. RT: B (95.3%)

Table 4.3-7 Characteristics of HIV infection in Group B.
RNA ribonucleic acid copies/ml blood sampled, PR protease, RT reverse transcriptase

4.3.7. Viral load dynamics of Group B

All five participants began taking antiretroviral medications soon after diagnosis with the intention of suppressing HIV viral load. All patients achieved an undetectable viral load by the time of their second study visit which was a median of 40 days post diagnosis (range 29-112). This time to undetectability was within 3 months of starting medication which is expected as per current guidelines. B003 took longest to achieve an undetectable viral load. This participant had the highest viral load at diagnosis and therefore the time taken to achieve viral suppression is in keeping with this finding. This is shown in Table 4.3-8 and Figure 4.3-1.

	Days to undetectable viral load
B001	32
B002	57
B003	112
B004	29
B005	40
Median	40

Table 4.3-8 Viral load dynamics Group B
Details of time taken to achieve an undetectable viral load since starting cART medication

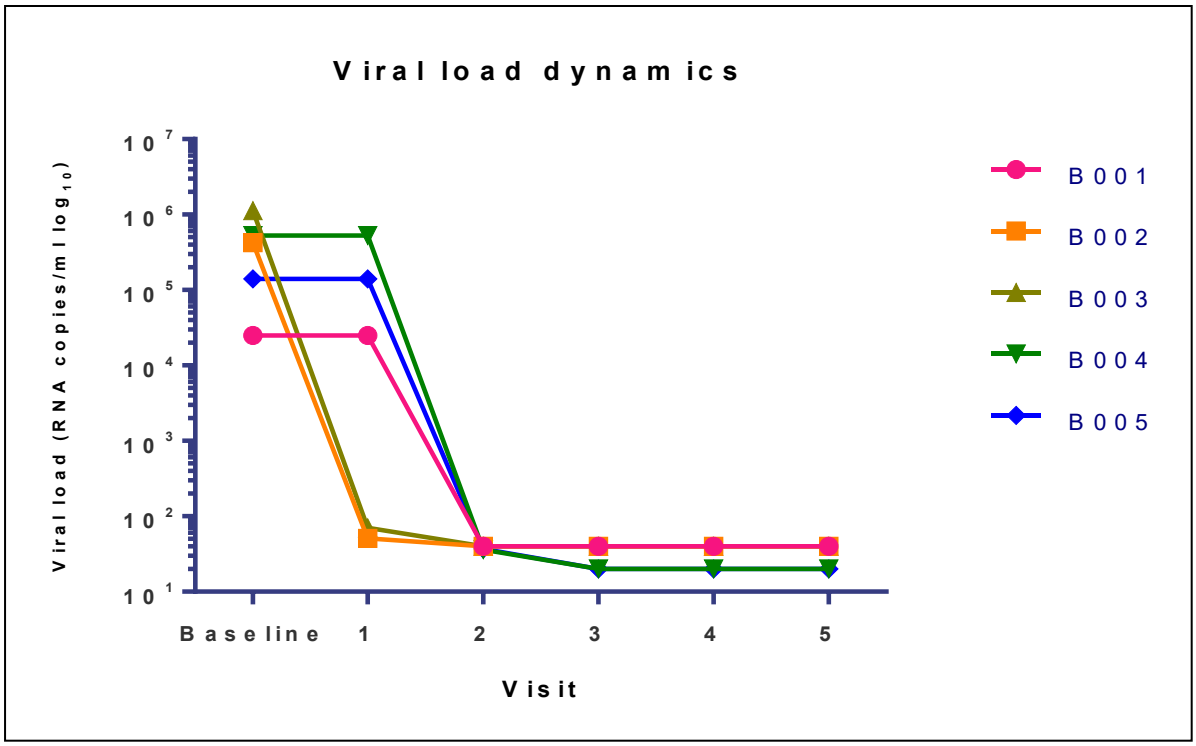


Figure 4.3-1 Group B viral load dynamics
Study visit (x-axis) and plasma viral load (y axis, RNA copies per ml in logarithmic scale)

4.4. gp160 library analysis of seroconverter serum aliquots

In this part of the study anti-Env responses were reviewed in five individuals who underwent seroconversion from HIV negative to positive. As this was a longitudinal study design, serum samples were collected from three timepoints to assess the immune response: prior to infection, early infection and later infection. This schedule is described in the materials and methods chapter.

All seronegative samples were confirmed initially by serologic testing using ARCHITECT HIV Ag/Ab Combo (Abbott Diagnostics) assay which tests for p24 antigen positivity (anti p24 MAb) and anti-HIV antibodies directed at gp41 of HIV-1 group M/O and gp36 of HIV-2. They were then tested by western blot to confirm true seronegative status, results on Table 4.3-3.

The post infection samples were again confirmed with the ARCHITECT HIV Ag/Ab Combo assay and HIV RNA sampling. Infection duration was estimated based on time since previous HIV testing and result from recent infection testing algorithm (RITA). This test measures the avidity of anti-HIV antibodies; lower scores indicate recent infection within the previous four months (92,325).

These samples did not undergo further positive tests e.g. ELISA or western blot; these tests may have facilitated classification of group B participants into the relevant Fiebig stage, or to examine serum binding to full glycoproteins or specific epitopes. However, the intention of this chapter was to review antibody binding to epitopes rather than whole Env structures.

By recruiting seronegative individuals and following seroconversion events, incident HIV infections were captured. All five group B members who were followed longitudinally had blood samples drawn prior to seroconversion when they were members of the seronegative cohort. These were the pre infection samples. The same gp160 yeast library was used to interrogate these samples. As previously described, yeast surface display of antigen represents a conformational epitope more akin to that seen in infection *in vivo*.

Serum aliquots were retrieved and adsorption CD20 performed as previously described. In contrast to the previous experiment, all samples were used individually and did not batch. The following samples were analysed: fifteen patient serum (pre, early and late infection from participants B001-B005), technical negative controls (autofluorescence, unstained and fluorescence minus one), a biological negative control (healthy laboratory samples), and a positive control (group E seropositive cART naïve participant).

Samples were prepared as described in materials and methods and the HIV gp160 envelope library was used. Each serum sample was added to an aliquot containing HIV-gp160 envelope library and sorted using a BD FACS ARIA III in a CL3 laboratory. The same gating strategy was used as described in the previous chapter to select yeast cells bound to patient serum and sorted approximately 50000 yeast cells per experiment. Successive rounds of sorting, enrichment, subsequent culture and re-sorting for each sample were performed.

4.4.1. Seroconverter serum FACS results

The fifteen experimental samples were analysed by FACS (BD FACS Aria III) and yield and percentage of total population of PE high populations assessed following each sort. The positive control showed a large population of PE high yeast cells, in keeping with the known serostatus of that sample.

The healthy control PE high yeast population was 0.25% and the positive control was 0.77% of the total population. All fifteen experimental samples showed a PE high population. Approximately 50,000 yeast cells were sorted into SDCAA and pen/strep collection media for each sample. Sorted cells were vortexed, refrigerated until the end of the experiment. Samples were transferred to an incubator to rest for one hour post sort and then transferred to SDCAA plates and liquid media for culture as previously described.

Table 4.4-1 below shows PE high yeast population for each patient sample.

Sample	PE high yeast population	Sample	PE high yeast population	Sample	PE high yeast population
NC	0.25%				
PC	0.77%				
Pre B001	0.62%	Early B001	0.44%	Late B001	0.28%
Pre B002	0.28%	Early B002	0.97%	Late B002	0.79%
Pre B003	0.21%	Early B003	0.23%	Late B003	0.17%
Pre B004	1.36%	Early B004	0.26%	Late B004	0.23%
Pre B005	0.23%	Early B005	0.47%	Late B005	0.24%
Median	0.28%	Median	0.44%	Median	0.24%
Range	0.21- 1.36	Range	0.23-0.97	Range	0.17-0.79

Table 4.4-1 Percentage of gp160 envelope expressing yeast cell reactive with patient sera
Table shows first FACS analysis of HIV gp160 library sorted by seroconverter serum samples from pre, early and late HIV infection

. NC negative biological control, PC positive control

4.4.2. Sequential enrichment plots

I performed two further rounds of FACS and culture on each patient yeast sample and reviewed the data plots. Each enrichment produced an increasingly PE high population for all fifteen patient samples (5 pre-infection, 5 early infection, 5 late infection) and the positive and healthy controls. This is shown in Figure 4.4-1, Figure 4.4-2, and Figure 4.4-3 below.

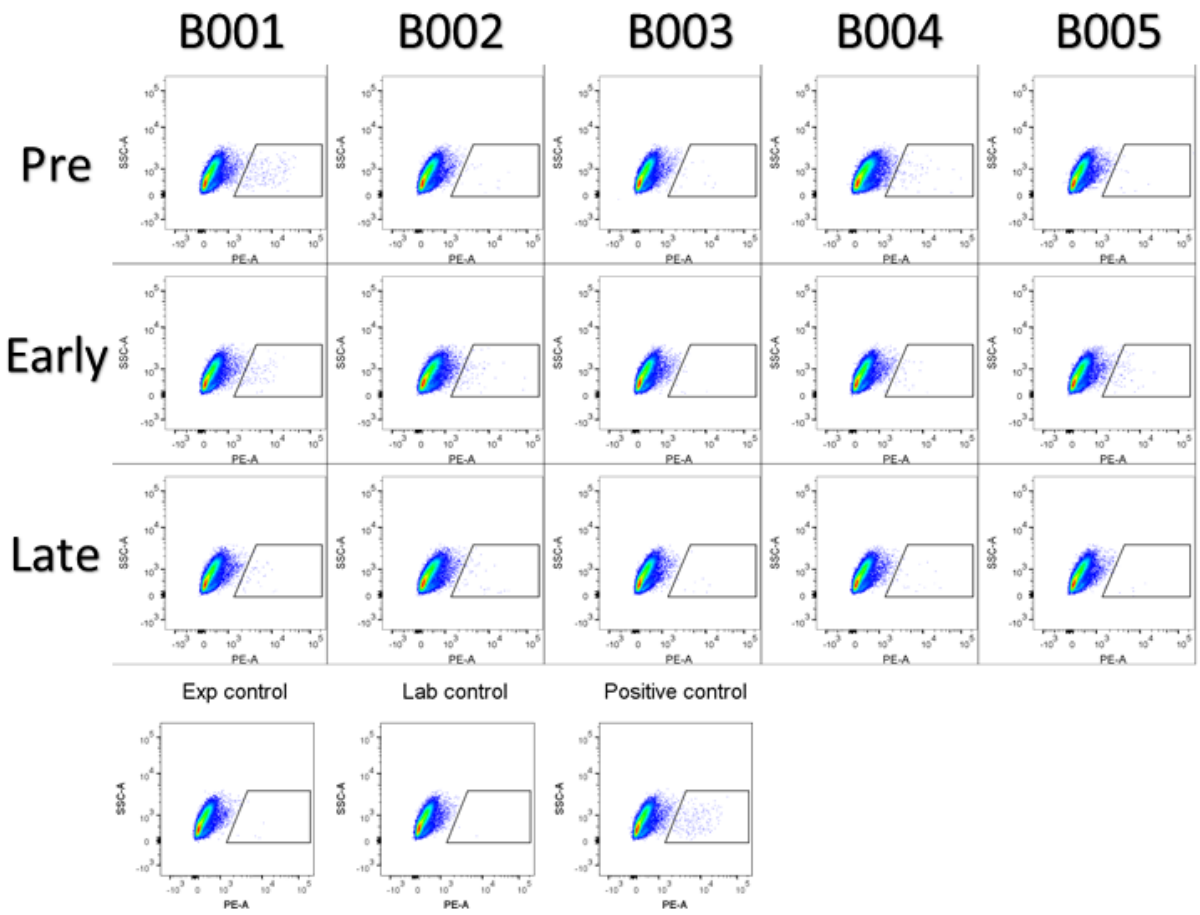


Figure 4.4-1 Flow cytometric dot plots of proportion of yeast cell expressing HIV gp160 envelope which react with patient sera before and during HIV infection after 1st round of FACS sorting

First row pre-infection, second row early infection, third row late infection, from B001-B005.Exp control- technical negative control, lab control- biological negative control, positive control as described.

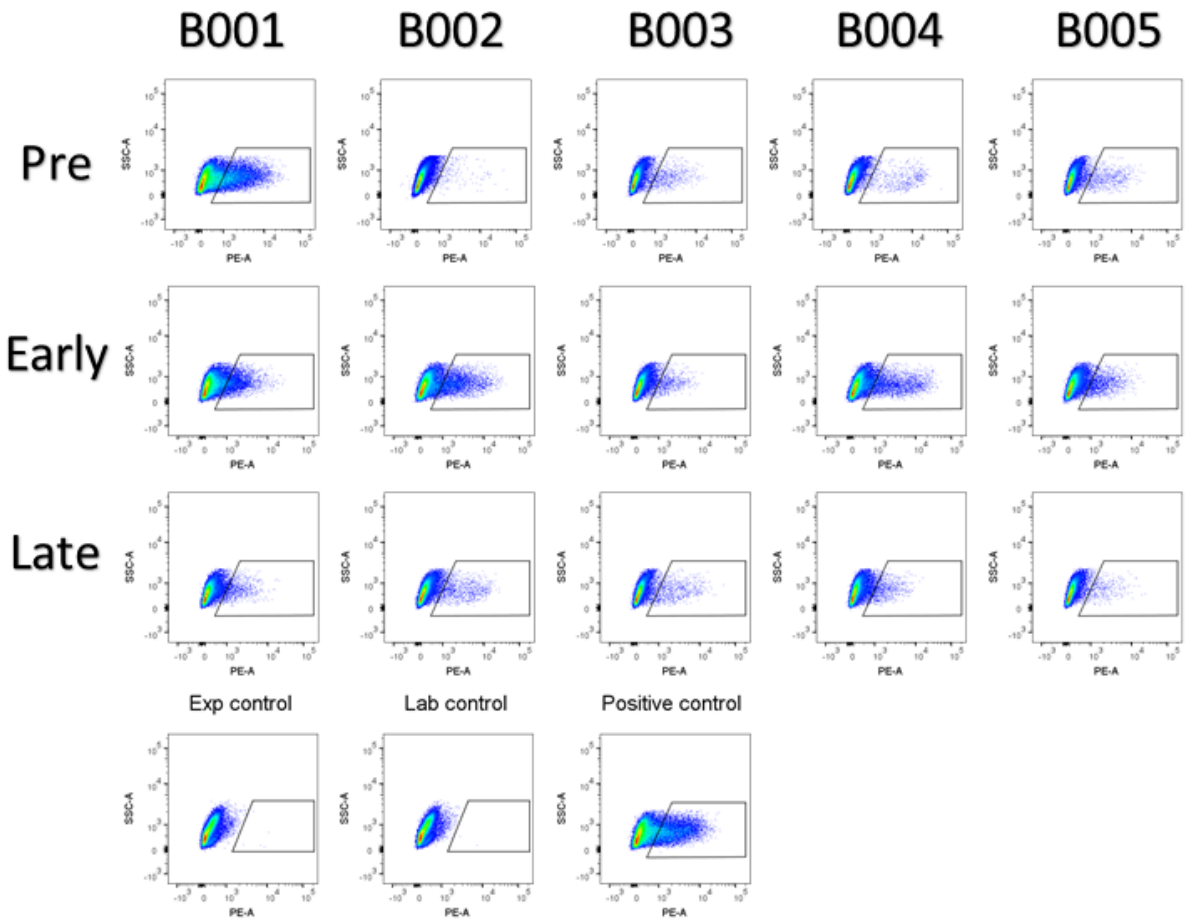


Figure 4.4-2 Flow cytometric dot plots of proportion of yeast cell expressing HIV gp160 envelope which react with patient sera before and during HIV infection after 2nd round of FACS sorting

First row pre-infection, second row early infection, third row late infection, from B001-B005.Exp control- technical negative control, lab control- biological negative control, positive control as described.

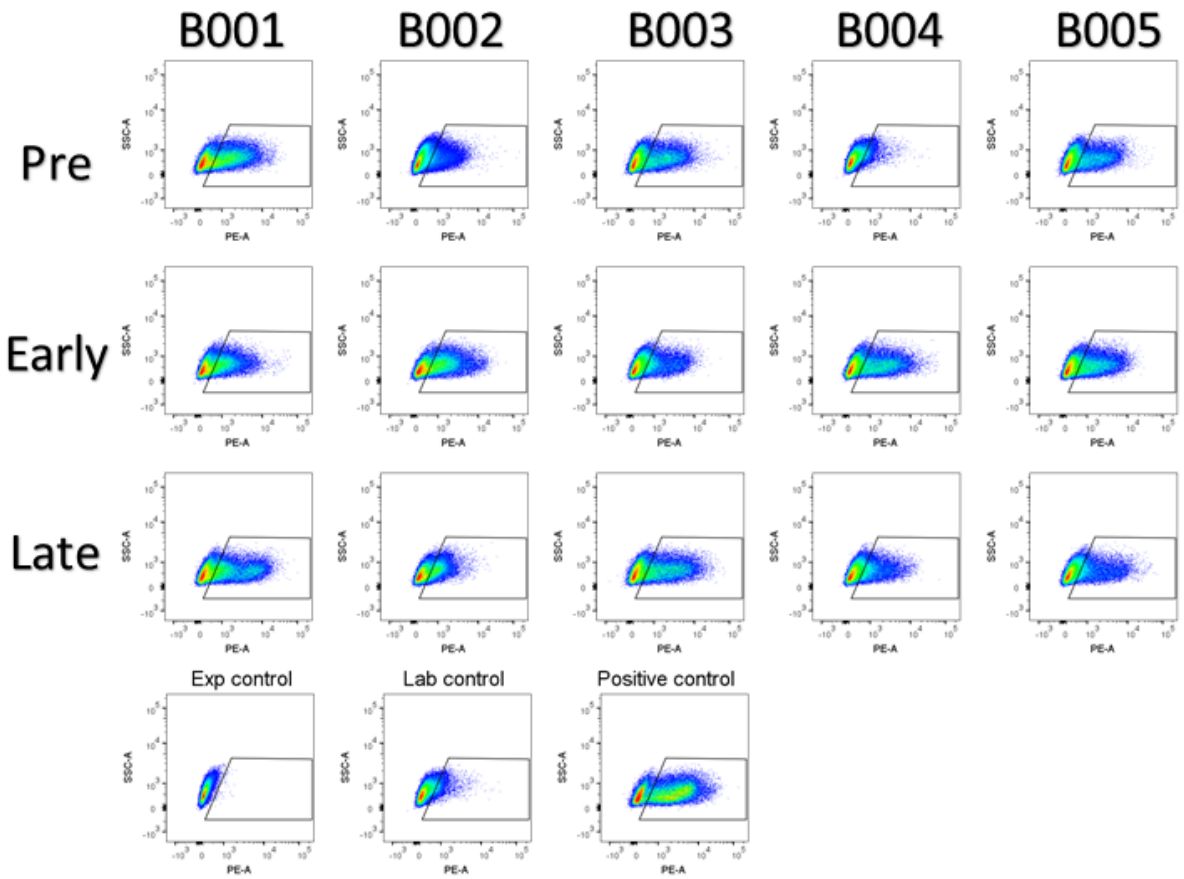


Figure 4.4-3 FACS analysis of seroconverter samples 3rd round flow cytometric dot plots of proportion of yeast cell expressing HIV gp160 envelope which react with patient sera before and during HIV infection after 3rd round of FACS sorting

First row pre-infection, second row early infection, third row late infection, from B001-B005.Exp control- technical negative control, lab control- biological negative control, positive control as described.

Figure 4.4-4 below shows the progressive increase in the PE high yeast population with successive round of flow sorting and culture (enrichment). Technical negative control (autofluorescence), positive control and experimental B003 preinfection samples are shown here for demonstrative purposes.

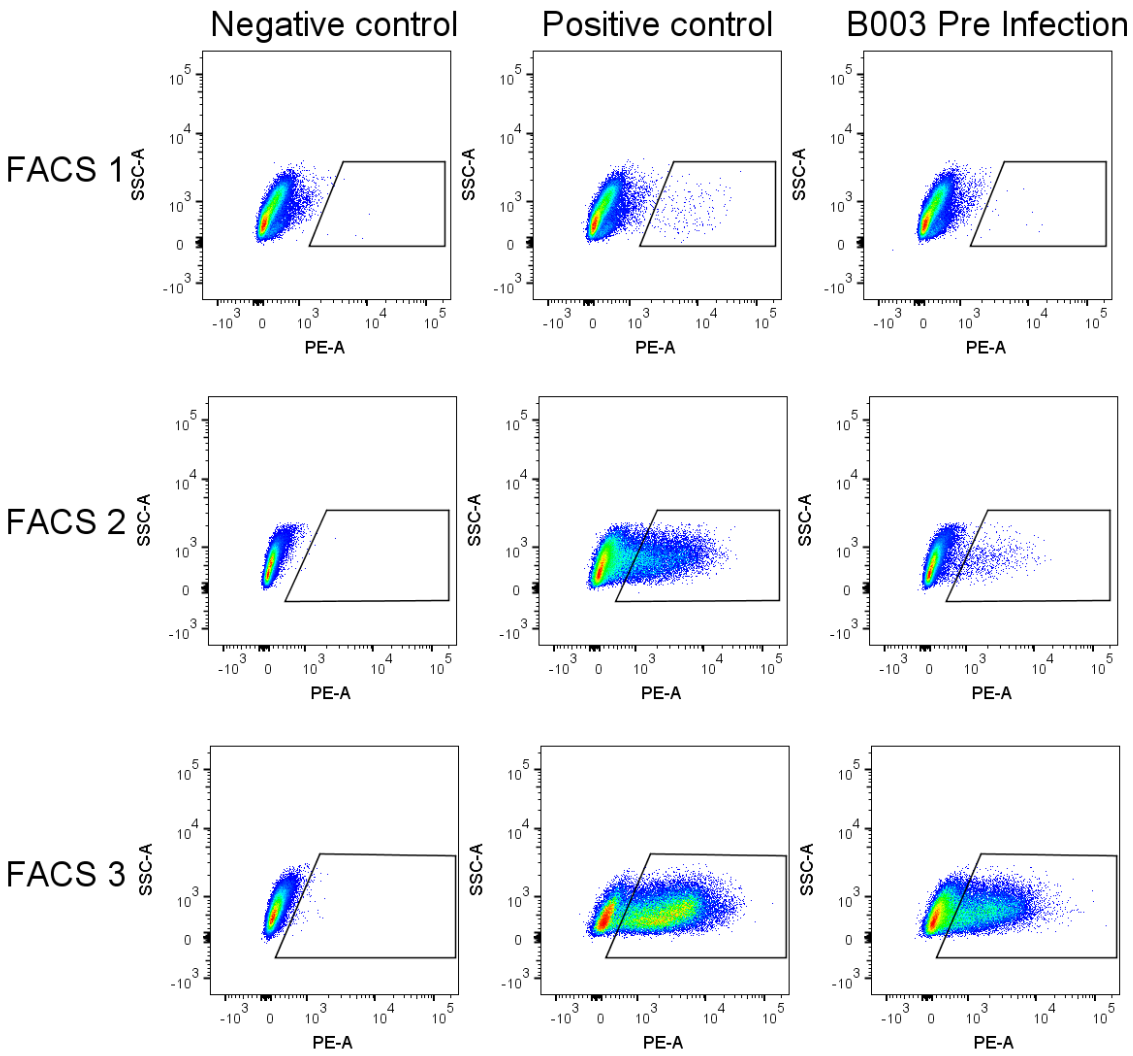


Figure 4.4-4 Sequential enrichment of yeast gp160 envelope positive cells which bind to patient sera
Figure showing progressive increase in PE high yeast population through successive enrichment. X axis PE- area, y axis side scatter area. Samples used for illustrative purposes- technical negative control, positive control and B003 pre infection.

4.4.3. Sequential enrichment graph

As shown, successive rounds enrichment produced an increasing PE high yeast population. These represent a more select population of yeast cells being sorted per experiment as the same patient serum samples were used each time. This sorted yeast population now contains yeast cells bearing epitopes selectively recognised by the patient's serum. Data from the flow cytometry analysis was recorded as percentage PE high of total yeast population per sort. With each successive enrichment, a greater population of the yeast was PE high, representing a greater volume of patient serum binding to surface bound yeast epitopes. All samples demonstrated enrichment, as did the positive control. These results are shown in Table 4.4-2 and Figure 4.4-4.

	NC	Lab C	PC		
1	0.15	0.25	0.77		
2	0.03	1.45	21.8		
3	0.07	11.5	65		
	PreB1	PreB2	PreB3	PreB4	PreB5
1	0.62	0.28	0.21	1.36	0.23
2	23.2	0.24	1.83	1.45	1.86
3	49.6	13.1	33.2	8.01	27.5
	Early1	Early2	Early3	Early4	Early5
1	0.44	0.97	0.23	0.26	0.47
2	11.5	11.1	2.05	8.32	4.5
3	39.3	48.2	25.1	37.4	38.4
	LateB1	LateB2	LateB3	LateB4	LateB5
1	0.28	0.79	0.17	0.23	0.24
2	3.18	2.93	2.11	2.83	1.12
3	43.1	35.2	40	25.9	23

Table 4.4-2 Percentage of gp160 envelope positive yeast cells which bind to control and patient sera following sequential FACS sort enrichment

Left column indicates sort round, numbers indicate PE high yeast population shown as a percentage of the total yeast population. NC technical negative control (autofluorescence), Lab C biological negative control, PC seropositive positive control.

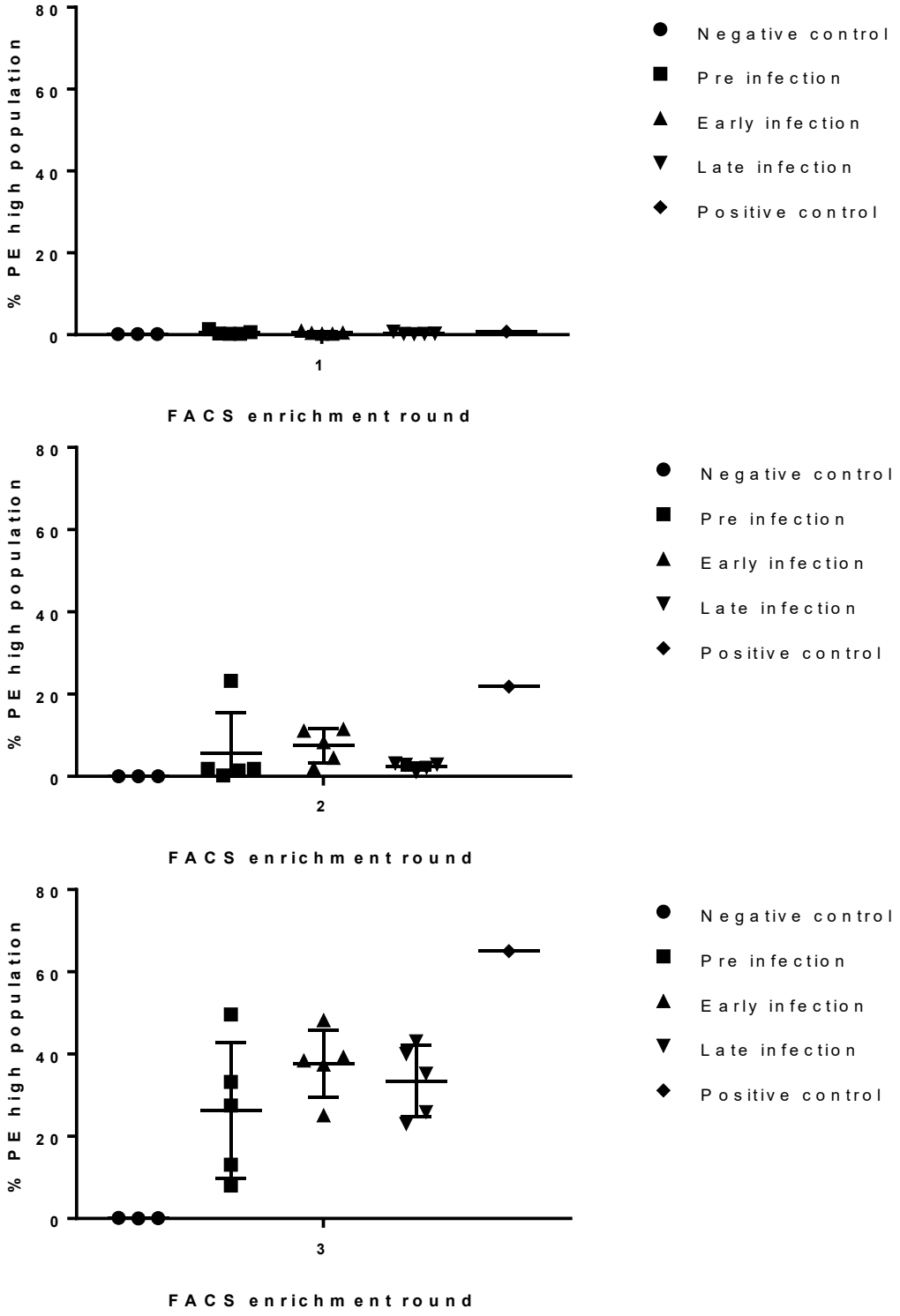


Figure 4.4-5 Mean and standard deviation (SD) of gp160 envelope positive yeast cells which bind to control and patient sera after sequential FACS sort enrichment

The graphs show the pre, early and late infection samples grouped according to enrichment round 1, 2, or 3. Controls include negative (technical- autofluorescence) and positive controls, patient serum samples pre/early/late B001-B005

4.4.4. Single clone analysis

I used single clone analysis to verify affinity of selected yeast populations and patient serum samples. As described, this process uses homogenous yeast cells bearing a common HIV envelope epitope for analysis of the respective patient serum. Sixteen individual clones were used to review the discrete antigenic regions responsible for antibody recognition. Single clone analysis also provided the base material for the next section of the project.

The criteria for a positive single clone population was as previously; if the PE high population peak was greater than biological negative control, this was considered significant. These clones were then processed for DNA extraction and sequencing to identify epitopes of interest. The gating strategy and controls for single clone analysis were as previously described.

Figure 4.4-6 shows the controls and gating strategy using negative biological and positive controls and serum/yeast pairing B003 late infection. The PE high population is shown on the x axis and side scatter shown on the y axis.

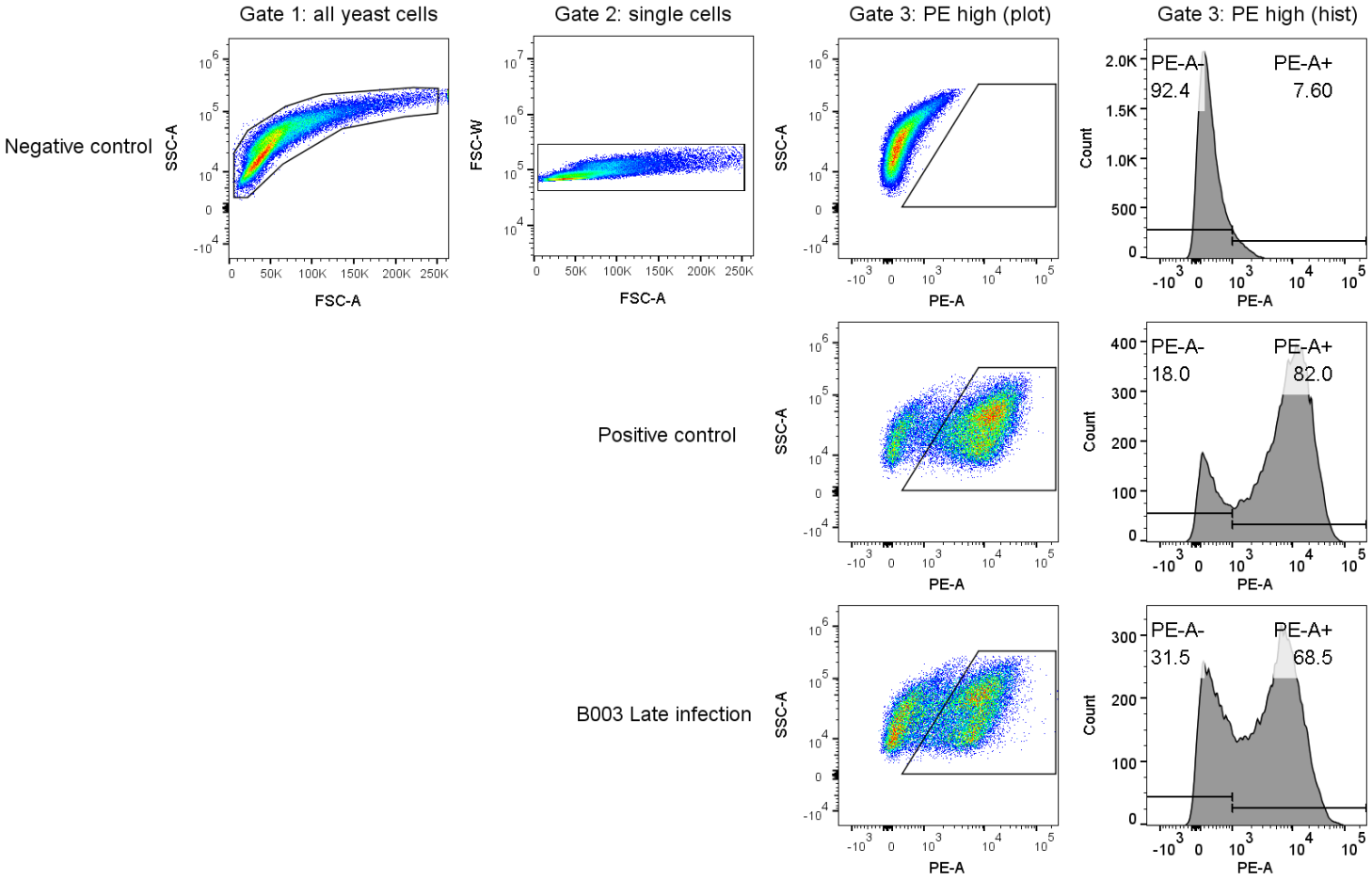


Figure 4.4-6 Single clone analysis gating and controls
Gating strategy and plots with histograms for single clone analysis of seroconverter serum. Negative control (biological), positive control and sample serum B003 late infection

I reviewed the single clone flow plots. Any yeast and serum plots with a PE high population greater than that of healthy controls were selected for further analysis. Not all patient yeast/serum groups had single clone samples with a greater frequency than the experimental controls and these were not submitted for sequence analysis.

Positive control, B003 and B005 pre infection, B003 and B004 early infection, and B001, B003 and B004 late infection histograms had a PE high population greater than negative/laboratory control.

The successful single clone analyses are shown in

Table 4.4-3 below, and Figure 4.4-7 and Figure 4.4-8 show selected histograms for yeast/serum pairings where the PE high histogram plot was greater than that of the biological control.

Sample	No. Samples with a PE yeast population greater than lab control	Selected for sequence analysis
Pre B1	1	No
Pre B2	5	No
Pre B3	13	Yes
Pre B4	5	No
Pre B5	15	Yes
Early 1	6	No
Early 2	4	No
Early 3	6	Yes
Early 4	12	Yes
Early 5	3	No
Late B1	12	Yes
Late B2	3	No
Late B3	15	Yes
Late B4	12	Yes
Late B5	6	No

Table 4.4-3 No of single yeast gp160 envelope clones which react with patient sera
Table shows instances where PE high population was greater than biological negative control sample

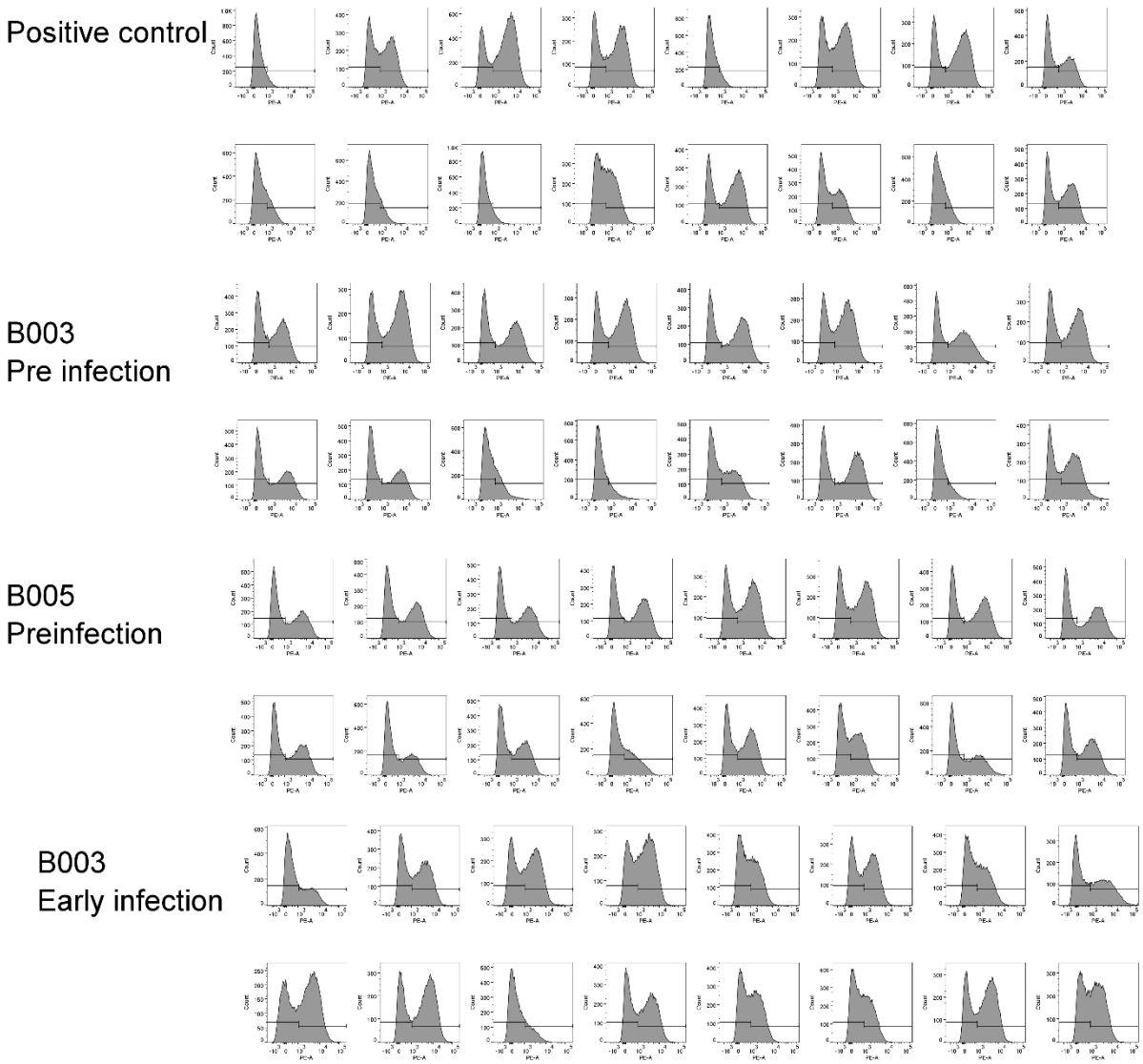


Figure 4.4-7 Representative histograms of single gp160 envelope yeast cells which react with patient sera (1)
Positive control, B003 and B005 pre infection, B003 early infection where PE high population was greater than negative/laboratory control

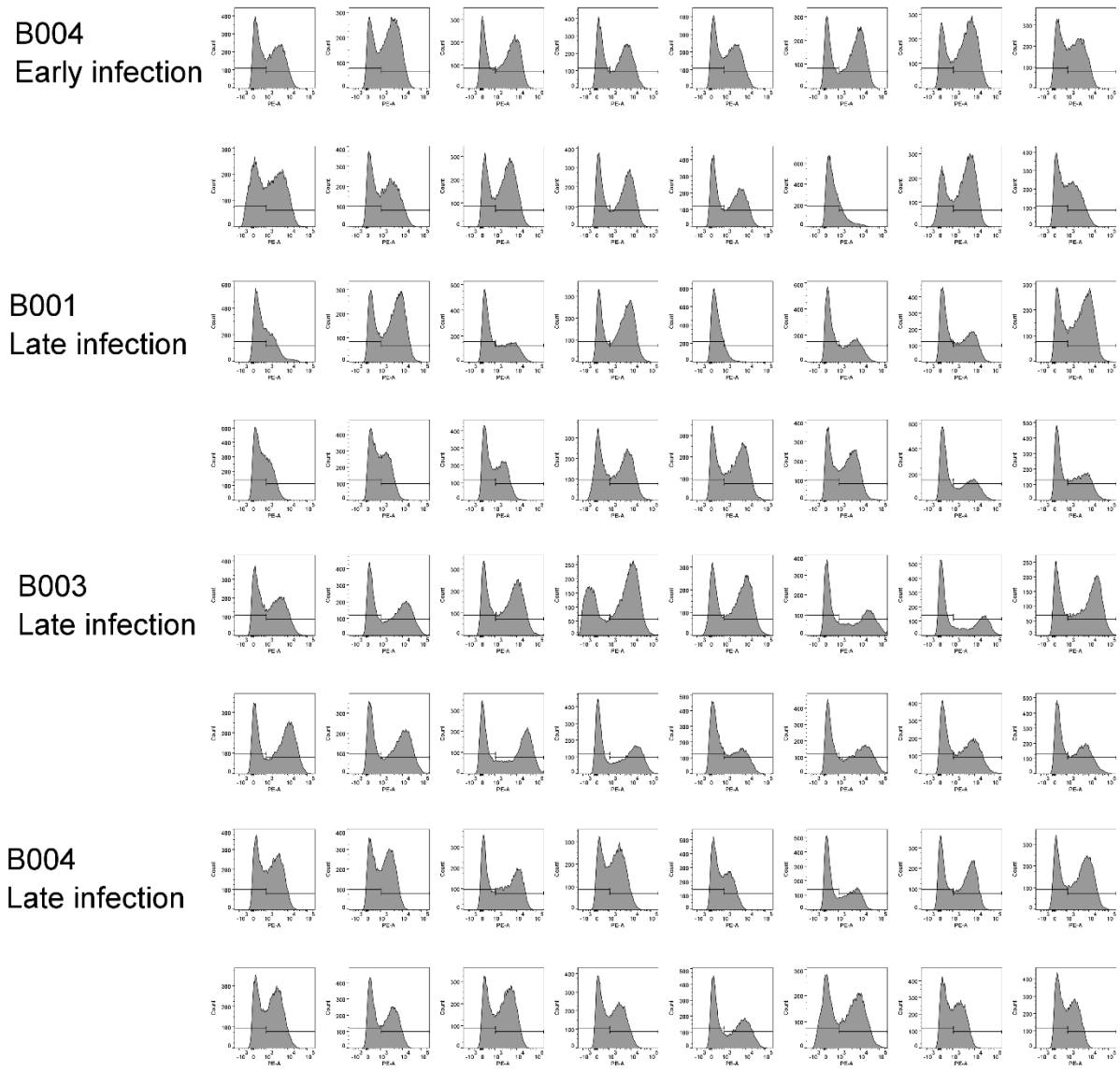


Figure 4.4-8 Representative histograms of single gp160 envelope yeast cells which react with patient sera (2)
B004 early infection, B001, B003 and B004 late infection histograms where PE high population was greater than negative/laboratory control

4.4.5. Sequential enrichment summary

The patient serum aliquots enriched with subsequent rounds of flow cytometry, representing a progressively refined yeast population bearing epitopes recognised by the patient serum antibodies. For each round of sorting, the biological controls were the healthy control and positive control samples. Table 4.4-4 below shows the increasingly PE high yeast population as a percentage of the total yeast population.

		%- yeast population PE high		
		1	2	3
Control	AF	0.18%	0.03%	0.04%
	US	0.18%	0.04%	0.18%
	FMO	0.15%	0.03%	0.07%
	Lab C	0.25%	1.45%	11.5%
	Pos C	0.77%	21.80%	65.00%
Sample	Pre B1	0.62%	23.20%	49.60%
	Pre B2	0.28%	0.24%	13.10%
	Pre B3	0.21%	1.83%	33.20%
	Pre B4	1.36%	1.45%	8.01%
	Pre B5	0.23%	1.86%	27.50%
	Early 1	0.44%	11.50%	39.30%
	Early 2	0.97%	11.10%	48.20%
	Early 3	0.23%	2.05%	25.10%
	Early 4	0.26%	8.32%	37.40%
	Early 5	0.47%	4.50%	38.40%
	Late B1	0.28%	3.18%	43.10%
	Late B2	0.79%	2.93%	35.20%
	Late B3	0.17%	2.11%	40.00%
	Late B4	0.23%	2.83%	25.90%
	Late B5	0.24%	1.12%	23.00%

Table 4.4-4 Summary table of proportion of yeast gp160 envelope yeast cells which react with patient sera following sequential FACS sort and enrichment

Table shows gp160 yeast library sorted by seroconverter participant serum samples

4.4.6. Sequence analysis plots

I aligned sorted yeast sequences to the parent gp160 reference sequence as described in section 4.4.7. The number of sequences retrieved per patient sample is documented in Table 4.4-5. The following pages display the aligned sequences in Figure 4.4-9, Figure 4.4-10, and Figure 4.4-11.

	Pre	Early	Late
B001	16	38	15
B002	24	34	49
B003	39	42	38
B004	41	48	34
B005	39	45	38

Table 4.4-5 Number of sequences available from 50 clones submitted

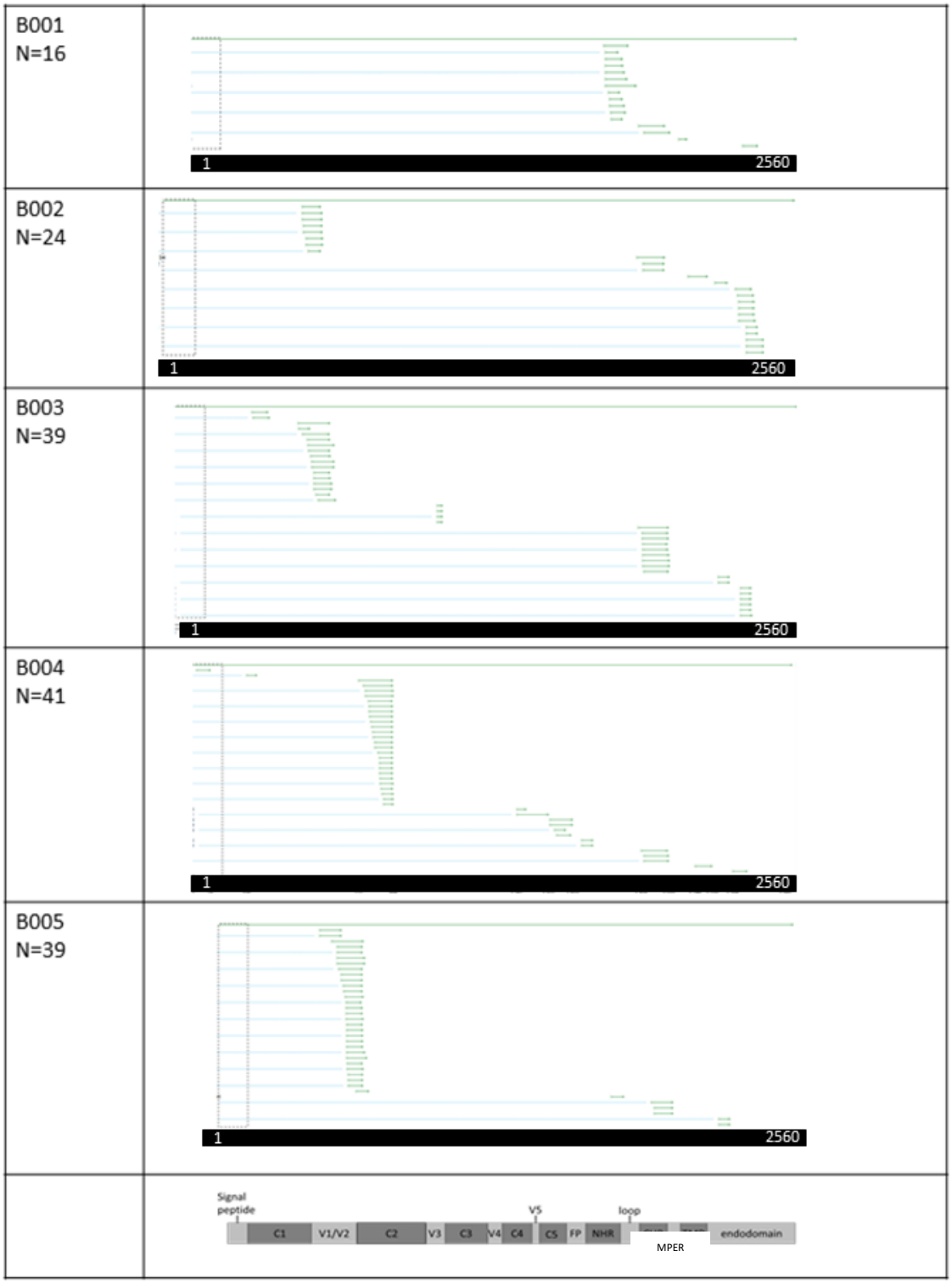


Figure 4.4-9 HIV gp160 library sorted by pre- infection samples
Sequences obtained from parent yeast sequences sorted by pre-infection yeast samples. HIV gp160 big and small libraries combined for use here. X-axis black bar indicates gp160 reference sequence HXB2 as previously. N = number of sequences returned from 50 sent clones. HIV envelope schematic shown below for illustrative purposes.

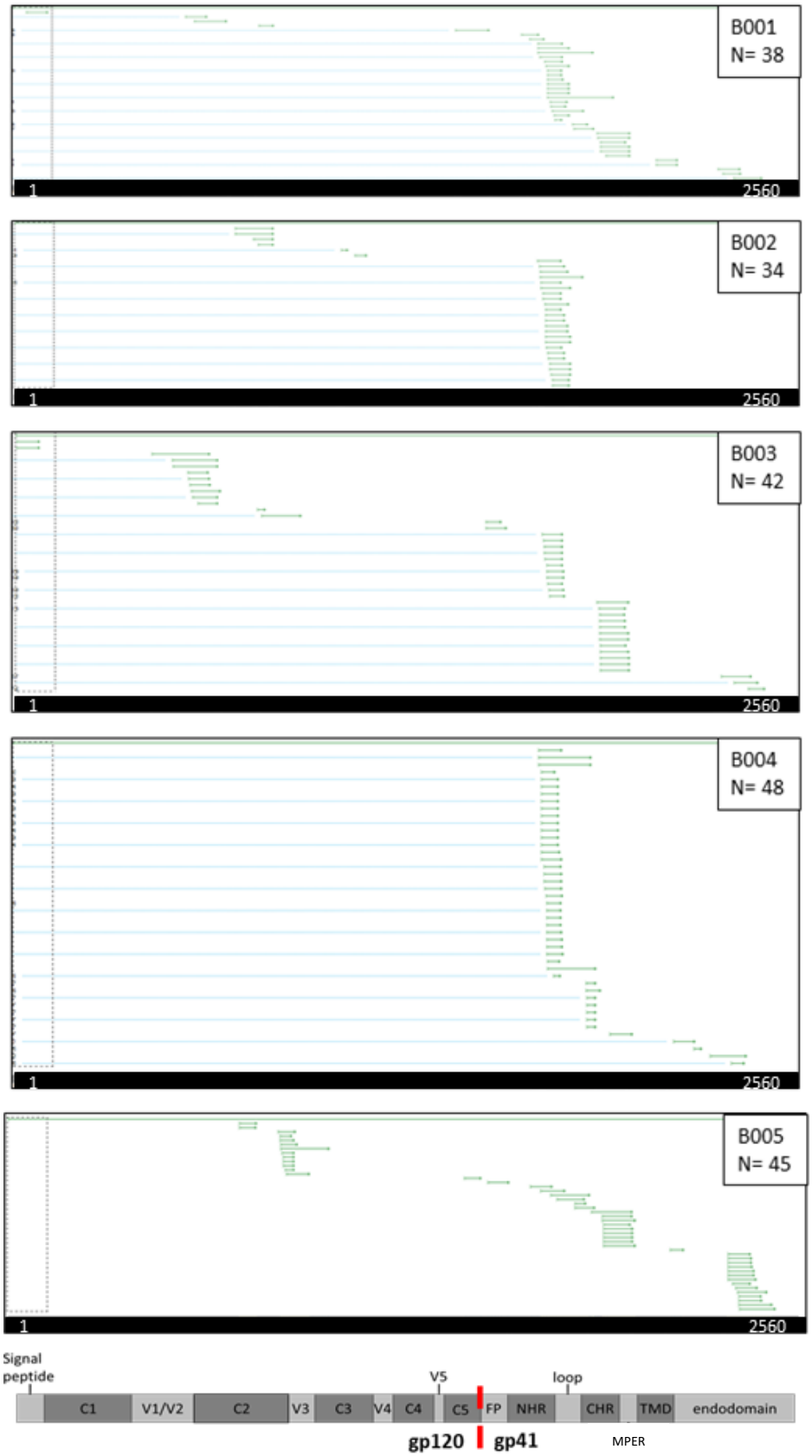


Figure 4.4-10 HIV gp160 library sorted by early infection samples

Sequences obtained from parent yeast sequences sorted by early infection yeast samples. HIV gp160 big and small libraries combined for use here. X-axis black bar indicates gp160 reference sequence HXB2 as previously. N = number of sequences returned from 50 sent clones. HIV envelope schematic shown below for illustrative purposes.

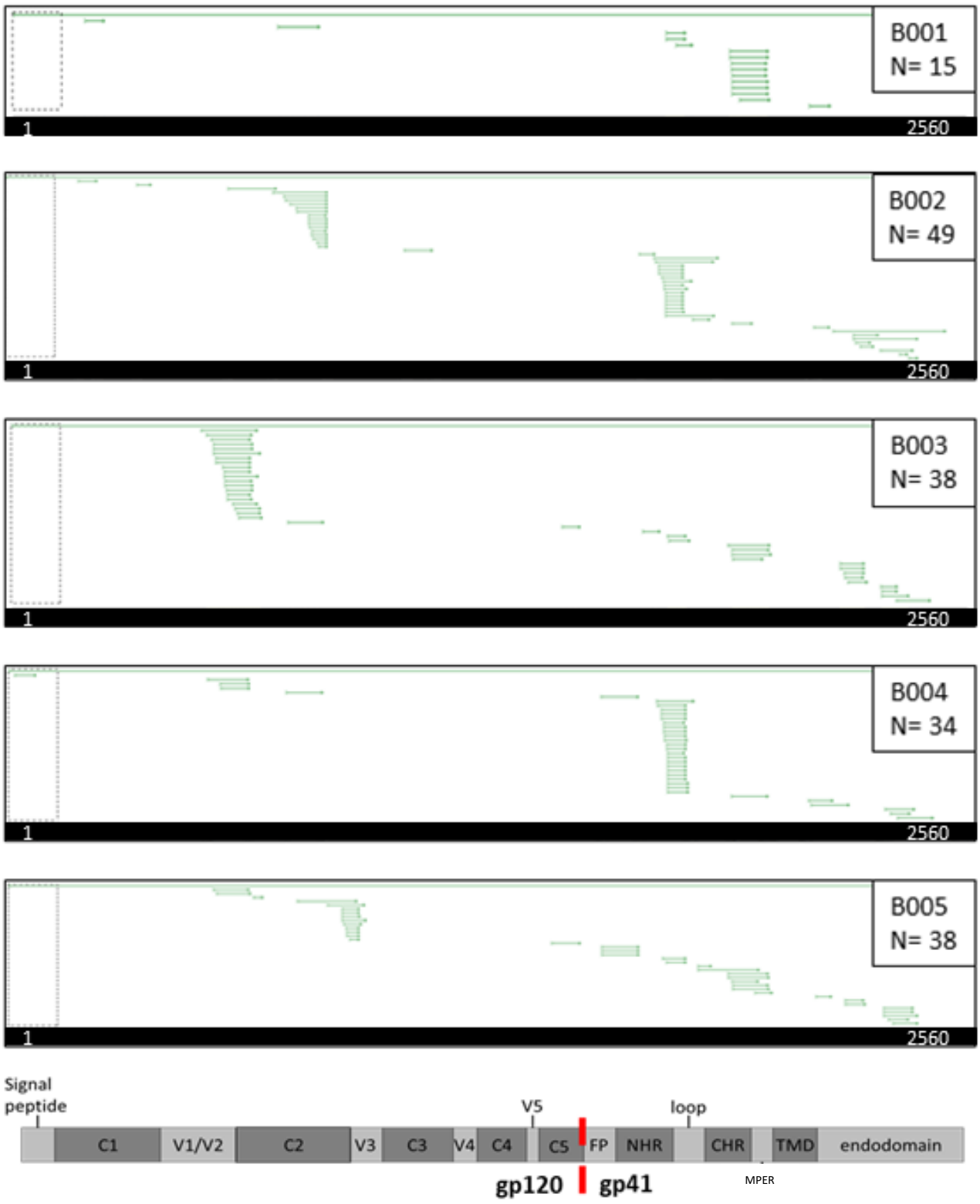


Figure 4.4-11 HIV gp160 library sorted by late infection samples
Sequences obtained from parent yeast sequences sorted by late infection yeast samples. HIV gp160 big and small libraries combined for use here. X-axis black bar indicates gp160 reference sequence HXB2 as previously. N = number of sequences returned from 50 sent clones. HIV envelope schematic shown below for illustrative purposes.

4.4.7. Sequence analysis histograms

I used an algorithm to determine the amino acid residue frequency at each position on the reference gp160 sequence HXB2 (282). The first part of the histogram review looked at the distribution of fragments on the parent sequence. The next part of the review identified major antigenic domains identified by serum samples. Epitope recognition was significant if the peak of the amino acid frequency curve was greater than greater than 5 residues. The area under the curve (AUC) for each epitope allowed direct comparison of proportion of sequences recognised by the participant serum, and a comparative analysis was performed using an unpaired t-test.

The figures below show amino acid frequencies for the two control samples (negative healthy control, seropositive control) and the fifteen seroconverter samples. Histogram curves were grouped in two different ways to allow comparison of findings; first by timepoint (pre, early, late; Figure 4.4-12) and then by participant number (B001-B005; Figure 4.4-13).

By arranging the data by timepoint, common antigenic regions of the Env responsible for the serum immune response were observed at the three time periods- pre, early and late infection.

When observing the sequences grouped by individual participant, specific patterns emerged showing regions of gp120 and gp41 recognised by patient serum samples repeatedly at sequential time points.

The positive and healthy control epitope recognition have been described in the previous chapter.

Timepoint serum recognition

On review of the sequence histograms arranged by timepoint (Figure 4.4-12), there is a key finding; gp160 epitopes are recognised by pre infection serum.

Pre infection serum samples recognised regions of both gp120 and gp41. Two regions of gp120 were identified; AA region 177-219 (B002, B003, B005) corresponding to the V1V2 and C2 regions, and the AA region 240-289 (B004) corresponding to the C2 region. Two regions of gp41 were recognised by pre infection serum; AA region 585-614 (B001) corresponding to the loop and C-helical region, and AA region 643-677 (B001, B003) corresponding to the C-helical and membrane proximal external region (MPER) regions.

The epitopes recognised by group B seronegative patient serum samples were similar to those recognised by the seronegative batched aliquots in chapter 3; these include the gp120 V1V2 and C2 regions, and the gp41 N helical region, C helical region, MPER and endodomain.

The epitopes of interest are also similar to that observed in the larger seronegative cohort study; the V1V2 loop and the C2 region. As previously discussed, the V1V2 region is of interest having been identified as a target epitope for vaccine induced ADCC responses in the RV144 trial. The C2 epitope is usually hidden and may be recognised due to the nature of yeast surface display technology.

Early and late serum samples recognised gp160 antigens in the gp41 region. As these samples were drawn at median duration of 123 (early) and 282 (late) days since infection, these findings are in keeping with the known initial antibody responses to HIV. These are typically anti-gp41, later evolving to more a heterogenous population as time since diagnosis passes (130).

Individual early infection serum samples recognised the gp120 V1V2 and C2 epitopes (B003 and B005). Two gp41 epitopes were recognised by the early infection samples; the N helical region and loop

domain (B001, B002, B003, B004), and the C helical and Membrane proximal external region regions (B001, B003).

Individual late infection serum recognised non overlapping gp120 epitopes; V1V2 region (B003), C2 region (B002), and later part of C2 region (B005).

No common gp120 epitope targeted by late serum but within a given patient (B003) there were gp120 epitopes recognised across all time points. This most likely represents variation in the time since diagnosis to date of blood sampling, and a developing humoral response to gp120 epitopes.

Late serum samples were obtained at different timepoints of infection for each participant. As shown in table 4.3.4, the time from infection and diagnosis to early and late samples was estimated based on recently infected testing algorithm and the most recently documented HIV negative test; the earlier of these two dates was considered the date of infection. Ideally, samples taken at fixed timepoints would have been used, but as date of infection was not available, and blood sampling was subject to participant's availability, all available samples were reviewed and selected those with similar estimated time since infection. This is the difference between animal models where infection challenges are scheduled according to a protocol, and real world observational studies where identifying infection and organising sampling require logistical efforts.

The late serum samples did recognise common gp41 epitopes; the N-helical, loop, and C-helical regions (B002 and B003) and the pre and transmembrane and endodomain (B001, B003, B005).

The positive control was an aliquot containing samples from patients with early HIV infection, who would be expected to show a predominantly gp41 antibody response (143). Clinic attendees are encouraged to undergo routine testing every three months, or more frequently if engaging in high risk behaviour. These findings are shown in Figure 4.4-12 below and Table 4.4-6 at the end of this section.

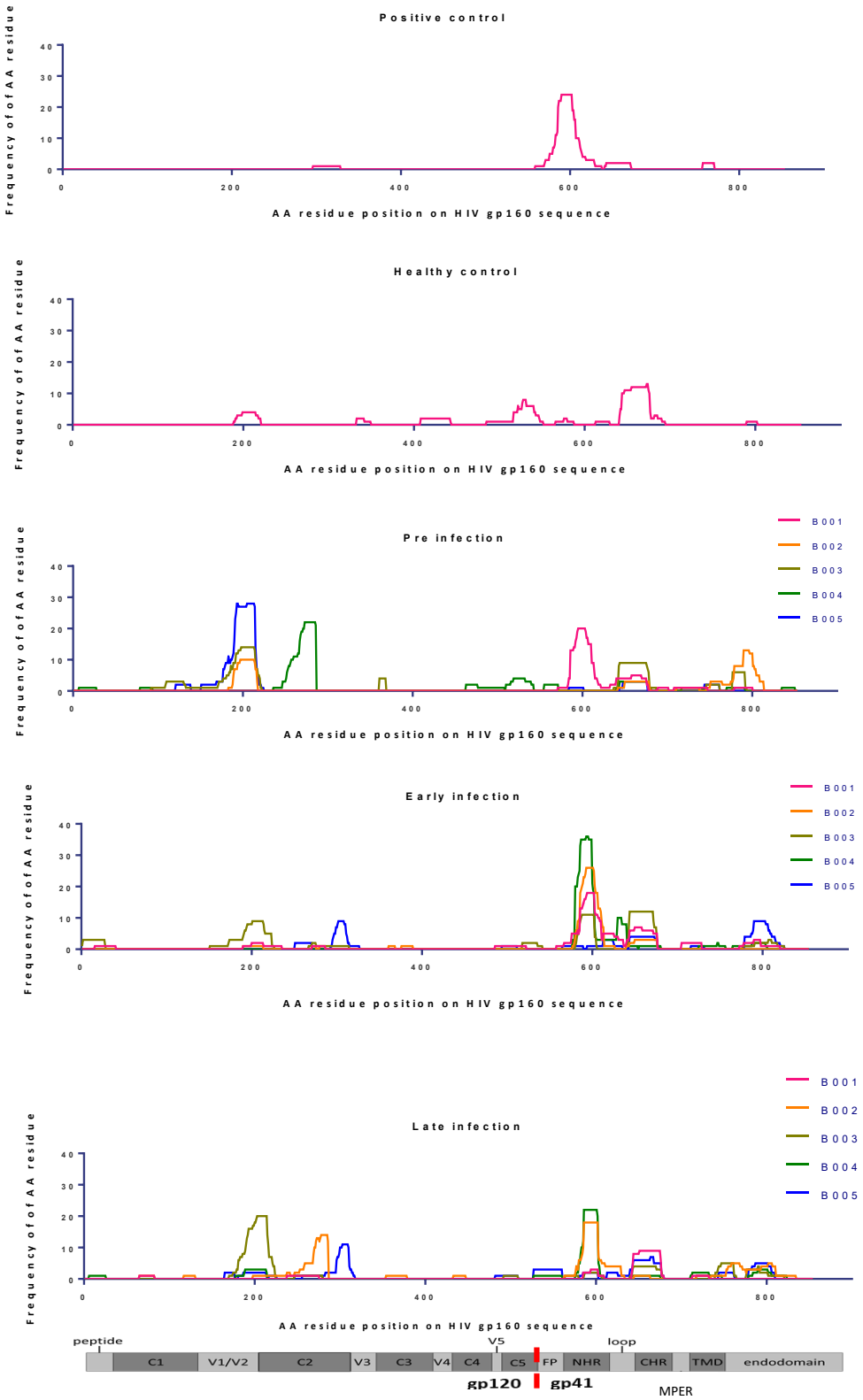


Figure 4.4-12 Control and seroconverter sequence analysis histogram- timepoints
Histograms of control (negative healthy, seropositive) and seroconverter samples arranged by infection status (pre, early and late). X axis shows amino acid position on HIV envelope sequence, y axis shows amino acid frequency at each position on the HIV-1 envelope parent sequence. Gp160 schematic shown at bottom for reference purposes

Participant serum recognition

I will now describe the epitopes recognition by pre and post infection serum samples for all five participants. My key finding here is that epitopes recognised by pre infection serum samples are recognised again by post infection serum

B001 pre, early and late infection serum samples recognised the gp41 region AA 571-678 with two distinct regions; the loop and C helical regions (571-628) and the C helical and transmembrane domains (628 678). **B002** pre and late infection serum samples recognised an overlapping region of gp41 AA 752 – 805 (transmembrane and endodomain). **B003** serum samples displayed pre and post overlapping areas of recognition. All three serum timepoints recognised a region of gp120 and gp41; AA 174 – 224 (V1V2 and C2 regions) and AA 639 – 688 (MPER and transmembrane domain). **B005** pre, early and late serum samples had one overlapping area of recognition on gp41; AA 639 – 680 (C helical region, Membrane proximal external region. **B004** serum samples had no pre and post infection overlapping regions. These findings are shown in Figure 4.4-13 below and Table 4.4-6 at the end of this section.

I consider the findings of overlapping pre and post infection recognition sites as pivotal for my thesis, as it supports the initial hypothesis of pre exposure to epitopes influencing future humoral responses, or the possibility of cross-reactivity of humoral responses to unrelated/non-HIV antigens. Seronegative and seropositive serum samples which select overlapping epitopes suggest persistent recognition of an epitope, and a response similar to prime and boost vaccination strategy. These findings suggest prior recognition of discrete HIV envelope surface proteins may be responsible for directing the evolution of the post infection serum antibody response.

This part of the study was purely observational. Due to the small size of the group and varying numbers of sequences retrieved, there were no attempts to draw statistical conclusions relating to epitope and risk exposure or demographics from the results.

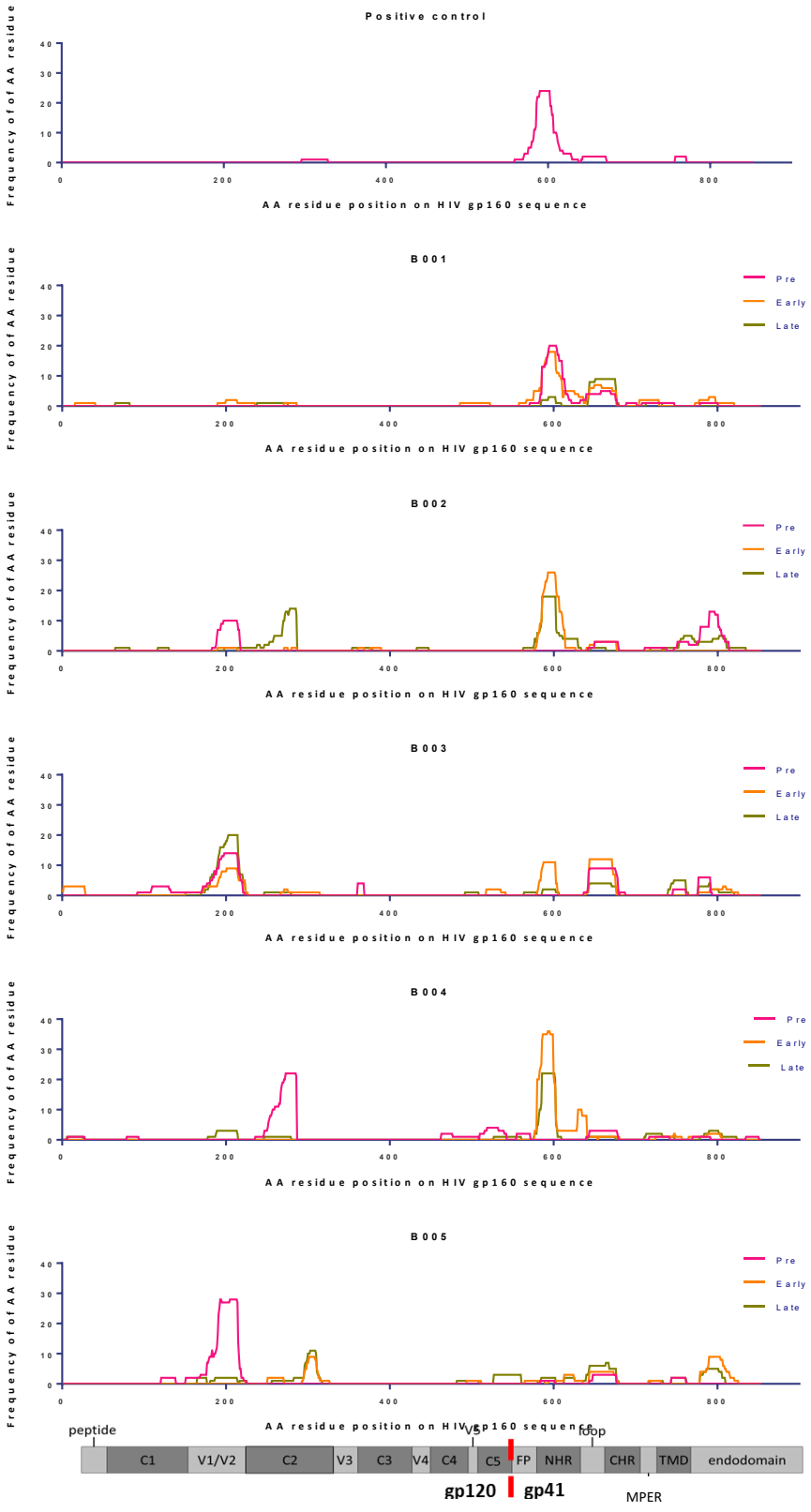


Figure 4.4-13 Control and seroconverter sequence analysis histogram- participant
Histograms of control (negative healthy, seropositive) and seroconverter samples arranged by participant. X axis shows amino acid position on HIV envelope sequence, y axis shows amino acid frequency at each position on the HIV-1 envelope parent sequence. Gp160 schematic shown at bottom for reference purposes

Participant	Env region	Epitope recognised	AA start	AA finish	Timepoint	AA peak	Pre/post infection overlap	Region	Sequence
B001	gp41	1	571	628	**Pre**	**20**	Yes	Loop, C helical region	KQLQARVLAVERYLRDQQLLGIWGCSGKLICTTAVPWNTSWSNKSMEEIWENMTWMQW
					Early	18			
					Late	3			
		2	628	678	**Pre**	**6**	Yes	C helical region, MPER	WEREIDNYTELIYGLLEKSQNQQEKNEQELLELDKWANLWNWFDITSWLW
					Early	8			
					Late	9			
B002	gp120	1	189	216	**Pre**	**10**	No	V1V2 region, C2 region	YMLINCNTSVITQACPKVSFEPIPIHFC
		2	252	287	Late	14	No	C2 region	VVSTQLLLNGSLAEEEIVIRSENIMD
	gp41	1	575	638	Early	25	Yes	N-helical region, loop, C-helical region	ARVLAVERYLRDQQLLGIWGCSGKLICTTAVPWNTSWSNKSMEEIWENMTWMQWEREIDNYTEL
					Late	18			
		2	752	805	**Pre**	**12**	Yes	Transmembrane, endodomain	LIWDDLRSLWLFIYHRLRDLLLIAARIVELLGRRGWEALKYWWNLLQYWRQELQ
					Late	5			
B003	gp120	1	174	224	**Pre**	**14**	Yes	V1V2 region, C2 region	FNTLDVVPIDNDDKSYMLINCNTSVITQACPKVSFEPIPIHFCTPAGFAII
					Early	9			
					Late	20			
	gp41	1	583	606	Early	11	Yes	N helical region, loop region	YLRDQQLLGIWGCSGKLICTTAVP
		2	639	688	**Pre**	**9**	Yes	MPER, TMD	IYGLLEKSQNQQEKNEQELLELDKWANLWNWFDITSWLWYIKLFIMIVGG
					Early	12			
					Late	4			
B004	gp120	1	240	289	**Pre**	**25**	No	C2	VSTVQCTHGIKPVVSTQLLLNGSLAEEEIVIRSENIMDNTKTIIVQLKEA
	gp41	1	575	604	Early	35	Yes	N helical region, loop domain	ARVLAVERYLRDQQLLGIWGCSGKLICTTA
					Late	22			
B005	gp120	1	176	222	**Pre**	**27**		V1V2 region C2 region	TLDVVPIDNDDKSYMLINCNTSVITQACPKVSFEPIPIHFCTPAGFA
	gp41	1	639	680	Pre	3	Yes	C helical region, MPER	IYGLLEKSQNQQEKNEQELLELDKWANLWNWFDITSWLWYIK.
					Early	9			
					Late	6			
		2	778	810	Early	14	No	Endodomain	IVELLGRRGWEALKYWWNLLQYWRQELQKSALS
					Late	5			

Table 4.4-6 Summary of gp160 epitope recognition by seroconverter serum

4.4.8. Single clone sequence analysis

I performed single clone analysis as previously described and selected those with a PE high population greater than negative (healthy) controls. These single clones were sequenced as they represented a homogenous population all bearing similar epitope, allowing me to create a library of specific epitope fragments for future use. Single clone sequence analysis was done on the samples shown below in Table 4.4-7.

Sample	No. Samples > lab control	Selected for sequence analysis
Pre B003	13	Yes
Pre B005	15	Yes
Early B003	6	Yes
Early B004	12	Yes
Late B001	12	Yes
Late B003	15	Yes
Late B004	12	Yes
Positive control	6	Yes

Table 4.4-7 Single clone analysis of seroconverter samples
Samples with PE high population greater than controls were submitted for sequencing

4.5. Major antigenic domain/determinant for selected samples

I selected participant B003 for further analysis of major antigenic determinants for two reasons: peak frequency of epitope recognition and single clone analysis. B003 pre, early and late samples had consistent and sequential recognition of HIV envelope protein with peak amino acid frequencies of 13, 6, and 15 respectively. In addition, the single clone analysis for all three serum timepoints demonstrates a reliable PE high population for the clones reviewed. For this part of the work, the major antigenic determinant (MAD) is discussed in terms of percentage total of the area under the curve (AUC), and region of gp160. The seropositive control was also shown for comparison.

Figure 4.5-1 and Table 4.5-1 show the MAD for the positive control and experimental B003 samples. One MAD was identified for the positive control serum, located in gp41. This is in keeping with the previously identified antigenic region for this sample as described in the previous chapter (Table 3.6-5). MAD were also located within overlapping regions of recognition. All three timepoints recognised gp120 and gp41 regions, corresponding to C2 and C-helical regions respectively.

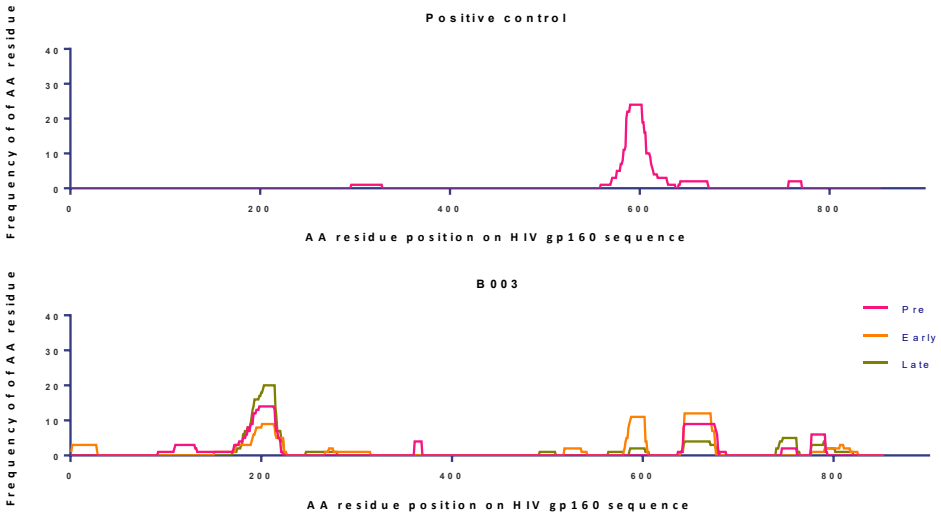


Figure 4.5-1 Sequence histograms for PC and B003
Histograms of positive control (seropositive) and B003 pre, early and late serum samples arranged by infection status. X axis shows amino acid position on HIV envelope sequence, y axis shows amino acid frequency at each position on the HIV-1 envelope parent sequence

	MAD	Total AA	AUC	AA start	AA finish	Width (AA)	Peak	AUC (%)	Env location	Sequence
PC	1	817	695	586	604	18	24	85.10%	NHR (gp41) Loop (gp41)	DQQLLGIWGCSGKLICTTA
Pre	1	1074	479	198	213	16	14	45.00%	C2 (gp120)	VITQACPKVSFEPIPI
	2	1074	334	641	666	26	9	31.00%	C-helix (gp41)	GLLEKSQNQQEKNEQELLELDKWANL
Early	1	1175	322	192	214	23	19	27.40%	C2 (gp120)	INCNTSVITQACPKVSFEPIPIH
	2	1175	380	644	671	28	12	32.30%	CHR (gp41) MPER (gp41)	EKSQNQQEKNEQELLELDKWANLWNWFD
Late	1	1062	599	198	215	18	20	56.40%	C2 (gp120)	VITQACPKVSFEPIPIHF
	2	1062	99	747	759	13	5	9.30%	Endodomain (gp41)	HGFLALIWDDLRS

Table 4.5-1 Summary table of major antigenic determinants for B003

Table shows information on major antigenic determinants considered significant in gp160 analysis in B003 pre early and late infection. PC seropositive control, MAD major antigenic determinant, AA amino acid, AUC area under the curve.

4.6. Direct comparison of all samples and stages

I proceeded to review each stage of the study group samples in grouped and individual format. This was to explore if there were similarities in recognition of the gp120 and 41 epitopes across the three stages of the study- pre, early and late infection. Gp41 epitope recognition by participant and domain was reviewed to see if patterns emerged.

This part of the study was purely descriptive and aims to outline the variations in serum recognition of HIV envelope epitope amongst the group B participants. As the group number is small (n=5) it was not possible to determine epitope frequency as it related to baseline demographics and risk exposure.

4.6.1. Individual gp120 vs gp41 responses

I reviewed the total number of selected sequences in the pre, early and late-infection groups which preferentially recognised either the gp120 epitope or the gp41 epitope. The selected fragments were separated into the proportions which recognised gp120 and gp41.

There was variation in individual responses. In pre infection samples, most individuals demonstrated recognition of both gp120 and 41, however B001 had no serum recognition of gp120. Early and late serum samples were directed against gp41 and gp120 epitopes respectively, which is in keeping with known antibody response in progressive HIV infection. This is shown in Table 4.6-1 and Figure 4.6-1.

	gp120	gp41	gp120	gp41	gp120	gp41
	Pre		Early		Late	
B001	0.0	100.0	12.4	87.7	13.2	86.8
B002	34.7	65.3	7.5	92.5	35.3	64.7
B003	57.4	42.6	38.7	61.3	63.4	36.6
B004	72.2	27.8	0.0	100.0	18.0	82.0
B005	86.5	13.5	23.0	77.0	37.0	63.0

Table 4.6-1 Pre, early and late infection sequence fragment review
Fragment location in gp160. Numbers are percentage proportions of total fragments recognised

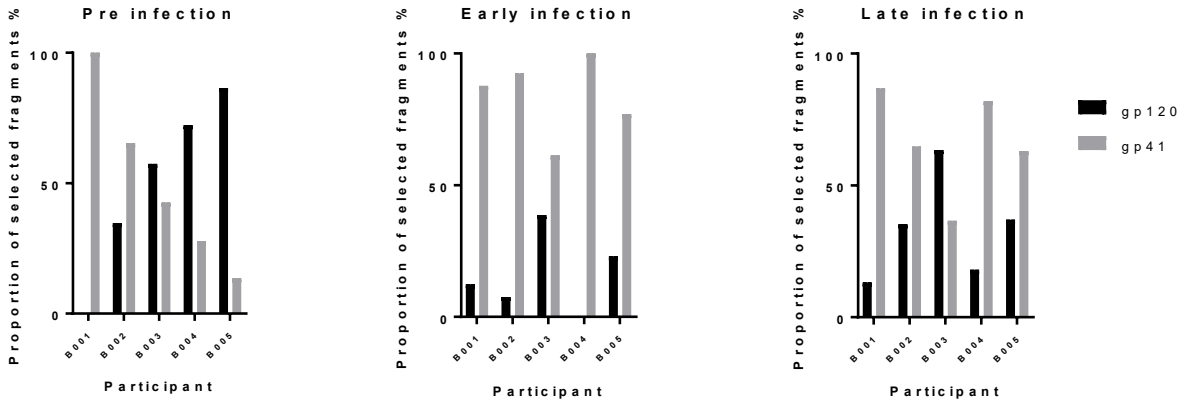


Figure 4.6-1 Seroconverter differential response to gp120 and gp41
X axis shows participant, y axis shows proportion of selected fragments as percentage of total. Gp120 black bars, gp41 grey bars.

4.6.2. All infection samples- gp120 individual epitope recognition

Summary of gp120 epitope recognition

I reviewed the epitope recognition at each stage of serum sampling for each of the recognised gp120 epitopes. This is shown in Table 4.6-2 and Figure 4.6-2.

The following epitopes had minimal recognition by participant serum at all stages of infection: signal protein, C1, C3, V4, C4, V5, C5. Two reasons were considered- perhaps a function of the yeast display system, or stearic hindrance to epitopes. The constant regions are targets for neutralising MAb. The anti-CDbs neutralising MAbs 1b12, HG16, VRC01 and VRC03 and anti-CD4 induced MAb 2G12 recognise discontinuous epitopes of C2-5 and V5 and the carbohydrate moieties in C2, C3, V4 respectively. Perhaps the fragmented nature of YSD does not allow for presentation discontinuous epitopes as they require long env sequences translated into folded protein structures (315). Alternatively, inaccessibility to certain epitopes *in vivo* may explain lack of anti-constant region serum binding. Phage display studies show C1 and C5 regions are accessible on monomeric gp120 but concealed on native gp120 viral surface by gp41. Hence this epitope may not be accessible *in vivo* HIV infection (326).

The V1V2 epitope was recognised by pre-infection serum with nearly 40% B005 pre-infection sorted fragments matching this epitope. There was minimal recognition by early infection serum and some recognition by late stage serum. As previously described in chapter three, this is an epitope of interest as ADCC mediating antibodies from RV144 directed towards epitopes at gp120 C1 region were associated with reduced HIV infection whereas anti-gp120 IgA Abs blocked binding and effects of ADCC (186). In seronegative samples, recognition of a pre-fusion V1V2 epitope may be due to exposure to epitopes in the absence of infection, as suggested by results in chapter 3.

There was minimal recognition of V1V2 by post infection samples, which may be due to differences of V1V2 presentation *in vivo*. In HIV infection, the V1V2 epitope undergoes structural changes after

binding to CD4 to allow the fusion peptide of gp41 to insert onto the host cell membrane (50,327). This may differ from the YSD presented V1V2 structure.

The C2 epitope was recognised by participant serum at all stages of sampling. Pre-infection serum recognised C2 with 63.1% and 52.6% of B004 and B005 fragments recognising this epitope. Early and late participant serum had moderate recognition of this epitope. B002 showed affinity for this epitope at pre and late infection sampling stages (27.1% and 29.4% respectively). B003 showed an affinity for this epitope at all three sampling stages (28.1% of pre, 21.5% of early and 45.1% of late infection sequenced fragments).

The V3 epitope was recognised by B005 early and late infection serum samples (13.7% and 14.7% of sequenced fragments respectively). V3 can induce anti-Env antibody responses (144,295,328), is a determinant of tropism/coreceptor usage for CCR5 or CXCR4 and may evolve over time resulting in altered tropism (53,329). So this level of epitope recognition is less than would have been expected, and the following was considered. Native trimer presents V3 with glycosylation at N332, which may not be present in a YSD model due to variations in glycosylation (330). In addition, native V3 may be shielded by V1V2 (331).

Other factors contributing to variations in recognition of previously described targets could include variation between YSD and *in vivo* glycosylation and an inability of seropositive serum to recognise non-glycosylated structure. Ideally, commercial anti-Env MAb binding to the yeast displayed trimer structure would have been reviewed to assess binding characteristics to yeast and proceed with fragmented trimer thereafter. Another factor could be the progressive glycosylation of the native Env trimer structure/V1V2 *in vivo* and corresponding evolving humoral response means less-glycosylated Env structures of YSD not recognised by later infection stage serum antibodies.

		SP	C1	V1V2	C2	V3	C3	V4	C4	V5	C5
Pre infection	B001	0	0	0	0	0	0	0	0	0	0
	B002	0	0	7.66	27.08	0	0	0	0	0	0
	B003	0	6.52	19.74	28.12	0	2.98	0	0	0	0
	B004	1.91	1.37	0	63.08	0	0	0	0	1.46	4.38
	B005	0	1.12	32.81	52.56	0	0	0	0	0	0
Early infection	B001	1.26	1.17	0.58	6.81	0	0	0	0	0	2.53
	B002	0	0	0.78	3.89	0	2.85	0	0	0	0
	B003	6.81	0	9.19	21.45	1.28	0	0	0	0	0
	B004	0	0	0	0	0	0	0	0	0	0
	B005	0	0	0	6.07	13.69	1.71	0	0	0	1.54
Late infection	B001	0	4.25	0	8.96	0	0	0	0	0	0
	B002	0	2.27	0.32	29.41	0	2.03	0	1.22	0	0
	B003	0	0	16.72	45.06	0	0	0	0	0	1.66
	B004	2.53	0	4.18	11.28	0	0	0	0	0	0
	B005	0	0	5.3	14.02	14.68	0	0	0	0	2.98

Table 4.6-2 gp120 epitope recognition

Numbers represent proportion of fragment as percentage of total fragments identified.

SP signal protein, epitope C1, V1V2, C2, V3, C3, V4, C4, V5, C5.

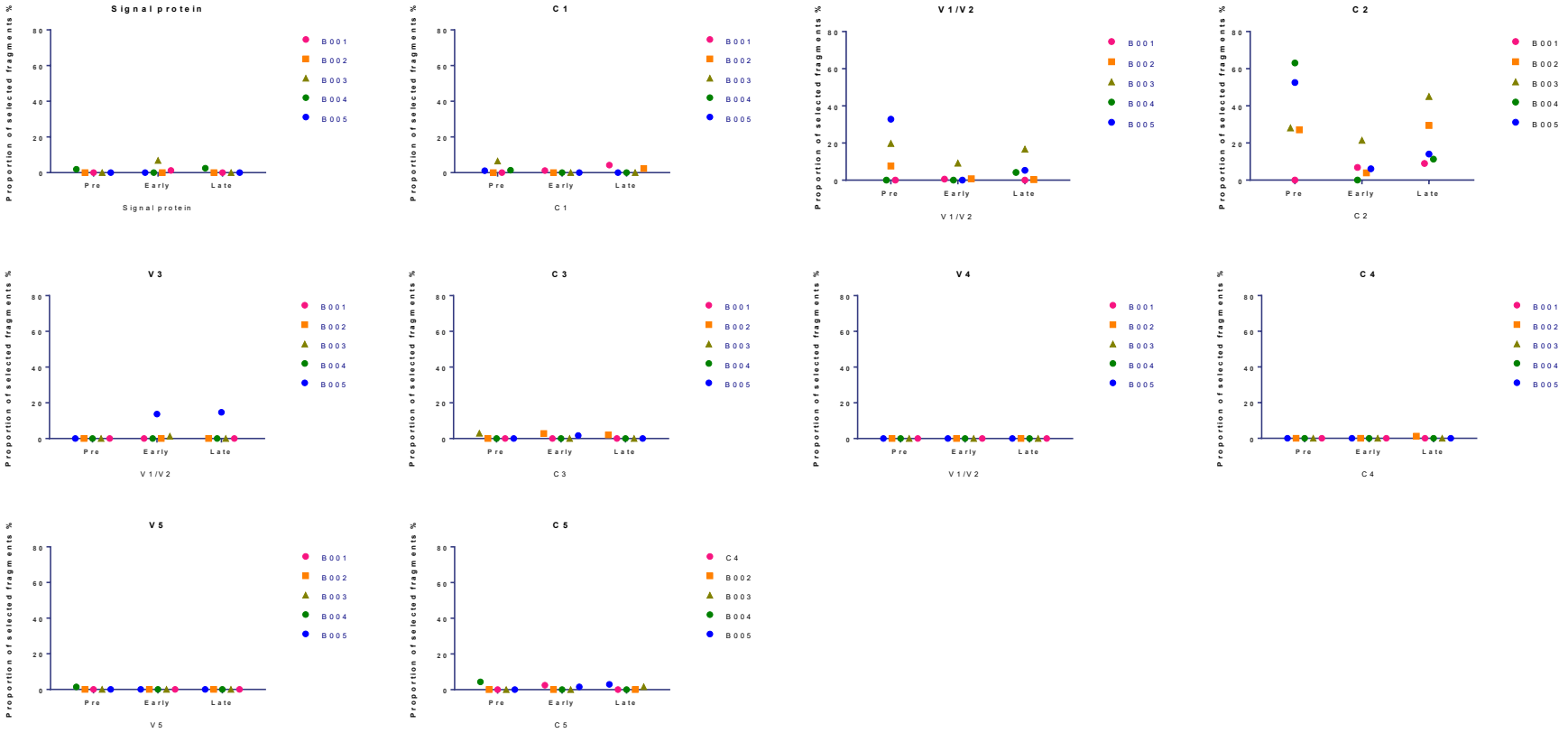


Figure 4.6-2 Seroconverter gp120 epitope recognition
Superimposed scatter plots showing affinity of patient serum samples for each gp120 epitope at each stage of study sampling. X axis shows pre, early and late infection for all 5 participants, y axis is proportion of fragment as percentage of total fragments identified.

SP signal protein, epitope C1, V1V2, C2, V3, C3, V4, C4, V5, C5.

4.6.3. All infection samples- gp41 epitope recognition

I reviewed the epitope recognition at each stage of serum sampling for each of the recognised gp41 epitopes. This is shown in Table 4.6-3 and Figure 4.6-3.

Pre infection serum most frequently recognised the endodomain, and the least recognised was the fusion protein region. Two participant serum samples showed a strong preference for particular epitopes; 50.3% of B001 recognised the loop region, and 50.9% of B002 recognised the endodomain region. These samples displayed an oligoclonal preference for their respective epitopes, compared to B003 and B004, which demonstrated broader recognition of most epitopes. C-helical region and membrane proximal external regions were recognised by most of the pre-infection serum samples.

Early infection serum had a broad response to all epitopes. The most frequently recognised epitope was the loop region, and the least was the transmembrane domain. 53.8% of B002 fragments recognised the loop region. B004 showed recognition of the N helical and loop regions (25.4% and 53.8% respectively), and B005 showed recognition of the endodomain (33.8% of fragments).

Late infection serum recognised a variety of gp41 epitopes. The most frequently recognised epitope was the endodomain, and the least recognised was the fusion protein. B001 serum preferentially recognised the C helical and membrane proximal external regions (38.0% and 31.8% respectively). B004 serum showed recognition of the N helical and loop regions (29.3% and 29.4% respectively).

To explain why early infection responses are broader and differ from those of pre infection, consider the following biological rationale. In seronegative serum responses, there are two mechanisms for epitope recognition; exposure to epitope in the absence of infection, or cross-reactivity with intestinal microbial antigens. In seropositive samples, exposure to replicating virus stimulates B-cell activity. The early group B participant samples were from an estimated four months post infection. Studies of B-cell activity at approximately 12 weeks post infection show induction of class switched polyclonal B-

cell populations and increased numbers of terminally differentiated cells in blood and GALT, creating a diverse population of antibodies including autologous neutralising antibodies (332)l.

Considering the epitopes individually, there were certain epitopes which generated more responses across all sampling stages. The N helical region, loop, C helical region, membrane proximal external region and endodomain were recognised at all stages of study sampling. Minimally recognised epitopes included the fusion protein and transmembrane domain.

The strongly recognised epitopes can be considered in the context of regions commonly targeted by immunisation strategies. The following gp41 regions- N helical region, loop, C helical region, MPER and the endodomain- were identified.

MPER recognition is of interest, as it is a highly conserved epitope known to stimulate formation of broadly neutralising antibodies capable of preventing infection in non-human primate models 2F5, 4E10, and 10E8 (253,254,333,334). MPER is highly conserved, lacks excessive N-glycosylation and plays a key role in viral fusion and infectivity. This suggests that as an epitope it is a target for vaccine strategies. However, incorporation of bnAb-specific MPER epitopes into vaccines results in non-neutralising antibodies, suggesting the epitopes necessary for neutralisation require extra features such as membrane presence or intermediate structural states to generate bnAbs (335,336)

Anti-MPER antibodies exhibit autoreactivity with host antigens; 2F5 and 4E10 to cardiolipin, 2F5 to kinureninase, 4E10 to splicing factor-3b subunit-3 and type I inositol triphosphate, and 10E8 to FAM84A protein. This suggests that if anti-host antigen antibodies occur, they may be suppressed by B-cell maturation pathways in order to maintain immunological tolerance of host antigens, thus impairing the serum antibody response to MPER (337).

		FP	NHR	loop	CHR	MPER	TMD	ED
Pre infection	B001	0	15.5	50.3	15.4	8.9	3.8	6
	B002	0	0	0	5.8	6.9	1.7	50.9
	B003	0	0	0	16.6	14.2	0.4	11.6
	B004	8.8	3.5	0	5.3	4.6	0.6	5.1
	B005	0	0.8	0.8	4.3	4.2	0	3.4
Early infection	B001	1.1	17.4	30.5	18.4	8.3	3.7	8.4
	B002	0	25.4	53.8	7.4	5.8	0	0
	B003	3.5	8.5	10.1	19.3	13	0	6.8
	B004	0	38.2	36.6	14.3	1.9	0	9.1
	B005	1.9	4.3	7.3	17.6	11.5	0.7	33.8
Late infection	B001	0	3.8	8.5	38	31.8	2.6	2.1
	B002	0	15.8	21.9	4.3	0.2	0.5	22.2
	B003	0	2.8	2.4	7.6	5.6	0	18.2
	B004	1.8	29.3	29.4	2.5	1.8	3	14.2
	B005	4.6	8.8	4.2	15.8	9.7	0.7	19.2

Table 4.6-3 gp41 epitope recognition

Numbers represent proportion of fragment as percentage of total fragments identified. FP fusion peptide, NHR N-helix, loop, CHR c-helix, MPER membrane proximal external region, TMD transmembrane domain, ED Endodomain.

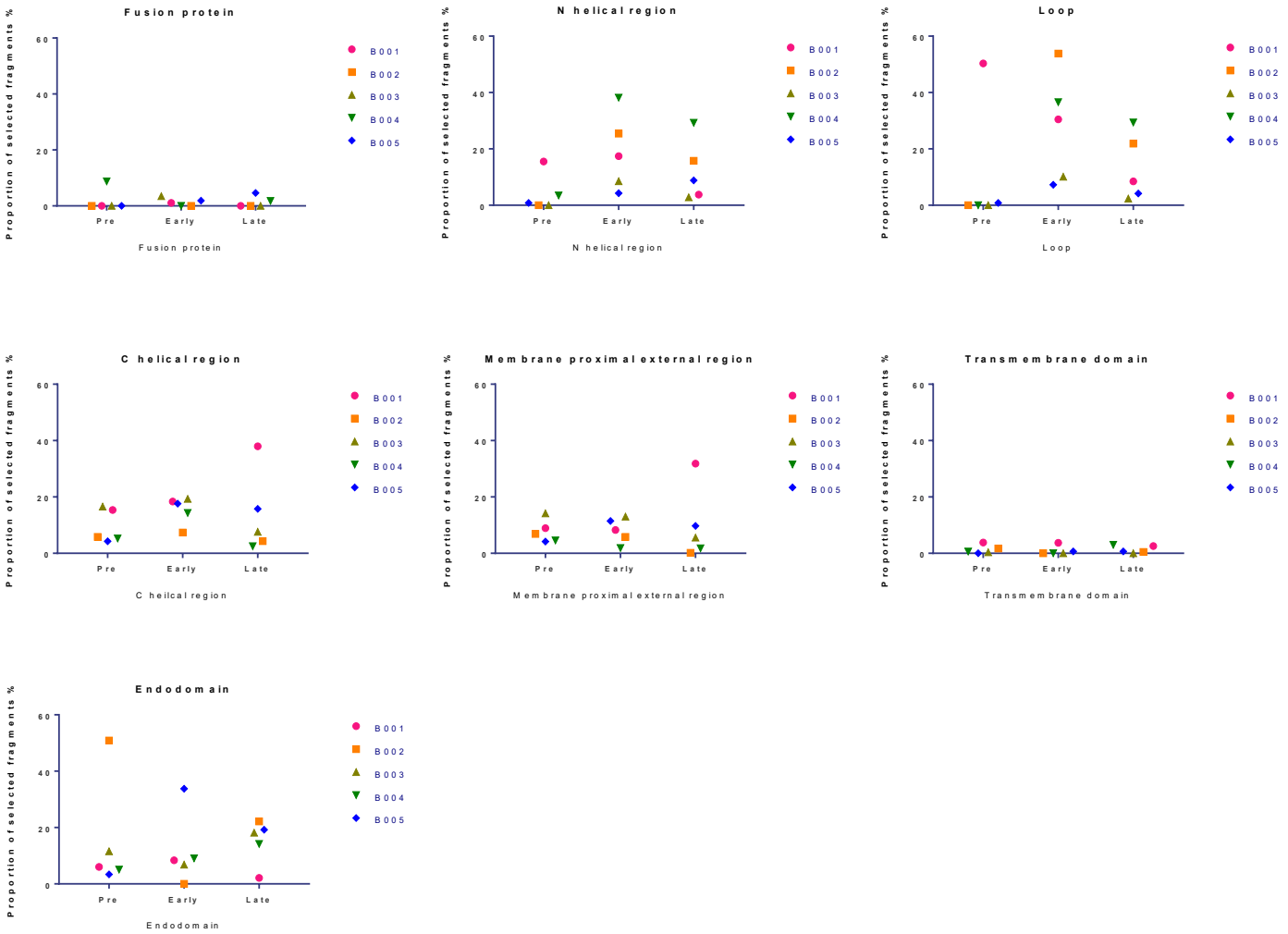


Figure 4.6-3 Seroconverter gp41 epitope recognition

Superimposed scatter plots showing affinity of patient serum samples for each gp41 epitope at each stage of study sampling. X axis shows pre, early and late infection for all 5 participants, y axis is proportion of fragment as percentage of total fragments identified. FP fusion peptide, NHR N-helix, loop, CHR c-helix, MPER membrane proximal external region, TMD transmembrane domain, ED Endodomain

4.7. Cross reactivity with gut microbiota

All pre-infection sequences which had a peak amino acid frequency of greater than five residues were selected (described in 2.5), and intestinal microbial antigen data detailing the *E.coli* bacterial RNA polymerase protein from the NCBI GenBank resource accessed 31/07/2019 (https://www.ncbi.nlm.nih.gov/protein/WP_001162094, accession no. WP_001162094). The BioEdit sequence alignment tool was used to review each gp41 epitope against the three protein subunits (alpha, beta 1, and beta 2.

4.7.1. Pre infection serum selected epitopes and *E.coli* RNA polymerase

There were five instances where epitopes selected by pre infection serum had structural similarities to *E.coli* RNA. These are described in Table 4.7-1, and used Pre infection B001 gp41-1 as an example.

The gp41-1 epitope was selected by B001 pre infection serum with a peak frequency of 20 residues. This epitope was located at amino acid positions 571- 628 (representing loop and C helical regions, sequence KQLQARVLAVERYLRDQQLLGIWGCSGKLICTTAVPWNTSWSNKSMEEIWENMTWMQW). The gp41-1 sequence was aligned to each of the three protein subunit sequences in BioEdit. The subunit beta 2 amino acid position 962 to 968 sequence (SGKLVIT) was similar to that seen in SGKLICTT gp41-1 (SGKLICT). This is shown in Figure 4.7-1 below. The five gp41/*E.coli* overlap instances and sequence details are shown in Table 4.7-1 below.

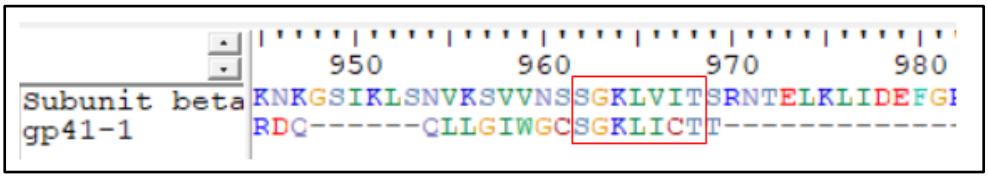


Figure 4.7-1 *E.coli* subunit beta AA and gp41-1 sequences aligned
Image shows *E.coli* and gp41 sequences aligned using BioEdit sequence editor. The scale represents amino acid residues and the red box shows the area of commonality

Epitope	Pre B001 gp41-1	Pre B001 gp41-2	Pre B002 gp41	Pre B003 gp41-2	Pre B005 gp41-1
Epitope location	571- 628:	628-678:	752-805:	639-688	639-680:
Epitope sequence	KQLQARVLAVERYLRDQQLLGI WGCSGKLICTTAVPWNTSWS NKSMEEIWENMTWMQW	WEREIDNYTELIYGLLEKSQNQ QEKNEQELLELDKWANLWN WFDITSWLW	LIWDDLRSLWLFIYHRLRDLLLI AARIVELLGRRGWEALKYWW NLLQYWRQELQ	IYGLLEKSQNQQEKNEQELLEL DKWANLWNWFDITSWLWYI KLFIMIVGG	IYGLLEKSQNQQEKNEQELLEL DKWANLWNWFDITSWLWYI K
Epitope region on gp41	Loop C helical region	C helical region MPER	Transmembrane domain Endodomain	MPER Transmembrane Endodomain	C helical region Transmembrane domain
Subunit alpha	No match	MATCH AA position 286 to 290 EVELL EQELL	No match	No match	No match
Subunit beta 1	No match	MATCH AA position 1197 to 1201 ELLKL ELLEL	No match	MATCH AA position 1197 to 1201 ELLKL ELLEL	No match
Subunit beta 2	MATCH AA position 962 to 968 SGKLVIT SGKLICT	No match	MATCH AA position 278 to 283 RLKRLL RLRDLL	No match	No match

Table 4.7-1 Pre infection serum gp41 epitopes

Pre infection epitopes Pre B001 gp41-1, Pre B001 gp41-2, Pre B002 gp41, Pre B003 gp41-2 and Pre B005 gp41-1 reviewed against *E.coli* RNA polymerase subunits alpha, beta 1, and beta 2. Included are gp41 sequence location, sequences, region, and matching *E.coli* RNA subunit

4.8. Summary

In summary, the work in this chapter demonstrates that seronegative humoral responses to HIV envelope antigens persist through seroconversion and recognise similar epitopes.

4.8.1. Serum antibody responses to HIV envelope antigens at pre, early and late infection

This chapter describes the work done on serum from seroconverting participants. The aims were to characterise serum antibody responses to HIV envelope antigens at pre, early and late infection, to identify the antigens recognised by host immune responses, and to examine common antigens.

I have demonstrated the presence of humoral immune responses against the HIV envelope protein, in all participant serum samples, both from pre and post seroconversion samples. While this is to be expected from seropositive samples, my key area of interest was in seronegative samples, as it builds on work from the previous chapter. As outlined, the group B sample size was too small to draw conclusions regarding exposure risk and anti-envelope responses, therefore no attempt has been made to attribute variation to these causes, suffice to say more work is needed here.

Two participants pre infection samples showed recognition of both gp120 and gp41 glycoproteins prior to HIV infection (B002, B003), and the remaining three recognised only one glycoprotein; (B001 gp41, B004 and B005 gp120).

The seropositive samples were, as expected for a developing immune response, with a predominantly gp41 response in early serum samples progressing to an equivocal gp120/41 response at later time point. While not novel, this finding supports the method used to interrogate participant immune response.

4.8.2. Identification of antigens recognised by host immune responses

Pre infection serum samples recognised epitopes of gp120 and gp41. Recalling the results from the previous chapter, pre infection samples had greater recognition of gp41, but this is a small study group

size and was not powered to detect differences in recognition based on demographics and HIV exposure risk.

Pre infection serum recognised the gp120 epitopes V1V2 and C2. These findings are in keeping with the epitopes of interest in the previous chapter. To recall the relevance of these structures, anti-V1V2 antibodies were associated with increased levels of IgG1 and IgG3 ADCC-mediated protection from infection in vaccine recipients in the RV144 trial (338), and the C2 epitope is usually hidden when *in vivo* conformation. The persistent finding of anti-V1V2 antibodies in seronegative participants validates the results of the previous chapter and confirms that batched aliquot analysis reflects individual serum components.

Pre infection serum recognised the following gp41 epitopes in order of decreasing frequency: endodomain, C helical region, and membrane proximal external region. The most frequently recognised epitope was the endodomain, and the least frequent the fusion protein region.

The presence of anti-endodomain antibodies in seronegative serum is of interest. This region of gp41 is approximately 100 amino acid residues in length and contains components responsible for viral function. This is shown in below in Figure 4.8-1 (339)

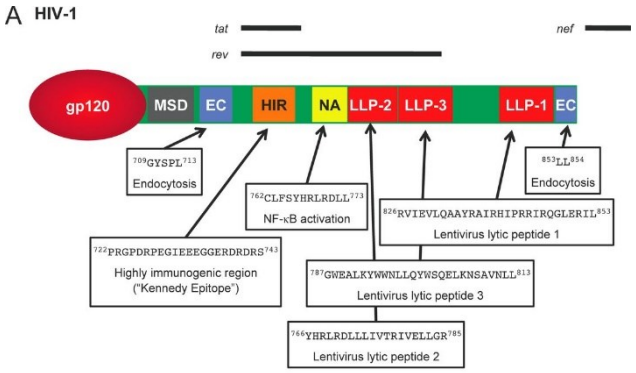


Figure 4.8-1 Schematic representation of gp41 endodomain
Reproduced from (17) (CC BY-NC 3.0). Black lines overlapping open reading frames (ORFs) of nef and the second exons of tat and rev in the proviral genome. MSD, membrane-spanning domain; EC, endocytosis; HIR, highly immunogenic region (Kennedy epitope); NA, NF-κB activation; LLP, lentivirus lytic peptides 2, 3, and 1

The endodomain provides stability for the envelope trimeric structure, supports viral replication, and may have direct cellular cytopathic effects (339). It also contains a highly immunogenic region known as the Kennedy epitope. Despite its proposed intracellular location, anti-Kennedy antibodies are frequently found in HIV patient serum (340,341).

Abortive infection results in apoptosis of cells, releasing intracellular debris including partially synthesised virions. These may act as epitope and adjuvant to stimulate a humoral response (81,82). In addition, partially degraded Env on the surface of cells may serve as an epitope for antibody responses (342).

The endodomain does not necessarily occupy a uniquely intracellular space .Serum from HIV patient serum contains anti-Kennedy antibodies- suggested this region has multiple membrane spanning domains occupying intra and extra cellular regions (339,343). Moreover, anti-Kennedy epitope MAbs can bind to Env-expressing cells, reinforcing an extracellular component available for epitope recognition (344)

One hypothesis suggests lentiviral lytic proteins 1, 2, and 3 embed themselves within a lipid bilayer resulting in partial exposure of the whole endodomain (345), and may explain why *in vivo* antibody responses are found against these presumed intra-cellular epitopes. The main endodomain epitope locations on the HXB2 reference sequence are shown in below (324)

Endodomain epitope	Start	Finish
Kennedy epitope	724	745
LLP-2	768	787
LLP-3	789	815
LLP-1	828	855

Table 4.8-1 Endodomain epitope locations
Start and finish locations of amino acid residues listed. LLP lentivirus lytic peptide

B002 and B003 pre infection sequences recognised portions of the endodomain at positions 752-805 and 639-688 respectively. The B002 endodomain region maps to the lentiviral lytic peptide-2, and the B003 maps to an endocytosis region.

As previously considered in this work, the presence of anti- intracellular epitope antibodies may be due to the conformational nature of yeast surface display. However, it may be that exposure to this highly immunogenic region stimulates an anti-endodomain response in the absence of established infection.

Another feature attributed to the endodomain is a role in function and replication. Studies reviewing truncation of this region show a decrease in susceptibility to neutralising antibodies (346). This suggests the endodomain plays a role in anti-HIV immunogenicity. With more time, this the work from this study could be brought forward to review the properties of these anti-endodomain antibodies and their functionality.

The other two epitopes identified by pre infection serum samples were the C-helical region (CHR) and the membrane proximal external region (MPER). The finding of anti-MPER antibodies is of interest as the MPER is a known target for broadly neutralising antibodies. This epitope is tryptophan rich and highly conserved across clades and connects the extracellular portion of envelope protein to the intracellular endodomain, playing a key role in facilitating viral fusion and entry into cells. For this reason, anti-MPER antibodies effect neutralising function and protect against viral challenge in non-human primate studies, and is described as a major gp41 neutralising determinant (337,347).

The site of MPER vulnerability is a 22 residue length sequence ALDKWASLWNWFDITNWLWYIK located at position 662-683 in the HIV envelope sequence. 2F5, 4E10, and 10E8 are naturally occurring broadly neutralising antibodies which target a variety of linear epitopes within this region (253,348). A portion of this highly conserved MPER epitope was recognised by three of my study participants at all stages of serum sampling; B001 (gp41 region AA 628-678), B003 (gp41 region AA 639-688), and B005 (gp41 region AA 639-680) (sequences previously listed in Table 4.4-6).

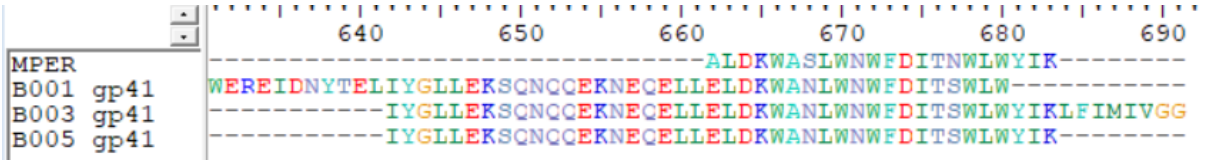


Figure 4.8-2 MPER and group B epitopes aligned
BioEdit aligned amino acid sequences; MPER membrane proximal external region vulnerable region 632 to 683. B001, B003 and B005 epitopes shown beneath.

The presence of these serum responses invites further analysis. This region is conserved across clades, however a feature of anti-MPER antibodies from HIV-infected patients is their preference for binding the intermediate and post-fusion MPER structure. In native formation, access to the envelope protein MPER structure is obstructed by two glycans at positions N88 and N625. As the pre fusion hairpin forms and transitions to the intermediate state, MPER is exposed and becomes a target for bnAbs (349).

Bringing this back to the B001, B003 and B005 epitopes, the fragmented nature of the yeast surface display means epitopes are more readily exposed. But how could anti-MPER antibodies form in the absence of established infection, given the necessary conformational change required for epitope exposure as experienced in viral infection as opposed to seronegative status? One theory for gp41 exposure in absence of viral membrane fusion is the formation of "junk Env(elope)". This is formed during viral budding from infected cells when gp120 dissociates from the intact gp160 trimer structure due to lack of inter-glycoprotein stability, leaving a gp41 stump (342,350). These stumps have been described as bnAb targets, but only in seropositive candidates (351). Review of the literature did not locate evidence to support the presence of viral proteins on cell surface membranes in the absence of infection and so a mechanism is proposed in the final discussion chapter **Error! Reference source not found.**.

Another consideration is the conformation of epitope display. As mentioned, YSD presents fragmented epitopes, therefore future work could focus on the binding of the B group anti-MPER antibodies to varying trimer conformations and review binding to native or intermediate/post fusion envelope trimers. In addition binding by MPER antibodies to different Env conformations by using commercially available anti-gp41/MPER MAb could be used to interrogate the responses found here and compare to target epitopes of known MAbs.

4.8.3. Overlapping epitope recognition

The pattern of responses recognising epitopes at progressive stages of the study timeline point to a possible role for preexposure to antigen that informs future humoral immune responses.

Samples where seronegative epitope recognition was echoed by post infection serum include B001 (gp41 epitope AA 571- 628, loop and small portion of C helical region), and B003 (gp120 epitope AA 174-224 V1V2 and C helical region, gp41 epitope AA 639-688, transmembrane domain). This is shown in Figure 4.4-13. This data was an important piece of this work and highlights the concept of antigens shaping a pre-exposed immune response that matures on contact with second antigen.

In this part of the study, it was not possible to determine if pre and post humoral responses were towards similar viral clades. Presuming viral quasispecies differ at each sexual exposure, the humoral response seen here is to similar antigen targets conserved across different viruses. Conserved epitopes are desirable vaccination targets (352), therefore if resulting antibodies are functionally useful, these regions could be considered as vaccine targets.

Another consideration about anti-epitope response is the persistence of antibody in the presence of viral suppression. As all B group candidates achieved an undetectable viral load within 90 days, it is interesting to note an ongoing anti-envelope response.

Anti-HIV antibodies develop during exposure to virus, and early treatment halts evolution of antibody responses. Seropositive individuals treated at early stages of infection who achieve viral suppression may abolish the formation of detectable HIV specific antibodies (353,354). Most involve young patients treated immediately, but some ultimately progress to seroconversion at later stages.

Anti-Env antibodies persist despite initiation of cART, but levels vary according to ongoing viral replication; viraemic individuals have high Env titres, elite controllers have lower Env titres, and those taking cART have lowest Env titres, supporting the concept of ongoing antigen exposure as necessary for maintenance of antibody levels (355).

Low levels of Env in virally suppressed patients may be due to persistence of Env expression in infected follicular T-cells within the B-cell follicle allowing direct stimulation of antibody producing cells (356).

The candidate selected for ongoing work was B003, who presented with the highest viral load, and took the longest to achieve viral suppression. The greater viral exposure during seroconversion and time to suppression may have been the reason for this individual's pronounced epitope recognition.

4.8.4. Intestinal microbiota

As outlined in the introduction section 1.11.2, there is evidence intestinal microbial antigens influences development of the serum antibody response to pathogens. Liao et al extracted $CD19^{+}$ $CD27^{hi}$ $CD38^{lo}$ $CD20^{lo/hi}$ plasmablasts/plasma cells from blood/bone marrow of acute HIV infected patients and performed RT-PCR to amplify rearranged variable regions of Ig heavy and light genes and compared these sequences to those induced by primary Env vaccination (gp120/NefTat/AS01B). They reported higher levels of somatic hypermutation seen in V_H and V_L of acute HIV patients, MAb produced from these sequences bound intestinal microbial antigens (IMA) with one MAb significantly mutated and demonstrating polyreactivity with gp41 and IMA. This suggested immature B-cell exposure to IMA in intestinal mucosa as a mechanism for polyreactivity with Env and IMA (260).

This was further explored by Trama et al who reviewed anti-HIV antibody responses in terminal ileal B cells. A whole cell gut lysate was probed with anti-gp41 monoclonal antibodies and the antigenic target determined to be a 37 kDa α subunit of recombinant E. coli RNA polymerase (263). This antigen was confirmed by Williams et al who noticed the *E.coli* α subunit H1 helix had structural similarities with a short segment of the gp41 HR1 region (264).

Williams et al then proposed this mechanism of polyreactivity as responsible for diversion of vaccine-induced antibodies away from protective immune responses. They reviewed the efficacy of HIV-1 DNA rAd5 boost vaccine with main components were *gag, pol, nef* and gp140 *env* genes. The resulting vaccine responses were mainly towards gp41 and were non-protective and mirrored by low frequencies of gp120-memory B cells in these patients; 0.05% population were gp120-specific memory B cells vs 0.28% gp140-specific memory B cells. As other studies using Env gp120 immunogens showed a memory B-cell population of 0.73%, the reduced was not attributed to a fault of immunogen.

The authors then searched for anti-gp41 unmutated common ancestor B cells. They identified B cells from the pre-vaccine samples with V_HDJ_H rearrangements matching those of the Env-specific memory B cells, indicating a clonal lineage. The resulting pre vaccine IgM MAb reacted with vaccine Env, MN gp41 and IMA, and the post vaccine MAb reacted with gp41 and IMA. There was greater binding to IMA of preMAb vs post MAb, and greater binding to Env of postMAb vs preMAb, suggesting Env vaccination induced polyreactive non-neutralising anti-gp41 responses from pre-existing B cells, and this response can cross react with IMA (264).

My work in this chapter describes serum selection of gp41 epitopes by pre infection serum samples. Considering the potential cross reactivity with intestinal microbiota, epitope sequences selected by seronegative serum were reviewed against reported immunogenic intestinal microbiota sequences.

There was common structural areas between epitopes recognised by pre infection serum and those of intestinal *E.coli* RNA sequences, with five instances of similar sequences, shown in Table 4.7-1. These similarities could explain the presence of anti-gp41 antibodies. Further work here could include fully demonstrating this using the *E.coli* protein constructs and monoclonal antibodies, but this has not been attempted here.

The possibility of the recognised gp41 epitopes and *E.coli* epitopes aligning due to chance must also be considered. One scoring system addresses this concern by calculating the strength of the alignment

between two sequences and could this be attributed to chance. The "chance" element here involves comparing the strength of alignment of the sequence of interest (in this case the gp41 epitope) and, and a randomly generated sequence of similar length sequences. This was done using the online reference NCBI protein basic local alignment sequence tool (NCBI protein BLAST, website https://blast.ncbi.nlm.nih.gov/Blast.cgi) and shown below in Table 4.8-2. The expectant (E) value is the chance that this sequence would occur randomly. The closer to zero the E value, the less likely this alignment is due to chance, and hence an increase in strength.

From the data below, the strongest alignment was Pre B002 gp41_1 (transmembrane domain and endodomain sub-epitope lentiviral lytic peptide-2) and the *E.coli* RNA polymerase subunit beta 2. Three of the alignments were between 0-1, indicating a very small chance these sequences aligned due to chance.

Name	E value
Pre B001 gp41_2 subunit alpha	2.10
Pre B001 gp41_2 subunit beta 1	0.97
Pre B003 gp41_2 subunit beta 1	0.97
Pre B001 gp41_1 subunit beta 2	3.70
Pre B002 gp41_1 subunit beta 2	0.64

Table 4.8-2 Review of gp41 epitope and *E.coli* alignment
Name: name of alignment, gp41 epitope with one of the three *E.coli* RNA polymerase subunits. E expectant value; possibility of alignment

To further explore the finding of cross reactivity with *E.coli* cells, *in vitro* binding to the sequences of interest could be reviewed by obtaining peptide sequences for ELISA or cellular display and participant serum binding reviewed. In addition, binding of known anti-MPER antibodies to these peptides could be reviewed to validate the findings.

4.8.5. Limitations

On reviewing this chapter, there are some limitations to consider. The proposed longitudinal follow-up blood sampling for group B was not possible beyond December 2016. This was a strategic decision, as focus turned to progressing the laboratory component of this work rather than the logistics of

obtaining further tissue samples. Considering the work involved, and following discussion with study supervisors, it was agreed there was adequate material to continue this project.

Another limitation was the number of subjects available for pre and post seroconversion analysis. As detailed, nine participants were approached for follow-up, but due to other commitments it was not possible to obtain tissue samples for all.

Another limitation was the stability of yeast clones once sorted. Yeast cultures may fall victim to bacterial contamination, and despite the creation of frozen stocks occasional batches of cultures were lost. Optimisation of media with addition of antimicrobial agents helped avoid this outcome.

4.8.6. Future work

Other avenues emerging from this work include further interrogation of endodomain epitopes responsible for pre infection humoral responses given the known immunogenicity of the Kennedy epitope and the existence of the anti-endodomain response. Also, exploration of anti-MPER antibodies in a cellular as opposed to yeast based method could elucidate which MPER configuration allows maximal binding of antibodies.

To demonstrate these are similar and not de novo, similar techniques to Williams et al (264) could be used; isolation of memory B cells specific for certain epitope e.g. MPER, and comparison of VHDJH¬ rearrangement sequence for the pre and post B cells. If these were similar it would imply clonal lineage responsible for initial exposure and subsequent antibody development and maturation.

To prove antigen pre-exposure drives future serum antibody responses, animal models could be vaccinated with isolated epitopes and humoral responses tracked to increasing amounts of epitope in similar manner to work presented here. Another model would be to review epitope recognition in seroconverters with no/minimal previous HIV exposure, but these candidates may be more difficult to locate.

Conclusion

In conclusion, these results show anti-HIV envelope responses are present in the serum of seronegative individuals, and similar epitopes are recognised by pre and post infection patient serum. Epitopes identified include the gp120 V1V2 and C2 epitopes, and the gp41 MPER, endodomain and loop regions. This aspect of my study is novel and has not been described previously for HIV-1. These anti-Env antibodies are further explored in the following chapter.

Chapter 5
Monoclonal antibody production

Chapter 5 Monoclonal antibody production

5.1. Introduction

Having demonstrated the existence of antibody responses to epitopes in seronegative participants, these antibodies were developed in large quantities to assess their function. The next part of the work describes how yeast clones of interest were selected by pre-infection serum to sort B cells and produce monoclonal antibodies specific to any specific yeast clone.

A method for producing monoclonal antibodies was first published in 1975 by Köhler and Milstein, who would later win the 1984 Nobel Prize in Medicine for this discovery (357). The technique used mice immunised by a specific antigen. The antigen-specific murine splenic B cells were then fused with murine myeloma cells to create hybridomas capable of antigen-specific antibody secretion for an indefinite period. Murine derived monoclonal antibodies were rarely used in human clinical trials as by their nature they were too immunogenic to be tolerated by the human immune system. Immunogenic monoclonal antibodies are undesirable as a treatment option, as the antibodies themselves become targets for the host immune system, leading to reduced therapeutic efficacy. Human derived antibodies manufactured by similar processes were developed during the early 1980's but were not widely developed due to difficulties with production processes (358). The key difficulty with murine (mouse developed), chimeric (murine variable and human constant region) and humanised (human with murine complementarity determining regions) monoclonal antibodies was the persistence of murine derived protein sequences.

Newer methods for B cell isolation monoclonal antibody production have gained popularity. These methods aim to produce antibodies with a greater proportion of human components to reduce immunogenicity and improve therapeutic efficacy. These include phage display systems, B cell cloning from immunised rabbits, and the single B cell isolation and cloning.

The method used in this chapter utilises both the yeast surface display system described in the materials and methods chapter, and a monoclonal antibody generating technique described by Smith et al (284). The yeast library identifies HIV envelope antigen specific antibodies at known time points in HIV infection (pre, early and late). These antibodies have been generated by B cells undergoing somatic hypermutation and maturation as a direct result of exposure to the HIV viral envelope (160). This B cell population was the target for the B cell baiting and potential isolation of multiple anti-HIV envelope antibodies. The isolated B cells are processed to extract heavy and light chain insert DNA sequences, which are then transfected into a human cell line. This method contrasts with previously described monoclonal antibody generation processes and has some distinct advantages.

Antibodies produced by the Smith method have a human Fc backbone and are expressed by a human cell line. Potential downstream therapeutic applications are not hindered by the steps required to transform phage or mice generated antibodies into those compatible with human tissue.

The advantage with using a yeast surface display system is the isolation of antigen specific B cells and antibodies. The Smith method used blood drawn from vaccinated individuals seven days post inoculation and identified plasmablasts by gating for a $CD19^{hi}CD20^{low}CD27^{hi}CD38^{hi}$. The method used gated for baiting and selecting $CD19^{hi}$ cells represents most of the B cell population except plasma and follicular dendritic cells. The yeast bait aims to select HIV envelope antigen specific B cells.

In the previous chapter, epitopes were identified which generated an immune response in seronegative and seropositive populations. Of interest are seronegative antibody responses which are echoed following seroconversion with recognition of the same epitopes. This chapter describes the process developed to extract B cells specific for these epitopes and produce the epitope-specific antibodies. The protocol aims capture a specific population of B cells, referred to as yeast antigen baiting. Briefly patient PBMCs were incubated with a yeast clone bearing a known epitope. B cells expressing the corresponding surface bound receptor would then bind the expressed yeast surface antigen. Fluorescence activated cell sorting (FACS) was used to identify and sort this double positive population onto 96-well plates, and extraction/cloning of B cell DNA to produce heavy and light chain pairs representing the B cell receptor/secreted antibody. Heavy and light chain pairs were transfected into a HEK293T cell line which was cultured to produce monoclonal antibodies for further analysis. Yeast clones were selected using principles from the previous chapter; if patient sera showed affinity for a yeast clone, it was selected it for B cell baiting.

5.2. Aims

The aim of this chapter was to develop a technique merging yeast surface display technology with fluorescence activated cell sorting, and to subsequently generate monoclonal antibodies using B cell expression cloning. From the previous results, it was decided to proceed with the analysis of one participants pre-infection anti-gp41response; B003 pre-infection serum was selected as it recognised a major antigenic determinant of the HIV gp41 epitope.

5.3. Basic experiment setup

5.3.1. Experimental controls and samples

Controls and experimental samples were prepared as described in the previous chapter. Each experiment consisted of ten controls and the desired number of experimental samples. This experiment setup was designed to closely resemble the flow sorting work done with patient serum, as the intention was to sort B cells of interest by antigen binding to surface antibody. Table 5.3-1 shows control and experimental aliquots. The experimental controls are described in the following pages.

PBMC controls	Unstained PBMC
	PBMC + CD3/14/16 FITC
	PBMC + CD19 APC
	PBMC + CD3/14/16 FITC + CD19 APC
Yeast controls	Unstained yeast
	Stained yeast
	Unstained yeast + stained yeast
	Unstained yeast + cell surface markers
	Stained yeast + cell surface markers
	PBMC + cell surface markers + unstained yeast
Experimental samples	PBMC with all lymphocyte cell surface markers and stained yeast

Table 5.3-1 FACS experiment setup
Table shows all control and experimental aliquots

The plots below in Figure 5.3-1 show the PBMC controls. The cell group of interest is the APC/CD19 high FITC/ CD3/14/16 low population shown in Q1 of row 2. This is the B cell population of interest.

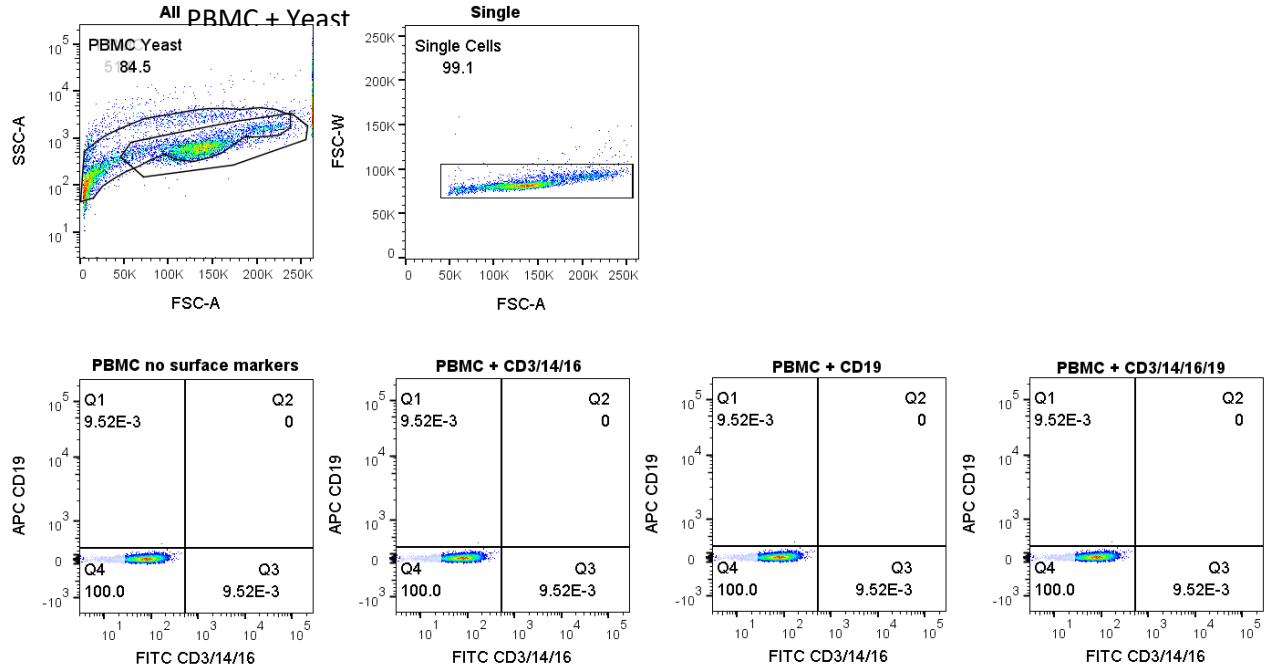


Figure 5.3-1 PBMC controls
Row 1: 1: x axis forward scatter area, y axis side scatter area; captures all PBMC. 2: x axis forward scatter area against y axis forward scatter width; single PBMC. Plots from 1 experiment, 250,000 to 300,000 cells sorted

Row 2: PBMC control samples for lymphocyte cell surface markers. X axis FITC CD3/14/16 representing dump channel, y axis APC CD19 representing B cells. 1: unstained PBMC with no cell surface markers. 2: PBMC stained for cell surface markers CD3/14/16 (FITC/dump channel, non B cells). 3: PBMC stained for cell surface marker CD19 (B cell population of interest, APC). 4: PBMCs stained for all cell surface markers (CD3/14/16 FITC, CD19 APC).

9.523E-3 = 009523

The yeast control samples consisted of separate aliquots of unstained yeast, stained yeast and unstained and stained mixed together (see Figure 5.3-2 below). This control demonstrated successful uptake of the dye into the yeast population. The fluorochrome Pacific Blue (BV421, Invitrogen) was selected for yeast dyeing to prevent spectral overlap with lymphocyte cell surface markers. The mixed unstained and stained yeast cell aliquot plot demonstrates clear separation of two yeast populations and successful yeast uptake of Pacific Blue dye.

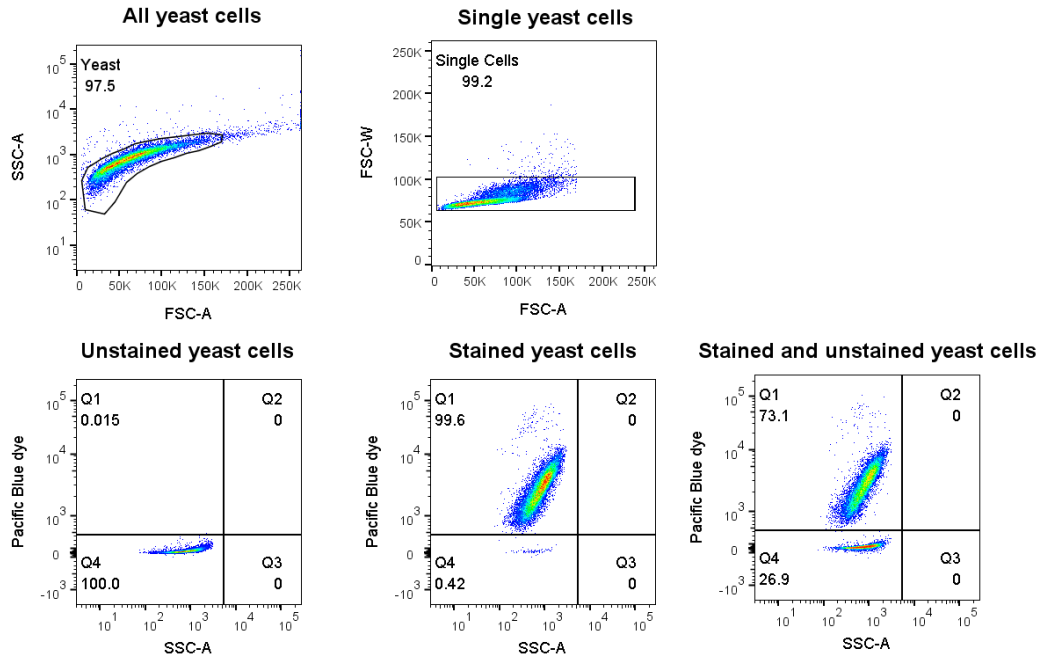


Figure 5.3-2 Yeast controls
Yeast cell gating strategy and populations. Plots from 1 experiment, 250,000 to 300,000 cells sorted

Row 1: 1 x axis forward scatter area y axis side scatter area; all yeast cells. 2: x axis forward scatter area y axis forward scatter width; single yeast cells.

Row 2: X axis side scatter area, y axis Pacific Blue 1: unstained yeast cells, 2: stained yeast cells, 3 mixed stained and unstained yeast cells.

The PBMC and yeast controls were used to assess non-specific yeast cell binding to PBMC and review non-specific PBMC affinity for yeast surface bound epitopes. These are shown in Figure 5.3-3.

Healthy volunteer PBMC were added to aliquots of stained and unstained E016 yeast clones. The cell surface markers CD3/14/16/19 were also added to replicate experimental conditions. The population of interest was the double positive CD19 high/Pacific Blue high Q2 window.

Most of the unstained yeast population inhabited Q4, and the stained population inhabited Q1, with a negligible population in Q2. This demonstrated an absence of significant non-specific PBMC and yeast cell binding. Subsequent experiments assessed successful PBMC/yeast cell binding.

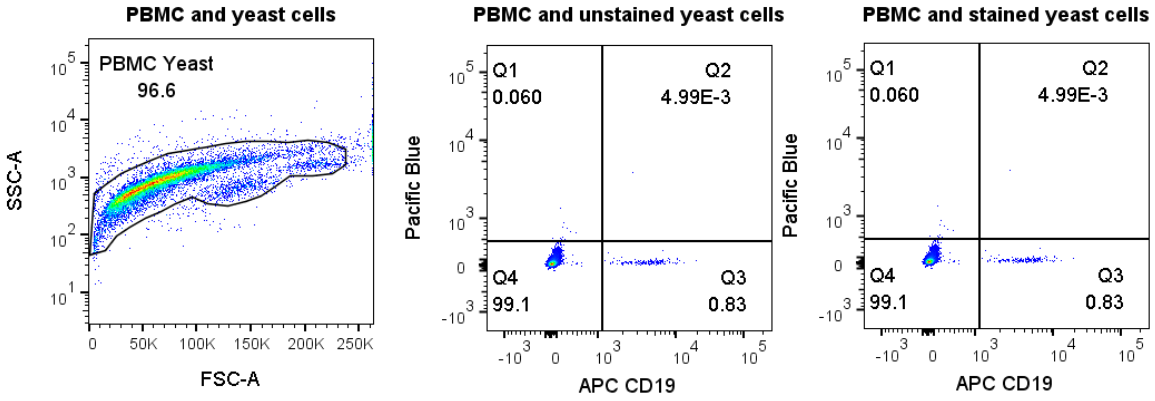


Figure 5.3-3 PBMC and yeast controls
FACS plots show unstained and stained yeast added to non-specific PBMCs and CD19 APC cell surface marker. Plots from 1 experiment, 250,000 to 300,000 cells sorted

Row 1: 1 x axis forward scatter area y axis side scatter area; all PBMC and yeast cells. 2 and 3: x axis APC CD19 y axis Pacific Blue for unstained and stained yeast cells.

4.99E-3 = 0.00499

PBMC and yeast cell ratio was optimised using increasing concentrations of yeast cells at ratios of 1:1, 1:5, 1:10 and 1:20. This was to assess if nonspecific yeast binding to PBMC influenced the efficacy of downstream sorting

The double positive APC high/Pacific Blue high population in Q2 was reviewed and found a progressive decrease in the total number of cells in Q2. At a ratio of 1:1, the double positive population is 1.08 e^{-4}% of the total cell count. This population becomes zero i.e. negligible progressively with increasing yeast ratios. At a yeast/PBMC ratio of 1:20, the Q2 cell population is 0. This stage of optimisation suggests that non-specific yeast and B cell binding does not occur at higher yeast cell concentrations. Following this review, each experiment used with approximately five million PBMC and five million yeast cells.

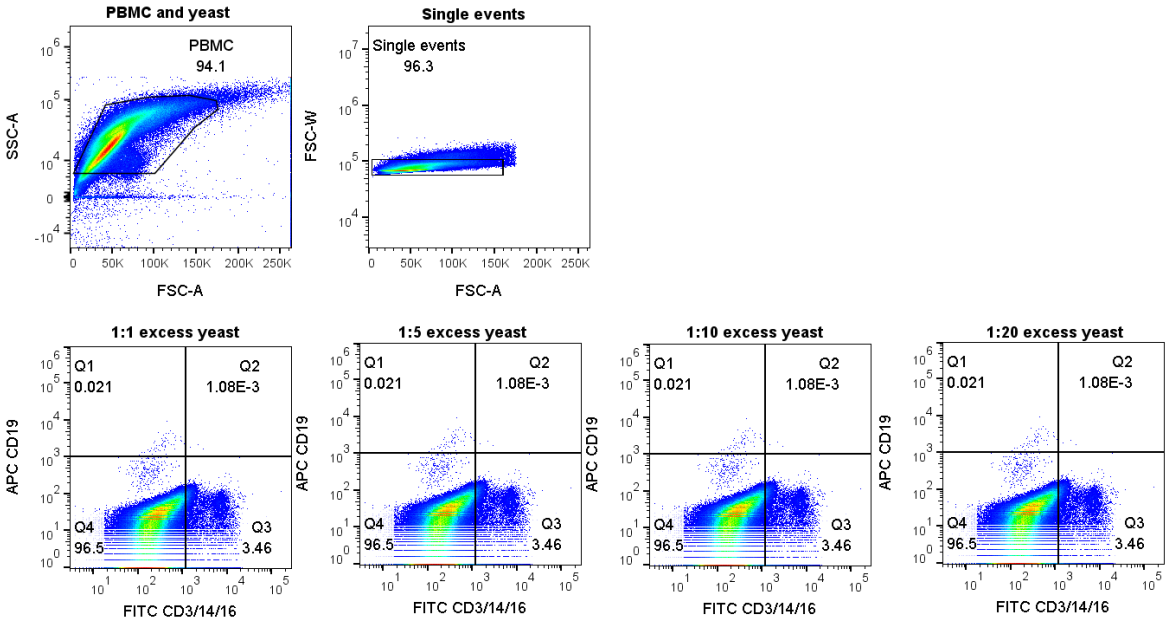


Figure 5.3-4 PBMC and yeast increasing ratio control
FACS plots with PBMC to an increasing yeast cell ratio. The figure shows PBMCs and stained yeast added to unstained yeast aliquots at ratio 1:1:1, 1:1:5, 1:1:10, and 1:1:20. Plots from 1 experiment, 250,000 to 300,000 cells sorted

Row 1: x axis forward scatter area y axis side scatter area. 1: all PBMC and yeast cells, 2: single events

Row 2: x axis FITC CD3/14/16 dump channel, y axis APC CD19 B cells. 1-4 yeast to PBMC ratio of 1:1, 1:5, 1:10 and 1:20

PBMC/lymphocyte cell surface marker binding to yeast cells was reviewed for the possibility of non-specific fluorochrome binding to yeast cells which would result in a non-specific double positive population.

Figure 5.3-5 below shows the lymphocyte cell surface markers CD3/14/16/19 added to yeast cells. The plots did not show a significant population of FITC (CD 3/14/16) or APC (CD19) high cells in Q6 and demonstrated negligible binding of PBMC cell surface markers to yeast.

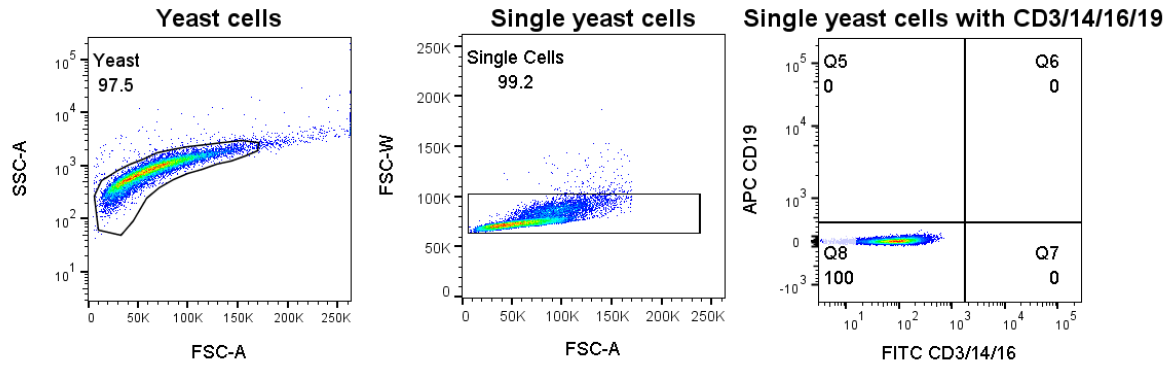


Figure 5.3-5 PBMC cell surface marker and unstained yeast cell control
FACS plots showing yeast mixed with CD19 APC cell surface marker. Flow cytometry profiles of unstained yeast cell and PBMC labelled with CD19 and combination FIC markers T, monocyte and NK cell markers. Plots from 1 experiment, 250,000 to 300,000 cells sorted

Row 1: 1 x axis forward scatter area y axis side scatter area, all yeast cells, 2: forward scatter area to width; single yeast cells, 3: x axis FITC CD19 y axis; single yeast cells with CD3/14/16 cell surface markers

5.3.2. Optimisation of sorting experiment

This section describes optimisation of the B cell baiting flow cytometry process using varying concentrations of cells and reagents.

5.3.2.1. Varying concentrations of yeast/PBMC cell surface cell marker

The effect of an increasing yeast cell ratio to PBMC and fluorochrome cell surface markers was reviewed. PBMCs with yeast cells at a ratio of 1:1, 1:10, 1:25, 1:50 and 1:100 were reviewed (data not shown here). On review, the number of APC+/Pacific Blue+ cells in Q2 remained similar despite an increasing yeast population. Following this review, a PBMC/yeast ratio of 1:1 was selected and the concentration of cell surface markers kept as described in the methods section.

5.3.2.2. Selection of appropriate positive control to optimise flow sorting

For this section of work, the performance of seropositive PBMCs sorted by selected yeast clones was reviewed. This was to evaluate if PBMCs binding yeast cells via cell surface receptor binding to yeast membrane displayed antigen. Seropositive participant samples were selected from group E to optimise the yeast antigen baiting experiment. These participants were E0016, E0017, E0018, E0019 and E0020. PBMCs were prepared and stained as previously described.

Three yeast clones with antigenic determinants defined in the previous chapter were selected. These clones were Pos-C01, Pos-C02, Pos-C06 representing an amino acid sequence located in the N helical region and loop (AA 559-628) within the HIV envelope subunit gp41. The yeast clones were cultured in SDCAA and SGCAA to promote surface expression of protein and then stained them with Pacific Blue dye. Eighteen samples were analysed in total to review which yeast epitope was most recognised by patient serum.

APC high/Pacific Blue high PBMC and yeast samples were sorted using the BD FACS Aria III. The gating strategy was as described in materials and methods section 2.6.8.7. For each sorting experiment, the Q2 window was the population of interest; a double positive APC high/Pacific Blue high population and represented CD19+ B cells bound to epitope on the surface of the yeast cells. For all but one of the seropositive participant samples (E018), the yeast clone with the greatest affinity for CD19 positive B cells was PosC-01. This clone was selected for all further optimisation and sorting. The PBMCs from participant E016 were also used for further work due to a sorted Q2 population of 0.077% of all cells in total. These results are shown in Table 5.3-2 and Figure 5.3-6.

	Yeast clone		
Participant	PosC-01	PosC-02	PosC-06
E016	0.077%	0.041%	0.047%
E017	0.025%	0.018%	0.011%
E018	0.013%	0.018%	0.003%
E019	0.015%	0.009%	0.010%
E020	0.029%	0.011%	0.013%
E019-5	0.002%	0.002%	0.002%

Table 5.3-2 Q2 cell population
Described as proportion of all cells sorted for all five participant PBMC and yeast clones

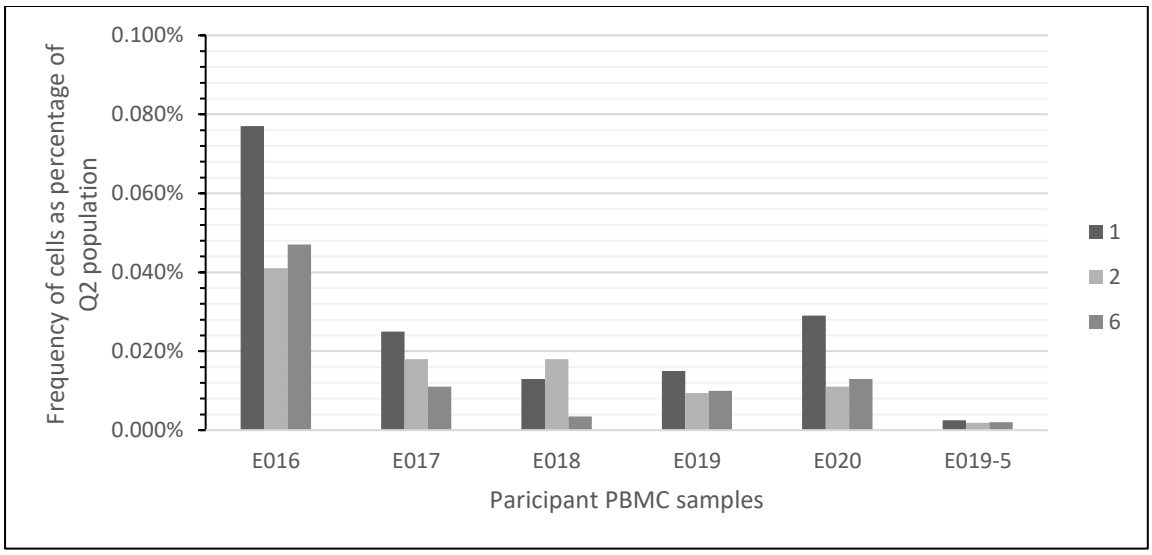


Figure 5.3-6 Double positive PBMC/yeast Q2 cell population
X axis participant, E019-5 was assayed at fivefold yeast-PBMC ratio. Y axis frequency of all cells as percentage/proportion of all cells sorted for each participant. Patient results are grouped, and individual yeast clones represented by shading as clone 1, 2, or 6.

5.3.2.3. Backgating on APC and FITC channels

The Q2 APC/Pacific Blue population was selected and backgated this using APC and FITC to ensure the population of PBMCs selected was APC high (representing CD19 B cells) and FITC low (representing other lymphocytes labelled with CD 3/14/16). The first plot has a Q2 with population of 0.061 (CD19 Pac Blue high yeast cells). This population is then backgated on FITC and APC and is shown in the second plot- all events are located within FITC low and APC high population. All E016-E020 Q2 plots were backgated and most cells found to be APC high/Pacific Blue high were FITC low/APC high. This is shown in Figure 5.3-7 and Figure 5.3-8.

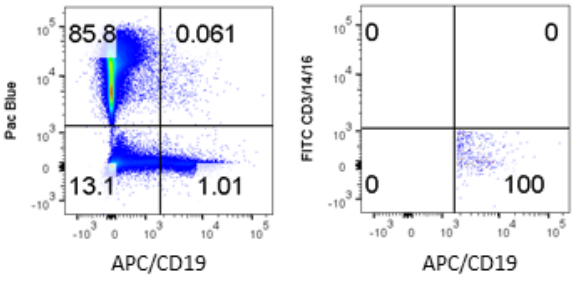


Figure 5.3-7 Backgating on APC and FITC channels
PBMC from seropositive participant E016 sorted with the HIV gp41 envelope clone PosC-01.1: x axis APC/CD19 representing B cells, y axis Pacific Blue representing yeast cells. 2: x axis APC/CD19 representing B cells, y axis FITC CD3/14/16 representing dump channel

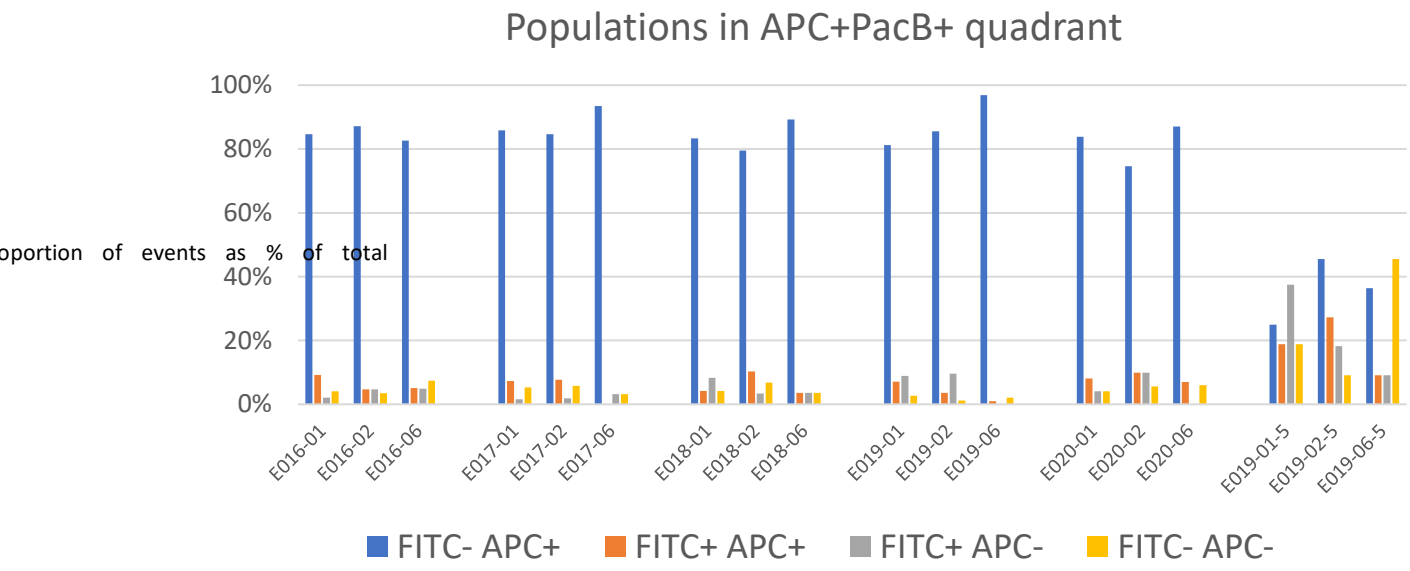


Figure 5.3-8 Backgated FITC/APC high Q2 population
Population backgated using APC and Pacific Blue. X axis participant and quadrant indicated by colour, y axis proportion of events as percentage of total population.

5.3.2.4. E016 optimisation

Study participant E016 PBMCs were used used for optimisation. E016 was a sample drawn from a participant with early HIV infection who had not yet started antiretroviral medication. PBMCs were stained with cell surface markers as previously described and added these to the dyed yeast clone PosC-01. The experimental controls and sample were set up as described previously. Three separate aliquots of PBMC and yeast clones were used for optimisation and designated these Positive control A, B, and C (PosC A, B, C). All samples were analysed by FACS (BD FACS Aria III) and gated as previously described.

The results showed 0.03 – 0.04% of all cells were yeast/PBMC dyad representing epitope/B cell surface receptor binding. This double positive population was sorted onto a 96-well plate containing catch buffer. Eighty double positive population and five bulk sort events (described below) were sorted onto the 96-well plate. The results from the APC high/Pacific Blue high Q2 window are displayed in Table 5.3-3 below.

	Q1: CD19- APC+	Q2: CD19+ APC+	Q3: CD19+ APC-	Q4: CD19- APC-
E016 PosC A	97.20%	**0.03%**	0.80%	2.01%
E016 PosC B	96.80%	**0.04%**	0.72%	2.43%
E016 PosC C	96.90%	**0.03%**	0.75%	2.33%

Table 5.3-3 Sorted population proportions
Figures are proportion of all selected PBMC and yeast cells

5.3.2.5. Index sorting of double positive population

Index cell sorting for these cell populations was reviewed. Index sorting records each sorted cell's phenotype and can be used to retrospectively analyse any cell sorted with this feature. This ensured sorted cells originated from the double positive population. This is shown in Table 5.3-4 and demonstrated the intended population was captured by this method. Having reviewed cell proportions from optimisation steps, the experimental stage of yeast cell baiting was next.

	Q1: CD19- APC+	Q2: CD19+ APC+	Q3: CD19+ APC-	Q4: CD19- APC-
E016 PosC A	97.20%	**0.03%**	0.80%	2.01%
E016 PosC A index	0%	**100%**	0%	0%
E016 PosC B	96.80%	**0.04%**	0.72%	2.43%
E016 PosC B index	0%	**100%**	0%	0%
E016 PosC C	96.90%	**0.03%**	0.75%	2.33%
E016 PosC C index	0%	**100%**	0%	0%

Table 5.3-4 Index sorting yield
Sorted populations as proportion of all selected PBMC and yeast cells. Q2 population of interest contains only CD19/APC high phenotype in keeping with the desired target sort population

5.4. Experimental B cell antigen baiting

Having optimised B cell sorting, experimental samples were sort. Samples and corresponding PBMCs were determined in the previous chapter. By using participant sera samples to sort yeast cells based on surface displayed epitope, it followed that the B cells responsible for secretion of these antibodies would display surface receptors complementary to those epitopes selected by serum samples.

To this point, the purpose was to isolate anti-Env epitope antibodies from pre infection samples by PBMC sampling. However, it must be remembered that most adult Ig-secreting cells are located in bone marrow.

Recalling the activation pathway of B cells, exposure to protein antigen requires activation by T helper cells in primary follicles resulting in formation of the germinal centre. Ongoing isotype switching and antibody maturation results in high affinity memory B cells and plasmablasts. The plasmablasts from follicles and mesenteric lymph nodes migrate to gut lamina propria and mesenteric surfaces, and those from lymph nodes or splenic follicles migrate to bone marrow at 2-3 weeks. Here, they differentiate to form plasma cells with a half-life of months-years, and bone marrow is now principle site of antibody production (127)

The ideal tissue type for sampling here would be plasmablasts from bone marrow, but the study would have relied on bone marrow sampling of all seronegative candidates in an effort to capture seroconversion events; this was not logistically possible. Another approach might have been to sort $CD19^{+}CD27^{+}CD38^{+}$ plasmablasts only, but they exist as a small population of 0·6–1·6% of in adult PBMC populations compared to 7·2–11·2% for $CD19^{+}$ B cells (359). Following this it was decided to select $CD19^{+}$ cells with paratope specificities identified by yeast epitopes.

Multiple PBMC and yeast clone combinations including one seronegative participant sample from the first chapter of results, A0181 were analysed. This sample was a component of the seronegative H9 aliquot sample. The bulk of my analysis focussed on longitudinal PBMC samples from participant B003 who displayed repeated epitope recognition at all timepoints. Relevant samples were selected for monoclonal antibody work. Table 5.4-1 shows PBMC and yeast clones (AA = amino acid).

PBMC used	Yeast clone	Epitope	AA position	AA sequence
Negative control (lab)	Pos C	Gp41	586-604	DQQLLGIWGCSGKLICTTA
Positive control E016	Pos C	Gp41	586-604	DQQLLGIWGCSGKLICTTA
Seronegative A0181	H9-01	gp 41	653-676	KLFIMIVGGLVGLRIVFAVLSIVNR
Seronegative B003	PreB3-03	gp 120	198-213	VITQACPKVSFEPIPI
Seronegative B003	PreB3-04	gp 41	643-676	LEKSQNQQEKNEQELLELDKWANLWNWFDITNWL
Seropositive B003 (early)	Early B3-02	gp 120	192-214	INCNTSVITQACPKVSFEPIPIH
Seropositive B003 (early)	Early B3-15	gp 41	644-671	EKSQNQQEKNEQELLELDKWANLWNWFD
Seropositive B003 (late)	Late B3-09	gp 120	198-215	VITQACPKVSFEPIPIHF

Table 5.4-1 Yeast clones selected for B cell baiting

5.4.1. Flow sorting plots- experimental

Serum/yeast pairs were sorted as listed above, and APC CD19 high/Pacific Blue high population- representing B cells bound to yeast epitopes recorded. The PBMC negative (lab/healthy) and positive control samples were prepared as previously.

All experimental samples contained a double positive population which was measured as a percentage of the total yeast population. This ranged from 0.01-0.23%. Index plots for each sample were reviewed and showed all sorted cells as being CD19 high/APC high.

These results are shown in Table 5.4-2 and Figure 5.4-1

	FITC low as frequency. of parent population	FITC low /Q2: CD19+/Pac Blue+	Index sort
PBMC (negative) control	37.50%	0.02%	
Positive control	64.10%	0.05%	
Seronegative A0181 H9-01	58.50%	0.21%	100%
Pre infection B003 gp41	92.90%	0.03%	100%
Pre infection B003 gp120	48.80%	0.23%	100%
Early infection B003 gp41	33.40%	0.06%	100%
Early infection B003 gp120	10.80%	0.22%	100%
Late infection B003 gp120	81.90%	0.01%	100%

Table 5.4-2 Summary of APC high/Pacific Blue high sorted population

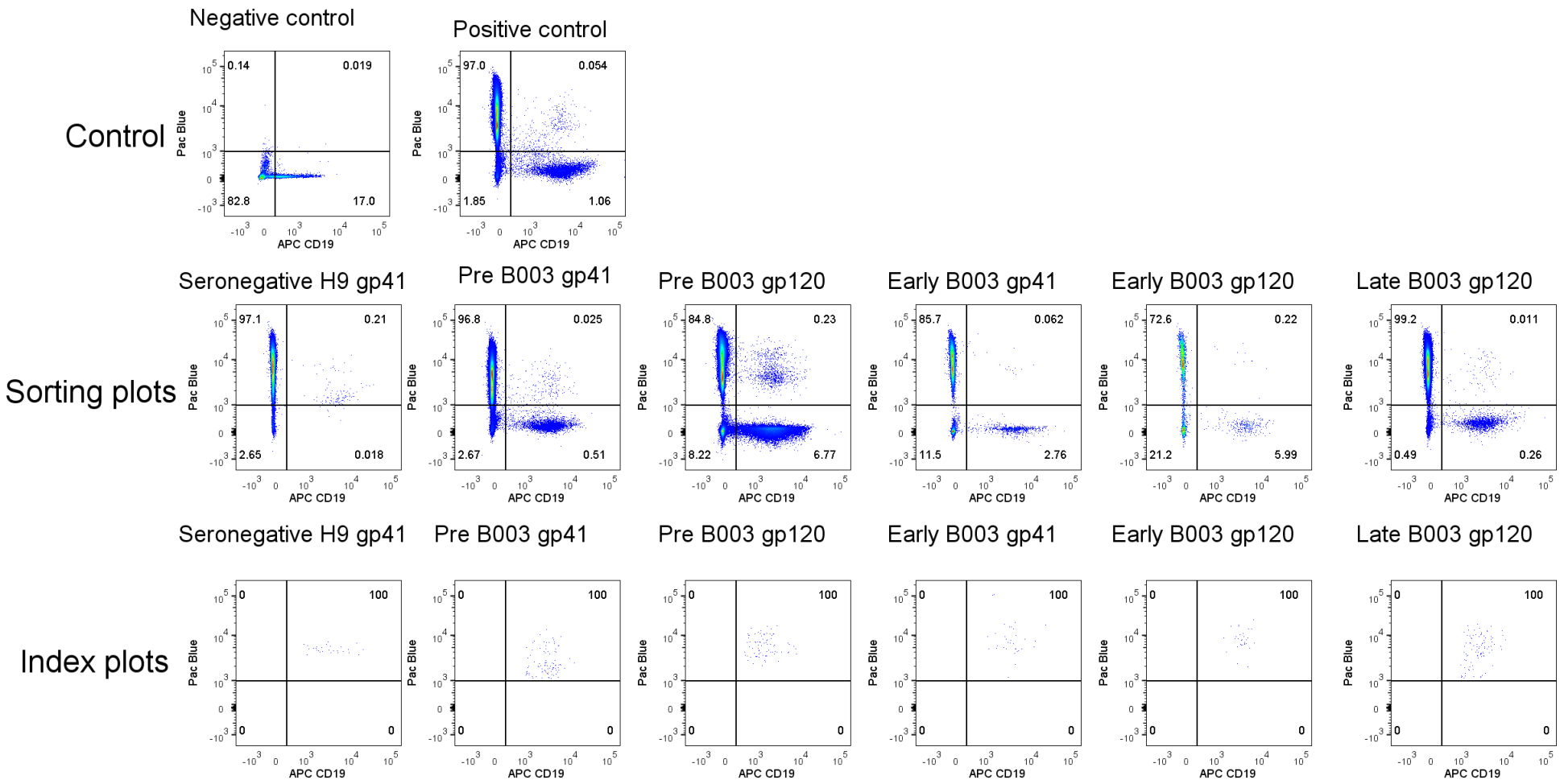


Figure 5.4-1 FACS plots for B cell baiting
X axis APC CD19 representing B cells, y axis Pacific Blue representing yeast cells

Row 1: controls; negative healthy and seropositive PBMC. Row 2: experimental sorted plots. Row 3: index plot for sorted cells. Q2 is population of interest representing PBMC/yeast cell dyad.

5.5. Monoclonal antibody optimisation

The sorted B cell/yeast population plates were stored at -80°C until required. For use, plates were retrieved and thawed in a sterile hood in the containment level 2 laboratory. The E016 yeast/PBMC samples were for optimisation.

5.5.1. Single cell reverse transcriptase (RT-PCR) and cloning polymerase chain reaction

Single cell RT-PCR was performed as previously described and then loaded PCR product onto TBE gel electrophoresis to confirm presence of the correct bands. Heavy and light chain wells were matched to ensure chain pairs were available for future work steps and documented well numbers for purification and cloning PCR steps and used the well number to identify all antibody products originating from this well. Kappa sequencing was performed (Genewiz, UK) to determine which primers were required for the subsequent kappa cloning PCR. Sequences were trimmed using BioEdit and uploaded to the IMGT website to identify the correct gene family specific primers for use in the cloning PCR step.

5.5.2. Cloning PCR

Any positive wells in the RT-PCR stage were then submitted for cloning PCR. The resulting PCR products were then analysed in a 1% TBE gel. The wells were noted, and heavy/light chain matched pairs were considered indicative of one yeast/PBMC dyad sorted per well and chain pairings recorded.

A total of 85 wells were sorted in total for the optimisation. Four wells (PosC 22, PosC 29, PosC 66 and Pos C B-05) contained a corresponding pair representing a potential monoclonal antibody product.

The TBE gel is shown in Figure 5.5-1 and the chain outcomes in Table 5.5-1.

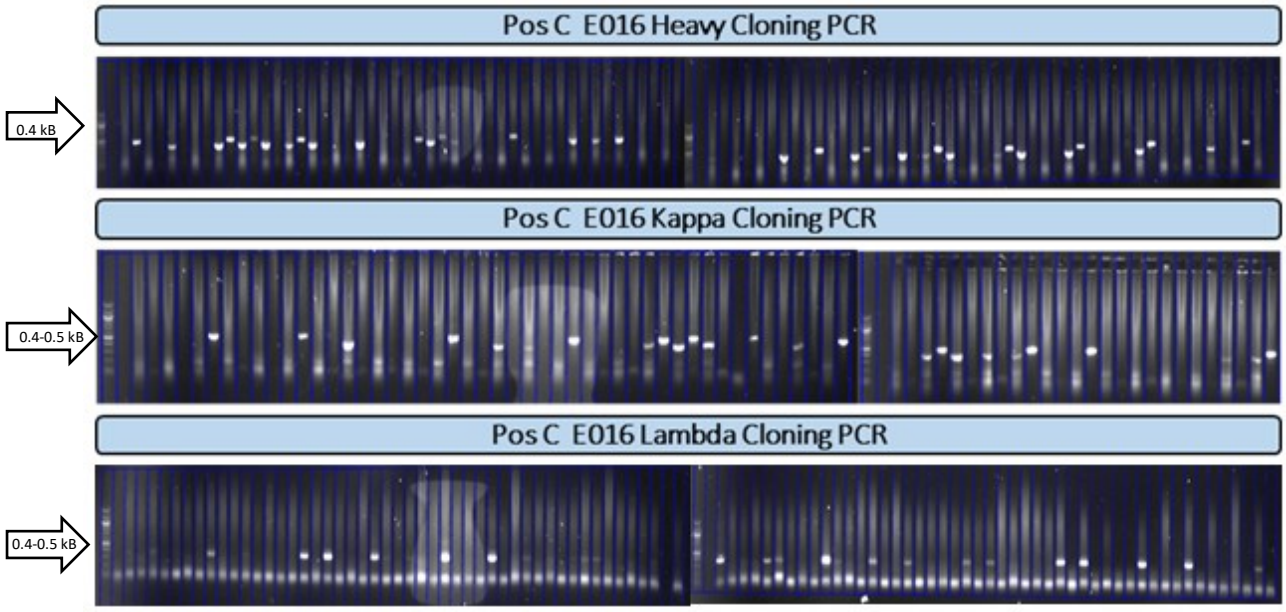


Figure 5.5-1 Positive control cloning PCR TBE gel analysis
TBE gel electrophoresis showing heavy and light (kappa and lambda) chains for PosC E016 PBMC and yeast sorting

	Total	% of sorted wells
Heavy	31	36.5%
Kappa	3	3.5%
Lambda	5	5.9%

Table 5.5-1 Outcomes for chain pairs
Total heavy, kappa and lambda chains located in TBE gel post cloning step

5.6. Monoclonal antibody- experimental results

5.6.1. Cloning PCR results

Table 5.6-1 below shows outcomes for cloning PCR steps. For the purposes of downstream monoclonal antibody production, considered wells into which one yeast/B cell dyad had been sorted were considered a successful sorting event. For each single double sort event, two potential antibodies are removed from further analysis. The table also shows the ratio of antibody light chain kappa to lambda ratio. For reference, healthy individuals usually have a kappa to lambda ratio of approximately 2:1 for immunoglobulin light chains, usually varying only in the context of disease (360).

Sample	No. wells sorted		No. chains	% sorted wells	No. light chains with heavy chain present	% total light chains	K:L ratio	Total potential Ab	Double sort events	Available Ab pairs
Seronegative	48	Heavy	14	29.17%			1.17	13.00	3.00	7
		Kappa	7	14.58%	7	53.85%				
		Lambda	10	20.83%	6	46.15%				
Pre B003 gp120	96	Heavy	10	10.42%			6.00	7.00	0.00	7
		Kappa	1	1.04%	6	85.71%				
		Lambda	6	6.25%	1	14.29%				
Pre B003 gp41	96	Heavy	65	67.71%			1.79	67.00	8.00	51
		Kappa	52	54.17%	43	64.18%				
		Lambda	24	25.00%	24	35.82%				
Early B003 gp120	96	Heavy	55	57.29%			1.56	41.00	2.00	37
		Kappa	25	26.04%	25	60.98%				
		Lambda	16	16.67%	16	39.02%				
Early B003 gp41	96	Heavy	63	65.63%			0.96	51.00	5.00	41
		Kappa	25	26.04%	25	49.02%				
		Lambda	26	27.08%	26	50.98%				
Late B003 gp120	96	Heavy	64	66.67%			4.43	38	1	36
		Kappa	31	32.29%	31	81.58%				
		Lambda	7	7.29%	7	18.42%				

Table 5.6-1 Cloning PCR outcomes

Listed in order are the sample details: number of wells sorted, chain insert type, no of each chain sorted and then as a percentage of total wells sorted, whether each light chain insert contained a corresponding heavy chain insert, and then as a percentage of the total, the kappa and lambda ratio, the total potential antibody pairings, the presence of double sort events, and finally the potential available antibody pairs. Double sort events indicate a well containing both kappa and lambda chains, where greater than one yeast/B cell dyad had been sorted into that well.

The seronegative A0181 H9-01 gp41 sample yielded thirteen chain insert pairs, six kappa and one lambda. All were single sort events and considered viable candidates.

The pre infection B003 gp120 sample yielded seven chain insert pairs; six kappa chains and one lambda chain, all with single sorting events. The overall yield of antibodies was comparatively low and was likely due to optimisation reasons, as successive experiments were yielded greater numbers of potential antibody pairs. The pre infection B003 gp41 sample yielded 67 chain insert pairs; 43 kappa chains and 24 lambda chains. This sample had 8 double sort events and so 51 antibodies were considered viable.

The early infection B003 gp120 sample yielded 41 chain insert pairs; 25 kappa and 16 lambda chains. There were two double sort events, yielding 37 potential antibody pairs. The early infection B003 gp41 sample yielded 51 chain insert pairs; 25 kappa and 26 lambda chains. There were five double sort events, yielding 41 potential antibody pairs.

The late infection B003 gp120 sample yielded 38 chain insert pairs; 31 kappa and 7 seven lambda chains. There was one double sort event, yielding 36 potential antibody pairs

5.6.2. Kappa chain sequence analysis

As discussed in the optimisation section of the PCR cloning process, kappa chain sequences were obtained to identify the correct gene family specific primers for downstream cloning.

Chains were named according to PBMC sample timepoint (P/E/L B3 as pre, early, late), epitope location (gp120 or gp41) and well of origin. Therefore, sample EB3gp41-76 is from early B003 PBMC, identifying and epitope on gp41, and the chain was in the 76th well of the TBE gel.

5.6.3. Flow sorting and PCR cloning yields

The outcomes for experimental samples are summarised in Figure 5.6-1. Outcomes are described as wells sorted, total wells containing either heavy or light chains, wells where the presence of one heavy and one light chain indicating a possible antibody, and the proportion of wells containing either a single or multiple yeast/PBMC dyad. The trend line shows the yield of antibodies described as a percentage of the total number of wells sorted. The graph describes each sorting experiment and the date it was undertaken, and the table beneath the graph give the absolute figures. All experiments contained 96 sorted events.

Pre infection seronegative PBMCs were sorted with clone PreB3-03 (gp120) and clone PreB3-04 (gp41), with sort yields of 7.4% and 61.5%. Seropositive PBMCs from two timepoints were sorted; late PBMCs were sorted with clone PoB3-09 (gp120) to give an antibody yield of 37.5%, and sorted early PBMC samples with clone AcB3-15 (gp41) and clone AcB3-02 (gp120), giving sort yields of 48.4% and 38.5%,

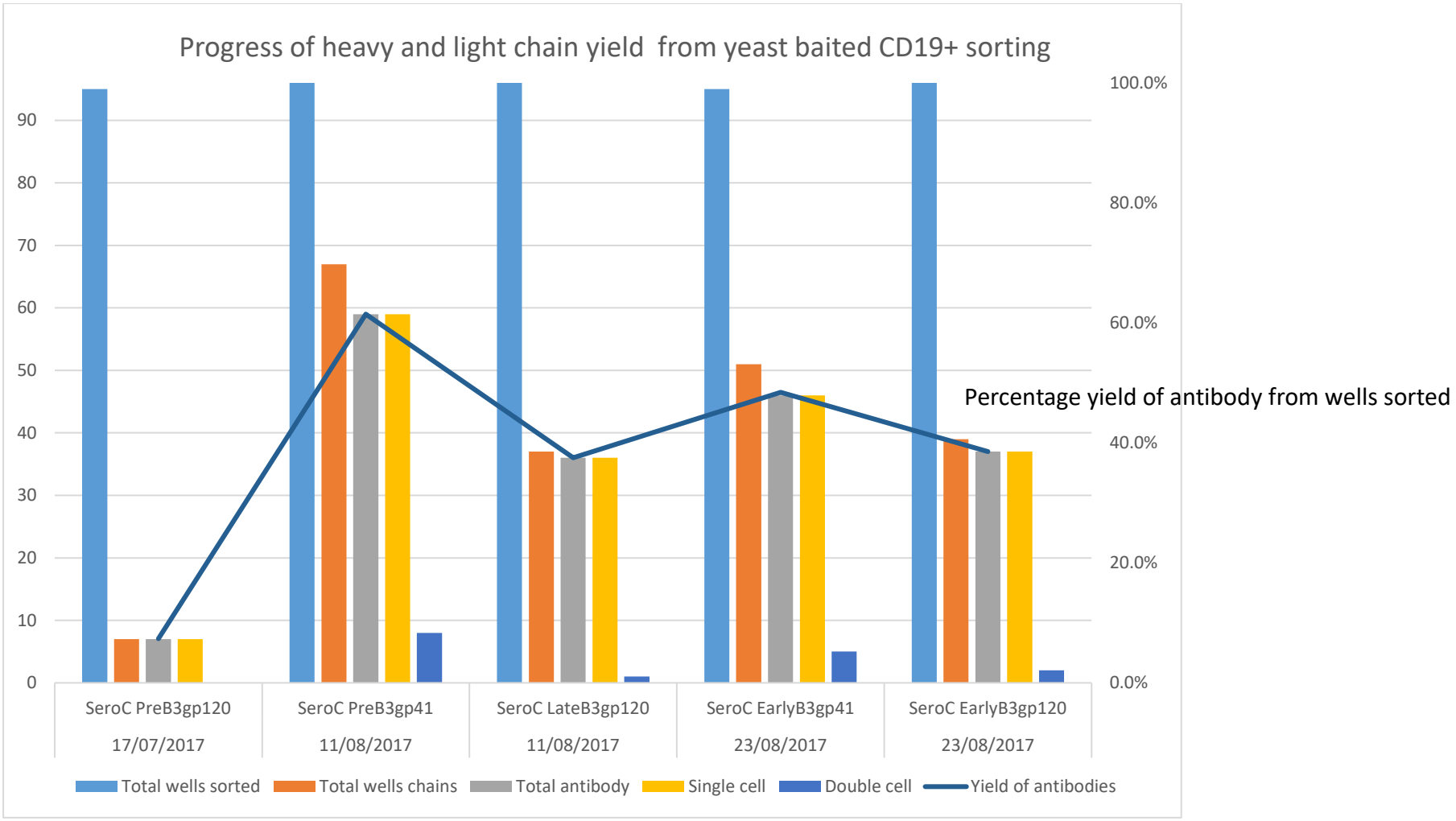


Figure 5.6-1 Yields from successive experiments
X axis experiment name and date, bars indicate the following; total wells sorted, total wells containing chains, total potential antibody pairs, single vs double sorted events, and yield of potential antibody pairs

In summary, the greatest yield of antibodies was produced from the seronegative PBMC from B003 sorted with the gp41 yeast clone PreB3-04; possible reasons include ongoing optimisation of the experimental processes.

SGCAA yeast cultures were harvested at an OD600 measurement of 2-5 to ensure an adequate cell density and cell number for sorting. The number of PBMCs was increased to 5 million per experiment which ensured a greater availability of candidate B cells for sorting.

For every step involving a 96-well PCR plate, the plate was centrifuged at 1000RPM for one minute to settle all contents to the bottom of the wells, as tiny reagent volumes meant they adhered easily to the inner surface walls of the wells.

For the PCR stages of the experiments, master mixes of all reagents were created save for PCR templates and enzymes, to ensure enzymes did not suffer degradation due to temperature or handling and added them at the final stage.

As outlined, the greatest yield from B cell yeast sorting was the B003 pre infection seronegative PBMC sorted with the gp41 yeast clone PreB3-04. These 51 potential antibody heavy and light chain pairs were selected for further workup and analysis.

5.6.4. PreB3 anti-gp41 monoclonal antibody production- digestion, ligation

A digestion reaction was performed on 51 candidate heavy and light chain inserts in preparation for ligation to the corresponding vector. The products underwent PCR purification and were run on a 1% TBE gel with a 1kb molecular reference ladder. Any visible bands present at the appropriate molecular weights were considered as successfully digested. A total of 38 chain insert pairs were harvested from the original 51 submitted for digestion. These consisted of 38 heavy, 15 lambda, and 23 kappa chain inserts. The other 13 heavy/light chain pairings did not appear on the gel and could not be analysed. A digestion was performed on the corresponding chain insert vectors. Two vectors were prepared for each chain insert; heavy 1 and 2, kappa 1 and 2, lambda 1 and 2. This is shown in Figure 5.6-2.

Insert and vector product concentrations were measured in preparation for ligation at a 3:1 ratio. Concentrations for this step are in the appendices. The ligated chain insert and vector constructs were used to transform DH5 alpha cells, incubated overnight. The following day colonies were harvested and cultured in preparation for DNA extraction and digest. This digest step was to ensure presence of PCR product post ligation that was then sent for sequencing analysis.

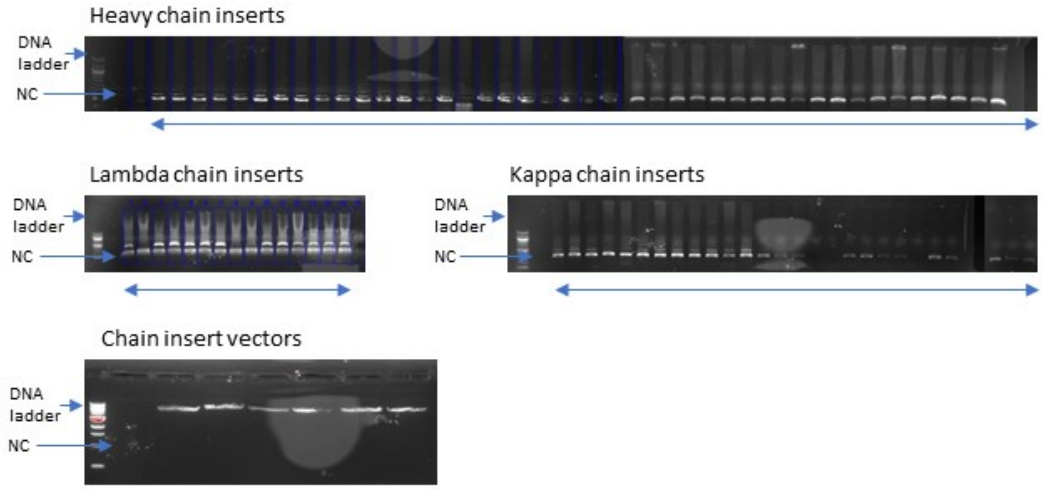


Figure 5.6-2 TBE digest gels;
Name and number of bands visible in brackets. 100bp DNA ladder and NC negative control. First two rows: heavy (38), lambda (15) kappa (23). Blue linear arrows = wells 1-48. Third row chain insert vectors H1,2, K1,2, L1,2. All insert kB sizes as previous

5.6.5. PreB3 anti-gp41 monoclonal antibody production- miniprep and digest outcome

Following the miniprep and digest stage, 38 chain insert pairs were sent for sequencing analysis (GeneWiz UK). 21 pairs returned viable sequences, the remaining 17 did not and were removed from future use.

The following 21 candidate antibody chain insert pairs were produced:

10, 14, 16, 17, 22, 27, 33, 38, 46, 48, 51, 54, 63, 64, 68, 77, 81, 83, 87, 89, 94.

To recap, the number assigned to each antibody relates to the well of the 96-well plate into which the original double positive yeast/PBMC dyad was sorted. Each antibody insert pair consisted of a heavy and light chain insert and is named according to the wells and the experiment from which they originated; H01-10 is heavy chain insert 10 from the first cloning and digestion experiment. The sequences were uploaded to the online IMGT database for analysis.

Information on antibody gene family, framework region and complementarity determining lengths for all anti-gp41 antibodies is shown in Table 5.6-2. From this point, chain insert pairs are referred to as antibody pairs.

Chain type	Insert name	V-gene and allele	J- gene and allele	D- gene and allele	FR lengths	CDR- lengths
Heavy	H01-10	IGHV3-43*01F	IGHJ5*02F	IGHD2-8*01 F	[25.17.38.11]	[8.8.X]
Light	K01-10	IGKV1-5*03F	IGKJ1*01F		[23.17.36.10]	[6.3.10]
Heavy	H01-14	IGHV1-18*04F	IGHJ4*02F	IGHD3-22*01 F	[25.17.38.11]	[8.8.15]
Light	L01-14	IGLV1-40*03F	IGLJ3*02F		[25.17.36.10]	[9.3.11]
Heavy	H01-16	IGHV3-43*01F	IGHJ6*02F	IGHD3-22*01 F	[25.17.38.11]	[8.8.21]
Light	K01-16	IGKV1-39*01F or IGKV1D-39*01F	IGKJ2*01F		[23.17.36.10]	[6.3.9]
Heavy	H01-17	IGHV1-46*01F or IGHV1-46*03F	IGHJ4*02F	IGHD3-3*01 F	[25.17.38.11]	[8.8.14]
Light	L01-17	IGLV2-23*02F	IGLJ2*01F or IGLJ3*01F		[25.17.36.10]	[9.3.10]
Heavy	H01-22	IGHV4-4*02F	IGHJ4*02F	IGHD6-19*01 F	[25.17.38.11]	[9.7.19]
Light	K01-22	IGKV1-39*01F	IGKJ1*01F		[23.17.36.10]	[6.3.9]
Heavy	H01-27	IGHV1-18*01F	IGHJ6*02F	IGHD5-18*01 F	[25.17.38.11]	[8.8.18]
Light	K-02-27	IGKV1-39*01F	IGKJ2*02F		[23.17.36.10]	[6.3.9]
Heavy	H02-33	IGHV3-53*01F	IGHJ6*02F	IGHD2-2*01 F	[25.17.38.11]	[8.7.14]
Light	K01-33	IGKV1-06*01F	IGKJ1*01F		[23.17.36.10]	[6.3.9]
Heavy	H01-38	IGHV4-30-4*07F	IGHJ5*02F	IGHD5-18*01 F	[25.17.38.11]	[10.7.13]
Light	K01-38	IGKV3-20*01F	IGKJ5*01F		[23.17.36.10]	[7.3.9]
Heavy	H01-46	IGHV4-4*02F	IGHJ4*02F	IGHD6-19*01 F	[25.17.38.11]	[9.7.19]C
Light	L01-46	IGLV2-14*01F	IGLJ3*02F		[25.17.36.10]	[9.3.10]
Heavy	H01-48	IGHV4-39*01F	IGHJ4*02F	IGHD2-21*02 F	[25.17.38.11]	[10.7.11]
Light	K02-48	IGKV1-06*01F	IGKJ1*01F		[23.17.36.10]	[6.3.9]
Heavy	H01-51	IGHV3-23*04F	IGHJ6*02F	IGHD2-15*01 F	[25.17.38.11]	[8.8.21]
Light	K-02-51	IGKV3-11*01F	IGKJ3*01F		[26.17.36.10]	[6.3.9]
Heavy	H02-54	IGHV1-3*01F	IGHJ5*02F	IGHD6-13*01 F	[25.17.38.11]	[8.8.17]
Light	K02-54	IGKV1-39*01F	IGKJ3*01F		[23.17.36.10]	[6.3.9]

Chain type	Insert name	V-gene and allele	J- gene and allele	D- gene and allele	FR lengths	CDR- lengths
Heavy	H01-63	IGHV3-15*01F	IGHJ4*02F	IGHD1-26*01 F	[25.17.38.11]	[8.10.10]
Light	K02-63	IGKV1-09*01F	IGKJ2*01F		[23.17.36.10]	[6.3.9]
Heavy	H02-64	IGHV4-39*01F	IGHJ6*02F	IGHD5-18*01 F	[25.17.38.11]	[10.7.21]
Light	K02-64	IGKV3-11*01F	IGKJ5*01F		[22.17.36.10]	[6.3.10]
Heavy	H01-68	IGHV3-30*04F or IGHV3-30-3*03F	IGHJ5*02F	IGHD4-11*01	[25.17.38.11]	[8.8.12]
Light	L02-68	IGLV2-14*01F	IGLJ3*02F		[25.17.36.10]	[9.3.10]
Heavy	H02-77	IGHV3-30*04F or IGHV3-30-3*03F	IGHJ6*02F	IGHD4-11*01	[25.17.38.11]	[8.8.18]
Light	K02-77	IGKV1-39*01F or IGKV1D-39*01F	IGKJ1*01F		[26.17.36.10]	[6.3.9]
Heavy	H01-81	IGHV3-30*04F or IGHV3-30-3*03F	IGHJ6*02F	IGHD2-21*01 F	[25.17.38.11]	[8.8.14]
Light	K02-81	IGKV1-09*01F	IGKJ4*01F		[22.17.36.10]	[6.3.9]
Heavy	H02-83	IGHV4-59*08F	IGHJ5*01F	IGHD1-7*01 F	[25.17.38.11]	[8.7.12]
Light	K02-83	IGKV1-9*01F	IGKJ4*01F		[26.17.36.10]	[6.3.9]
Heavy	H01-87	IGHV4-39*01F	IGHJ4*02F	IGHD3-22*01 F	[25.17.38.11]	[10.7.15]
Light	K02-87	IGKV3-20*01F	IGKJ4*01F		[23.17.36.10]	[7.3.9]
Heavy	H01-89	IGHV1-46*01F or IGHV1-46*03F	IGHJ5*02F	IGHD2-2*01 F	[25.17.38.11]	[8.8.24]
Light	L02-89	IGLV1-51*01F	IGLJ2*01F or IGLJ3*01F		[25.17.36.10]	[8.3.12]
Heavy	H01-94	IGHV1-18*04F	IGHJ3*02F	IGHD1-1*01 F	[25.17.38.11]	[8.8.10]
Light	L02-94	IGLV2-14*01F	IGLJ3*02F		[25.17.36.10]	[9.3.10]

Table 5.6-2 Antibody gene family, framework region and complementarity determining lengths for all anti-gp41 antibodies (continued)

The tables contain information describing the antibodies retrieved. This includes the variable (V), joining (J) and diversity (D) gene and allele for each heavy chain, the V and J gene and allele for each light chain, the length in amino acids of each of the four framework regions for each variable chain regions (FR length; 1, 2, 3, 4), the length in amino acids of each of the three complementarity determining region amino acids for each chain (CDR length; 1, 2, 3).

5.6.6. Transfection of HEK293 cells

HEK293 were prepared cells for culture and passaged them as described previously. Transfections were performed in duplicate to increase possible yields. The 6-well culture plates were prepared for the 21 antibody pairs, and cell wells assessed to ensure adherence on the day on transfection. The correct amounts of heavy and light chain vectors and inserts were calculated and added to PEI and D10 media, this mixture added to the corresponding well and media changed to serum free. After five days of culture in an incubator, supernatant was harvested and transferred to a labelled cryovial.

5.6.7. ELISA screening of supernatants

An enzyme-linked immunosorbent assay (ELISA) was used to screen supernatants from transfections 1 and 2 for antibodies. The plate setup is shown in Table 5.6-3 with controls occupying columns 1 and 2 and row H. The ELISA assay screened supernatant for presence of IgG and used a colour change to measure antibody concentration. A 96-well plate was coated with a target-specific capture antibody, (anti-human CD93 monoclonal antibody) which bound human IgG. The supernatant was added to 96-well plate and any IgG present bound to the capture antibody. The detection antibody, protein-specific biotinylated anti-human antibody (horseradish peroxidase) was added to detect presence of primary antibody; A substrate solution was added and underwent enzymatic colour change. The level of colour change was quantified by measuring the optical density of the solution, results compared to a standard curve, and the corresponding antibody concentration calculated

	1	2	3	4	5	6	7	8	9	10	11	12
A	NS	NS	10	14	16	17	22	27	33	38	46	48
B	1:2	1:2	10	14	16	17	22	27	33	38	46	48
C	1:4	1:4	10	14	16	17	22	27	33	38	46	48
D	1:8	1:8	51	54	63	64	68	77	81	83	87	89
E	1:16	1:16	51	54	63	64	68	77	81	83	87	89
F	1:32	1:32	51	54	63	64	68	77	81	83	87	89
G	1:64	1:64	94	94	94							
H	0	0	D	D	D							

Table 5.6-3 ELISA plate setup

NS = neat standard, D = serum free media. Numbers indicate antibodies

The ELISA readouts for transfection 1 and 2 are shown in Table 5.6-4 and Table 5.6-5. Transfection 1 yielded four well groups with an OD greater than controls- 27, 51, 77, 83, and transfection 2 yielded eight well groups with OD's greater than controls- 17, 22, 27, 46, 63, 77, 83, 87. Two transfections were performed to increase the yield of antibodies.

	1	2	3	4	5	6	7	8	9	10	11	12
A	0.51	0.572	0.058	0.056	0.057	0.062	0.081	0.119	0.054	0.068	0.066	0.056
B	0.413	0.392	0.056	0.055	0.053	0.061	0.083	0.178	0.053	0.055	0.067	0.055
C	0.265	0.253	0.055	0.057	0.055	0.072	0.083	0.128	0.054	0.055	0.068	0.055
D	0.173	0.165	1.212	0.061	0.055	0.057	0.055	0.475	0.054	0.76	0.058	0.058
E	0.112	0.103	1.172	0.056	0.078	0.054	0.05	0.442	0.053	0.811	0.054	0.057
F	0.075	0.079	1.152	0.057	0.055	0.054	0.054	0.489	0.054	0.722	0.056	0.061
G	0.07	0.069	0.056	0.054	0.055	0.054	0.054	0.055	0.055	0.054	0.054	0.055
H	0.053	0.061	0.054	0.054	0.054	0.056	0.052	0.053	0.058	0.056	0.056	0.06

Table 5.6-4 ELISA plate readout for transfection 1
Highlighted wells are those with OD greater than standards and correspond to monoclonal antibodies 27, 51, 77, 83

	1	2	3	4	5	6	7	8	9	10	11	12
A	0.808	0.817	0.052	0.052	0.051	0.064	0.080	0.077	0.054	0.055	0.089	0.057
B	0.450	0.391	0.053	0.055	0.057	0.064	0.103	0.088	0.056	0.054	0.089	0.059
C	0.278	0.239	0.053	0.052	0.054	0.066	0.096	0.081	0.055	0.054	0.057	0.055
D	0.169	0.159	0.051	0.055	0.266	0.057	0.055	0.224	0.054	0.563	0.069	0.059
E	0.113	0.102	0.050	0.050	0.268	0.056	0.053	0.225	0.056	0.536	0.066	0.058
F	0.087	0.075	0.052	0.051	0.270	0.056	0.054	0.236	0.056	0.534	0.068	0.059
G	0.067	0.064	0.056	0.054	0.051	0.057	0.056	0.058	0.055	0.056	0.059	0.057
H	0.063	0.060	0.052	0.053	0.053	0.054	0.055	0.055	0.055	0.054	0.060	0.059

Table 5.6-5 ELISA plate readout for transfection 2
Highlighted wells are those with OD greater than standards and correspond to monoclonal antibodies 17, 22, 27, 46, 63, 77, 83, 87

The optical density of the standards (columns 1 and 2) was used to create a mean optical density for each concentration which allowed the construction of a standard curve of concentration against optical density. As the three most dilute standards fell below a mean OD of 0.01, they were omitted from the standard curve. This is shown in Table 5.6-6 and Figure 5.6-3.

	Standard 1 OD	Standard 2 OD	Concentration of standard solution (ng/ml)	Mean OD
A	0.510	0.572	0.5	0.541
B	0.413	0.392	0.25	0.403
C	0.265	0.253	0.125	0.259
D	0.173	0.165	0.063	0.169
E	0.112	0.103	0.031	0.108
F	0.075	0.079	0.016	0.077
G	0.07	0.069	0.008	0.07
H	0.053	0.061	0	0.057

Table 5.6-6 Standards for ELISA and mean optical density
Standard 1 and 2 optical density and concentration of each standard solution in ng/ul

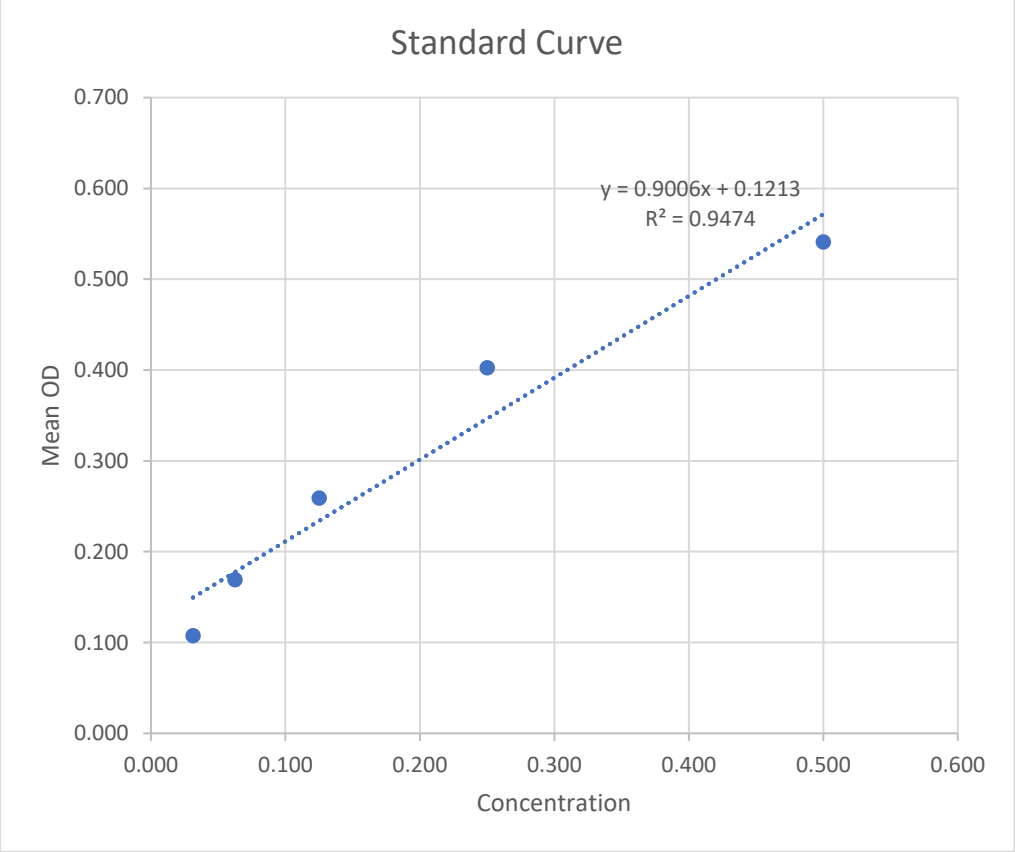


Figure 5.6-3 Standard curve to determine IgG concentration
X axis displays concentration of known standards (ng/ml) against optical density. Equation of the line shown as R2

This allowed calculation of monoclonal antibody concentrations. The mean and standard deviation for the optical density readings was calculated and the equation of the line used to solve x (MAb concentration) from y (optical density). The transfection 1 equation of the line was y = 0.9006x + 0.1213; R^2 = 0.9474, and transfection 2 equation of the line was y = 1.4969x + 0.0606; R^2 = 0.999. These results are shown in Table 5.6-7 and Figure 5.6-4.

	Monoclonal antibody	OD value (Y) using the average of 3 readings	Standard deviation of the OD readings	X (concentration) value calculated from Y (ng/ml)
Transfection 1	27	0.142	0.032	0.023
	51	1.179	0.031	1.174
	77	0.469	0.251	0.386
	83	0.764	0.385	0.714
Transfection 2	17	0.065	0.001	0.003
	22	0.093	0.012	0.022
	27	0.082	0.006	0.014
	46	0.078	0.018	0.012
	63	0.268	0.002	0.139
	77	0.228	0.104	0.112
	83	0.544	0.277	0.323
	87	0.068	0.005	0.005

Table 5.6-7 ELISA concentration calculations
Monoclonal antibody concentration (ng/ml) from OD450 of transfection solution

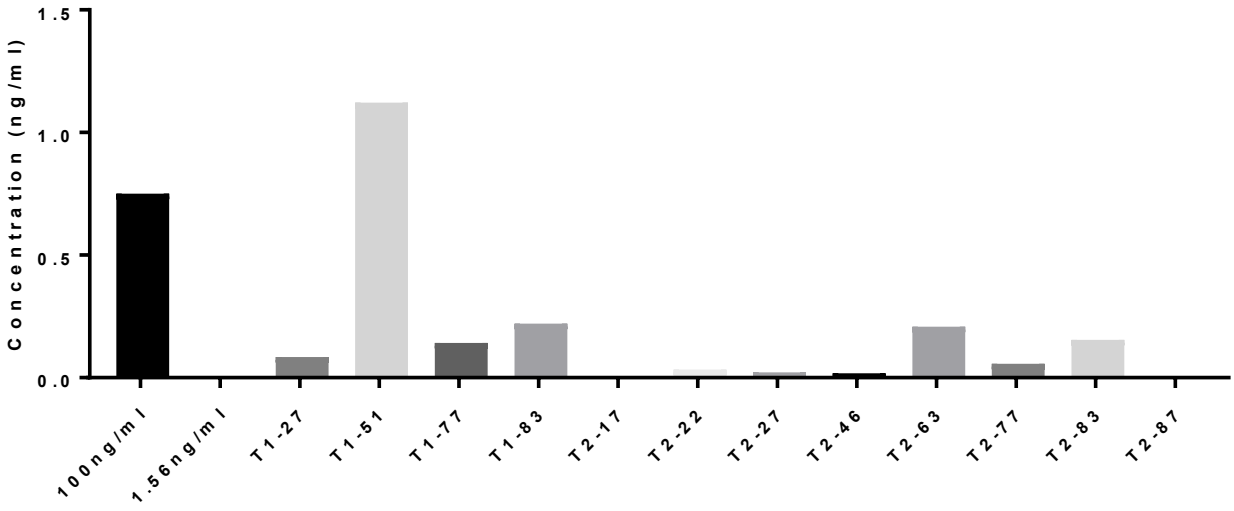


Figure 5.6-4 Monoclonal antibody concentrations
X axis shows neat standard at 100ng/ml and 1:64 diluted standard at 1.56ng/ml, and all experimental monoclonal antibody results. Y axis is concentration in ng/ml

The ELISA results confirmed presence of antibody and estimate the concentration. The yield of antibodies transfections 1 and 2 were as follows: Transfection 1: 27, 51, 77, 83 (named T1-XX), and Transfection 2: 17, 22, 27, 46, 63, 77, 83, 87 (named T2-XX). The following antibodies were selected for anti-HIV envelope affinity studies: T1-27, T1-51, T1-77, T1-83 (transfection 1) and T2-17, T2-22, T2-46, T2-63, T2-87 (transfection 2).

5.6.8. Sodium dodecyl sulphate (SDS) polyacrylamide gel electrophoresis

An SDS-PAGE was used gel to analyse the molecular weights of the antibodies. The four monoclonal antibodies from transfection 1 (27, 51, 77 and 83) and a protein standard ladder (10 – 250 kiloDaltons) were loaded onto the gel and ran this for 40 minutes at 200V, the gel retrieved and stained, and viewed using the Gel-Doc XR light box. On inspection, the antibodies had separated into heavy and light chains. A protein ladder was used as standard to estimate chain insert molecular weights. Heavy chain inserts had a molecular weight of 50-75 kiloDaltons, and light chains 10 kiloDaltons. Figure 5.6-5 shows the gel on the right with a reference ladder to the left.

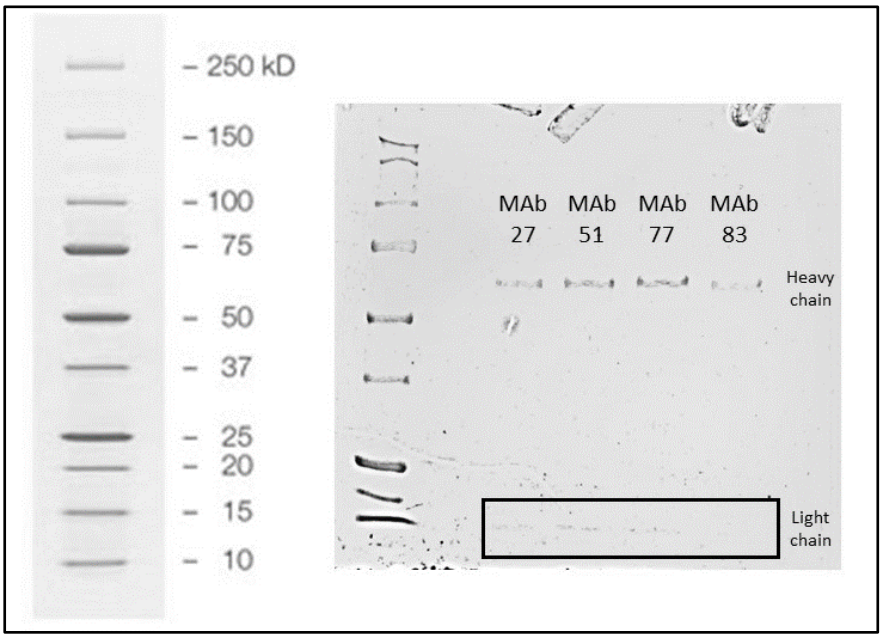


Figure 5.6-5 SDS-PAGE gel of transfection 1
Gel shows antibodies 27, 51, 77 and 83 from transfection 1. Left panel- kilodalton reference ladder

5.6.9. Monoclonal antibody anti-HIV specificity screening

FACS was used to assess each monoclonal antibody affinity for HIV envelope proteins. A 96-well plate was used to perform primary labelling of the HIV gp140 coated CEM.NKr cells and then added a secondary anti-human IgG- FITC conjugated antibody. Following incubations and washes, cell aliquots were placed in individual FACS tubes and these FACS analysis. This produces CEM.NKr covered in HIV gp140 epitopes which can bind experimental monoclonal antibody, which then bind anti-human FITC conjugated IgG as the secondary antibody. Figure 5.6-6 shows the controls and gating strategy used for anti-HIV specificity screening, and Figure 5.6-7 shows the control and experimental FACS plots for the antibodies screened.

A total of nine antibodies were analysed for anti-HIV specificity - T2-17, T2-22, T1-27, T2-46, T1-51, T2-63, T1-77, T1-83, T2-87-. Each was tested in triplicate to reduce variation due to operator error and calculated the average of the three results, displayed below in Table 5.6-8 and Figure 5.6-8. Multiple t-tests were performed with IgG negative control as the baseline comparator to describe the data shown in Table 5.6-9.

Ideally, mAb binding to the yeast clone of interest would have been reviewed, however several months had passed between yeast sorting and mAb production, and the original yeast clones were contaminated. Another strategy would have been to review mAb binding to an ELISA coated using known specific epitopes/peptides or gp140 structures.

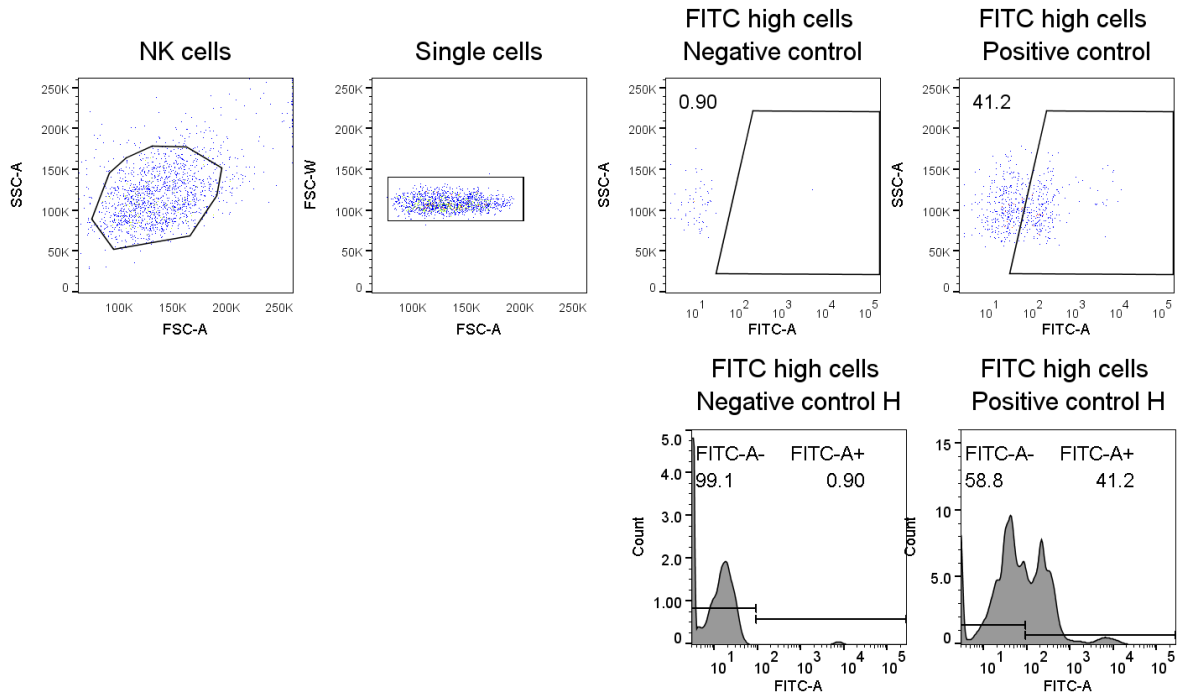


Figure 5.6-6 Transfection controls

Experimental controls for transfection. The FITC high population is displayed as plot and histogram to assess the mean fluorescence intensity (MFI) and distribution of the cell data. As the positive population is normally distributed, the MFI is used for the analysis.

Row 1: Plots. 1 x axis forward scatter area, y axis side scatter area; natural killer cells (NK). 2: forward scatter area y axis forward scatter width: single NK cells.3 and 4: x axis FITC-A and y axis side scatter area for negative biological IgG control and seropositive HIVIG control

Row 2: Histograms; x axis FITC-A and y axis side scatter area for negative biological IgG control and seropositive HIVIG control

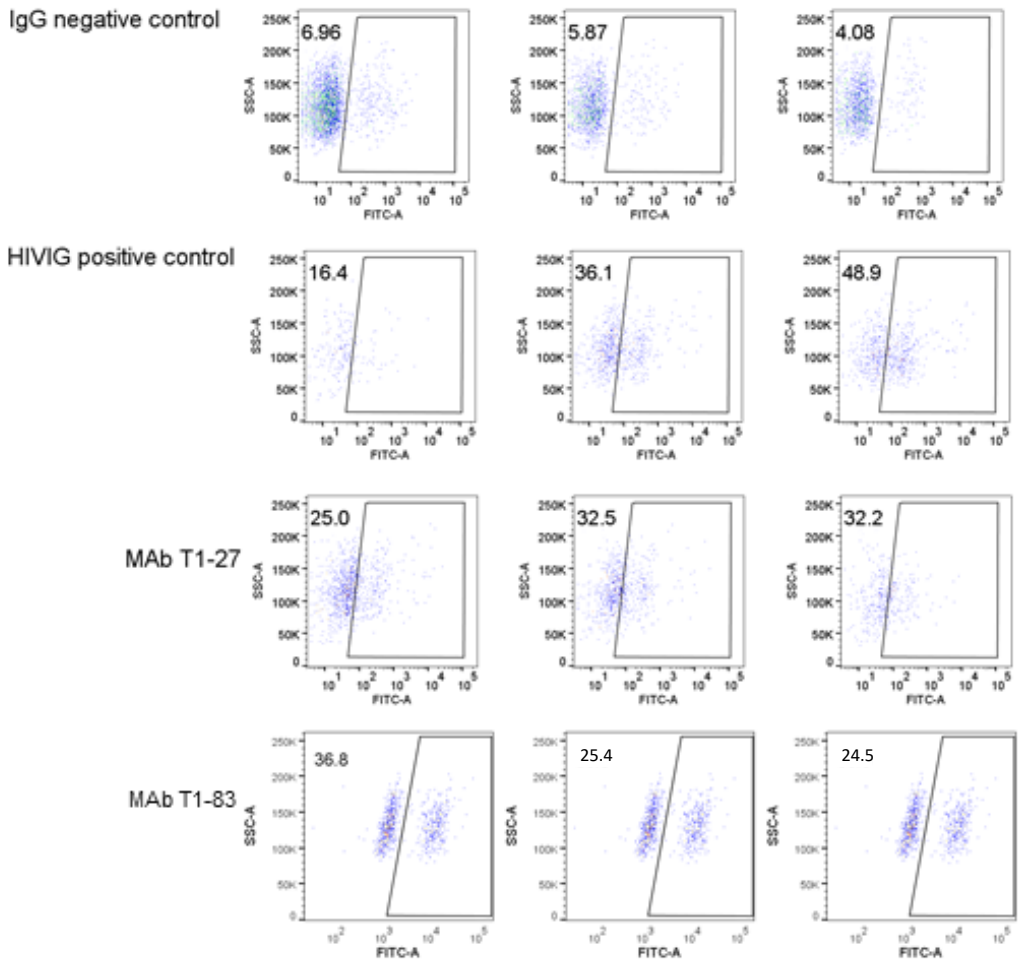


Figure 5.6-7 Monoclonal antibody anti-HIV specificity screening FACS plots
X axis FITC-A, y axis side scatter area. Two controls- IgG negative and HIVIG positive controls shown first. Plots show indirect binding of control and monoclonal HIV antibodies to gp140 coated CEM NKr cells

Positive monoclonal antibodies, T1-27 and T1-83

Monoclonal antibody	Mean fluorescence intensity	Average mean fluorescence intensity
Autofluorescence	0	0
Fluorescence minus one	0	
Unstained	0	
IgG control 1	5.03	4.8
IgG control 2	4.98	
IgG control 3	4.26	
HIVIG positive control 1	16.40	33.8
HIVIG positive control 2	36.10	
HIVIG positive control 3	48.90	
T2_17_01	9.38	12.6
T2_17_02	19.10	
T2_17_03	9.26	
T2_22_01	10.20	7.7
T2_22_02	8.66	
T2_22_03	4.15	
T1_27-01	25.00	29.9
T1_27-02	32.50	
T1_27-03	32.20	
T2_46_01	1.75	0.9
T2_46_02	0.93	
T2_46_03	0.00	
T1_51-01	11.00	7.5
T1_51-02	7.75	
T1_51-03	3.85	
T2_63_01	4.65	4.7
T2_63_02	5.04	
T2_63_03	4.33	
T1_77-01	7.55	9.9
T1_77-02	10.60	
T1_77-03	11.40	
T1_83-01	36.00	28.6
T1_83-02	25.40	
T1_83-03	24.50	
T2_87_01	1.71	1.5
T2_87_02	1.27	
T2_87_03	1.55	

Table 5.6-8 Analysis of mean fluorescence intensity of control and HIV monoclonal antibodies to gp140 coated CEM.NKr cells

Results of monoclonal antibodies assayed using FACS and gp140 coated CEM.NKr cells. Cut off for positive binding taken as any value greater then negative control IgG MFI of 4.8

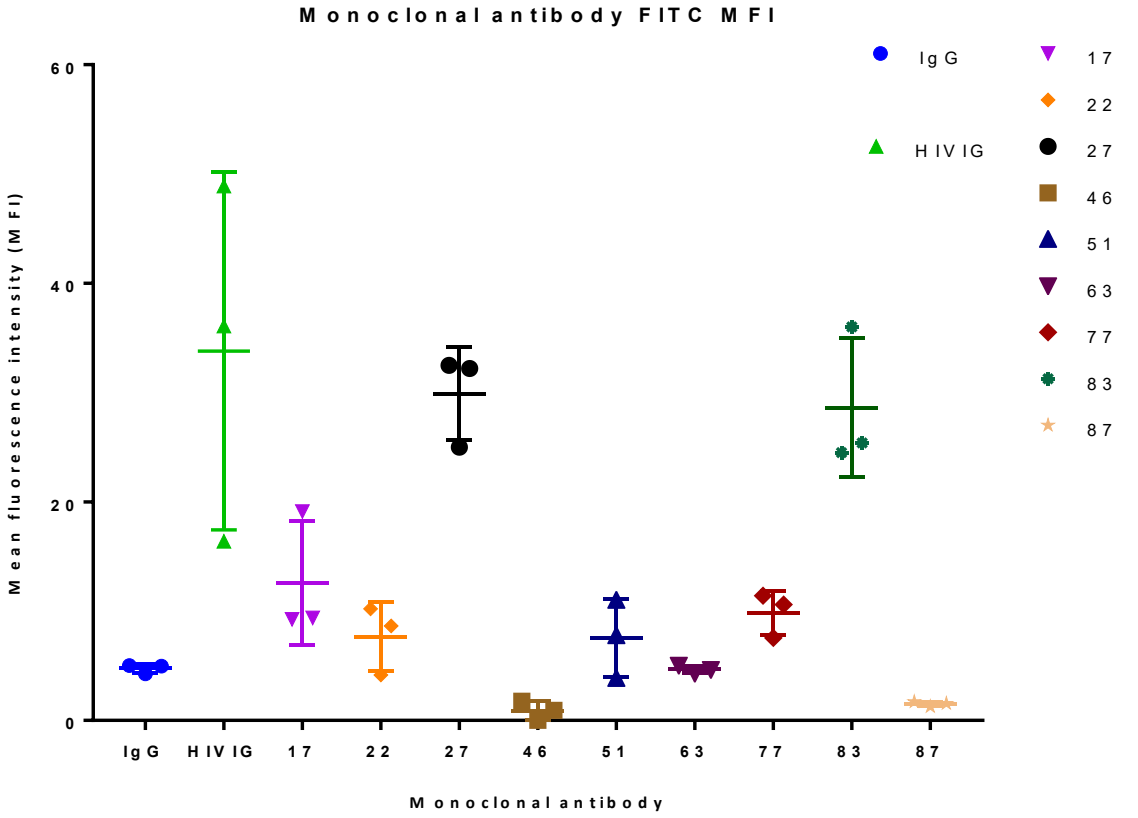


Figure 5.6-8 Mean and standard deviation of mean fluorescence intensity of control and HIV monoclonal antibodies to gp140 coated CEM.NKr cells
X axis controls (negative healthy IgG and positive control HIVIG), and experimental antibodies). All experimental antibodies colour coded by key at right panel.

Comparison	P value	P value summary	Significantly different (P < 0.05)?	95% confidence interval
HIVIG	0.0951	ns	No	-12.52 to 70.61
T2-17	0.1313	ns	No	-5.747 to 21.39
T2-22	0.205	ns	No	-3.849 to 9.676
T1-27	**0.0104**	*	**Yes**	14 to 36.29
T2-46	**0.0059**	**	**Yes**	-5.145 to -2.582
T1-51	0.2707	ns	No	-5.148 to 10.7
T2-63	0.6309	ns	No	-0.7217 to 0.555
T1-77	0.0644	ns	No	-0.7558 to 10.94
T1-83	**0.0214**	*	**Yes**	8.615 to 39.14
T2-87	**0.0079**	**	**Yes**	-4.499 to -1.995

Table 5.6-9 Paired t-tests for comparison of control and experimental monoclonal antibodies
Analysis of multiple comparisons for each monoclonal antibody MFI against negative control IgG. Multiple t-tests used to compare all monoclonal antibodies against IgG

On review, some conclusions can be drawn regarding the controls and the experimental antibodies.

The negative control IgG had an MFI of 4.8, and this value was used as the cut-off value to determine all experimental sample positivity. The positive control HIVIG MFI was 33.8 (CI -12.52 to 70.61), which was significantly greater than that of IgG (p = 0.0033). HIVIG is a polyclonal preparation of antibodies and hence the MFI for this control was greater. In conclusion, HIVIG was a good positive control for this experiment.

Four of the monoclonal antibodies had an MFI which differed significantly from the negative control. Two of these antibodies (T2-46 and T2-87) had minimal MFI with both significantly less than IgG. T1-27 and T1-83 had MFI greater than IgG and closer to that of the positive control HIVIG. T1-27 average MFI was 29.9 (95% confidence interval 14 to 36.29, p = 0.0104) and T1-83 average MFI was 28.6 (95% confidence interval 8.615 to 39.14, p = 0.0214).

5.7. Review of HIV specific monoclonal antibody properties

Antibody properties to account for variations in epitope binding were selected to review the two antibodies with the greatest HIV gp140 affinity.

5.7.1. Gene family usage

Gene family usage was reviewed, and with only two antibodies of interest, statistical analysis and conclusions was not attempted. High affinity antibodies used differing heavy chain V, J, and D genes. For light chains, both antibodies used VH1. These findings are shown in Table 5.7-1.

Chain type	Insert name	Variable gene and allele	Joining gene and allele	Diversity gene and allele
Heavy	H27	IGHV1-18*01 F	IGHJ6*02 F	IGHD5-18*01 F
Heavy	H83	IGHV4-59*08 F	IGHJ5*01 F or IGHJ5*02 F	IGHD1-7*01 F
Light	K27	IGKV 1-39*01 F	IGKJ 2*02 F	
Light	K83	IGKV1-9*01 F	IGKJ4*01 F	

Table 5.7-1 MAb gene family usage
Experimental monoclonal antibodies T1-27 and 83 V, D, J gene family usage.

5.7.2. Variable region analysis

As described in the introduction, variable regions give antibodies unique characteristics. Each heavy and light chain contains a variable region, which is composed of two key structures- the framework region (FR) and the complementarity determining region (CDR). FR remain conserved across antibody groups, but CDR are hypervariable with individual characteristics. CDR3 is the most variable structure.

5.7.2.1. Framework region (FR) analysis

The amino acid length of the framework regions of the two high affinity monoclonal antibodies was reviewed. There was no difference between the framework region lengths for heavy chain inserts; all possessed framework regions of similar amino acid length. For the light chain inserts, minimal variability was present in the 1st framework region (FR1). T1-27 and T1-83 kappa light chains had an FR1 of 23 and 26 AA respectively. These findings are in keeping with known properties of framework regions, which tend to be conserved, in contrast to the complementarity determining regions. Table 5.7-2 and Figure 5.7-1 show the properties of each monoclonal antibody framework region.

	FR1	FR2	FR3	FR4
H27	25	17	38	11
H83	25	17	38	11
K27	23	17	36	10
K83	26	17	36	10

Table 5.7-2 MAb heavy and light chain framework regions
Lengths in amino acid residues

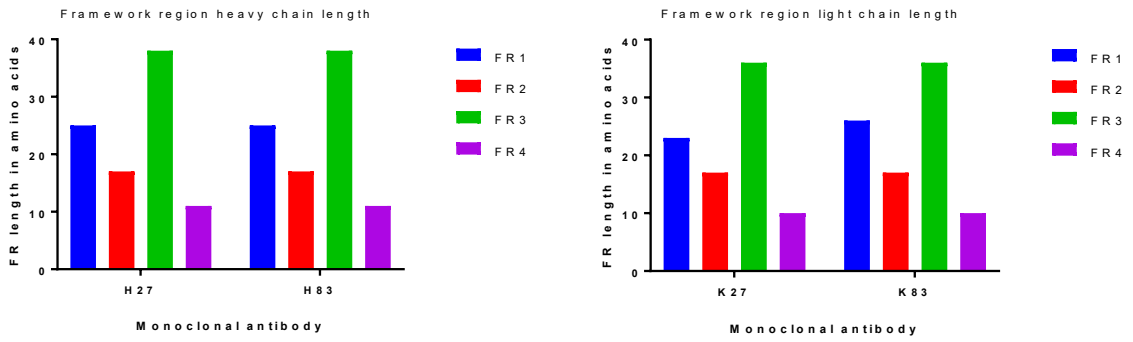


Figure 5.7-1 Amino acid length of pre infection HIV heavy and light chain framework regions
Lengths in amino acid residues

5.7.2.2. Complementarity determining region (CDR) analysis

Antibody CDR are unique structures of varying lengths, which may explain the high affinity for HIV gp140 displayed by T1-27 and T1-83. Heavy chain CDR 1 and 2 lengths did not vary greatly across the monoclonal antibodies. Median CDR1 length was 8.75 AA (range 8-10, SD 1.07), median length CDR2 7.25 AA (range 7-8, SD 0.5). The CDR3 length for heavy chains were reviewed. T1-27 and T1-83 had long heavy chain CDR3 (18 and 12 respectively). For light chains, both kappa chain CDR3 lengths were 9 amino acids long. These data are shown in Table 5.7-3 and Figure 5.7-2.

Chain type	Insert name	CDR-IMGT lengths		
		CDR1	CDR2	CDR3
Heavy	H01-27	8	8	18
Heavy	H02-83	8	7	12
Light	K02-27	6	3	9
Light	K02-83	6	3	9

Table 5.7-3 MAb heavy and light chain complementarity determining regions
Length in amino acid residues

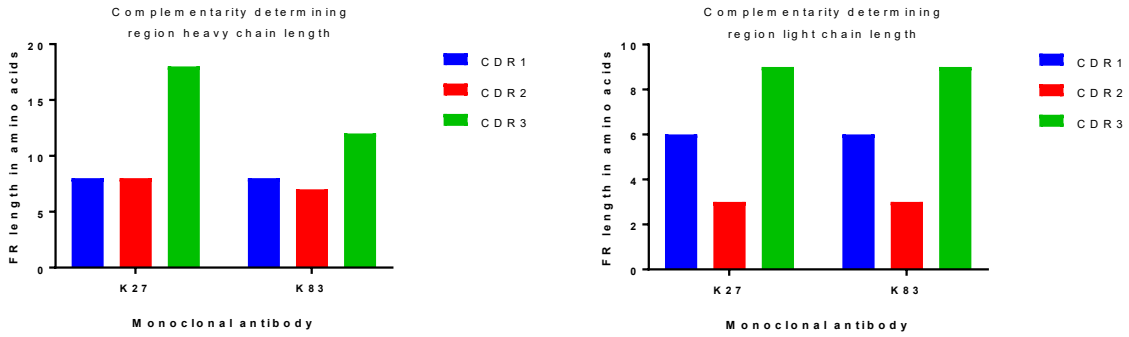


Figure 5.7-2 Amino acid of pre-infection HIV monoclonal MAb heavy and light chain complementarity determining regions
Length in amino acid residues

5.9. Functional assay using rapid fluorometric ADCC assay

One antibody, T1-27 was selected for assessment by RFADCC. The negative (1) and positive controls (2) used were IgG, A32 and HIVIG respectively. Percentage ADCC was defined as the proportion of CEM.NKr cells which had lost intracellular CFSE expression but retained membranous PKH-26 expression. Plots are representative of experimental conditions where each antibody was assessed in triplicate. There was no discernible ADCC activity mediated by T1-27, as the percentage population in Q1 was similar to that of the negative control. This is shown in Figure 5.9-1 and Figure 5.9-2.

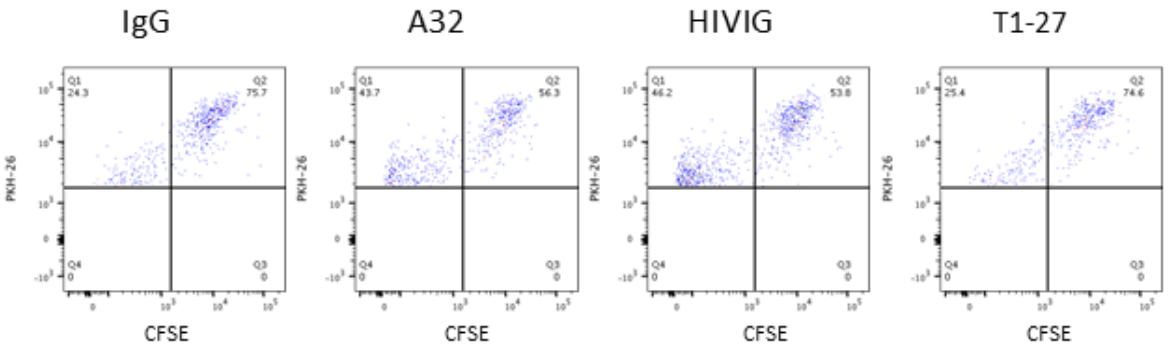


Figure 5.9-1 RFDACC results- plots
X axis aliquots, y axis ADCC as percentage of total cell population. Three plots showing IgG negative control, A32 and HIVIG positive controls and experimental monoclonal antibody T1-27 RFADCC assays. Q1 is quadrant of interest indicating lysed cells. X axis CFSE, y axis PKH-26.

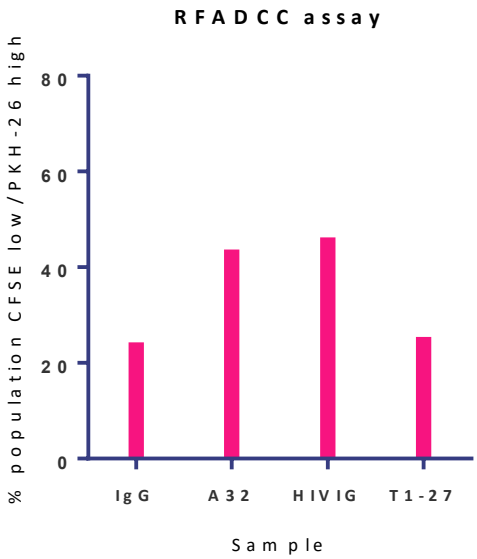


Figure 5.9-2 RFDACC results- graph
X axis aliquot, y axis percentage ADCC expressed as CFSE low PKH-26 high population in Q1 of plots.

5.10. Summary

This chapter describes my attempts to generate monoclonal antibodies by harvesting B cells baited by yeast-surface bound HIV envelope fragments. This method has not previously been described in the literature.

5.10.1.B cell antigen baiting and monoclonal antibody production

Optimisation of this process resulted in greater yields of antibodies per plate sorted throughout successive rounds of experiments. This was most likely due to better experimental technique and familiarity with the procedures.

One consideration of the overall yield from this process is the fragility of B cells and RNA during processing. The frequency of recovery of antibody secreting cells from cryopreserved samples can be equivocal to that of fresh samples, but retention of flow cytometry cell surface markers may be reduced (361). In addition, dead cells can pick up dyes and contribute to increased non-specific background (362). Future work could include the use of a live/dead stain to differentiate viable cells.

The recovery of RNA from frozen tissue may also influence the yield of monoclonal antibody. Two options for RNA recovery are to either thaw tissue on ice (which I did) or use ground homogenised frozen tissue. Reports from other sites suggest there is more degradation and less retrievable RNA in thawed tissue (21% intact in thawed vs. 95% intact in frozen) (363–365).

The Smith paper on which this work is based anticipates expected antibody yields of 20 antibodies per half plate (42 wells) of sorted B cells. Reasons for the fall in yield include flow and PCR limitations. The authors draw attention to the instability of the B cell's genetic material once captured within the sorting plate well. This was mitigated by preparation of catch buffer in 96-well plates which were centrifuged and frozen until the point of use. The flow cytometer plate mounting platform was also called to maintain stability of sorted products. Once sorting was complete, plates were immediately centrifuged and frozen. One difference in my work was the use of full 96-well plates as opposed to

half filling the plates. This extended time taken to fill plates may have contributed to degradation of product.

The Smith paper also describes the occasion of empty wells not filled by the sorter. This may be due to a machine calibration to leave wells empty rather than fill with a doublet. Certainly, in my results, there were double sorting episodes clearly indicated by the [presence of lambda and kappa light chains in one well. From this, it is also possible that some wells contained double sorted lambda and kappa chains which affected downstream processing. Another reported limitation is during PCR processing, where non amplification of the V gene segments may originate from V genes not covered by the set of primers. In addition, use of a primer pool for kappa sequencing may have saved time.

The authors conclude that from their initial 42 well sorted plate, an expected yield would be 10-16 valid transfectable heavy and light chain inserts. This represents a sorted well to antibody chain pair yield of 23.8-38.1%. In my work, initial antibody yields from a fully sorted 96-well plate was 4.2-14.6% potential transfectable antibody chain pairs. This subsequently improved to 37.5-61.5%. A reason for the variation in my antibody yields may have been trying to manage multiple rounds of experiments at different time points. Following optimisation with seropositive PBMC and related yeast clones, PBMCs from multiple infection timepoints were sorted. As work proceeded, the scale of the project to manufacture antibodies from all infection timepoints would require a significant amount of time became apparent. At this stage, focus turned to identifying pre infection anti-gp41 specific B cells as this was the population of interest identified at the beginning of the project.

The PreB3-04 clone covers the gp41 sequence 643-676 which spans the MPER site of vulnerability discussed in the previous chapter. This region is well conserved across HIV viral clades and was considered a reasonable epitope to have used for B cell baiting.

5.10.2.Monoclonal antibody anti-HIV specificity

The assay used to review monoclonal antibody affinity for HIV envelope protein used gp140 coated CEM.NKr cells as a target. As seen in the results section, two of nine antibodies demonstrated gp140 affinity significantly greater than the controls. Ideally with more time the transfection process would be repeated and the experiments performed with larger volumes of cell culture to improve the antibody yield. These large volume experiments are ongoing in our laboratory at present using the source material generated here.

The two antibodies T1-27 and T1-83 demonstrated HIV specificity and proves the hypothesis that anti-HIV antibodies are present in HIV-exposed seronegative individuals and that these antibodies are specific to gp41 envelope proteins.

In retrospect, regarding the positive control, use of a known monoclonal antibody rather than HIVIG might have been a more appropriate, as one of the three positive control samples failed to show significant binding to the cell-displayed gp140.

5.10.3.Monoclonal antibody properties

Various antibody properties to elucidate reasons for the anti-HIV activity of T1-27 and T1-83 were explored. These observations were not assessed by statistical methods as the number of antibodies produced was too small. The gene families used by the V/D/J genes of the heavy chain and V/J genes of the light chain inserts were varied with no pattern emerging. Framework region lengths were of similar in the high affinity antibodies. Complementarity determining regions 1 and 2 were of similar length in heavy and light chains and in keeping with expected dimensions. HCDR1 was 10-16 AA (normal 8-10), and HCDR2 was 7-8 (normal 8-15), light chains included LCDR1 with 6-9 AA (normal 10-17) and LCDR2 with 3 (normal 3-8) (366). The 3rd complementarity determining regions of the antibody light chains were 6 amino acids long which is similar to lengths of anti-HIV antibodies published previously (260).

As previously outlined, the heavy chain CDR3 (CDRH3) is responsible for inter-antibody antigen binding site specificities. Human HCDR3 length is usually 12 amino acids long with can range from 4 to 35 residues (367). The HCDR3 lengths found in the monoclonal antibodies generated in this study range from 12 to 19 amino acid residues, and these longer CDR3 regions were found in high affinity antibodies.

Previously it has been shown that antibody affinity for HIV is associated with long heavy chain CDR3 regions in three monoclonal antibodies with proven anti-HIV activity. The CD4 binding site targeting monoclonal antibody b12, and the anti-gp41 membrane proximal external region monoclonal antibodies 2F5 and 4E10 were shown to have heavy chain CDR3 regions of approximately 15 residues. Three of the four antibodies isolated have CDR3 regions of 15 residues or greater, but this was not associated with increased affinity for the target epitope.

Long HCDR3 are seen in many HIV-specific bnAbs and provide a structural advantage in accessing glycan-obstructed or recessed epitopes (178). Initially these were thought to arise from extensive rounds of somatic hypermutation (151). There is evidence to suggest they arise at original recombination events, and are selected from the naïve reservoir as opposed to arising from de novo insertions during somatic hypermutations, as suggested by the presence of long HCDR3 in healthy unexposed controls (368).

I was unable to account for the variations in HIV gp140 affinity due to antibody structural properties. This project is being continued in our laboratory at present, with large scale quantities of these monoclonal antibodies being produced. This may reveal more information about binding qualities and may result in improved affinity for target epitopes.

5.10.4.Functional assay using Rapid Fluorometric ADCC

Only one of the two high gp140 affinity antibodies, T1-27, was submitted for functional analysis. There was no evidence of ADCC mediated by this antibody. Reasons may have included minimal quantities of available monoclonal antibody, or poor quality product. While this is disappointing, it would be

worth considering other functional assays such as neutralisation to assess this antibody's characteristics. Again, this step was limited by time constraints, but future work could focus on assaying these two antibodies across a wider spectrum of functionality.

5.10.5.Assessment of mAb binding specificity

Another strategy to assess the mAb produced would be to assess binding to a variety of constructs to demonstrate these mAb were specific for the epitopes described in chapter four. Assays could have included mAb binding to HIV-infected cells, or mAb binding to ELISA coated with either peptides of the sequences identified in chapter four or known commercially available Env structures.

5.11. Summary

The aims of this chapter were to develop a technique merging yeast surface display technology with fluorescence activated cell sorting to sort B cells of interest. From this, monoclonal antibodies were generated using B cell expression cloning, and their affinity for HIV envelope protein demonstrated, proving specificity.

Structure and function of the two HIV-specific monoclonal antibodies were assessed to elucidate reasons for variations in binding affinity and function, but results were unable to account for the differences, and no functional activities were demonstrated.

Chapter 6
Discussion and Conclusion

5.12. Discussion

The intention of this project was to review host immune response to the HIV surface envelope protein (Env), and to describe the response at various time points- seronegative people exposed to but not infected by HIV, and seropositive people at early and later stages of HIV infection. Once these antibodies were identified, a B cell sorting technique was developed to produce monoclonal antibodies, which, in future, could allow precise epitope mapping. The hypothesis suggested the presence of anti-Env immune responses in seronegative individuals either from previous exposure to Env protein in the absence of established infection, or from pre-education of the immune system by gut microbiota. These pre-existing responses could influence development of anti-Env responses during a future HIV seroconversion event.

The project was conceived during a period of increasing HIV diagnoses among men who have sex with men (MSM). As most of these diagnoses were made at a clinic within our NHS foundation trust, this was an opportunity to capture HIV seroconversion events based on identifying individuals likely seroconvert. All individuals considered high risk for HIV acquisition were invited to participate in risk reduction strategies developed by the clinic which included increased frequency of HIV testing, access to counselling sessions, provision of barrier protection and advice on substance use. Moreover, any individuals recruited to this study who were not yet formally identified as high risk patients were directed towards these resources. At no point were high risk individuals denied access to services in the interest of the study.

Approximately 300 participants were recruited to this study during a period of 45 weeks. From 238 seronegative group A recruits (seronegative MSM attending for routine sexual health screening), nine individuals transferred to group B once they were identified as having seroconverted (newly diagnosed HIV infection confirmed with HIV RNA sampling), and six of the nine agreed to participation and serial phlebotomy as per the study schedule. Monthly blood draws were not always possible for logistical reasons. Where feasible, efforts were made to coordinate study visits with routine clinical

care appointment. Where extra visits were required to comply with the proposed phlebotomy study schedule, time constraints meant not all individuals were available to attend as planned.

All B group study participants were in employment, and further absence from work to attend study visits was not heavily pursued. However, most group B participants were eager to support this research and often voluntarily attended for extra visits before and after normal working hours. It is to their credit that this study was able to gather such a valuable resource of information and tissue samples. In total, for the five group B seroconverter participants who were analysed in further detail, of a total of 35 scheduled study visits, 28 were completed (median number of study visits completed 6, range 3-7). This represents an 80% study visit completion rate.

On reviewing the recruitment strategy, the seroconversion rate was well below that proposed by the UK PROUD study which reported an incidence rate of 9.1 new HIV infections per 100-person years (113). Here, the high risk group was defined as six or greater sexual partners and the presence of a rectal sexually transmitted infection. There were three seroconversion events in the high risk patient group during a 34 month period of follow-up, equating to three events per 213 years of follow-up, or an incidence rate of 1.4 new HIV infections per 100-person years.

Reduced rate of HIV acquisition was due to a fall in incident HIV infection in men who have sex with men. PROUD recruited patients from 2012 to 2014, whereas this study recruited patients from 2015 to 2016. These data were described by Nwokolo et al in 2017 (275). Annual Public Health England data on new HIV infection MSM showed a steady increase since 2007, and data from 2016 showed an overall decrease of 18% in new HIV diagnoses, with a decrease of 21% in MSM. This was most pronounced in London, with a 29% decrease in new MSM infections, compared to 11% reported from testing sites outside the capital. The study recruitment clinic reported an 80% decrease in new MSM infections, despite an increase in HIV testing during the same period. This was a remarkable achievement due to multifaceted approaches to HIV treatment and prevention. This clinic prioritises access to therapy for people with newly diagnosed HIV infection, and most patients begin

antiretroviral treatment within seven days of diagnosis. The clinic also supported seronegative patients who used pre-exposure prophylaxis as a risk reduction strategy. As a group, MSM and the wider LGBTIQA+ (lesbian, gay, bisexual, transgender, intersex, queer/questioning, asexual and others) community have worked tirelessly to raise awareness and improve access to the healthcare services which benefit their community. More must be done to support other communities which may not recognise the healthcare issues that disproportionately target them.

In addition, a reduction in a community viral load could contribute to a reduction in HIV transmission and incidence (369). The UK has managed to achieve the UNAIDS 90-90-90 target (92) with 92% of PLWH aware of their status (92%, credible interval (Crl) 88 to 94%), with 98% of those diagnosed in receipt of treatment and 90% of those who are virally suppressed (97%). Meeting these targets has also contributed to a reduction in onward HIV transmission.

This study reviewed incident seroconversion in one specific community group, men who have sex with men, and was conceived in an era where young MSM continued to experience an increase in new HIV diagnoses. This clinic diagnosed one in every three HIV infections in London and provided care for one in every four newly diagnosed HIV infections in the UK. Therefore, this study addressed a very accessible population, making use of frequent health attenders. The previously cited report by Public Health England acknowledges other community groups where HIV testing uptake requires improvement, particularly heterosexual women of black and minority ethnic groups, and people living outside urban centres. Therefore, while this study focused on a specific community, the hope is that the work presented on immune responses that can be applied across a broader spectrum

Considering the change in incident HIV infection in MSM and the ensuing reduction in expected numbers of patients seroconverting to HIV, could there have been ways to increase number of group B participants? Retrospectively, an earlier start to the project may have improved these figures. Otherwise, as HIV diagnoses continue to fall in all sections of the community, it is difficult to propose methods for increased recruitment of seroconverting participants. In conclusion, our rate of

seroconversion was below that which was initially expected. However the nature of the work involved in this project was such that the numbers seroconverting provided adequate material to work with.

Methods

Within our research group there was expertise in yeast surface display technology reviewing of host responses to simian immunodeficiency virus (303), severe acute respiratory syndrome (SARS) and Middle Eastern respiratory syndrome (MERS-CoV) (data not published). The creation of the HIV-Env protein library was a novel task but was supported by these colleagues.

On completion of the project, there are some areas where processes could be improved. Firstly, the initial design of the yeast surface display system used two libraries of varying sizes. The “small” library fragments were 100-300bp, and the “big” library fragments were 100-500bp in length. The big library was preferential to the small, and on reflection it was not necessary to create two. From an optimisation perspective, it was useful to understand the experimental conditions responsible for each batch of fragment size.

Another feature of working with yeast was the vulnerability of clones to bacterial contamination. Advised storage of yeast is at 4°C for 2-4 weeks in SDCAA culture, or frozen glycerol stocks at -80°C. With refrigerated stocks, despite use of anti-microbial containing culture media, bacterial contamination occurred towards the end of storage periods, creating a pressure to use fresh aliquots and protect and secure sorted aliquots.

Yeast surface display technology has now been available for two decades. As described in the introduction, it compares favourably to other protein engineering techniques due to a eukaryotic expression system and suitability for fluorescence activated cells sorting. A limitation of yeast surface display is the breadth of screening diversity. Flow cytometers can typically screen 50,000 yeast cells per second, resulting in an upper limit of 10^8 or 10^9 yeast cells per library sort. This is compared to 10^{12} – 10^{14} for phage and ribosome display libraries. However, the quality of yeast libraries can be improved

through techniques including magnetic activated cell sorting which removes poor quality protein epitopes (370).

Another concern of yeast technology is the post-translational modification of surface bound proteins. Yeast use a high mannose glycosylation mechanism resulting in proteins with a short half-life *in vivo* (371). However, as this project was *in vitro* with no intended therapeutic application, it was not felt to be of concern. Future directions involving humanized glycosylation could address this.

For the purposes of this project, yeast surface display was a robust technology and provides a way to interrogate antibody response to pathogens. It provided an array of epitopes allowing assessment of antibodies present within patient serum at given timepoints. Individual yeast clones of interest provided a reliable method to review serum responses and formed the basis of the B cell baiting method.

As B cell baiting was a novel technique, the concept of B cell baiting with yeast was discussed with colleagues in our research group who had pre-exiting expertise with yeast cell sorting and B cell cloning. The experience gained in yeast surface display technology formed the basis for the baiting material.

The optimisation steps used seropositive PBMC baited with yeast clones. As seropositive serum samples had identified yeast bound HIV-Env epitopes, it was feasible to consider the possibility of PBMC binding similar epitopes using cell surface receptors. The samples used for optimisation were seropositive PBMCs from group E participants which avoided using experimental aliquots unnecessarily. A good availability of candidate PBMC and yeast clones allowed optimisation using various combinations. As shown in chapter five, the actual yields of sorted cells, PCR products and subsequent antibody chain inset candidates took time to develop with sequential experiments. In retrospect, I suspect repeating the processes with more time and practice could yield greater numbers

of candidate monoclonal antibodies. Further optimisation of this B cell baiting technique could include using peptide bait based on the epitopes identified by the seronegative patient sera samples.

The advantages of this method is using known epitopes to bait participant B cells. Any epitope identified by screening patient sera can theoretically be reproduced by capturing the B cell of interest using this baiting technique. Theoretically, this method could be extended to other pathogens if paired participant PBMC and serum samples are available.

A drawback is time taken from inception to product yield. Yeast clones must be cultured for one week, meaning serial sorting and culture takes one month. Another consideration is the technical expertise of other involved personnel. Yeast flow sorting success relies on the expertise of the sort facility manager and a degree of confidence in sorting both B cells and yeast cells. At the planning stages of this project, in depth discussions were had with a dedicated facility manager covering all aspect of sorting from sample preparation to post sorting machine care, which helped this project due to the reliance on sorting in all stages of the work.

The B cell cloning technique described in the methods (284) can be completed in 28 days, but took longer to complete all stages of the protocol. In practice, multiple candidate antibodies from various infection timepoints were assayed simultaneously in the hope of successful monoclonal antibodies. With more time and confidence, B cell baiting, and cloning could be completed in 60 days, depending on number of successive rounds of yeast sorting and culturing.

The seronegative results chapter looked at the presence of anti-HIV-Env response in seronegative MSM and sought to determine of HIV exposure influenced the scale of the response. The groups were divided into high and low risk according to the UK PROUD criteria based on an individual's reported number of sexual partners, and the presence of a sexually transmitted rectal infection.

The results supported the hypothesis that individuals with greater levels of HIV exposure were more likely to develop anti-HIV responses and demonstrated two points. Firstly, anti-gp41 responses are

present in seronegative MSM, and presence varies according to levels of exposure to HIV. Secondly, yeast surface display (YSD) technology provides a method of examining humoral immune responses against HIV.

The advantages of YSD have been discussed previously in this results chapter, to recap; YSD allows precise epitope mapping of known protein structure, presents these epitopes in a eukaryotic fashion, and may display cryptic epitopes not typically displayed *in vivo*, nor in cellular/ELISA based assays. Differences in glycosylation between YSD and *in vivo* viral production may hinder identification of glycosylation-dependent epitopes, and future work could include enzymatic additions to more accurately match that seen *in vivo*.

As discussed, Carrillo et al reported on anti-Env IgG and IgA responses in HESN, but no variation in magnitude according to their presumed HIV exposure (225). The results presented here suggest high risk HIV exposed seronegative MSM have greater recognition of HIV gp41. Deviation from the published data may be explained by the risk stratification adopted each study. All recruits to this study were MSM as compared to heterosexual couples. Secondly, I reviewed a larger number of HESN (50 high risk and 50 low risk compared to 27 couples). Thirdly, the nature of risk exposure was different. In this study, a high risk sexual exposure was defined according to PROUD-UK criteria; multiple sexual partners and the presence of a rectal sexually transmitted infection. This differs from the referenced study where monogamous couples were recruited and reported only 56% reported unprotected sexual intercourse. Finally, the referenced study reported 66% of the HESN seropositive partners had an undetectable viral load at time of enrolment, and the median viral load in the remaining partners was approximately 5000-50000 copies HIV RNA/ml. Data from the pivotal HPTN 052 study showed suppression of an individual's viral load reduced risk of transmission to seronegative partners (95). In this study, serostatus of all partners were not known, and despite the recent achievement of the UNAIDS 90-90-90 target in the UK, individuals engaging in unprotected sex with multiple unknown partners probably have greater viral exposure than HESN in serodiscordant monogamous

relationships. Therefore, a reduced amount of available circulating virus in the Carrillo couplings could explain the differences between previously reported humoral responses and the findings observed here.

Considering the HESN in this study displayed anti-MPER responses, it would be interesting to track development of this response in seronegative individuals who have recently become sexually active to review if this response occurs within the same timeframe, as specific anti-MPER responses occur approximately one year post seroconversion (36,66,130).

In conclusion, the presence of anti-Env humoral responses in highly exposed seronegative individuals and provided the foundation for the next part of the work. These results showed the proportion of epitope recognition was approximately twice as much in high compared to low-risk participant sera (gp160 library HR 74.57, LR 53.46, HR:LR 1.39; gp41 library HR 75.75, LR 35.1, HR:LR 2.16).

Anti-Env immune responses were examined at pre, early and late infection in five individuals and responses to HIV-Env epitopes was found at all three timepoints. The epitopes recognised by the seroconverter pre-infection samples were similar to those seen in the seronegative cohort, validating the YSD method when used with batched and individual aliquots, and indicated the epitopes selected by seronegative serum are similar across both seronegative exposed and healthy control groups.

The hypothesis pre-existing exposure to HIV-Env generated serum epitope responses that influenced future immune response development was borne out by participant samples. Anti-Env responses were selected based on previously published data describing initial antibody responses to gp41 epitopes (36,130). As all seronegative samples had some degree of HIV-Env recognition, and the most frequently recognised epitopes (gp120 V1V2, C2, gp41 MPER and endodomain) were similar across all risk groups, it may be the case that it is the immunogenicity of the epitope itself rather than the degree of exposure which provokes response.

It may also be the case that these immunogenic epitopes are presented differently to that experienced *in vivo* by B cells, as previously discussed in the context of YSD vs mammalian epitope presentation, and presentation of fragmented epitopes may be an over-simplification. Yeast surface display presents a fragmented epitope which may be recognised by a narrow subset of B cell receptors, whereas the natural history of infection may require antigens presented to multiple naïve B cells which produces the *in vivo* humoral response. Given more time, I would have liked to explore the anti-Env response in healthy controls, as this would help determine the significance and magnitude of the anti-Env response in genuinely unexposed individuals.

The nature of viral exposure required to generate the humoral response merits discussion. As touched upon in the summary in chapter four, anti-Env responses must be considered in terms of a three dimensional structure. Anti-Env responses in seronegative individuals coupled with the major antigenic determinant locations in typically cryptic regions suggests exposure to non-intact trimeric structure occurs in abortive infection attempts.

Sexual transmission of HIV does not occur at every opportunity. As quoted in the introduction chapter, the rate of HIV infection per sexual act is approximately 0.001, 0.003, and 0.01 for female-to-male, male-to-female, and male-to-male respectively (per contact transmission on logarithmic scale) (103). The mucosal barrier offers protection as transmission via vaginal and rectal intercourse is more likely due to a single viral quasispecies, as opposed to injection drug users where multiple virions may be responsible for infection. Numerous HIV virions may breach a mucosal barrier but fail to establish infection, with failed attempts including infection with defective or less fit virions (36). Therefore, viral exposure occurs in the absence of established infection.

To consider exposure to cryptic epitopes and generation of immune responses, the concept of ineffective cellular infection and cryptic epitope exposure may be responsible for epitope recognition in seronegative individuals. These methods could be explained by abortive $CD4^{+}$T cell infection resulting in caspase-1 mediated pyroptosis, where intense inflammatory reactions cause programmed

cell death, releasing intracellular contents including degraded cellular debris and drives further inflammation by the release of pro-inflammatory cytokines (81,82). This innate inflammatory reaction, which is not necessarily epitope specific, may act as an adjuvant to formation of a humoral response. Another theory is the formation of "junk Env" occurring in ineffective processing of HIV glycoproteins to produce gp41 stumps on cell surfaces.

There was sequence similarity of epitopes recognised by seronegative pre-infection samples and *Ecoli* RNA polymerase subunit motifs. This had been described by Liao et al (263) who reported one 4-amino acid residue motif commonality in an unmutated common ancestor antibody. This work builds on these findings and goes further; epitope sequences selected by seronegative sera were compared to the published microbiota epitopes to identify regions of similarity. Areas of variation could be explained by somatic hypermutation of an evolving antibody response. To further explore these responses, an assay designed to review participant sera binding to cell-based gp41 antigen would confirm the anti-Env specificity of these responses. In addition, the mAb produced from the work in chapter five could be assayed for gp41 binding and confirmed by competitive assays with known commercial anti-gp41 mAb.

To consider; are intestinal microbial antigens responsible for these gp41-directed responses? Or abortive HIV-1 exposure as discussed earlier? Structural similarity of these epitopes could be due to chance or given the nature of lentiviruses and their ability to integrate into host DNA, another explanation could be prior inclusion of lentiviral sequences in *Ecoli* RNA polymerase. Viruses are the most abundant and diverse genetic entities present on earth, with the potential to infect all life forms. During infection, viral DNA or reverse transcribed RNA may become incorporated into host genome creates a heritable genetic legacy in all progeny from the host (372–375). This is a particular characteristic of retroviruses and could explain sequence similarity between elements of a retroviral pathogen (HIV) and a bacterial protein (*Ecoli* RNA polymerase). Further work here would be to screen HESN sera for anti- *Ecoli* RNA polymerase responses. As most people should have anti-*Ecoli* RNA

polymerase serum responses, it would be interesting to see any variation in HESN vs normal population.

The final results chapter described development of a novel technique to bait B cells of interest in preparation for B cell cloning. From the work detailed in results chapter four, serial responses of B003 at pre, early and late infection serum were reviewed, and sera recognised gp120 and gp41 epitopes at all timepoints. The yeast clone selected to bait B cells covered the highly conserved MPER region (aa643-676, sequence LEKSQNQQEKNEQELLELDKWANLWNWFDITNWL) and had been recognised by B003 pre-infection serum. As the B cell population of interest was small, preservation of the target cell population was aided by epitope-specific serum-yeast sorting to identify the key epitope of interest.

The final antibody yield in chapter five was low, with only two HIV specific antibodies, but the results show a novel method to extract epitope specific B cells for specific monoclonal antibody generation. Future optimisation would aim to increase the epitope-specific B cell population. Methods could include screening PBMC using whole Env trimer or peptides based on epitopes of interest. As mentioned in chapter five, bulk sorting was attempted but no there was no improvement in sorted cell yield. Further work here could review the generated antibodies in terms of antibody engineering. As the extracted antibody was MPER region specific, alteration of the Fab region sequence to enhance binding properties, or the Fc portion to explore a variety of effector functions could be reviewed.

In conclusion, to review the intentions of the project; I have described anti-Env responses in seronegative populations, tracked serial anti-Env responses in a group of five seroconverting participants and shown similarity in epitopes recognised in the humoral response to established infection, and developed a novel technique to extract B cells and generate monoclonal antibodies. I have also demonstrated similarities in recognised Env epitopes and amino acid sequences of the E coli proteins, contributing to the current literature and proposing a mechanism for this finding.

References

Chapter 6 References

1. US Centers for Disease Control and Prevention. Follow-up on Kaposi's sarcoma and pneumocystis pneumonia. MMWR 1981. 1981.

2. US Centers for Disease Control and Prevention. Update on Kaposi's sarcoma and opportunistic infections in previously healthy persons--United States. MMWR 1982. 1982.

3. US Centers for Disease Control and Prevention. Epidemiologic Aspects of the Current Outbreak of Kaposi's Sarcoma and Opportunistic Infections. N Engl J Med [Internet]. 1982 Jan 28;306(4):248–52. Available from: https://doi.org/10.1056/NEJM198201283060432

4. Barré-Sinoussi F, Chermann JC, Rey F, Nugeyre MT, Chamaret S, Gruest J, et al. Isolation of a T-lymphotropic retrovirus from a patient at risk for acquired immune deficiency syndrome (AIDS). Science. 1983 May;220(4599):868–71.

5. Gallo RC, Sarin PS, Gelmann EP, Robert-Guroff M, Richardson E, Kalyanaraman VS, et al. Isolation of human T-cell leukemia virus in acquired immune deficiency syndrome (AIDS). Science. 1983 May;220(4599):865–7.

6. Broder S, Gallo RC. A pathogenic retrovirus (HTLV-III) linked to AIDS. N Engl J Med. 1984 Nov;311(20):1292–7.

7. Gallo RC, Salahuddin SZ, Popovic M, Shearer GM, Kaplan M, Haynes BF, et al. Frequent detection and isolation of cytopathic retroviruses (HTLV-III) from patients with AIDS and at risk for AIDS. Science. 1984 May;224(4648):500–3.

8. UNAIDS. Global HIV & AIDS statistics — 2019 fact sheet [Internet]. 2019. Available from: https://www.unaids.org/en/resources/fact-sheet

9. UNAIDS. Global HIV & AIDS statistics — 2018 fact sheet [Internet]. 2018. Available from:

https://www.unaids.org/en/resources/fact-sheet

10. WHO. World Health Organisation [Internet]. HIV/AIDS. 2016 [cited 2016 Jul 7]. Available from: http://www.who.int/gho/hiv/en/

11. UNAIDS. UNAIDS Data 2018 [Internet]. 2018. Available from: https://www.unaids.org/sites/default/files/media_asset/unaids-data-2018_en.pdf

12. US Centers for Disease Control and Prevention. HIV and Gay and Bisexual Men. [Internet]. 2019. Available from: https://www.cdc.gov/hiv/group/msm/index.html

13. Baral S, Burrell E, Scheibe A, Brown B, Beyrer C, Bekker L-G. HIV risk and associations of HIV infection among men who have sex with men in peri-urban Cape Town, South Africa. BMC Public Health. 2011 Oct;11:766.

14. Sanders EJ, Graham SM, Okuku HS, van der Elst EM, Muhaari A, Davies A, et al. HIV-1 infection in high risk men who have sex with men in Mombasa, Kenya. AIDS. 2007 Nov;21(18):2513–20.

15. Wade AS, Kane CT, Diallo PAN, Diop AK, Gueye K, Mboup S, et al. HIV infection and sexually transmitted infections among men who have sex with men in Senegal. AIDS. 2005 Dec;19(18):2133–40.

16. Beyrer C, Baral SD, van Griensven F, Goodreau SM, Chariyalertsak S, Wirtz AL, et al. Global epidemiology of HIV infection in men who have sex with men. Lancet. 2012;380(9839):367–77.

17. Popovic M, Sarngadharan MG, Read E, Gallo RC. Detection, isolation, and continuous production of cytopathic retroviruses (HTLV-III) from patients with AIDS and pre-AIDS. Science. 1984 May;224(4648):497–500.

18. Painter M CK. HIV and Retroviruses; Encyclopedia of Microbiology. 2019. 613–628 p.

19. Varmus H. Retroviruses. Science (80-) [Internet]. 1988 Jun 10;240(4858):1427 LP – 1435.

Available from: http://science.sciencemag.org/content/240/4858/1427.abstract

20. Campbell RS, Robinson WF. The comparative pathology of the lentiviruses. J Comp Pathol. 1998 Nov;119(4):333–95.

21. Frankel AD, Young JA. HIV-1: fifteen proteins and an RNA. Annu Rev Biochem. 1998;67:1–25.

22. Watts JM, Dang KK, Gorelick RJ, Leonard CW, Bess Jr JW, Swanstrom R, et al. Architecture and secondary structure of an entire HIV-1 RNA genome. Nature [Internet]. 2009;460(7256):711–6. Available from: https://doi.org/10.1038/nature08237

23. Coffin JM, Hughes SH, Varmus HE. Retroviral Virions and Genomes--Retroviruses. Cold Spring Harbor Laboratory Press; 1997.

24. Suzuki Y, Craigie R. The road to chromatin—nuclear entry of retroviruses. Nat Rev Microbiol. 2007;5(3):187–96.

25. Schröder ARW, Shinn P, Chen H, Berry C, Ecker JR, Bushman F. HIV-1 integration in the human genome favors active genes and local hotspots. Cell. 2002;110(4):521–9.

26. Ji H, Moore DP, Blomberg MA, Braiterman LT, Voytas DF, Natsoulis G, et al. Hotspots for unselected Ty1 transposition events on yeast chromosome III are near tRNA genes and LTR sequences. Cell. 1993 Jun;73(5):1007–18.

27. Kirchner J, Connolly CM, Sandmeyer SB. Requirement of RNA polymerase III transcription factors for in vitro position-specific integration of a retroviruslike element. Science. 1995 Mar;267(5203):1488–91.

28. Demeulemeester J, De Rijck J, Gijsbers R, Debyser Z. Retroviral integration: Site matters: Mechanisms and consequences of retroviral integration site selection. Bioessays. 2015 Nov;37(11):1202–14.

29. Lusic M, Siliciano RF. Nuclear landscape of HIV-1 infection and integration. Nat Rev Microbiol. 2017 Feb;15(2):69–82.

30. Brown PO, Bowerman B, Varmus HE, Bishop JM. Correct integration of retroviral DNA in vitro. Cell. 1987 May;49(3):347–56.

31. Ellison V, Abrams H, Roe T, Lifson J, Brown P. Human immunodeficiency virus integration in a cell-free system. J Virol. 1990 Jun;64(6):2711–5.

32. Farnet CM, Haseltine WA. Integration of human immunodeficiency virus type 1 DNA in vitro. Proc Natl Acad Sci U S A. 1990 Jun;87(11):4164–8.

33. Kreiss JK, Kitchen LW, Prince HE, Kasper CK, Essex M. Antibody to human T-lymphotropic virus type III in wives of hemophiliacs. Evidence for heterosexual transmission. Ann Intern Med. 1985 May;102(5):623–6.

34. Piot P, Quinn TC, Taelman H, Feinsod FM, Minlangu KB, Wobin O, et al. Acquired immunodeficiency syndrome in a heterosexual population in Zaire. Lancet (London, England). 1984 Jul;2(8394):65–9.

35. Redfield RR, Markham PD, Salahuddin SZ, Sarngadharan MG, Bodner AJ, Folks TM, et al. Frequent transmission of HTLV-III among spouses of patients with AIDS-related complex and AIDS. JAMA. 1985 Mar;253(11):1571–3.

36. Cohen MS, Shaw GM, McMichael AJ, Haynes BF. Acute HIV-1 Infection. N Engl J Med [Internet]. 2011 May 19;364(20):1943–54. Available from: https://www.ncbi.nlm.nih.gov/pubmed/21591946

37. Korenromp EL, White RG, Orroth KK, Bakker R, Kamali A, Serwadda D, et al. Determinants of the Impact of Sexually Transmitted Infection Treatment on Prevention of HIV Infection: A

Synthesis of Evidence from the Mwanza, Rakai, and Masaka Intervention Trials. J Infect Dis [Internet]. 2005 Feb 1;191(Supplement_1):S168–78. Available from: https://doi.org/10.1086/425274

38. Plummer FA, Simonsen JN, Cameron DW, Ndinya-Achola JO, Kreiss JK, Gakinya MN, et al. Cofactors in Male-Female Sexual Transmission of Human Immunodeficiency Virus Type 1. J Infect Dis [Internet]. 1991 Feb 1;163(2):233–9. Available from: https://doi.org/10.1093/infdis/163.2.233

39. Wawer MJ, Gray RH, Sewankambo NK, Serwadda D, Li X, Laeyendecker O, et al. Rates of HIV-1 transmission per coital act, by stage of HIV-1 infection, in Rakai, Uganda. J Infect Dis. 2005 May;191(9):1403–9.

40. Keele BF, Giorgi EE, Salazar-Gonzalez JF, Decker JM, Pham KT, Salazar MG, et al. Identification and characterization of transmitted and early founder virus envelopes in primary HIV-1 infection. Proc Natl Acad Sci U S A. 2008;105(21):7552–7.

41. Daar ES, Moudgil T, Meyer RD, Ho DD. Transient high levels of viremia in patients with primary human immunodeficiency virus type 1 infection. N Engl J Med. 1991 Apr;324(14):961–4.

42. Clark SJ, Saag MS, Decker WD, Campbell-Hill S, Roberson JL, Veldkamp PJ, et al. High titers of cytopathic virus in plasma of patients with symptomatic primary HIV-1 infection. N Engl J Med. 1991 Apr;324(14):954–60.

43. Fiebig EW, Wright DJ, Rawal BD, Garrett PE, Schumacher RT, Peddada L, et al. Dynamics of HIV viremia and antibody seroconversion in plasma donors: implications for diagnosis and staging of primary HIV infection. AIDS. 2003 Sep;17(13):1871–9.

44. Little SJ, McLean AR, Spina CA, Richman DD, Havlir D V. Viral dynamics of acute HIV-1 infection. J Exp Med. 1999 Sep;190(6):841–50.

45. Essex M, Allan J, Kanki P, McLane MF, Malone G, Kitchen L, et al. Antigens of human T-lymphotropic virus type III/lymphadenopathy-associated virus. Ann Intern Med. 1985 Nov;103(5):700–3.

46. Burton DR, Mascola JR. Antibody responses to envelope glycoproteins in HIV-1 infection. Nat Immunol. 2015;16(6):571–6.

47. Reardon PN, Sage H, Dennison SM, Martin JW, Donald BR, Alam SM, et al. Structure of an HIV-1-neutralizing antibody target, the lipid-bound gp41 envelope membrane proximal region trimer. Proc Natl Acad Sci U S A [Internet]. 2014;111(4):1391–6. Available from: http://www.ncbi.nlm.nih.gov/pubmed/24474763

48. Choe H, Martin KA, Farzan M, Sodroski J, Gerard NP, Gerard C. Structural interactions between chemokine receptors, gp120 Env and CD4. Semin Immunol. 1998 Jun;10(3):249–57.

49. Hiv.lanl.gov. HIV molecular immunology database [Internet]. Available from: https://www.hiv.lanl.gov/content/immunology/ab_search

50. Kwong PD, Wyatt R, Robinson J, Sweet RW, Sodroski J, Hendrickson WA. Structure of an HIV gp120 envelope glycoprotein in complex with the CD4 receptor and a neutralizing human antibody. Nature. 1998 Jun;393(6686):648–59.

51. Choe H, Farzan M, Sun Y, Sullivan N, Rollins B, Ponath PD, et al. The β-chemokine receptors CCR3 and CCR5 facilitate infection by primary HIV-1 isolates. Cell. 1996;85(7):1135–48.

52. Connor RI, Sheridan KE, Ceradini D, Choe S, Landau NR. Change in coreceptor use correlates with disease progression in HIV-1--infected individuals. J Exp Med. 1997 Feb;185(4):621–8.

53. Joseph SB, Swanstrom R. The evolution of HIV-1 entry phenotypes as a guide to changing target cells. J Leukoc Biol. 2018 Mar;103(3):421–31.

54. McGaughey GB, Barbato G, Bianchi E, Freidinger RM, Garsky VM, Hurni WM, et al. Progress towards the development of a HIV-1 gp41-directed vaccine. Curr HIV Res [Internet]. 2004;2(2):193–204. Available from: http://www.ncbi.nlm.nih.gov/pubmed/15078183

55. Blumenthal R, Durell S, Viard M. HIV entry and envelope glycoprotein-mediated fusion. J Biol Chem. 2012;287(49):40841–9.

56. Tagliamonte M, Tornesello ML, Buonaguro FM, Buonaguro L. Conformational HIV-1 envelope on particulate structures: a tool for chemokine coreceptor binding studies. J Transl Med. 2011;9 Suppl 1:S1.

57. Yasen A, Herrera R, Rosbe K, Lien K, Tugizov SM. Release of HIV-1 sequestered in the vesicles of oral and genital mucosal epithelial cells by epithelial-lymphocyte interaction. PLoS Pathog. 2017 Feb;13(2):e1006247.

58. Cavrois M, Neidleman J, Kreisberg JF, Greene WC. In vitro derived dendritic cells trans-infect CD4 T cells primarily with surface-bound HIV-1 virions. PLoS Pathog. 2007 Jan;3(1):e4.

59. Neidleman JA, Chen JC, Kohgadai N, Müller JA, Laustsen A, Thavachelvam K, et al. Mucosal stromal fibroblasts markedly enhance HIV infection of CD4+ T cells. PLoS Pathog. 2017 Feb;13(2):e1006163.

60. Rodriguez-Garcia M, Shen Z, Barr FD, Boesch AW, Ackerman ME, Kappes JC, et al. Dendritic cells from the human female reproductive tract rapidly capture and respond to HIV. Mucosal Immunol. 2017 Mar;10(2):531–44.

61. Collins KB, Patterson BK, Naus GJ, Landers D V, Gupta P. Development of an in vitro organ culture model to study transmission of HIV-1 in the female genital tract. Nat Med. 2000 Apr;6(4):475–9.

62. Gupta P, Collins KB, Ratner D, Watkins S, Naus GJ, Landers D V, et al. Memory CD4(+) T cells are the earliest detectable human immunodeficiency virus type 1 (HIV-1)-infected cells in the female genital mucosal tissue during HIV-1 transmission in an organ culture system. J Virol. 2002 Oct;76(19):9868–76.

63. McKinnon LR, Nyanga B, Chege D, Izulla P, Kimani M, Huibner S, et al. Characterization of a human cervical CD4+ T cell subset coexpressing multiple markers of HIV susceptibility. J Immunol. 2011 Dec;187(11):6032–42.

64. Hladik F, Sakchalathorn P, Ballweber L, Lentz G, Fialkow M, Eschenbach D, et al. Initial events in establishing vaginal entry and infection by human immunodeficiency virus type-1. Immunity. 2007;26(2):257–70.

65. Zhang Z, Schuler T, Zupancic M, Wietgrefe S, Staskus KA, Reimann KA, et al. Sexual transmission and propagation of SIV and HIV in resting and activated CD4+ T cells. Science. 1999 Nov;286(5443):1353–7.

66. McMichael AJ, Borrow P, Tomaras GD, Goonetilleke N, Haynes BF. The immune response during acute HIV-1 infection: clues for vaccine development. Nat Rev Immunol. 2010;10(1):11–23.

67. Ribeiro RM, Qin L, Chavez LL, Li D, Self SG, Perelson AS. Estimation of the initial viral growth rate and basic reproductive number during acute HIV-1 infection. J Virol. 2010 Jun;84(12):6096–102.

68. Gohda J, Ma Y, Huang Y, Zhang Y, Gu L, Han Y, et al. HIV-1 replicates in human osteoclasts and enhances their differentiation in vitro. Retrovirology. 2015;12(1):1–10.

69. Lee B, Sharron M, Montaner LJ, Weissman D, Doms RW. Quantification of CD4, CCR5, and CXCR4 levels on lymphocyte subsets, dendritic cells, and differentially conditioned monocyte-

derived macrophages. Proc Natl Acad Sci. 1999;96(9):5215–20.

70. Mitchell BI, Laws EI, Ndhlovu LC. Impact of Myeloid Reservoirs in HIV Cure Trials. Curr HIV/AIDS Rep [Internet]. 2019;16(2):129–40. Available from: https://doi.org/10.1007/s11904-019-00438-5

71. Folks T, Kelly J, Benn S, Kinter A, Justement J, Gold J, et al. Susceptibility of normal human lymphocytes to infection with HTLV-III/LAV. J Immunol. 1986 Jun;136(11):4049–53.

72. Finzi D, Blankson J, Siliciano JD, Margolick JB, Chadwick K, Pierson T, et al. Latent infection of CD4+ T cells provides a mechanism for lifelong persistence of HIV-1, even in patients on effective combination therapy. Nat Med. 1999 May;5(5):512–7.

73. Shan L, Deng K, Gao H, Xing S, Capoferri AA, Durand CM, et al. Transcriptional Reprogramming during Effector-to-Memory Transition Renders CD4(+) T Cells Permissive for Latent HIV-1 Infection. Immunity. 2017 Oct;47(4):766-775.e3.

74. Zack JA, Kim SG, Vatakis DN. HIV restriction in quiescent $CD4^+$ T cells. Retrovirology. 2013 Apr;10:37.

75. Pace MJ, Graf EH, Agosto LM, Mexas AM, Male F, Brady T, et al. Directly infected resting CD4+T cells can produce HIV Gag without spreading infection in a model of HIV latency. PLoS Pathog. 2012;8(7):e1002818.

76. Chavez L, Calvanese V, Verdin E. HIV Latency Is Established Directly and Early in Both Resting and Activated Primary CD4 T Cells. PLoS Pathog. 2015 Jun;11(6):e1004955.

77. Hosmane NN, Kwon KJ, Bruner KM, Capoferri AA, Beg S, Rosenbloom DIS, et al. Proliferation of latently infected CD4(+) T cells carrying replication-competent HIV-1: Potential role in latent reservoir dynamics. J Exp Med [Internet]. 2017/03/24. 2017 Apr 3;214(4):959–72. Available

from: https://www.ncbi.nlm.nih.gov/pubmed/28341641

78. Mohri H, Bonhoeffer S, Monard S, Perelson AS, Ho DD. Rapid turnover of T lymphocytes in SIV-infected rhesus macaques. Science. 1998 Feb;279(5354):1223–7.

79. Chun T-W, Justement JS, Pandya P, Hallahan CW, McLaughlin M, Liu S, et al. Relationship between the size of the human immunodeficiency virus type 1 (HIV-1) reservoir in peripheral blood CD4+ T cells and CD4+:CD8+ T cell ratios in aviremic HIV-1-infected individuals receiving long-term highly active antiretroviral therapy. J Infect Dis. 2002 Jun;185(11):1672–6.

80. Moir S, Chun T-W, Fauci AS. Pathogenic mechanisms of HIV disease. Annu Rev Pathol. 2011;6:223–48.

81. Doitsh G, Cavrois M, Lassen KG, Zepeda O, Yang Z, Santiago ML, et al. Abortive HIV infection mediates CD4 T cell depletion and inflammation in human lymphoid tissue. Cell [Internet]. 2010 Nov 24;143(5):789–801. Available from: https://www.ncbi.nlm.nih.gov/pubmed/21111238

82. Doitsh G, Galloway NLK, Geng X, Yang Z, Monroe KM, Zepeda O, et al. Cell death by pyroptosis drives CD4 T-cell depletion in HIV-1 infection. Nature. 2014 Jan;505(7484):509–14.

83. Grossman Z, Meier-Schellersheim M, Paul WE, Picker LJ. Pathogenesis of HIV infection: what the virus spares is as important as what it destroys. Nat Med. 2006 Mar;12(3):289–95.

84. Barber DL, Wherry EJ, Masopust D, Zhu B, Allison JP, Sharpe AH, et al. Restoring function in exhausted CD8 T cells during chronic viral infection. Nature. 2006 Feb;439(7077):682–7.

85. Medicine TC of E. HIV Testing in the Emergency Department [Internet]. 2012. Available from: https://www.rcem.ac.uk/docs/College Guidelines/5z6. HIV Testing in the Emergency Department (Revised Oct 2012).pdf

86. National Institute for Health and Care Excellence [NICE]. NG60. 2016.

87. WHO. 90–90–90 - An ambitious treatment target to help end the AIDS epidemic [Internet]. 2017. Available from: http://www.unaids.org/en/resources/documents/2017/90-90-90

88. Trust TH. New PHE stats show UK has reached UN's HIV target for 2020 [Internet]. 2018. Available from: https://www.tht.org.uk/news/new-phe-stats-show-uk-has-reached-uns-hiv-target-2020-terrence-higgins-trust-response

89. Hubert JB, Burgard M, Dussaix E, Tamalet C, Deveau C, Le Chenadec J, et al. Natural history of serum HIV-1 RNA levels in 330 patients with a known date of infection. The SEROCO Study Group. AIDS. 2000 Jan;14(2):123–31.

90. Fischl MA, Richman DD, Grieco MH, Gottlieb MS, Volberding PA, Laskin OL, et al. The efficacy of azidothymidine (AZT) in the treatment of patients with AIDS and AIDS-related complex. A double-blind, placebo-controlled trial. N Engl J Med. 1987;317(4):185–91.

91. Hammer SM, Katzenstein DA, Hughes MD, Gundacker H, Schooley RT, Haubrich RH, et al. A trial comparing nucleoside monotherapy with combination therapy in HIV-infected adults with CD4 cell counts from 200 to 500 per cubic millimeter. AIDS Clinical Trials Group Study 175 Study Team. N Engl J Med. 1996;335(15):1081–90.

92. Nash S, Desai S, Croxford S, Guerra L, Lowndes C, Connor N GO. Progress towards ending the HIV epidemic in the United Kingdom: 2018 report. [Internet]. 2018. Available from: https://assets.publishing.service.gov.uk/government/uploads/system/uploads/attachment_data/file/759408/HIV_annual_report_2018.pdf

93. Palella FJ, Delaney KM, Moorman AC, Loveless MO, Fuhrer J, Satten GA, et al. Declining morbidity and mortality among patients with advanced human immunodeficiency virus infection. HIV Outpatient Study Investigators. N Engl J Med [Internet]. 1998;338(13):853–60. Available from: http://www.ncbi.nlm.nih.gov/pubmed/9516219

94. Lundgren JD, Babiker AG, Gordin F, Emery S, Grund B, Sharma S, et al. Initiation of Antiretroviral Therapy in Early Asymptomatic HIV Infection. N Engl J Med. 2015 Aug;373(9):795–807.

95. Cohen MS, Chen YQ, McCauley M, Gamble T, Hosseinipour MC, Kumarasamy N, et al. Prevention of HIV-1 infection with early antiretroviral therapy. N Engl J Med. 2011;365(6):493–505.

96. Das M, Chu PL, Santos GM, Scheer S, Vittinghoff E, McFarland W, et al. Decreases in community viral load are accompanied by reductions in new HIV infections in San Francisco. PLoS One. 2010;5(6):e11068.

97. Granich RM, Gilks CF, Dye C, De Cock KM, Williams BG. Universal voluntary HIV testing with immediate antiretroviral therapy as a strategy for elimination of HIV transmission: a mathematical model. Lancet. 2009;373(9657):48–57.

98. Grulich AE, van Leeuwen MT, Falster MO, Vajdic CM. Incidence of cancers in people with HIV/AIDS compared with immunosuppressed transplant recipients: a meta-analysis. Lancet [Internet]. 2007;370(9581):59–67. Available from: http://www.ncbi.nlm.nih.gov/pubmed/17617273

99. Bedimo RJ, McGinnis KA, Dunlap M, Rodriguez-Barradas MC, Justice AC. Incidence of non-AIDS-defining malignancies in HIV-infected versus noninfected patients in the HAART era: impact of immunosuppression. J Acquir Immune Defic Syndr [Internet]. 2009;52(2):203–8. Available from: http://www.ncbi.nlm.nih.gov/pubmed/19617846

100. Shahbaz S, Manicardi M, Guaraldi G, Raggi P. Cardiovascular disease in human immunodeficiency virus infected patients: A true or perceived risk? World J Cardiol. 2015;7(10):633–44.

101. Cotter AG, Mallon PW. HIV infection and bone disease: implications for an aging population.

Sex Heal. 2011;8(4):493–501.

102. Campbell LJ, Ibrahim F, Fisher M, Holt SG, Hendry BM, Post FA. Spectrum of chronic kidney disease in HIV-infected patients. HIV Med. 2009;10(6):329–36.

103. Royce RA, Seña A, Cates W, Cohen MS. Sexual Transmission of HIV. N Engl J Med [Internet]. 1997 Apr 10;336(15):1072–8. Available from: https://doi.org/10.1056/NEJM199704103361507

104. Weller S, Davis K. Condom effectiveness in reducing heterosexual HIV transmission. Cochrane Database Syst Rev. 2002;(1):Cd003255.

105. Smith DK, Herbst JH, Zhang X, Rose CE. Condom effectiveness for HIV prevention by consistency of use among men who have sex with men in the United States. J Acquir Immune Defic Syndr. 2015;68(3):337–44.

106. Williams JR, Alary M, Lowndes CM, Behanzin L, Labbe AC, Anagonou S, et al. Positive impact of increases in condom use among female sex workers and clients in a medium HIV prevalence epidemic: modelling results from Project SIDA1/2/3 in Cotonou, Benin. PLoS One. 2014;9(7):e102643.

107. Muyindike W, Fatch R, Steinfield R, Matthews LT, Musinguzi N, Emenyonu NI, et al. Contraceptive use and associated factors among women enrolling into HIV care in southwestern Uganda. Infect Dis Obs Gynecol. 2012;2012:340782.

108. HIV testing and risk behaviors among gay, bisexual, and other men who have sex with men - United States. MMWR Morb Mortal Wkly Rep. 2013 Nov;62(47):958–62.

109. Paz-Bailey G, Mendoza MCB, Finlayson T, Wejnert C, Le B, Rose C, et al. Trends in condom use among MSM in the United States: the role of antiretroviral therapy and seroadaptive

strategies. AIDS. 2016 Jul;30(12):1985–90.

110. Jin F, Prestage GP, Matthews G, Zablotska I, Rawstorne P, Kippax SC, et al. Prevalence, incidence and risk factors for hepatitis C in homosexual men: data from two cohorts of HIV-negative and HIV-positive men in Sydney, Australia. Sex Transm Infect. 2010;86(1):25–8.

111. Rodger AJ, Cambiano V, Bruun T, Vernazza P, Collins S, Degen O, et al. Risk of HIV transmission through condomless sex in serodifferent gay couples with the HIV-positive partner taking suppressive antiretroviral therapy (PARTNER): final results of a multicentre, prospective, observational study. Lancet (London, England). 2019 Jun;393(10189):2428–38.

112. Baeten JM, Donnell D, Ndase P, Mugo NR, Campbell JD, Wangisi J, et al. Antiretroviral prophylaxis for HIV prevention in heterosexual men and women. N Engl J Med. 2012 Aug;367(5):399–410.

113. McCormack S, Dunn DT, Desai M, Dolling DI, Gafos M, Gilson R, et al. Pre-exposure prophylaxis to prevent the acquisition of HIV-1 infection (PROUD): effectiveness results from the pilot phase of a pragmatic open-label randomised trial. Lancet [Internet]. 2016 Jul 7;387(10013):53–60. Available from: http://dx.doi.org/10.1016/S0140-6736(15)00056-2

114. Kaplan EH, Heimer R. A model-based estimate of HIV infectivity via needle sharing. J Acquir Immune Defic Syndr. 1992;5(11):1116–8.

115. Organisation WH. Portugal on fast track to achieve HIV targets ahead of 2020 deadline [Internet]. 2018. Available from: http://www.euro.who.int/en/countries/portugal/news/news/2018/7/portugal-on-fast-track-to-achieve-hiv-targets-ahead-of-2020-deadline

116. Reardon S. The US opioid epidemic is driving a spike in infectious diseases. Vol. 571, Nature. England; 2019. p. 15–6.

117. CDC. Plenary Session. In: National HIV Prevention Conference. 2019.

118. Mandelbrot L, Tubiana R, Le Chenadec J, Dollfus C, Faye A, Pannier E, et al. No perinatal HIV-1 transmission from women with effective antiretroviral therapy starting before conception. Clin Infect Dis. 2015 Dec;61(11):1715–25.

119. BHIVA. BHIVA guidelines on the management of HIV in pregnancy and postpartum 2018. 2018.

120. McHenry L, Khoshnood M. Blood money: Bayer's inventory of HIV-contaminated blood products and third world hemophiliacs. Account Res. 2014;21(6):389–400.

121. BBC. UK contaminated blood scandal [Internet]. 2019. Available from: https://www.bbc.co.uk/news/topics/c6gz70808ext/uk-contaminated-blood-scandal

122. Transplant NB and. Tests we carry out on your blood [Internet]. 2019. Available from: https://www.blood.co.uk/the-donation-process/further-information/tests-we-carry-out/

123. Piot P, Abdool Karim SS, Hecht R, Legido-Quigley H, Buse K, Stover J, et al. Defeating AIDS--advancing global health. Lancet. 2015;386(9989):171–218.

124. FAGRAEUS A. The plasma cellular reaction and its relation to the formation of antibodies in vitro. J Immunol. 1948 Jan;58(1):1–13.

125. COOPER MD, PETERSON RD, GOOD RA. DELINEATION OF THE THYMIC AND BURSAL LYMPHOID SYSTEMS IN THE CHICKEN. Nature. 1965 Jan;205:143–6.

126. LeBien TW, Tedder TF. B lymphocytes: how they develop and function. Blood [Internet]. 2008 Sep 1;112(5):1570–80. Available from: https://www.ncbi.nlm.nih.gov/pubmed/18725575

127. Murphy K, Travers P, Walport M. Janeway's Immunobiology . Seventh Edition. Garland Science. 2008.

128. Vanderven HA, Jegaskanda S, Wheatley AK, Kent SJ. Antibody-dependent cellular cytotoxicity and influenza virus. Curr Opin Virol. 2017 Feb;22:89–96.

129. Tay MZ, Wiehe K, Pollara J. Antibody-Dependent Cellular Phagocytosis in Antiviral Immune Responses. Front Immunol [Internet]. 2019 Feb 28;10:332. Available from: https://www.ncbi.nlm.nih.gov/pubmed/30873178

130. Mouquet H. Antibody B cell responses in HIV-1 infection. Trends Immunol. 2014 Nov;35(11):549–61.

131. Moir S, Fauci AS. B cells in HIV infection and disease. Nat Rev Immunol. 2009 Apr;9(4):235–45.

132. Moir S, Malaspina A, Pickeral OK, Donoghue ET, Vasquez J, Miller NJ, et al. Decreased survival of B cells of HIV-viremic patients mediated by altered expression of receptors of the TNF superfamily. J Exp Med [Internet]. 2004 Sep 6;200(5):587–99. Available from: https://www.ncbi.nlm.nih.gov/pubmed/15353552

133. Malaspina A, Moir S, Ho J, Wang W, Howell ML, O'Shea MA, et al. Appearance of immature/transitional B cells in HIV-infected individuals with advanced disease: correlation with increased IL-7. Proc Natl Acad Sci U S A. 2006 Feb;103(7):2262–7.

134. Moir S, Fauci AS. Insights into B cells and HIV-specific B-cell responses in HIV-infected individuals. Immunol Rev. 2013 Jul;254(1):207–24.

135. Moir S, Fauci AS. Pathogenic mechanisms of B-lymphocyte dysfunction in HIV disease. J Allergy Clin Immunol [Internet]. 2008/06/10. 2008 Jul;122(1):12–21. Available from: https://www.ncbi.nlm.nih.gov/pubmed/18547629

136. Moir S, Fauci AS. B-cell exhaustion in HIV infection: the role of immune activation. Curr Opin HIV AIDS. 2014 Sep;9(5):472–7.

137. Moir S, Buckner CM, Ho J, Wang W, Chen J, Waldner AJ, et al. B cells in early and chronic HIV infection: evidence for preservation of immune function associated with early initiation of antiretroviral therapy. Blood [Internet]. 2010/09/13. 2010 Dec 16;116(25):5571–9. Available from: https://www.ncbi.nlm.nih.gov/pubmed/20837780

138. Planchais C, Hocqueloux L, Ibanez C, Gallien S, Copie C, Surenaud M, et al. Early Antiretroviral Therapy Preserves Functional Follicular Helper T and HIV-Specific B Cells in the Gut Mucosa of HIV-1-Infected Individuals. J Immunol. 2018 May;200(10):3519–29.

139. Tanko RF, Soares AP, Müller TL, Garrett NJ, Samsunder N, Abdool Karim Q, et al. Effect of Antiretroviral Therapy on the Memory and Activation Profiles of B Cells in HIV-Infected African Women. J Immunol [Internet]. 2016/12/30. 2017 Feb 1;198(3):1220–8. Available from: https://www.ncbi.nlm.nih.gov/pubmed/28039305

140. Wilson EMP, Sereti I. Immune restoration after antiretroviral therapy: the pitfalls of hasty or incomplete repairs. Immunol Rev [Internet]. 2013 Jul;254(1):343–54. Available from: https://www.ncbi.nlm.nih.gov/pubmed/23772630

141. Xu W, Santini PA, Sullivan JS, He B, Shan M, Ball SC, et al. HIV-1 evades virus-specific IgG2 and IgA responses by targeting systemic and intestinal B cells via long-range intercellular conduits. Nat Immunol [Internet]. 2009/08/02. 2009 Sep;10(9):1008–17. Available from: https://www.ncbi.nlm.nih.gov/pubmed/19648924

142. de Bree GJ, Lynch RM. B cells in HIV pathogenesis. Curr Opin Infect Dis. 2016;29(1):23–30.

143. Tomaras GD, Yates NL, Liu P, Qin L, Fouda GG, Chavez LL, et al. Initial B-cell responses to transmitted human immunodeficiency virus type 1: virion-binding immunoglobulin M (IgM) and IgG antibodies followed by plasma anti-gp41 antibodies with ineffective control of initial viremia. J Virol [Internet]. 2008;82(24):12449–63. Available from:

http://www.ncbi.nlm.nih.gov/pubmed/18842730

144. Davis KL, Gray ES, Moore PL, Decker JM, Salomon A, Montefiori DC, et al. High titer HIV-1 V3-specific antibodies with broad reactivity but low neutralizing potency in acute infection and following vaccination. Virology. 2009;387(2):414–26.

145. Wei X, Decker JM, Wang S, Hui H, Kappes JC, Wu X, et al. Antibody neutralization and escape by HIV-1. Nature. 2003 Mar;422(6929):307–12.

146. Richman DD, Wrin T, Little SJ, Petropoulos CJ. Rapid evolution of the neutralizing antibody response to HIV type 1 infection. Proc Natl Acad Sci U S A. 2003 Apr;100(7):4144–9.

147. Hraber P, Seaman MS, Bailer RT, Mascola JR, Montefiori DC, Korber BT. Prevalence of broadly neutralizing antibody responses during chronic HIV-1 infection. AIDS. 2014 Jan;28(2):163–9.

148. Gray ES, Madiga MC, Hermanus T, Moore PL, Wibmer CK, Tumba NL, et al. The neutralization breadth of HIV-1 develops incrementally over four years and is associated with CD4+ T cell decline and high viral load during acute infection. J Virol. 2011 May;85(10):4828–40.

149. Bandawe GP, Moore PL, Werner L, Gray ES, Sheward DJ, Madiga M, et al. Differences in HIV type 1 neutralization breadth in 2 geographically distinct cohorts in Africa. J Infect Dis. 2015 May;211(9):1461–6.

150. Gray ES, Moore PL, Choge IA, Decker JM, Bibollet-Ruche F, Li H, et al. Neutralizing antibody responses in acute human immunodeficiency virus type 1 subtype C infection. J Virol. 2007 Jun;81(12):6187–96.

151. Bonsignori M, Zhou T, Sheng Z, Chen L, Gao F, Joyce MG, et al. Maturation Pathway from Germline to Broad HIV-1 Neutralizer of a CD4-Mimic Antibody. Cell [Internet]. 2016/03/03. 2016 Apr 7;165(2):449–63. Available from: https://www.ncbi.nlm.nih.gov/pubmed/26949186

152. Klein F, Diskin R, Scheid JF, Gaebler C, Mouquet H, Georgiev IS, et al. Somatic mutations of the immunoglobulin framework are generally required for broad and potent HIV-1 neutralization. Cell. 2013 Mar;153(1):126–38.

153. Aasa-Chapman MMI, Hayman A, Newton P, Cornforth D, Williams I, Borrow P, et al. Development of the antibody response in acute HIV-1 infection. AIDS. 2004 Feb;18(3):371–81.

154. Stiegler G, Kunert R, Purtscher M, Wolbank S, Voglauer R, Steindl F, et al. A potent cross-clade neutralizing human monoclonal antibody against a novel epitope on gp41 of human immunodeficiency virus type 1. AIDS Res Hum Retroviruses. 2001;17(18):1757–65.

155. Trkola A, Pomales AB, Yuan H, Korber B, Maddon PJ, Allaway GP, et al. Cross-clade neutralization of primary isolates of human immunodeficiency virus type 1 by human monoclonal antibodies and tetrameric CD4-IgG. J Virol. 1995;69(11):6609–17.

156. Moog C, Dereuddre-Bosquet N, Teillaud JL, Biedma ME, Holl V, Van Ham G, et al. Protective effect of vaginal application of neutralizing and nonneutralizing inhibitory antibodies against vaginal SHIV challenge in macaques. Mucosal Immunol. 2014;7(1):46–56.

157. Butler AL, Fischinger S, Alter G. The Antibodiome-Mapping the Humoral Immune Response to HIV. Curr HIV/AIDS Rep. 2019 Apr;16(2):169–79.

158. Mikell I, Sather DN, Kalams SA, Altfeld M, Alter G, Stamatatos L. Characteristics of the earliest cross-neutralizing antibody response to HIV-1. PLoS Pathog. 2011 Jan;7(1):e1001251.

159. Sagar M, Wu X, Lee S, Overbaugh J. Human immunodeficiency virus type 1 V1-V2 envelope loop sequences expand and add glycosylation sites over the course of infection, and these modifications affect antibody neutralization sensitivity. J Virol. 2006 Oct;80(19):9586–98.

160. Liao H-X, Lynch R, Zhou T, Gao F, Alam SM, Boyd SD, et al. Co-evolution of a broadly neutralizing

HIV-1 antibody and founder virus. Nature [Internet]. 2013/04/03. 2013 Apr 25;496(7446):469–76. Available from: https://www.ncbi.nlm.nih.gov/pubmed/23552890

161. Casado C, Colombo S, Rauch A, Martínez R, Günthard HF, Garcia S, et al. Host and viral genetic correlates of clinical definitions of HIV-1 disease progression. PLoS One. 2010 Jun;5(6):e11079.

162. Pereyra F, Jia X, McLaren PJ, Telenti A, de Bakker PIW, Walker BD, et al. The major genetic determinants of HIV-1 control affect HLA class I peptide presentation. Science. 2010 Dec;330(6010):1551–7.

163. Laguette N, Sobhian B, Casartelli N, Ringeard M, Chable-Bessia C, Ségéral E, et al. SAMHD1 is the dendritic- and myeloid-cell-specific HIV-1 restriction factor counteracted by Vpx. Nature. 2011 May;474(7353):654–7.

164. Neil SJD, Zang T, Bieniasz PD. Tetherin inhibits retrovirus release and is antagonized by HIV-1 Vpu. Nature. 2008 Jan;451(7177):425–30.

165. Stremlau M, Owens CM, Perron MJ, Kiessling M, Autissier P, Sodroski J. The cytoplasmic body component TRIM5alpha restricts HIV-1 infection in Old World monkeys. Nature. 2004 Feb;427(6977):848–53.

166. Sheehy AM, Gaddis NC, Choi JD, Malim MH. Isolation of a human gene that inhibits HIV-1 infection and is suppressed by the viral Vif protein. Nature. 2002 Aug;418(6898):646–50.

167. Laher F, Ranasinghe S, Porichis F, Mewalal N, Pretorius K, Ismail N, et al. HIV Controllers Exhibit Enhanced Frequencies of Major Histocompatibility Complex Class II Tetramer(+) Gag-Specific CD4(+) T Cells in Chronic Clade C HIV-1 Infection. J Virol. 2017 Apr;91(7).

168. Dinges WL, Richardt J, Friedrich D, Jalbert E, Liu Y, Stevens CE, et al. Virus-specific CD8+ T-cell responses better define HIV disease progression than HLA genotype. J Virol. 2010;84(9):4461–

8.

169. Braibant M, Brunet S, Costagliola D, Rouzioux C, Agut H, Katinger H, et al. Antibodies to conserved epitopes of the HIV-1 envelope in sera from long-term non-progressors: prevalence and association with neutralizing activity. AIDS. 2006 Oct;20(15):1923–30.

170. González N, McKee K, Lynch RM, Georgiev IS, Jimenez L, Grau E, et al. Characterization of broadly neutralizing antibody responses to HIV-1 in a cohort of long term non-progressors. PLoS One. 2018;13(3):e0193773.

171. Crowell TA, Gebo KA, Blankson JN, Korthuis PT, Yehia BR, Rutstein RM, et al. Hospitalization Rates and Reasons Among HIV Elite Controllers and Persons With Medically Controlled HIV Infection. J Infect Dis [Internet]. 2014/12/15. 2015 Jun 1;211(11):1692–702. Available from: https://www.ncbi.nlm.nih.gov/pubmed/25512624

172. Wu X, Zhang Z, Schramm CA, Joyce MG, Kwon YD, Zhou T, et al. Maturation and Diversity of the VRC01-Antibody Lineage over 15 Years of Chronic HIV-1 Infection. Cell. 2015;161(3):470–85.

173. Simek MD, Rida W, Priddy FH, Pung P, Carrow E, Laufer DS, et al. Human immunodeficiency virus type 1 elite neutralizers: individuals with broad and potent neutralizing activity identified by using a high-throughput neutralization assay together with an analytical selection algorithm. J Virol. 2009 Jul;83(14):7337–48.

174. Moore PL, Williamson C, Morris L. Virological features associated with the development of broadly neutralizing antibodies to HIV-1. Trends Microbiol. 2015 Apr;23(4):204–11.

175. McCoy LE, Burton DR. Identification and specificity of broadly neutralizing antibodies against HIV. Immunol Rev. 2017 Jan;275(1):11–20.

176. Burton DR, Pyati J, Koduri R, Sharp SJ, Thornton GB, Parren PW, et al. Efficient neutralization of primary isolates of HIV-1 by a recombinant human monoclonal antibody. Science. 1994 Nov;266(5187):1024–7.

177. Kwong PD, Mascola JR, Nabel GJ. Broadly neutralizing antibodies and the search for an HIV-1 vaccine: the end of the beginning. Nat Rev Immunol. 2013;13(9):693–701.

178. Sok D, Burton DR. Recent progress in broadly neutralizing antibodies to HIV. Nat Immunol. 2018 Nov;19(11):1179–88.

179. McCoy LE. The expanding array of HIV broadly neutralizing antibodies. Retrovirology. 2018 Oct;15(1):70.

180. Steichen JM, Kulp DW, Tokatlian T, Escolano A, Dosenovic P, Stanfield RL, et al. HIV Vaccine Design to Target Germline Precursors of Glycan-Dependent Broadly Neutralizing Antibodies. Immunity. 2016 Sep;45(3):483–96.

181. Chung AW, Navis M, Isitman G, Centre R, Finlayson R, Bloch M, et al. Activation of NK cells by ADCC responses during early HIV infection. Viral Immunol. 2011 Apr;24(2):171–5.

182. Su B, Dispinseri S, Iannone V, Zhang T, Wu H, Carapito R, et al. Update on Fc-Mediated Antibody Functions Against HIV-1 Beyond Neutralization. Front Immunol. 2019;10:2968.

183. Forthal DN, Landucci G, Daar ES. Antibody from patients with acute human immunodeficiency virus (HIV) infection inhibits primary strains of HIV type 1 in the presence of natural-killer effector cells. J Virol. 2001 Aug;75(15):6953–61.

184. Gómez-Román VR, Patterson LJ, Venzon D, Liewehr D, Aldrich K, Florese R, et al. Vaccine-elicited antibodies mediate antibody-dependent cellular cytotoxicity correlated with significantly reduced acute viremia in rhesus macaques challenged with SIVmac251. J Immunol.

2005 Feb;174(4):2185–9.

185. Wren LH, Chung AW, Isitman G, Kelleher AD, Parsons MS, Amin J, et al. Specific antibody-dependent cellular cytotoxicity responses associated with slow progression of HIV infection. Immunology. 2013 Feb;138(2):116–23.

186. Haynes BF, Gilbert PB, McElrath MJ, Zolla-Pazner S, Tomaras GD, Alam SM, et al. Immune-correlates analysis of an HIV-1 vaccine efficacy trial. N Engl J Med [Internet]. 2012 Apr 5;366(14):1275–86. Available from: https://www.ncbi.nlm.nih.gov/pubmed/22475592

187. Barouch DH, Stephenson KE, Borducchi EN, Smith K, Stanley K, McNally AG, et al. Protective Efficacy of a Global HIV-1 Mosaic Vaccine Against Heterologous SHIV Challenges in Rhesus Monkeys. Cell. 2013;155(3).

188. Ackerman ME, Dugast A-S, McAndrew EG, Tsoukas S, Licht AF, Irvine DJ, et al. Enhanced phagocytic activity of HIV-specific antibodies correlates with natural production of immunoglobulins with skewed affinity for FcγR2a and FcγR2b. J Virol. 2013 May;87(10):5468–76.

189. Forthal DN, Moog C. Fc receptor-mediated antiviral antibodies. Curr Opin HIV AIDS. 2009 Sep;4(5):388–93.

190. Halstead SB, O'Rourke EJ. Dengue viruses and mononuclear phagocytes. I. Infection enhancement by non-neutralizing antibody. J Exp Med. 1977 Jul;146(1):201–17.

191. Mayr L, Su B, Moog C. Role of nonneutralizing antibodies in vaccines and/or HIV infected individuals. Curr Opin HIV AIDS. 2017 May;12(3):209–15.

192. Dugast AS, Stamatatos L, Tonelli A, Suscovich TJ, Licht AF, Mikell I, et al. Independent evolution of Fc- and Fab-mediated HIV-1-specific antiviral antibody activity following acute infection. Eur

J Immunol. 2014;44(10):2925–37.

193. Ackerman ME, Mikhailova A, Brown EP, Dowell KG, Walker BD, Bailey-Kellogg C, et al. Polyfunctional HIV-Specific Antibody Responses Are Associated with Spontaneous HIV Control. PLoS Pathog [Internet]. 2016 Jan 8;12(1):e1005315–e1005315. Available from: https://www.ncbi.nlm.nih.gov/pubmed/26745376

194. Pinto LA, Sullivan J, Berzofsky JA, Clerici M, Kessler HA, Landay AL, et al. ENV-specific cytotoxic T lymphocyte responses in HIV seronegative health care workers occupationally exposed to HIV-contaminated body fluids. J Clin Invest. 1995 Aug;96(2):867–76.

195. Cheynier R, Langlade-Demoyen P, Marescot MR, Blanche S, Blondin G, Wain-Hobson S, et al. Cytotoxic T lymphocyte responses in the peripheral blood of children born to human immunodeficiency virus-1-infected mothers. Eur J Immunol. 1992 Sep;22(9):2211–7.

196. Clerici M, Giorgi J V, Chou CC, Gudeman VK, Zack JA, Gupta P, et al. Cell-mediated immune response to human immunodeficiency virus (HIV) type 1 in seronegative homosexual men with recent sexual exposure to HIV-1. J Infect Dis. 1992 Jun;165(6):1012–9.

197. Clerici M, Levin JM, Kessler HA, Harris A, Berzofsky JA, Landay AL, et al. HIV-specific T-helper activity in seronegative health care workers exposed to contaminated blood. JAMA. 1994 Jan;271(1):42–6.

198. Borrow P, Lewicki H, Hahn BH, Shaw GM, Oldstone MB. Virus-specific CD8+ cytotoxic T-lymphocyte activity associated with control of viremia in primary human immunodeficiency virus type 1 infection. J Virol [Internet]. 1994 Sep 1;68(9):6103 LP – 6110. Available from: http://jvi.asm.org/content/68/9/6103.abstract

199. Musey L, Hughes J, Schacker T, Shea T, Corey L, McElrath MJ. Cytotoxic-T-cell responses, viral load, and disease progression in early human immunodeficiency virus type 1 infection. N Engl

J Med. 1997 Oct;337(18):1267–74.

200. Fowke KR, Nagelkerke NJ, Kimani J, Simonsen JN, Anzala AO, Bwayo JJ, et al. Resistance to HIV-1 infection among persistently seronegative prostitutes in Nairobi, Kenya. Lancet (London, England). 1996 Nov;348(9038):1347–51.

201. Tomescu C, Abdulhaqq S, Montaner LJ. Evidence for the innate immune response as a correlate of protection in human immunodeficiency virus (HIV)-1 highly exposed seronegative subjects (HESN). Clin Exp Immunol [Internet]. 2011 May;164(2):158–69. Available from: https://www.ncbi.nlm.nih.gov/pubmed/21413945

202. Carrington M, O'Brien SJ. The influence of HLA genotype on AIDS. Annu Rev Med. 2003;54:535–51.

203. MacDonald KS, Fowke KR, Kimani J, Dunand VA, Nagelkerke NJ, Ball TB, et al. Influence of HLA supertypes on susceptibility and resistance to human immunodeficiency virus type 1 infection. J Infect Dis. 2000 May;181(5):1581–9.

204. Philpott S, Weiser B, Tarwater P, Vermund SH, Kleeberger CA, Gange SJ, et al. CC chemokine receptor 5 genotype and susceptibility to transmission of human immunodeficiency virus type 1 in women. J Infect Dis [Internet]. 2003/01/29. 2003 Feb 15;187(4):569–75. Available from: https://www.ncbi.nlm.nih.gov/pubmed/12599073

205. Marmor M, Sheppard HW, Donnell D, Bozeman S, Celum C, Buchbinder S, et al. Homozygous and heterozygous CCR5-Delta32 genotypes are associated with resistance to HIV infection. J Acquir Immune Defic Syndr. 2001 Aug;27(5):472–81.

206. Boulet S, Sharafi S, Simic N, Bruneau J, Routy J-P, Tsoukas CM, et al. Increased proportion of KIR3DS1 homozygotes in HIV-exposed uninfected individuals. AIDS. 2008 Mar;22(5):595–9.

207. Martin MP, Qi Y, Gao X, Yamada E, Martin JN, Pereyra F, et al. Innate partnership of HLA-B and KIR3DL1 subtypes against HIV-1. Nat Genet [Internet]. 2007/05/13. 2007 Jun;39(6):733–40. Available from: https://www.ncbi.nlm.nih.gov/pubmed/17496894

208. Boulet S, Kleyman M, Kim JY, Kamya P, Sharafi S, Simic N, et al. A combined genotype of KIR3DL1 high expressing alleles and HLA-B*57 is associated with a reduced risk of HIV infection. AIDS. 2008 Jul;22(12):1487–91.

209. Tallon BJM, Bruneau J, Tsoukas CM, Routy J-P, Kiani Z, Tan X, et al. Time to seroconversion in HIV-exposed subjects carrying protective versus non protective KIR3DS1/L1 and HLA-B genotypes. PLoS One [Internet]. 2014 Oct 17;9(10):e110480–e110480. Available from: https://www.ncbi.nlm.nih.gov/pubmed/25330014

210. Scott-Algara D, Truong LX, Versmisse P, David A, Luong TT, Nguyen N V, et al. Cutting edge: increased NK cell activity in HIV-1-exposed but uninfected Vietnamese intravascular drug users. J Immunol. 2003 Dec;171(11):5663–7.

211. Montoya CJ, Velilla PA, Chougnet C, Landay AL, Rugeles MT. Increased IFN-gamma production by NK and CD3+/CD56+ cells in sexually HIV-1-exposed but uninfected individuals. Clin Immunol. 2006 Aug;120(2):138–46.

212. Ghadially H, Keynan Y, Kimani J, Kimani M, Ball TB, Plummer FA, et al. Altered dendritic cell-natural killer interaction in Kenyan sex workers resistant to HIV-1 infection. AIDS. 2012 Feb;26(4):429–36.

213. Tomescu C, Duh F-M, Lanier MA, Kapalko A, Mounzer KC, Martin MP, et al. Increased plasmacytoid dendritic cell maturation and natural killer cell activation in HIV-1 exposed, uninfected intravenous drug users. AIDS [Internet]. 2010 Sep 10;24(14):2151–60. Available from: https://www.ncbi.nlm.nih.gov/pubmed/20647906

214. Hasselrot K, Bratt G, Duvefelt K, Hirbod T, Sandstrom E, Broliden K. HIV-1 exposed uninfected men who have sex with men have increased levels of salivary CC-chemokines associated with sexual behavior. AIDS. 2010 Jun;24(10):1569–75.

215. Levinson P, Kaul R, Kimani J, Ngugi E, Moses S, MacDonald KS, et al. Levels of innate immune factors in genital fluids: association of alpha defensins and LL-37 with genital infections and increased HIV acquisition. AIDS. 2009 Jan;23(3):309–17.

216. Ranki A, Mattinen S, Yarchoan R, Broder S, Ghrayeb J, Lahdevirta J, et al. T-cell response towards HIV in infected individuals with and without zidovudine therapy, and in HIV-exposed sexual partners. AIDS. 1989 Feb;3(2):63–9.

217. Beretta A, Furci L, Burastero S, Cosma A, Dinelli ME, Lopalco L, et al. HIV-1-specific immunity in persistently seronegative individuals at high risk for HIV infection. Immunol Lett. 1996 Jun;51(1–2):39–43.

218. Mazzoli S, Trabattoni D, Lo Caputo S, Piconi S, Ble C, Meacci F, et al. HIV-specific mucosal and cellular immunity in HIV-seronegative partners of HIV-seropositive individuals. Nat Med. 1997 Nov;3(11):1250–7.

219. Restrepo C, Rallon NI, del Romero J, Rodriguez C, Hernando V, Lopez M, et al. Low-level exposure to HIV induces virus-specific T cell responses and immune activation in exposed HIV-seronegative individuals. J Immunol. 2010 Jul;185(2):982–9.

220. Alimonti JB, Kimani J, Matu L, Wachihi C, Kaul R, Plummer FA, et al. Characterization of CD8 T-cell responses in HIV-1-exposed seronegative commercial sex workers from Nairobi, Kenya. Immunol Cell Biol. 2006 Oct;84(5):482–5.

221. Kaul R, Rowland-Jones SL, Kimani J, Fowke K, Dong T, Kiama P, et al. New insights into HIV-1 specific cytotoxic T-lymphocyte responses in exposed, persistently seronegative Kenyan sex

workers. Immunol Lett. 2001 Nov;79(1–2):3–13.

222. Kuebler PJ, Shaw BI, Leadabrand KS, Mehrotra ML, Grant RM, Kallas EG, et al. Brief Report: HIV-1 gp120 T-Cell Responses Correspond to Infection Outcomes in the Global iPrEx Chemoprophylaxis Trial. J Acquir Immune Defic Syndr. 2016 Jun;72(2):184–8.

223. Nguyen M, Pean P, Lopalco L, Nouhin J, Phoung V, Ly N, et al. HIV-specific antibodies but not t-cell responses are associated with protection in seronegative partners of HIV-1-infected individuals in Cambodia. J Acquir Immune Defic Syndr. 2006 Aug;42(4):412–9.

224. Tudor D, Derrien M, Diomede L, Drillet AS, Houimel M, Moog C, et al. HIV-1 gp41-specific monoclonal mucosal IgAs derived from highly exposed but IgG-seronegative individuals block HIV-1 epithelial transcytosis and neutralize CD4(+) cell infection: an IgA gene and functional analysis. Mucosal Immunol. 2009;2(5):412–26.

225. Carrillo J, Restrepo C, Rallon NI, Massanella M, del Romero J, Rodriguez C, et al. HIV exposed seronegative individuals show antibodies specifically recognizing native HIV envelope glycoprotein. AIDS. 2013 Jun;27(9):1375–85.

226. Letvin NL, Rao SS, Dang V, Buzby AP, Korioth-Schmitz B, Dombagoda D, et al. No evidence for consistent virus-specific immunity in simian immunodeficiency virus-exposed, uninfected rhesus monkeys. J Virol [Internet]. 2007/08/08. 2007 Nov;81(22):12368–74. Available from: https://www.ncbi.nlm.nih.gov/pubmed/17686853

227. Camara M, Dieye TN, Seydi M, Diallo AA, Fall M, Diaw PA, et al. Low-level CD4+ T cell activation in HIV-exposed seronegative subjects: influence of gender and condom use. J Infect Dis. 2010 Mar;201(6):835–42.

228. Palmer CD, Tomassilli J, Sirignano M, Romero-Tejeda M, Arnold KB, Che D, et al. Enhanced immune activation linked to endotoxemia in HIV-1 seronegative MSM. AIDS. 2014

Sep;28(14):2162–6.

229. Barouch DH. The Quest for an HIV-1 Vaccine — Moving Forward. N Engl J Med. 2013;

230. Kim JH, Excler J-L, Michael NL. Lessons from the RV144 Thai phase III HIV-1 vaccine trial and the search for correlates of protection. Annu Rev Med. 2015;66:423–37.

231. Bonsignori M, Pollara J, Moody MA, Alpert MD, Chen X, Hwang K-K, et al. Antibody-dependent cellular cytotoxicity-mediating antibodies from an HIV-1 vaccine efficacy trial target multiple epitopes and preferentially use the VH1 gene family. J Virol [Internet]. 2012/08/15. 2012 Nov;86(21):11521–32. Available from: https://www.ncbi.nlm.nih.gov/pubmed/22896626

232. Rerks-Ngarm S, Pitisuttithum P, Nitayaphan S, Kaewkungwal J, Chiu J, Paris R, et al. Vaccination with ALVAC and AIDSVAX to prevent HIV-1 infection in Thailand. N Engl J Med [Internet]. 2009;361(23):2209–20. Available from: http://www.ncbi.nlm.nih.gov/pubmed/19843557

233. Forthal D, Hope TJ, Alter G. New paradigms for functional HIV-specific nonneutralizing antibodies. Curr Opin HIV AIDS [Internet]. 2013;8(5):393–401. Available from: http://www.ncbi.nlm.nih.gov/pubmed/23924999

234. Gray GE, Huang Y, Grunenberg N, Laher F, Roux S, Andersen-Nissen E, et al. Immune correlates of the Thai RV144 HIV vaccine regimen in South Africa. Sci Transl Med. 2019 Sep;11(510).

235. Laher F, Moodie Z, Cohen KW, Grunenberg N, Bekker L-G, Allen M, et al. Safety and immune responses after a 12-month booster in healthy HIV-uninfected adults in HVTN 100 in South Africa: A randomized double-blind placebo-controlled trial of ALVAC-HIV (vCP2438) and bivalent subtype C gp120/MF59 vaccines. PLoS Med. 2020 Feb;17(2):e1003038.

236. UNAIDS. Press statement- HVTN 702 clinical trial of an HIV vaccine stopped [Internet]. 2020. Available from:

https://www.unaids.org/en/resources/presscentre/pressreleaseandstatementarchive/2020/february/20200204_vaccine

237. Zhao LP, Fiore-Gartland A, Carpp LN, Cohen KW, Rouphael N, Fleurs L, et al. Landscapes of binding antibody and T-cell responses to pox-protein HIV vaccines in Thais and South Africans. PLoS One. 2020;15(1):e0226803.

238. Tolbert WD, Van V, Sherburn R, Tuyishime M, Yan F, Nguyen DN, et al. Recognition Patterns of the C1/C2 Epitopes Involved in Fc-Mediated Response in HIV-1 Natural Infection and the RV114 Vaccine Trial. MBio. 2020 Jun;11(3).

239. Flynn NM, Forthal DN, Harro CD, Judson FN, Mayer KH, Para MF. Placebo-controlled phase 3 trial of a recombinant glycoprotein 120 vaccine to prevent HIV-1 infection. J Infect Dis. 2005;191(5):654–65.

240. Pitisuttithum P, Gilbert P, Gurwith M, Heyward W, Martin M, van Griensven F, et al. Randomized, double-blind, placebo-controlled efficacy trial of a bivalent recombinant glycoprotein 120 HIV-1 vaccine among injection drug users in Bangkok, Thailand. In: J Infect Dis. United States; 2006. p. 1661–71.

241. McElrath MJ, De Rosa SC, Moodie Z, Dubey S, Kierstead L, Janes H, et al. HIV-1 vaccine-induced immunity in the test-of-concept Step Study: a case-cohort analysis. Lancet [Internet]. 2008;372(9653):1894–905. Available from: http://www.ncbi.nlm.nih.gov/pubmed/19012957

242. Gray GE, Allen M, Moodie Z, Churchyard G, Bekker LG, Nchabeleng M, et al. Safety and efficacy of the HVTN 503/Phambili study of a clade-B-based HIV-1 vaccine in South Africa: a double-blind, randomised, placebo-controlled test-of-concept phase 2b study. Lancet Infect Dis. 2011;11(7):507–15.

243. Carrillo J, Clotet B, Blanco J. Antibodies and Antibody Derivatives: New Partners in HIV

Eradication Strategies. Front Immunol [Internet]. 2018 Oct 23;9:2429. Available from: https://www.ncbi.nlm.nih.gov/pubmed/30405624

244. Margolis DM, Koup RA, Ferrari G. HIV antibodies for treatment of HIV infection. Immunol Rev. 2017 Jan;275(1):313–23.

245. Spivak AM, Planelles V. Novel Latency Reversal Agents for HIV-1 Cure. Annu Rev Med. 2018 Jan;69:421–36.

246. Archin NM, Liberty AL, Kashuba AD, Choudhary SK, Kuruc JD, Crooks AM, et al. Administration of vorinostat disrupts HIV-1 latency in patients on antiretroviral therapy. Nature. 2012 Jul;487(7408):482–5.

247. Sgarbanti M, Battistini A. Therapeutics for HIV-1 reactivation from latency. Curr Opin Virol. 2013 Aug;3(4):394–401.

248. Deeks SG. HIV: Shock and kill. Vol. 487, Nature. England; 2012. p. 439–40.

249. Saayman S, Ali SA, Morris K V, Weinberg MS. The therapeutic application of CRISPR/Cas9 technologies for HIV. Expert Opin Biol Ther [Internet]. 2015/04/12. 2015 Jun;15(6):819–30. Available from: https://www.ncbi.nlm.nih.gov/pubmed/25865334

250. Dash PK, Kaminski R, Bella R, Su H, Mathews S, Ahooyi TM, et al. Sequential LASER ART and CRISPR Treatments Eliminate HIV-1 in a Subset of Infected Humanized Mice. Nat Commun. 2019 Jul;10(1):2753.

251. Hutter G, Nowak D, Mossner M, Ganepola S, Mussig A, Allers K, et al. Long-term control of HIV by CCR5 Delta32/Delta32 stem-cell transplantation. N Engl J Med. 2009 Feb;360(7):692–8.

252. Gupta RK, Abdul-Jawad S, McCoy LE, Mok HP, Peppa D, Salgado M, et al. HIV-1 remission following CCR5Delta32/Delta32 haematopoietic stem-cell transplantation. Nature. 2019

Apr;568(7751):244–8.

253. Hessell AJ, Rakasz EG, Tehrani DM, Huber M, Weisgrau KL, Landucci G, et al. Broadly neutralizing monoclonal antibodies 2F5 and 4E10 directed against the human immunodeficiency virus type 1 gp41 membrane-proximal external region protect against mucosal challenge by simian-human immunodeficiency virus SHIVBa-L. J Virol. 2010;84(3):1302–13.

254. Bomsel M, Tudor D, Drillet AS, Alfsen A, Ganor Y, Roger MG, et al. Immunization with HIV-1 gp41 subunit virosomes induces mucosal antibodies protecting nonhuman primates against vaginal SHIV challenges. Immunity. 2011;34(2):269–80.

255. Santra S, Tomaras GD, Warrier R, Nicely NI, Liao HX, Pollara J, et al. Human Non-neutralizing HIV-1 Envelope Monoclonal Antibodies Limit the Number of Founder Viruses during SHIV Mucosal Infection in Rhesus Macaques. PLoS Pathog [Internet]. 2015;11(8):e1005042. Available from: http://www.ncbi.nlm.nih.gov/pubmed/26237403

256. Kong R, Xu K, Zhou T, Acharya P, Lemmin T, Liu K, et al. Fusion peptide of HIV-1 as a site of vulnerability to neutralizing antibody. Science. 2016 May;352(6287):828–33.

257. van Gils MJ, van den Kerkhof TLGM, Ozorowski G, Cottrell CA, Sok D, Pauthner M, et al. An HIV-1 antibody from an elite neutralizer implicates the fusion peptide as a site of vulnerability. Nat Microbiol. 2016 Nov;2:16199.

258. Ou L, Kong W-P, Chuang G-Y, Ghosh M, Gulla K, O'Dell S, et al. Preclinical Development of a Fusion Peptide Conjugate as an HIV Vaccine Immunogen. Sci Rep. 2020 Feb;10(1):3032.

259. Chaplin DD. Overview of the immune response. J Allergy Clin Immunol. 2010 Feb;125(2 Suppl 2):S3-23.

260. Liao HX, Chen X, Munshaw S, Zhang R, Marshall DJ, Vandergrift N, et al. Initial antibodies binding to HIV-1 gp41 in acutely infected subjects are polyreactive and highly mutated. J Exp Med [Internet]. 2011;208(11):2237–49. Available from: http://www.ncbi.nlm.nih.gov/pubmed/21987658

261. Weitkamp J-H, Kallewaard N, Kusuhara K, Bures E, Williams J V, LaFleur B, et al. Infant and adult human B cell responses to rotavirus share common immunodominant variable gene repertoires. J Immunol. 2003 Nov;171(9):4680–8.

262. Su LF, Kidd BA, Han A, Kotzin JJ, Davis MM. Virus-specific CD4(+) memory-phenotype T cells are abundant in unexposed adults. Immunity. 2013 Feb;38(2):373–83.

263. Trama AM, Moody MA, Alam SM, Jaeger FH, Lockwood B, Parks R, et al. HIV-1 envelope gp41 antibodies can originate from terminal ileum B cells that share cross-reactivity with commensal bacteria. Cell Host Microbe [Internet]. 2014;16(2):215–26. Available from: http://www.ncbi.nlm.nih.gov/pubmed/25121750

264. Williams WB, Liao HX, Moody MA, Kepler TB, Alam SM, Gao F, et al. HIV-1 VACCINES. Diversion of HIV-1 vaccine-induced immunity by gp41-microbiota cross-reactive antibodies. Science (80-) [Internet]. 2015;349(6249):aab1253. Available from: http://www.ncbi.nlm.nih.gov/pubmed/26229114

265. Zimmermann P, Curtis N. The influence of the intestinal microbiome on vaccine responses. Vaccine. 2018 Jul;36(30):4433–9.

266. Jamieson AM. Influence of the microbiome on response to vaccination. Hum Vaccin Immunother. 2015;11(9):2329–31.

267. Cram JA, Fiore-Gartland AJ, Srinivasan S, Karuna S, Pantaleo G, Tomaras GD, et al. Human gut microbiota is associated with HIV-reactive immunoglobulin at baseline and following HIV

vaccination. PLoS One. 2019;14(12):e0225622.

268. Long JE, Drayson MT, Taylor AE, Toellner KM, Lord JM, Phillips AC. Morning vaccination enhances antibody response over afternoon vaccination: A cluster-randomised trial. Vaccine. 2016 May;34(24):2679–85.

269. Long JE, Ring C, Drayson M, Bosch J, Campbell JP, Bhabra J, et al. Vaccination response following aerobic exercise: can a brisk walk enhance antibody response to pneumococcal and influenza vaccinations? Brain Behav Immun. 2012;26(4):680–7.

270. Miller E, Andrews N, Waight P, Findlow H, Ashton L, England A, et al. Safety and immunogenicity of coadministering a combined meningococcal serogroup C and Haemophilus influenzae type b conjugate vaccine with 7-valent pneumococcal conjugate vaccine and measles, mumps, and rubella vaccine at 12 months of age. Clin Vaccine Immunol. 2011 Mar;18(3):367–72.

271. Elliman D, Bedford H. Safety and efficacy of combination vaccines. Vol. 326, BMJ (Clinical research ed.). 2003. p. 995–6.

272. England PH. Complete routine immunisation schedule. 2019.

273. Agallou M, Athanasiou E, Koutsoni O, Dotsika E, Karagouni E. Experimental Validation of Multi-Epitope Peptides Including Promising MHC Class I- and II-Restricted Epitopes of Four Known Leishmania infantum Proteins [Internet]. Vol. 5, Frontiers in Immunology . 2014. p. 268. Available from: https://www.frontiersin.org/article/10.3389/fimmu.2014.00268

274. Nezafat N, Eslami M, Negahdaripour M, Rahbar MR, Ghasemi Y. Designing an efficient multi-epitope oral vaccine against Helicobacter pylori using immunoinformatics and structural vaccinology approaches. Mol Biosyst. 2017 Mar;13(4):699–713.

275. Nwokolo N, Hill A, McOwan A, Pozniak A. Rapidly declining HIV infection in MSM in central London. lancet HIV. 2017 Nov;4(11):e482–3.

276. FDA. ARCHITECT HIV Ag/Ab Combo [Internet]. Available from: https://www.fda.gov/media/116836/download

277. Pavie J, Rachline A, Loze B, Niedbalski L, Delaugerre C, Laforgerie E, et al. Sensitivity of five rapid HIV tests on oral fluid or finger-stick whole blood: a real-time comparison in a healthcare setting. PLoS One. 2010 Jul;5(7):e11581.

278. Boder ET, Wittrup KD. Yeast surface display for screening combinatorial polypeptide libraries. Nat Biotechnol. 1997;15(6):553–7.

279. Chao G, Lau WL, Hackel BJ, Sazinsky SL, Lippow SM, Wittrup KD. Isolating and engineering human antibodies using yeast surface display. Nat Protoc. 2006;1(2):755–68.

280. Grimm SK, Battles MB, Ackerman ME. Directed evolution of a yeast-displayed HIV-1 SOSIP gp140 spike protein toward improved expression and affinity for conformational antibodies. PLoS One. 2015;10(2):e0117227.

281. Hall TA. BioEdit: a user-friendly biological sequence alignment editor and analysis program for Windows 95/98/NT. Nucl Acids Symp. 1999;41:95–98.

282. Zuo T, Shi X, Liu Z, Guo L, Zhao Q, Guan T, et al. Comprehensive analysis of pathogen-specific antibody response in vivo based on an antigen library displayed on surface of yeast. J Biol Chem. 2011;286(38):33511–9.

283. Luo K, Li S, Jiang L, Zuo T, Qing J, Shi X, et al. Combinatorial library-based profiling of the antibody response against hepatitis C virus in humans. J Gen Virol. 2015 Jan;96(Pt 1):52–63.

284. Smith K, Garman L, Wrammert J, Zheng N-Y, Capra JD, Ahmed R, et al. m. Nat Protoc.

2009;4(3):372–84.

285. Wardemann H, Yurasov S, Schaefer A, Young JW, Meffre E, Nussenzweig MC. Predominant autoantibody production by early human B cell precursors. Science. 2003 Sep;301(5638):1374–7.

286. Tiller T, Meffre E, Yurasov S, Tsuiji M, Nussenzweig MC, Wardemann H. Efficient generation of monoclonal antibodies from single human B cells by single cell RT-PCR and expression vector cloning. J Immunol Methods [Internet]. 2007/10/31. 2008 Jan 1;329(1–2):112–24. Available from: https://www.ncbi.nlm.nih.gov/pubmed/17996249

287. Graham FL, Smiley J, Russell WC, Nairn R. Characteristics of a human cell line transformed by DNA from human adenovirus type 5. J Gen Virol. 1977 Jul;36(1):59–74.

288. Ferrari G, Pollara J, Kozink D, Harms T, Drinker M, Freel S, et al. An HIV-1 gp120 envelope human monoclonal antibody that recognizes a C1 conformational epitope mediates potent antibody-dependent cellular cytotoxicity (ADCC) activity and defines a common ADCC epitope in human HIV-1 serum. J Virol. 2011 Jul;85(14):7029–36.

289. NIH. NIH AIDS Reagent Program [Internet]. 2014. p. 14–5. Available from: https://www.aidsreagent.org/reagentdetail.cfm?t=Polyclonal_Antibodies&id=157

290. Gomez-Roman VR, Florese RH, Patterson LJ, Peng B, Venzon D, Aldrich K, et al. A simplified method for the rapid fluorometric assessment of antibody-dependent cell-mediated cytotoxicity. J Immunol Methods [Internet]. 2006;308(1–2):53–67. Available from: http://www.ncbi.nlm.nih.gov/entrez/query.fcgi?cmd=Retrieve&db=PubMed&dopt=Citation&list_uids=16343526

291. Imagawa DT, Lee MH, Wolinsky SM, Sano K, Morales F, Kwok S, et al. Human immunodeficiency virus type 1 infection in homosexual men who remain seronegative for prolonged periods. N

Engl J Med. 1989 Jun;320(22):1458–62.

292. Gibbons J, Cory JM, Hewlett IK, Epstein JS, Eyster ME. Silent infections with human immunodeficiency virus type 1 are highly unlikely in multitransfused seronegative hemophiliacs. Blood. 1990 Nov;76(10):1924–6.

293. Ferrer-Le-Coeur F, Mariotti M, Hivert P, Satre EP, Bouchardeau F, Couroucé AM, et al. No evidence of HIV-1 infection in seronegative hemophiliacs and in seronegative partners of seropositive hemophiliacs through polymerase chain reaction (PCR) and anti-NEF serology. Thromb Haemost. 1991 May;65(5):478–82.

294. Brettler DB, Somasundaran M, Forsberg AF, Krause E, Sullivan JL. Silent human immunodeficiency virus type 1 infection: a rare occurrence in a high-risk heterosexual population. Blood. 1992 Nov;80(9):2396–400.

295. Moore JP, Ho DD. Antibodies to discontinuous or conformationally sensitive epitopes on the gp120 glycoprotein of human immunodeficiency virus type 1 are highly prevalent in sera of infected humans. J Virol. 1993 Feb;67(2):863–75.

296. Aiuti F, Ensoli F, Fiorelli V, Mezzaroma I, Pinter E, Guerra E, et al. Silent HIV infection. Vaccine. 1993;11(5):538–41.

297. McChesney MB, Collins JR, Lu D, Lu X, Torten J, Ashley RL, et al. Occult systemic infection and persistent simian immunodeficiency virus (SIV)-specific CD4(+)-T-cell proliferative responses in rhesus macaques that were transiently viremic after intravaginal inoculation of SIV. J Virol. 1998 Dec;72(12):10029–35.

298. Dittmer U, Stahl-Hennig C, Coulibaly C, Nisslein T, Lüke W, Fuchs D, et al. Repeated exposure of rhesus macaques to low doses of simian immunodeficiency virus (SIV) did not protect them against the consequences of a high-dose SIV challenge. J Gen Virol. 1995 Jun;76 (Pt 6):1307–

15.

299. Regoes RR. The role of exposure history on HIV acquisition: insights from repeated low-dose challenge studies. PLoS Comput Biol. 2012;8(11):e1002767.

300. DeGruttola V, Seage GR 3rd, Mayer KH, Horsburgh CRJ. Infectiousness of HIV between male homosexual partners. J Clin Epidemiol. 1989;42(9):849–56.

301. Vittinghoff E, Douglas J, Judson F, McKirnan D, MacQueen K, Buchbinder SP. Per-contact risk of human immunodeficiency virus transmission between male sexual partners. Am J Epidemiol. 1999 Aug;150(3):306–11.

302. Jin F, Jansson J, Law M, Prestage GP, Zablotska I, Imrie JCG, et al. Per-contact probability of HIV transmission in homosexual men in Sydney in the era of HAART. AIDS. 2010 Mar;24(6):907–13.

303. Guo J, Zuo T, Cheng L, Wu X, Tang J, Sun C, et al. Simian immunodeficiency virus infection evades vaccine-elicited antibody responses to V2 region. J Acquir Immune Defic Syndr [Internet]. 2015;68(5):502–10. Available from: http://www.ncbi.nlm.nih.gov/pubmed/25622057

304. Bonsignori M, Hwang K-K, Chen X, Tsao C-Y, Morris L, Gray E, et al. Analysis of a clonal lineage of HIV-1 envelope V2/V3 conformational epitope-specific broadly neutralizing antibodies and their inferred unmutated common ancestors. J Virol. 2011 Oct;85(19):9998–10009.

305. Mata-Fink J, Kriegsman B, Yu HX, Zhu H, Hanson MC, Irvine DJ, et al. Rapid conformational epitope mapping of anti-gp120 antibodies with a designed mutant panel displayed on yeast. J Mol Biol. 2013 Jan;425(2):444–56.

306. Shental-Bechor D, Levy Y. Effect of glycosylation on protein folding: A close look at

thermodynamic stabilization. Proc Natl Acad Sci [Internet]. 2008 Jun 17;105(24):8256 LP – 8261. Available from: http://www.pnas.org/content/105/24/8256.abstract

307. De Pourcq K, De Schutter K, Callewaert N. Engineering of glycosylation in yeast and other fungi: current state and perspectives. Appl Microbiol Biotechnol [Internet]. 2010;87(5):1617–31. Available from: https://doi.org/10.1007/s00253-010-2721-1

308. Mathew E, Zhu H, Connelly SM, Sullivan MA, Brewer MG, Piepenbrink MS, et al. Display of the HIV envelope protein at the yeast cell surface for immunogen development. PLoS One. 2018;13(10):e0205756.

309. Li F, Finnefrock AC, Dubey SA, Korber BTM, Szinger J, Cole S, et al. Mapping HIV-1 vaccine induced T-cell responses: bias towards less-conserved regions and potential impact on vaccine efficacy in the Step study. PLoS One. 2011;6(6):e20479.

310. Fiore-Gartland A, Manso BA, Friedrich DP, Gabriel EE, Finak G, Moodie Z, et al. Pooled-Peptide Epitope Mapping Strategies Are Efficient and Highly Sensitive: An Evaluation of Methods for Identifying Human T Cell Epitope Specificities in Large-Scale HIV Vaccine Efficacy Trials. PLoS One. 2016;11(2):e0147812.

311. Scala G, Chen X, Liu W, Telles JN, Cohen OJ, Vaccarezza M, et al. Selection of HIV-Specific Immunogenic Epitopes by Screening Random Peptide Libraries with HIV-1-Positive Sera. J Immunol [Internet]. 1999 May 15;162(10):6155 LP – 6161. Available from: http://www.jimmunol.org/content/162/10/6155.abstract

312. Benatuil L, Perez JM, Belk J, Hsieh C-M. An improved yeast transformation method for the generation of very large human antibody libraries. Protein Eng Des Sel [Internet]. 2010 Feb 3;23(4):155–9. Available from: https://doi.org/10.1093/protein/gzq002

313. Feldhaus MJ, Siegel RW, Opresko LK, Coleman JR, Feldhaus JMW, Yeung YA, et al. Flow-

cytometric isolation of human antibodies from a nonimmune Saccharomyces cerevisiae surface display library. Nat Biotechnol. 2003 Feb;21(2):163–70.

314. Interpretation and use of the western blot assay for serodiagnosis of human immunodeficiency virus type 1 infections. MMWR Suppl. 1989 Jul;38(7):1–7.

315. Zolla-Pazner S, Cardozo T. Structure–function relationships of HIV-1 envelope sequence-variable regions refocus vaccine design. Nat Rev Immunol. 2010;10(7):527–35.

316. Morales JF, Morin TJ, Yu B, Tatsuno GP, O'Rourke SM, Theolis RJ, et al. HIV-1 envelope proteins and V1/V2 domain scaffolds with mannose-5 to improve the magnitude and quality of protective antibody responses to HIV-1. J Biol Chem. 2014 Jul;289(30):20526–42.

317. Zolla-Pazner S, Powell R, Yahyaei S, Williams C, Jiang X, Li W, et al. Rationally Designed Vaccines Targeting the V2 Region of HIV-1 gp120 Induce a Focused, Cross-Clade-Reactive, Biologically Functional Antibody Response. J Virol. 2016 Dec;90(24):10993–1006.

318. Gottardo R, Bailer RT, Korber BT, Gnanakaran S, Phillips J, Shen X, et al. Plasma IgG to linear epitopes in the V2 and V3 regions of HIV-1 gp120 correlate with a reduced risk of infection in the RV144 vaccine efficacy trial. PLoS One. 2013;8(9):e75665.

319. Jones AT, Chamcha V, Kesavardhana S, Shen X, Beaumont D, Das R, et al. A Trimeric HIV-1 Envelope gp120 Immunogen Induces Potent and Broad Anti-V1V2 Loop Antibodies against HIV-1 in Rabbits and Rhesus Macaques. J Virol. 2018 Mar;92(5).

320. Rong R, Li B, Lynch RM, Haaland RE, Murphy MK, Mulenga J, et al. Escape from autologous neutralizing antibodies in acute/early subtype C HIV-1 infection requires multiple pathways. PLoS Pathog. 2009;5(9):e1000594.

321. McCoy LE, van Gils MJ, Ozorowski G, Messmer T, Briney B, Voss JE, et al. Holes in the Glycan

Shield of the Native HIV Envelope Are a Target of Trimer-Elicited Neutralizing Antibodies. Cell Rep. 2016 Aug;16(9):2327–38.

322. England PH. RITA metadata, 2nd version. 2013.

323. BHIVA. BHIVA guidelines for the routine investigation and monitoring of adult HIV-1-positive individuals (2019 interim update) [Internet]. 2019. Available from: https://www.bhiva.org/file/DqZbRxfzlYtLg/Monitoring-Guidelines.pdf

324. Peeters M. Recombinant HIV sequences: their role in the global epidemic [Internet]. 2000. Available from: https://www.hiv.lanl.gov/content/sequence/HIV/REVIEWS/PEETERS2000/Peeters.html

325. Suligoi B, Galli C, Massi M, Di Sora F, Sciandra M, Pezzotti P, et al. Precision and accuracy of a procedure for detecting recent human immunodeficiency virus infections by calculating the antibody avidity index by an automated immunoassay-based method. J Clin Microbiol. 2002 Nov;40(11):4015–20.

326. Ditzel HJ, Parren PW, Binley JM, Sodroski J, Moore JP, Barbas CF 3rd, et al. Mapping the protein surface of human immunodeficiency virus type 1 gp120 using human monoclonal antibodies from phage display libraries. J Mol Biol. 1997 Apr;267(3):684–95.

327. Wyatt R, Sodroski J. The HIV-1 envelope glycoproteins: fusogens, antigens, and immunogens. Science. 1998 Jun;280(5371):1884–8.

328. Sok D, Pauthner M, Briney B, Lee JH, Saye-Francisco KL, Hsueh J, et al. A Prominent Site of Antibody Vulnerability on HIV Envelope Incorporates a Motif Associated with CCR5 Binding and Its Camouflaging Glycans. Immunity. 2016 Jul;45(1):31–45.

329. Nelson JA, Baribaud F, Edwards T, Swanstrom R. Patterns of changes in human

immunodeficiency virus type 1 V3 sequence populations late in infection. J Virol. 2000 Sep;74(18):8494–501.

330. Jiang X, Burke V, Totrov M, Williams C, Cardozo T, Gorny MK, et al. Conserved structural elements in the V3 crown of HIV-1 gp120. Nat Struct Mol Biol. 2010;17(8):955.

331. Pancera M, Zhou T, Druz A, Georgiev IS, Soto C, Gorman J, et al. Structure and immune recognition of trimeric pre-fusion HIV-1 Env. Nature. 2014 Oct;514(7523):455–61.

332. Levesque MC, Moody MA, Hwang K-K, Marshall DJ, Whitesides JF, Amos JD, et al. Polyclonal B cell differentiation and loss of gastrointestinal tract germinal centers in the earliest stages of HIV-1 infection. PLoS Med. 2009 Jul;6(7):e1000107.

333. Mascola JR, Stiegler G, VanCott TC, Katinger H, Carpenter CB, Hanson CE, et al. Protection of macaques against vaginal transmission of a pathogenic HIV-1/SIV chimeric virus by passive infusion of neutralizing antibodies. Nat Med. 2000;6(2):207–10.

334. Pegu A, Yang Z, Boyington JC, Wu L, Ko S-Y, Schmidt SD, et al. Neutralizing antibodies to HIV-1 envelope protect more effectively in vivo than those to the CD4 receptor. Sci Transl Med. 2014 Jul;6(243):243ra88.

335. Alam SM, Morelli M, Dennison SM, Liao H-X, Zhang R, Xia S-M, et al. Role of HIV membrane in neutralization by two broadly neutralizing antibodies. Proc Natl Acad Sci U S A. 2009 Dec;106(48):20234–9.

336. Frey G, Peng H, Rits-Volloch S, Morelli M, Cheng Y, Chen B. A fusion-intermediate state of HIV-1 gp41 targeted by broadly neutralizing antibodies. Proc Natl Acad Sci U S A. 2008 Mar;105(10):3739–44.

337. Molinos-Albert LM, Clotet B, Blanco J, Carrillo J. Immunologic Insights on the Membrane

Proximal External Region: A Major Human Immunodeficiency Virus Type-1 Vaccine Target. Front Immunol [Internet]. 2017 Sep 19;8:1154. Available from: https://www.ncbi.nlm.nih.gov/pubmed/28970835

338. Rerks-Ngarm S, Pitisuttithum P, Nitayaphan S, Kaewkungwal J, Chiu J, Paris R, et al. Vaccination with ALVAC and AIDSVAX to prevent HIV-1 infection in Thailand. N Engl J Med. 2009;361(23):2209–20.

339. Postler TS, Desrosiers RC. The Tale of the Long Tail: the Cytoplasmic Domain of HIV-1 gp41. J Virol [Internet]. 2013 Jan 1;87(1):2 LP – 15. Available from: http://jvi.asm.org/content/87/1/2.abstract

340. Kennedy RC, Henkel RD, Pauletti D, Allan JS, Lee TH, Essex M, et al. Antiserum to a synthetic peptide recognizes the HTLV-III envelope glycoprotein. Science. 1986 Mar;231(4745):1556–9.

341. Postler TS, Martinez-Navio JM, Yuste E, Desrosiers RC. Evidence against Extracellular Exposure of a Highly Immunogenic Region in the C-Terminal Domain of the Simian Immunodeficiency Virus gp41 Transmembrane Protein. J Virol [Internet]. 2012 Jan 15;86(2):1145 LP – 1157. Available from: http://jvi.asm.org/content/86/2/1145.abstract

342. Crooks ET, Tong T, Osawa K, Binley JM. Enzyme digests eliminate nonfunctional Env from HIV-1 particle surfaces, leaving native Env trimers intact and viral infectivity unaffected. J Virol. 2011 Jun;85(12):5825–39.

343. Hollier MJ, Dimmock NJ. The C-terminal tail of the gp41 transmembrane envelope glycoprotein of HIV-1 clades A, B, C, and D may exist in two conformations: an analysis of sequence, structure, and function. Virology. 2005 Jul;337(2):284–96.

344. Steckbeck JD, Sun C, Sturgeon TJ, Montelaro RC. Topology of the C-terminal tail of HIV-1 gp41: differential exposure of the Kennedy epitope on cell and viral membranes. PLoS One. 2010

Dec;5(12):e15261.

345. Viard M, Ablan SD, Zhou M, Veenstra TD, Freed EO, Raviv Y, et al. Photoinduced reactivity of the HIV-1 envelope glycoprotein with a membrane-embedded probe reveals insertion of portions of the HIV-1 Gp41 cytoplasmic tail into the viral membrane. Biochemistry. 2008 Feb;47(7):1977–83.

346. White E, Wu F, Chertova E, Bess J, Roser JD, Lifson JD, et al. Truncating the gp41 Cytoplasmic Tail of Simian Immunodeficiency Virus Decreases Sensitivity to Neutralizing Antibodies without Increasing the Envelope Content of Virions. Silvestri G, editor. J Virol [Internet]. 2018 Feb 1;92(3):e01688-17. Available from: http://jvi.asm.org/content/92/3/e01688-17.abstract

347. Salzwedel K, West JT, Hunter E. A conserved tryptophan-rich motif in the membrane-proximal region of the human immunodeficiency virus type 1 gp41 ectodomain is important for Env-mediated fusion and virus infectivity. J Virol. 1999;73(3):2469–80.

348. Muster T, Steindl F, Purtscher M, Trkola A, Klima A, Himmler G, et al. A conserved neutralizing epitope on gp41 of human immunodeficiency virus type 1. J Virol. 1993;67(11):6642–7.

349. Cerutti N, Loredo-Varela JL, Caillat C, Weissenhorn W. Antigp41 membrane proximal external region antibodies and the art of using the membrane for neutralization. Curr Opin HIV AIDS. 2017 May;12(3):250–6.

350. Moore JP, McKeating JA, Weiss RA, Sattentau QJ. Dissociation of gp120 from HIV-1 virions induced by soluble CD4. Science. 1990 Nov;250(4984):1139–42.

351. Williams KL, Stumpf M, Naiman NE, Ding S, Garrett M, Gobillot T, et al. Identification of HIV gp41-specific antibodies that mediate killing of infected cells. PLoS Pathog [Internet]. 2019 Feb 19;15(2):e1007572–e1007572. Available from: https://www.ncbi.nlm.nih.gov/pubmed/30779811

352. Sahay B, Nguyen CQ, Yamamoto JK. Conserved HIV Epitopes for an Effective HIV Vaccine. J Clin Cell Immunol [Internet]. 2017/08/30. 2017 Aug;8(4):518. Available from: https://www.ncbi.nlm.nih.gov/pubmed/29226015

353. Kassutto S, Johnston MN, Rosenberg ES. Incomplete HIV type 1 antibody evolution and seroreversion in acutely infected individuals treated with early antiretroviral therapy. Clin Infect Dis. 2005 Mar;40(6):868–73.

354. Ananworanich J, Puthanakit T, Suntarattiwong P, Chokephaibulkit K, Kerr SJ, Fromentin R, et al. Reduced markers of HIV persistence and restricted HIV-specific immune responses after early antiretroviral therapy in children. AIDS. 2014 Apr;28(7):1015–20.

355. Keating SM, Pilcher CD, Jain V, Lebedeva M, Hampton D, Abdel-Mohsen M, et al. HIV Antibody Level as a Marker of HIV Persistence and Low-Level Viral Replication. J Infect Dis [Internet]. 2017 May 11;216(1):72–81. Available from: https://doi.org/10.1093/infdis/jix225

356. Fukazawa Y, Lum R, Okoye AA, Park H, Matsuda K, Bae JY, et al. B cell follicle sanctuary permits persistent productive simian immunodeficiency virus infection in elite controllers. Nat Med. 2015 Feb;21(2):132–9.

357. Kohler G, Milstein C. Continuous cultures of fused cells secreting antibody of predefined specificity. Nature. 1975 Aug;256(5517):495–7.

358. Nelson AL, Dhimolea E, Reichert JM. Development trends for human monoclonal antibody therapeutics. Nat Rev Drug Discov. 2010 Oct;9(10):767–74.

359. Morbach H, Eichhorn EM, Liese JG, Girschick HJ. Reference values for B cell subpopulations from infancy to adulthood. Clin Exp Immunol. 2010 Nov;162(2):271–9.

360. Katzmann JA, Clark RJ, Abraham RS, Bryant S, Lymp JF, Bradwell AR, et al. Serum reference

intervals and diagnostic ranges for free kappa and free lambda immunoglobulin light chains: relative sensitivity for detection of monoclonal light chains. Clin Chem. 2002 Sep;48(9):1437–44.

361. Kyu SY, Kobie J, Yang H, Zand MS, Topham DJ, Quataert SA, et al. Frequencies of human influenza-specific antibody secreting cells or plasmablasts post vaccination from fresh and frozen peripheral blood mononuclear cells. J Immunol Methods. 2009 Jan;340(1):42–7.

362. Smith MJ, Packard TA, O'Neill SK, Hinman RM, Rihanek M, Gottlieb PA, et al. Detection and Enrichment of Rare Antigen-specific B Cells for Analysis of Phenotype and Function. J Vis Exp. 2017 Feb;(120).

363. Botling J, Edlund K, Segersten U, Tahmasebpoor S, Engström M, Sundström M, et al. Impact of thawing on RNA integrity and gene expression analysis in fresh frozen tissue. Diagn Mol Pathol. 2009 Mar;18(1):44–52.

364. Ji X, Wang M, Li L, Chen F, Zhang Y, Li Q, et al. The Impact of Repeated Freeze–Thaw Cycles on the Quality of Biomolecules in Four Different Tissues. Biopreserv Biobank [Internet]. 2017 Sep 20;15(5):475–83. Available from: https://doi.org/10.1089/bio.2017.0064

365. Scientific TF. Effect of Freeze-Thawing of Tissue on RNA Integrity [Internet]. Available from: https://www.thermofisher.com/uk/en/home/references/ambion-tech-support/rna-isolation/tech-notes/effect-of-freeze-thawing-of-tissue-on-rna-integrity.html

366. North B, Lehmann A, Dunbrack Jr RL. A new clustering of antibody CDR loop conformations. J Mol Biol [Internet]. 2010/10/28. 2011 Feb 18;406(2):228–56. Available from: https://www.ncbi.nlm.nih.gov/pubmed/21035459

367. Johnson G, Wu TT. Preferred CDRH3 lengths for antibodies with defined specificities. Int Immunol. 1998 Dec;10(12):1801–5.

368. Briney BS, Willis JR, Crowe JEJ. Human peripheral blood antibodies with long HCDR3s are established primarily at original recombination using a limited subset of germline genes. PLoS One. 2012;7(5):e36750.

369. Herbeck J, Tanser F. Community viral load as an index of HIV transmission potential. lancet HIV. 2016 Apr;3(4):e152-4.

370. Cherf GM, Cochran JR. Applications of Yeast Surface Display for Protein Engineering. Methods Mol Biol [Internet]. 2015;1319:155–75. Available from: https://www.ncbi.nlm.nih.gov/pubmed/26060074

371. Wildt S, Gerngross TU. The humanization of N-glycosylation pathways in yeast. Nat Rev Microbiol. 2005 Feb;3(2):119–28.

372. Moiani A, Paleari Y, Sartori D, Mezzadra R, Miccio A, Cattoglio C, et al. Lentiviral vector integration in the human genome induces alternative splicing and generates aberrant transcripts. J Clin Invest [Internet]. 2012/04/23. 2012 May;122(5):1653–66. Available from: https://www.ncbi.nlm.nih.gov/pubmed/22523069

373. Bushman F, Lewinski M, Ciuffi A, Barr S, Leipzig J, Hannenhalli S, et al. Genome-wide analysis of retroviral DNA integration. Nat Rev Microbiol. 2005 Nov;3(11):848–58.

374. Belshaw R, Pereira V, Katzourakis A, Talbot G, Paces J, Burt A, et al. Long-term reinfection of the human genome by endogenous retroviruses. Proc Natl Acad Sci U S A [Internet]. 2004/03/25. 2004 Apr 6;101(14):4894–9. Available from: https://www.ncbi.nlm.nih.gov/pubmed/15044706

375. Feschotte C, Gilbert C. Endogenous viruses: insights into viral evolution and impact on host biology. Nat Rev Genet [Internet]. 2012 Mar 16;13:283. Available from: https://doi.org/10.1038/nrg3199

Appendices

Chapter 7 Appendices

Supplemental material 1 Permissions for image use
Supplemental material 2 Permissions for image use
Supplemental material 3 Nanodrop readings for PCR products
Supplemental material 4 RNA polymerase sequences

Supplemental material 1 Permissions for image use

SPRINGER NATURE LICENSE
TERMS AND CONDITIONS

Jul 19, 2019

This Agreement between Katie McFaul ("You") and Springer Nature ("Springer Nature") consists of your license details and the terms and conditions provided by Springer Nature and Copyright Clearance Center.

License Number	4632571150475
License date	Jul 19, 2019
Licensed Content Publisher	Springer Nature
Licensed Content Publication	Nature Immunology
Licensed Content Title	Antibody responses to envelope glycoproteins in HIV-1 infection
Licensed Content Author	Dennis R Burton, John R Mascola
Licensed Content Date	May 19, 2015
Licensed Content Volume	16
Licensed Content Issue	6
Type of Use	Thesis/Dissertation
Requestor type	academic/university or research institute
Format	print and electronic
Portion	figures/tables/illustrations
Number of figures/tables/illustrations	2
High-res required	no
Will you be translating?	no
Circulation/distribution	<501
Author of this Springer Nature content	no
Title	Dr
Institution name	Imperial College London
Expected presentation date	Nov 2019
Portions	Figure 1: Schematic of some of the forms of Env protein that may be present on infectious HIV-1 and available to elicit Ab responses, Figure 2: Structure of the HIV-1 Env trimer,
Requestor Location	Katie McFaul 24 Petergate Wandsworth London, London, City of SW11 2UE United Kingdom Attn: Katie McFaul
Total	0,00 GBP

Terms and Conditions

Springer Nature Customer Service Centre GmbH
Terms and Conditions

This agreement sets out the terms and conditions of the licence (the **Licence**) between you and **Springer Nature Customer Service Centre GmbH** (the **Licensor**). By clicking 'accept' and completing the transaction for the material (**Licensed Material**), you also confirm your acceptance of these terms and conditions.

1. Grant of License

1. 1. The Licensor grants you a personal, non-exclusive, non-transferable, world-wide licence to reproduce the Licensed Material for the purpose specified in your order only. Licences are granted for the specific use requested in the order and for no other use, subject to the conditions below.

1. 2. The Licensor warrants that it has, to the best of its knowledge, the rights to license reuse of the Licensed Material. However, you should ensure that the material you are requesting is original to the Licensor and does not carry the copyright of another entity (as credited in the published version).

1. 3. If the credit line on any part of the material you have requested indicates that it was reprinted or adapted with permission from another source, then you should also seek permission from that source to reuse the material.

2. Scope of Licence

2. 1. You may only use the Licensed Content in the manner and to the extent permitted by these Ts&Cs and any applicable laws.

2. 2. A separate licence may be required for any additional use of the Licensed Material, e.g. where a licence has been purchased for print only use, separate permission must be obtained for electronic re-use. Similarly, a licence is only valid in the language selected and does not apply for editions in other languages unless additional translation rights have been granted separately in the licence. Any content owned by third parties are expressly excluded from the licence.

2. 3. Similarly, rights for additional components such as custom editions and derivatives require additional permission and may be subject to an additional fee. Please apply to Journalpermissions@springernature.com/bookpermissions@springernature.com for these rights.

2, 4, Where permission has been granted **free of charge** for material in print, permission may also be granted for any electronic version of that work, provided that the material is incidental to your work as a whole and that the electronic version is essentially equivalent to, or substitutes for, the print version.

2, 5, An alternative scope of licence may apply to signatories of the STM Permissions Guidelines, as amended from time to time.

3. Duration of Licence

3. 1. A licence for is valid from the date of purchase ('Licence Date') at the end of the relevant period in the below table:

Scope of Licence	Duration of Licence
Post on a website	12 months
Presentations	12 months
Books and journals	Lifetime of the edition in the language purchased

4. Acknowledgement

4, 1, The Licensor's permission must be acknowledged next to the Licenced Material in print. In electronic form, this acknowledgement must be visible at the same time as the figures/tables/illustrations or abstract, and must be hyperlinked to the journal/book's homepage. Our required acknowledgement format is in the Appendix below.

5. Restrictions on use

5. 1. Use of the Licensed Material may be permitted for incidental promotional use and minor editing privileges e.g. minor adaptations of single figures, changes of format, colour and/or style where the adaptation is credited as set out in Appendix 1 below. Any other changes including but not limited to, cropping, adapting, omitting material that affect the meaning, intention or moral rights of the author are strictly prohibited.

5. 2. You must not use any Licensed Material as part of any design or trademark.

5. 3. Licensed Material may be used in Open Access Publications (OAP) before publication by Springer Nature, but any Licensed Material must be removed from OAP sites prior to final publication.

6. Ownership of Rights

6. 1. Licensed Material remains the property of either Licensor or the relevant third party and any rights not explicitly granted herein are expressly reserved.

7. Warranty

IN NO EVENT SHALL LICENSOR BE LIABLE TO YOU OR ANY OTHER PARTY OR ANY OTHER PERSON OR FOR ANY SPECIAL, CONSEQUENTIAL, INCIDENTAL OR INDIRECT DAMAGES, HOWEVER CAUSED, ARISING OUT OF OR IN CONNECTION WITH THE DOWNLOADING, VIEWING OR USE OF THE MATERIALS REGARDLESS OF THE FORM OF ACTION, WHETHER FOR BREACH OF CONTRACT, BREACH OF WARRANTY, TORT, NEGLIGENCE, INFRINGEMENT OR OTHERWISE (INCLUDING, WITHOUT LIMITATION, DAMAGES BASED ON LOSS OF PROFITS, DATA, FILES, USE, BUSINESS OPPORTUNITY OR CLAIMS OF THIRD PARTIES), AND WHETHER OR NOT THE PARTY HAS BEEN ADVISED OF THE POSSIBILITY OF SUCH DAMAGES. THIS LIMITATION SHALL APPLY NOTWITHSTANDING ANY FAILURE OF ESSENTIAL PURPOSE OF ANY LIMITED REMEDY PROVIDED HEREIN.

8. Limitations

8. 1. ***BOOKS ONLY:*** Where **'reuse in a dissertation/thesis'** has been selected the following terms apply: Print rights of the final author's accepted manuscript (for clarity, NOT the published version) for up to 100 copies, electronic rights for use only on a personal website or institutional repository as defined by the Sherpa guideline (www.sherpa.ac.uk/romeo/).

9. Termination and Cancellation

9, 1, Licences will expire after the period shown in Clause 3 (above).

9, 2, Licensee reserves the right to terminate the Licence in the event that payment is not received in full or if there has been a breach of this agreement by you.

Appendix 1 — Acknowledgements:

For Journal Content:
Reprinted by permission from **[the Licensor]**: [**Journal Publisher** (e.g. Nature/Springer/Palgrave)] **[JOURNAL NAME]** [**REFERENCE CITATION** (Article name, Author(s) Name), [**COPYRIGHT**] (year of publication)

For **Advance Online Publication papers:**
Reprinted by permission from **[the Licensor]**: [**Journal Publisher** (e.g. Nature/Springer/Palgrave)] **[JOURNAL NAME]** [**REFERENCE CITATION** (Article name, Author(s) Name), [**COPYRIGHT**] (year of publication), advance online publication, day month year (doi: 10.1038/sj.[JOURNAL ACRONYM].)

For Adaptations/Translations:
Adapted/Translated by permission from [**the Licensor**]: [**Journal Publisher** (e.g. Nature/Springer/Palgrave)] [**JOURNAL NAME**] [**REFERENCE CITATION** (Article name, Author(s) Name), [**COPYRIGHT**] (year of publication)

Note: For any republication from the British Journal of Cancer, the following credit line style applies:

Reprinted/adapted/translated by permission from [**the Licensor**]: on behalf of Cancer Research UK: : [**Journal Publisher** (e.g. Nature/Springer/Palgrave)] [**JOURNAL NAME**] [**REFERENCE CITATION** (Article name, Author(s) Name), [**COPYRIGHT**] (year of publication)

For **Advance Online Publication** papers:
Reprinted by permission from The [**the Licensor**]: on behalf of Cancer Research UK: [**Journal Publisher** (e.g. Nature/Springer/Palgrave)] [**JOURNAL NAME**] [**REFERENCE CITATION** (Article name, Author(s) Name), [**COPYRIGHT**] (year of publication), advance online publication, day month year (doi: 10.1038/sj.[JOURNAL ACRONYM])

For Book content:
Reprinted/adapted by permission from [**the Licensor**]: [**Book Publisher** (e.g. Palgrave Macmillan, Springer etc) [**Book Title**] by [**Book author**(s)] [**COPYRIGHT**] (year of publication)

Other Conditions:

Version 1.2

Questions? customercare@copyright.com or +1-855-239-3415 (toll free in the US) or +1-978-646-2777.

Supplemental material 2 Permissions for image use

ELSEVIER LICENSE
TERMS AND CONDITIONS

Jul 22, 2019

This Agreement between Katie McFaul ("You") and Elsevier ("Elsevier") consists of your license details and the terms and conditions provided by Elsevier and Copyright Clearance Center.

License Number	4634390427582
License date	Jul 22, 2019
Licensed Content Publisher	Elsevier
Licensed Content Publication	Trends in Immunology
Licensed Content Title	Antibody B cell responses in HIV-1 infection
Licensed Content Author	Hugo Mouquet
Licensed Content Date	Nov 1, 2014
Licensed Content Volume	35
Licensed Content Issue	11
Licensed Content Pages	13
Start Page	549
End Page	561
Type of Use	reuse in a thesis/dissertation
Portion	figures/tables/illustrations
Number of figures/tables/illustrations	1
Format	both print and electronic
Are you the author of this Elsevier article?	No
Will you be translating?	No
Original figure numbers	Figure 2: sites of vulnerability on HIV-1 envelope glycoprotein
Title of your thesis/dissertation	Dr
Publisher of new work	Imperial College London
Expected completion date	Nov 2019
Estimated size (number of pages)	1
Requestor Location	Katie McFaul 24 Petergate Wandsworth London, London, City of SW11 2UE United Kingdom Attn: Katie McFaul
Publisher Tax ID	GB 494 6272 12
Total	0,00 GBP
Terms and Conditions	

Supplemental material 3 Nanodrop readings for PCR products

Digested library product concentrations for envelope and gp41 big and small libraries	Volume (µl)	Conc (ng/µl)	260/80 ratio	260/30 ratio	Total (ng)
HIV Env small library	50	55.8	1.88	1.9	2790
HIV Env big library	50	68.4	1.95	2.1	3420
gp41 small library	50	25.7	1.87	2.31	1285
gp41 big library	50	30.6	1.88	2.31	1530
A-tailed PCR library fragments	Volume (µl)	Conc (ng/µl)	260/80 ratio	260/30 ratio	Total (ng)
HIV Env small library	50	36.6	1.92	2.51	1830
HIV Env big library	50	64.5	1.86	2.39	3225
gp41 small library	50	22.9	1.69	1.72	1145
gp41 big library	50	30.6	1.88	1.9	1300
pCTCON2-T vector digest concentration	Volume (µl)	Conc (ng/µl)	260/80 ratio	260/30 ratio	Total (ng)
pCTCON2-T	25	273	1.87	2.17	8190
Ligated fragments and vector yield	Volume (µl)	Conc (ng/µl)	260/80 ratio	260/30 ratio	Total (ng)
HIV Env small library + vector	50	85.4	1.92	2.19	4270
HIV Env big library + vector	50	99.3	2.04	2.36	4965
gp41 small library + vector	50	65.7	1.79	1.95	3285
gp41 big library + vector	50	69.1	1.77	2.01	3455
Library fragment plasmid DNA concentrations	Volume (µl)	Conc (ng/µl)	260/80 ratio	260/30 ratio	Total (ng)
HIV Env small library plasmid	500	962.6	1.89	1.06	481300
HIV Env big library plasmid	500	1175.7	2	1.89	587850
gp41 small library plasmid	500	856.3	1.79	1.95	428150
gp41 big library plasmid	500	894.5	1.77	2.01	447250

Ul microlitre, Conc concentration, 260/80 and 260/30 ratio indicate quality and contamination of product, ng nanogram

Supplemental material 4 RNA polymerase sequences

Subunit alpha	MQGSVTEFLKPRLVDIEQVSSTHAKVTLEPLERGFGHTLGNALRRILLSSMPGCAVTEVEIDGVLHEYSTKEGVQEDILEILLNLKGLAVRVQGKDEVILTLNKSGIGPVTAADITHDGDVEIVKPQHVICHLTDENASISMRIKVQRGRGYV PASTRIHSEEDERPIGRLLVDACYSPVERIAYNVEAARVEQRTDLDKLVIEMETNGTIDPEEAIRRAATILAEQLEAFVDLRDVRQPEVKEEKPEFDPILLRPVDDLELTVRSANCLKAEAIHYIGDLVQRTEVELLKTPNLGKKSLTEIKDVLASR GLSLGMRLENWPPASIADE
Subunit beta 1	MVYSYTEKKRIRKDFGKRPQVLDVPYLLSIQLDSFQKFIEQDPEGQYGLEAAFRSVFPIQSYSGNSELQYVSYRLGEPVFDVQECQIRGVTYSAPLRVKLRLVIYEREAPEGTVKDIKEQEVYMGEIPLMTDNGTFVINGTERVIVSQLHRSP GVFFDSDKGKTHSSGKVLYNARIIPYRGSWLDFEFDPKDNLFVRIDRRRKLPATIILRALNYTTEQILDLFFEKVIFEIRDNKLQMELVPERLRGETASFDIEANGKVYVEKGRRITARHIRQLEKDDVKLIEVPVEYIAGKVVAKDYIDESTGELI CAANMELSLDLLAKLSQSGHKRIETLFTNDLDHGPYISETLRVDPTNDRLSALVEIYRMMRPGEPPTREAAESLFENLFFSEDRYDLSAVGRMKFNRSLLREEIEGSGILSKDDIIDVMKKLIDIRNGKGEVDDIDHLGNRRIRSVGEMAENQ FRVGLVRVERAVKERLSLGDLDTLMPQDMINAKPISAAVKEFFGSSQLSQFMDQNNPLSEITHKRRISALGPGGLTRERAGFEVRDVHPTHYGRVCPIETPEGPNIGLINSLSVYAQTNEYGFLETPYRKVTDGVVTDEIHYLSAIEEGNYVI AQANSNLDEEGHFVEDLVTCRSKGESSLFSRDQVDYMDVSTQQVVSVGASLIPFLEHDDANRALMGANMQRQAVPTLRADKPLVGTGMERAVAVDSGVTAVAKRGGVVQYVDASRIVIKVNEDEMYPGEAGIDIYNLTKYTRSNQ NTCINQMPCVSLGEPVERGDVLADGPSTDLGELALGQNMRVAFMPWNGYNFEDSILVSERVVQEDRFTTIHIQELACVSRDTKLGPEEITADIPNVGEAALSKLDESGIVYIGAEVTGGDILVGKVTPKGETQLTPEEKLLRAIFGEKASDV KDSSLRVPNGVSGTVIDVQVFTRDGVEKDKRALEIEEMQLKQAKKDLSEELQILEAGLFSRIRAVLVAGGVEAEKLDKLPRDRWLELGLTDEEKQNQLEQLAEQYDELKHEFEKKLEAKRRKITQGDDLAPGVLKIVKVYLAVKRRIQPGDK MAGRHGNKGVISKINPIEDMPYDENGTPVDIVLNPLGVPSRMNIGQILETHLGMAAKGIGDKINAMLKQQQEVAKLREFIQRAYDLGADVRQKVDLSTFSDEEVMRLAENLRKGMPIATPVFDGAKEAEIKELLKLGDLPTSGQIRLYD GRTGEQFERPVTVGYMYMLKLNHLVDDKMHARSTGSYSLVTQQPLGGKAQFGGQRFGEMEVWALEAYGAAYTLQEMLTVKSDDVNGRTKMYKNIVDGNHQMEPGMPESFNVLLKEIRSLGINIELEDE
Subunit beta 2	MKDLLKFLKAQTKTEEFDAIKIALASPDMIRSWSFGEVKKPETINYRTFKPERDGLFCARIFGPVKDYECLCGKYKRLKHRGVICEKCGVEVTQTKVRRERMGHIELASPTAHIWFLKSLPSRIGLLLDMPLRDIERVLYFESYVVIEGGMTNL ERQQILTEEQYLDALEEFGDEFDAKMGAEAIQALLKSMDLEQECEQLREELNETNSETKRKKLTKRIKLLEAFVQSGNKPEWMILTVLPVLPPDLRPLVPLDGGRFATSDLNDLYRRVINRNNRLKRLLDLAAPDIIVRNEKRMLQEAVDAL LDNGRRGRAITGSNKRPLKSLADMIKGKQGRFRQNLLKRVDYSGRSVITVGPYLRLHQCGLPKKMALELFKPFIYGKLELRGAKKMVEREEAVVWDILDEVIREHPVLLNRAPTLHRLGIQAFEPVLIEGKAIQLHPLVCAAYNADFDGDQ MAVHVPLTLEAQLEARALMMSTNNILSPANGEPIIVPSQDVVLGLYYMTRDCVNAKGEGMVLTGPKEAERLYRSGLASLHARVKVRITEYEKDANGELVAKTSLKDTTVGRAILWMIVPKGLPYSIVNQALGKKAISKMLNTCYRILGLK PTVIFADQIMYTGFAYAARSGASVGIDDMVIPEKKHEIISEAEAEVAEIQEQFQSGLVTAGERYNKVIDIWAAANDRVSKAMMDNLQTETVINRDGQEEKQVSFNSIYMMADSGARGSAAQIRQLAGMRGLMAKPDGSIIETPITANF REGLNVLQYFISTHGARKGLADTALKTANSGYLTRRLVDVAQDLVVTEDDCGTHEGIMMTPVIEGGDVKEPLRDRVLGRVTAEDVLKPGTADILVPRNTLLHEQWCDLLEENSVDAVKVRSVVSCDTDFGVCAHCYGRDLARGHIINKG EAIGVIAAQSIGEPGTQLTMRTFHIGGAASRAAAESSIQVKNKGSIKLSNVKSVVNSSGKLVITSRNTELKLIDEFGRTKESYKVPYGAVLAKGDGEQVAGGETVANWDPHTMPVITEVSGFVRFTDMIDGQTITRQTDELTGLSSLVVLDS AERTAGGKDLRPALKIVDAQGNDVLIPGTDMPAQYFLPGKAIVQLEDGVQISSGDTLARIPQESGGTKDITGGLPRVADLFEARRPKEPAILAEISGIVSFGKETKGKRRLVITPVDGSDPYEEMIPKWRQLNVFEGERVERGDVISDGPEA PHDILRLRGVHAVTRYIVNEVQDVYRLQGVKINDKHIEVIVRQMLRKATIVNAGSSDFLEGEQVEYSRVKIANRELEANGKVGATYSRDLLGITKASLATESFISAASFQETTRVLTEAAVAGKRDELRGLKENVIVGRLIPAGTGYAYHQDR MRRRAAGEAPAAPQVTAEDASASLAELLNAGLGGSDNE

Sequence information for alpha, beta 1 and 2 subunit protein components of E coli RNA polymerase